THE JOURNAL
OF
CHEMICAL PHYSICS

VOLUME 3 NOVEMBER, 1935 NUMBER 11

The Difference in Vapor Pressures of Ortho and Para Deuterium[1, 2]

F. G. BRICKWEDDE AND R. B. SCOTT, *National Bureau of Standards*
AND
H. S. TAYLOR, *Princeton University*

(Received September 2, 1935)

The difference between the vapor pressures, $\Delta P(e-n)$, of the 20.4°K equilibrium mixture and the normal mixture of the ortho and para varieties of D_2 were determined from 15° to 20.4°K. $\Delta P(e-n)$ varied from 0.3 mm of Hg at 15°K to 3.8 mm at 20.4°. $\Delta P(e-n)$ for deuterium is small as compared with $\Delta P(e-n)$ hydrogen, but $[\Delta P(\text{ortho-para})/P(n)]$ for deuterium is approximately equal to $[\Delta P(\text{para-ortho})/P(n)]$ for hydrogen at the same temperature. Further measurements were made on the uncatalyzed change with time of the vapor pressure of liquid normal deuterium. The change for deuterium is *less* than one mm of Hg in 200 hours, whereas the vapor pressure of liquid normal hydrogen increases one mm in 4 hours. This large difference in rates is attributable to the difference in magnetic moments of the proton and deuteron. If Wigner's theory of the ortho-para conversion by paramagnetic molecules in the gaseous phase is extended to the liquid phase to calculate the relative rates of change of the vapor pressures of liquid normal deuterium and liquid normal hydrogen, a ratio of 1/1000 is obtained for the ratio of the rate of change for deuterium to the rate of change for hydrogen.

THE difference between the vapor pressures of ortho and para deuterium in relation to the corresponding difference for hydrogen is in itself interesting, but it also seems important because the physical basis of the vapor pressure difference, even for hydrogen has not been made clear. Moreover vapor pressures of the ortho and para varieties have not been reported for any solid.

In Table I are listed properties of molecular hydrogen and deuterium that are useful in the interpretation of the differences between the vapor pressures of ortho and para varieties of these isotopes. The arrows indicate the relative orientations of the spins of the protons and the deuterons, the spins being $\frac{1}{2}$ and 1, respectively. The equilibrium concentrations of $p-H_2$ and $o-D_2$, the molecules with lowest rotational energy, $J=0$, increase as we proceed to lower temperatures.

The ortho-para deuterium vapor pressure differences were calculated from the measured vapor pressures of the normal mixture, $n-D_2$, and the 20.4°K temperature equilibrium mixture, $e-D_2$. The $e-D_2$ mixture was established by means of a zinc chromite catalyst, $ZnCrO_2$, placed in the bottom of a vapor pressure tube in which deuterium was condensed. The zinc chromite catalyst was prepared from zinc ammonium chromate which was obtained by mixing equimolecular proportions of dilute solutions of zinc nitrate and ammonium chromate. The solution was made slightly alkaline with ammonia and the

[1] Published with the approval of the Director of the National Bureau of Standards of the Department of Commerce.

[2] The results contained in this paper were reported in part at the symposium on *Heavy Hydrogen and Its Compounds* before a joint session of Section C of the American Association for the Advancement of Science and the American Physical Society in Pittsburgh, December 28, 1934.

TABLE I.

HYDROGEN	FERMI-DIRAC STATISTICS	ORTHO	PARA
	J (ROTATIONAL QUANTUM NUMBER)	ODD	EVEN
	CONCENTRATION[1] at 300°K (n-H_2)	0.75	0.25
	at 20°K (e-H_2)	0.002	0.998
DEUTERIUM	BOSE-EINSTEIN STATISTICS	ORTHO	PARA
	J (ROTATIONAL QUANTUM NUMBER)	EVEN	ODD
	CONCENTRATION[2] at 300°K (n-D_2)	0.667	0.333
	at 20°K (e-D_2)	0.978	0.022

[1] Harkness and Deming, J. Am. Chem. Soc. **54**, 2850 (1932).
[2] Johnston and Long, J. Chem. Phys. **2**, 389 (1934).

resulting precipitate washed, filtered and dried. The product was heated for 5 hours at 450°C and was then reduced by hydrogen at 400°C for 24 hours. The final product was a pale green powder which, by evacuation at 400°C, could be largely freed from traces of water which might interact with deuterium and thus contaminate it with hydrogen. Before use, it received a high temperature treatment with deuterium to convert any residual water to deuterium oxide. Zinc chromite, thus prepared is strongly paramagnetic and has been found to be an excellent agent for conversion of o-H_2 to p-H_2 at liquid-air temperatures.[3] Although not so efficient as chromium oxide gel[4] in the conversion process, it is superior to the latter in the present work owing to its small residual water content.

DESCRIPTION OF THE APPARATUS

Fig. 1 represents diagrammatically the apparatus used in making the vapor pressure measurements. In a liquid hydrogen cryostat were immersed three vapor pressure tubes connected with oil-lubricated (n-butyl phthalate) mercury manometers. Normal hydrogen was condensed in one tube and normal deuterium in the other two, one of which contained the $ZnCrO_2$ catalyst.

The temperature of the liquid hydrogen bath in the inner Dewar vessel was varied by means of a vacuum pump. With the aid of a fine adjustment valve and an oil-filled differential manometer it was possible to maintain the pressure in the vapor space over the liquid hydrogen bath constant to ± 0.2 mm of mercury. Since the liquid hydrogen bath was not stirred mechanically, special precautions were taken to insure that the hydrogen and deuterium condensates whose vapor pressures were being measured were at the same temperature. The manometer tubes running down through the cryostat bath were vacuum-jacketed except at their lower ends. These projected into a Bakelite tube across the lower end of which was a heater for boiling the cryostat bath. The heater prevented superheating of the bath, and set up circulation through the Bakelite tube.

Temperatures were calculated from the hydrogen vapor pressures by means of the following vapor pressure equation[5] for normal hydrogen

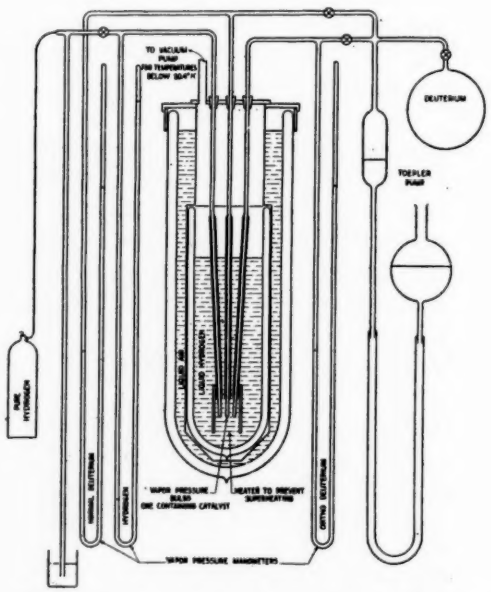

FIG. 1. Apparatus used in the measurement of the vapor pressures of deuterium.

[3] H. Diamond, Thesis, Princeton University, 1935.
[4] Howard, Trans. Faraday Soc. **30**, 278 (1934).

[5] This equation was deduced as the best fit for the experimental data on (1) the vapor pressure of liquid hydrogen, (2) the latent heat of vaporization, and (3) deviations of the molecular volume of the vapor from that

used in the previous paper:[6]

$$\log_{10} P(\text{mm of Hg}) = 4.6633 - 44.7291/T + 0.02023T. \quad (1)$$

Since the vapor pressure of normal hydrogen increases with time the measured vapor pressures were corrected by using the relation previously determined.[6] As it was also observed that small amounts of solid oxygen greatly increased the rate of conversion, the normal hydrogen which contained 0.02 percent air, as it flowed from a cylinder, was passed over copper gauze at 600°C and then through a liquid air trap.

The $e-D_2$ mixture was established by pumping the deuterium several times in and out of its vapor pressure tube containing the $ZnCrO_2$ at 20.4°K. Pumping was continued until the vapor pressure was not changed by further adsorption and desorption from the catalyst.

Experimental and Calculated Results

Vapor pressures of liquid and solid *n*-deuterium

The vapor pressures of the normal deuterium used in this investigation are related to those of liquid normal hydrogen by the following equations:

$$\log_{10} P(n-D_2 \text{ liquid}) = -1.3376 + 1.3004 \log_{10} P(n-H_2), \quad (2)$$

$$\log_{10} P(n-D_2 \text{ solid}) = -1.9044 + 1.5143 \log_{10} P(n-H_2). \quad (3)$$

Table II.

1 Age of condensed states (hrs.)	2 Observed vapor pressure of hydrogen (mm Hg)	3 Vapor pressure of normal hydrogen (calc.) (mm Hg)	4 Vapor pressure of normal deuterium (obs.) (mm Hg)
1.75	751.9	751.4	252.4
2.33	654.2	653.5	210.7
2.70	557.1	556.5	170.9
3.5	364.2	363.7	93.9
3.8	278.8	278.3	39.8
.9	741.9	741.6	248.1
1.5	549.9	549.6	168.2
1.8	489.7	489.4	144.4
2.2	414.3	414.0	114.4
2.7	385.7	385.3	102.6

of an ideal gas. All published vapor pressure measurements were considered, but this equation agrees best with the most recent Leiden measurements. (van Agt and Onnes, Leiden Comm. No. 176b (1925)).

[6] Scott, Brickwedde, Urey and Wahl, J. Chem. Phys. **2**, 454 (1934).

Table III. *Calculated boiling points and triple points.*

	Vapor pressure (mm Hg) $n-H_2$	Vapor pressure (mm Hg) $n-D_2$
23.59°K (Boiling point of $n-D_2$)	1753	760
20.38 (Boiling point of $n-H_2$)	760	256.2
18.71 (Triple point of $n-D_2$)	448	128.7
13.92 (Triple point of $n-H_2$)	54	5.2

With Eq. (1), these become

$$\log_{10} P(n-D_2 \text{ liquid}) = 4.7266 - 58.1657/T + 0.02630T, \quad (4)$$

$$\log_{10} P(n-D_2 \text{ solid}) = 5.1572 - 67.7333/T + 0.03063T. \quad (5)$$

These equations represent the lowest vapor pressure data yet obtained for deuterium and fit three of our samples prepared at different times.

In Table II are recorded two series of determinations of the vapor pressures of normal hydrogen and deuterium. The observed vapor pressures are given in columns 2 and 4. Column 3 is obtained from column 2 by correcting for the change[6] with time of the vapor pressure of the hydrogen resulting from the conversion of ortho to para hydrogen.

In Table III are listed the vapor pressures of normal hydrogen and deuterium at their boiling and triple points calculated from these equations. The values differ slightly from those of the earlier paper because the later measurements were made of purer deuterium. The vapor pressure of $n-D_2$ at 20.38°K reported here is 1.3 mm lower and the triple point temperature 0.13° higher than the previous values.[6]

Vapor Pressure Differences for Normal and Temperature (20.4°K) Equilibrium Deuterium

In Table IV are recorded observed differences between the vapor pressures of $e-D_2$ and $n-D_2$. These are plotted[7] in Fig. 2. The measurements

[7] Fig. 2 does not imply that the vapor pressures of the liquid and solid phases of $e-D_2$ at its triple point are not equal. At the high temperature end of the lower temperature curve is the triple point of $e-D_2$ and at the low temperature end of the higher temperature curve is the triple point of $n-D_2$. Between these two points the curve is continuous but the interval between the triple-point temperatures (Table V) is too small to represent on Fig. 2.

Separate lines were drawn through the observations for the liquid and solid phases because there is no reason for

TABLE IV. *Experimental observations of* $\Delta P(e\cdot D_2 - n\cdot D_2)$ *(mm Hg).*

Dec. 13, 1934				Dec. 14, 1934		Dec. 15, 1934			
Series #1		Series #2		Series #3		Series #4		Series #5	
$P(n\cdot D_2)$	ΔP	$P(n\cdot D_2)$	ΔP	$P(n\cdot D_2)$	ΔP	$P(n\cdot D_2)$	ΔP	$P(n\cdot D_2)$	ΔP
247.17	3.66	35.76	0.74	247.80	3.69	253.01	3.58	84.38	1.20
208.86	2.92	75.74	1.48	203.37	3.35	204.98	2.76	205.11	3.09
178.63	2.41	140.60	1.98	178.76	2.80	180.82	2.46	250.52	3.93
157.46	2.18	179.44	2.69	150.60	2.38	153.34	2.23	250.43	4.03
122.10	1.71	245.67	3.44	102.29	1.85	125.20	2.50	248.99	3.58
103.21	1.61			80.02	1.44	91.78	1.77		
75.56	1.36			60.58	0.97	74.60	1.33		
62.20	1.10			38.65	0.67	60.65	0.99		
37.77	0.76			18.08	0.37	41.18	0.76		
19.40	0.73			252.34	3.38	24.65	0.55		
				251.56	3.62				

of series No. 1 and No. 2 were made on $e-D_2$ in a vapor pressure tube without catalyst, after D_2 had been converted to the equilibrium mixture in the tube containing the $ZnCrO_2$. The observations of the other series were made with $e-D_2$ in the presence of the catalyst. It was found that the presence of the $ZnCrO_2$ produced no appreciable change in the vapor pressure.

To prove that the observed ΔP's are to be attributed to a change in the ortho-para concentration and are not in error due to a contamination of the $e-D_2$ with hydrogen, the $e-D_2$ was pumped from its vapor pressure tube into a flask in which it was converted to $n-D_2$ by a hot platinum filament, at the end of each day's observations, and the vapor pressure of the converted $n-D_2$ was compared next day with a sample of unconverted $n-D_2$. The differences between the vapor pressures of the converted $n-D_2$ and the unconverted $n-D_2$ scattered to positive and negative values without any definite indication of a hydrogen contamination even after a second conversion to $e-D_2$ and reconversion to $n-D_2$.

Although the D_2 used for this investigation probably was purer than any other previously used for vapor pressure determinations, it may have contained a small but constant HD impurity. Since HD does not have ortho and para varieties, it should not have affected our results to any greater extent than in proportion to its concentration.

The vapor pressures of the 20.4°K equilibrium mixture of the ortho and para varieties of the deuterium used in this investigation are related to those of liquid normal hydrogen by the following equations:

$$\log_{10} P(e_{20.4^\circ} - D_2 \text{ liquid}) = -1.3302 + 1.3000 \log_{10} P(n-H_2), \quad (6)$$

$$\log_{10} P(e_{20.4^\circ} - D_2 \text{ solid}) = -1.8873 + 1.5106 \log_{10} P(n-H_2). \quad (7)$$

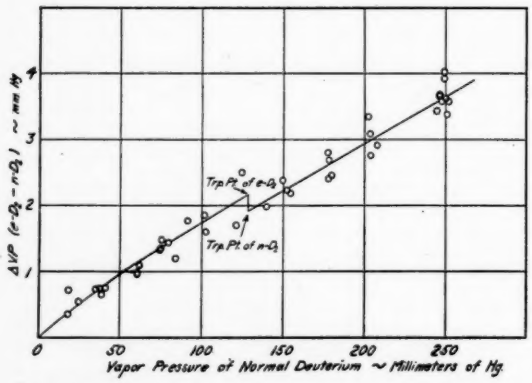

FIG. 2. The vapor pressure difference of 20.4°K temperature equilibrium deuterium $(e-D_2)$ and normal deuterium $(n-D_2)$.

TABLE V. *Triple-point temperatures and pressures.*

	$n-D_2$	$e-D_2$	$n-H_2$	$e-H_2$*
T°K	18.71	18.67	13.92	13.79
P (mm Hg)	128.7	128.4	54.	53.

* Bonhoeffer and Harteck, Zeits. f. physik. Chemie **B4**, 113 (1929).

a single line. The meeting of the lines of Fig. 2 would imply that $e-D_2$ and $n-D_2$ have the same triple-point temperatures. The ortho-para vapor pressure difference of solid hydrogen has not been investigated, but $e-H_2$ has a lower triple-point temperature than $n-H_2$ (Table V). Therefore, the ΔP curve for hydrogen must be similar to that for deuterium (Fig. 2).

TABLE VI.

	Hydrogen (mm Hg)				Deuterium (mm Hg)			
$T°K$	$P(n\cdot H_2)$	$\Delta P(e\cdot H_2-n\cdot H_2)$	$\Delta P(p\cdot H_2-o\cdot H_2)$	$\frac{\Delta P(p\cdot H_2-o\cdot H_2)}{P(n\cdot H_2)}$	$P(n\cdot D_2)$	$\Delta P(e\cdot D_2-n\cdot D_2)$	$\Delta P(o\cdot D_2-p\cdot D_2)$	$\frac{\Delta P(o\cdot D_2-p\cdot D_2)}{P(n\cdot D_2)}$
15	96.6	5.1	6.8	0.070	12.6	0.3	0.8	0.063
16	155.4	7.6	10.2	.066	25.9	0.5	1.7	.065
17	237.7	10.8	14.4	.061	49.4	0.9	2.9	.060
18	348.7	14.8	19.8	.057	88.2	1.6	4.9	.055
18.67[a]	442.5	18.1	24.2	.055	126.5	2.2	6.7	.053
18.71[b]	447.5	18.3	24.5	.055	128.7	1.9	6.2	.048
19	493.7	19.7	26.3	.053	146.3	2.2	6.9	.047
20	678.3	25.0	33.4	.049	221.0	3.2	10.4	.047
20.38	760.0	27.1	36.2	.048	256.2	3.8	12.1	.047

[a] Triple point of $e-D_2$.
[b] Triple point of $n-D_2$.

With Eq. (1), these become

$$\log_{10} P(e_{20.4°}-D_2 \text{ liquid}) = 4.7321 - 58.1478/T + 0.02630T, \quad (8)$$

$$\log_{10} P(e_{20.4°}-D_2 \text{ solid}) = 5.1571 - 67.5678/T + 0.03056T. \quad (9)$$

In Table V are listed the triple point temperatures and pressures of $n-D_2$, $e-D_2$, $n-H_2$ and $e-H_2$.

In Table VI values for deuterium based on the curves of Fig. 2 are compared with corresponding values for hydrogen derived from the observations of Keesom, Bijl and van der Horst.[8] $\Delta P(o\cdot D_2-p\cdot D_2)$ and $\Delta P(p\cdot H_2-o\cdot H_2)$ were calculated from $\Delta P(e-n)$ on the assumption of Raoult's law. The smaller difference between the vapor pressures of $e-D_2$ and $n-D_2$ as compared with the corresponding difference for hydrogen is accounted for by the smaller percentage change in concentration and by a smaller difference between the vapor pressures of the ortho and para varieties. The difference between the vapor pressures of $p-H_2$ and $o-H_2$, $\Delta P(p\cdot H_2-o\cdot H_2)$, is about 3 times the corresponding difference $\Delta P(o\cdot D_2-p\cdot D_2)$ at 20.4°K and 5.7 times at 15°K. However, the ratio $\Delta P/P(n.)$ is approximately the same for hydrogen and deuterium at the same temperature. (See Table VI.)

Heats of Vaporization

As it is customary to use vapor pressure data with the Clausius-Clapeyron equation to calculate latent heats, we have attempted to use our data to calculate the difference between the latent heats $\Delta L(n-e)$ of the normal and equilibrium mixtures of ortho and para varieties. In this calculation use was made of the following equation of state of hydrogen, which is very closely that used in the previous paper:

$$pV(\text{liters per mole}) = RT - 0.0381(1+1150/T^2)p. \quad (10)$$

In the absence of any data on the equation of state of deuterium at liquid hydrogen temperatures, this same equation was used for deuterium as well. Substituting in the Clausius-Clapeyron equation for the volume of the saturated vapor from the above equation, the following relation for the difference between the latent heats $\Delta L(n-e)$ of the normal and equilibrium mixtures was obtained:

$$\Delta L(n-e) = R\frac{d \ln_e P_e/P_n}{d(1/T)} + T\left[v+0.0381\left(1+\frac{1150}{T^2}\right)\right]\frac{d\Delta P(e-n)}{dT}. \quad (11)$$

Here v is the molecular volume of the condensed state. For liquid hydrogen[9] it is 28.43 cm³, for solid deuterium[10] 23.15 cm³ and for liquid deuterium it was assumed to be 25.2 cm³ or 11.5 percent smaller than that of liquid hydrogen. For liquid hydrogen the *observations* of Keesom, Bijl and van der Horst[11] were used. The two derivatives of Eq. (11) were determined graphically.

[8] Keesom, Bijl and van der Horst, Royal Academy of Sciences, Amsterdam **34₂**, 1223 (1931); also Leiden Communication No. 217a.

[9] *International Critical Tables*, Vol. I, p. 102.
[10] Clusius and Bartholomé, Zeits. f. tech. Physik **15**, 545 (1934).
[11] Keesom, Bijl and van der Horst, Proc. Amst. Acad. Sci. **34₂**, 1229 (1931).

TABLE VII. *Differences between heats of vaporization.*

	TEMP. RANGE	$\Delta L(n-e_{20.4°})$	$\Delta L(p-o)$
Solid D_2	16°–18.71°K	0.6±0.5	1.8±1.5
Liquid D_2	18.71°–20.4°K	0.0±0.5	0.0±1.5
Liquid H_2	16°–20.4°K	2.3±0.5	−3.1±0.7

The results are tabulated in Table VII together with values of $\Delta L(p-o)$ calculated from $\Delta L(n-e)$ upon the assumption that ortho and para varieties form ideal solutions. The difference in signs of $\Delta L(p-o)$ for H_2 and D_2 arises from the interchange of the terms ortho and para to designate the rotating and nonrotating varieties of hydrogen and deuterium. The ± values are estimated probable errors.

It is interesting that $\Delta L(p-o)$ for liquid D_2 is not more nearly equal to $\Delta L(o-p)$ for liquid hydrogen.

The differences between the external latent heats of vaporization are small as compared with the values of Table VII. Since $\Delta Pv(p-o)$ for the condensed phases is negligibly small, the ΔL values of Table VII are also the differences between the internal energies of the condensed states.

ON THE UNCATALYZED CHANGE OF THE VAPOR PRESSURE OF LIQUID DEUTERIUM WITH TIME

Scott, Brickwedde, Urey and Wahl[8] investigated the uncatalyzed change with time of the vapor pressures of liquid hydrogen and liquid deuterium resulting from the ortho-para conversion in the liquid state. The vapor pressure of normal hydrogen at 20.38°K increases at the rate of one mm of Hg in 4 hours, whereas the change for deuterium is less than one mm in 200 hours. The vapor pressure increase of liquid hydrogen follows the law of a bimolecular reaction, which Cremer and Polanyi[12] found to fit their thermal conductivity measurements of the increase of $p-H_2$ in liquid hydrogen. Since the $p-H_2$ molecules have neither nuclear nor rotational magnetic moments, they have no magnetic field to effect a realignment of the nuclei of the ortho molecules with which they collide. Conversion in liquid hydrogen, therefore, results only from collisions of two ortho molecules. The $o-H_2$ molecules having a nuclear magnetic moment of 5.8 Bohr nuclear magnetons (BNM)[13] and a rotational magnetic moment of 0.85 BNM have resultant moments of 6.6, 5.9, and 5.0, averaging 5.8 BNM.

It is not to be expected that the conversion of $p-D_2$ to $o-D_2$ in liquid deuterium will follow the simple bimolecular change of hydrogen. Five-sixths of the $o-D_2$ molecules have a nuclear magnetic moment of 1.5 BNM[13] and the remaining sixth has a zero moment; there is no rotational moment. The $p-D_2$ molecules have a nuclear magnetic moment of 0.75 and a rotational moment of 0.42 BNM.[14] The resultant moments of $p-D_2$ are 1.2, 0.9, and 0.3, averaging 0.8 BNM. It is seen, therefore, that not only does the para to ortho deuterium conversion result from collisions of para and ortho molecules as well as collisions of para molecules, with each other, but that actually the para-ortho collisions are more effective since the magnetic moments of the ortho molecules are greater than those of para molecules.

Wigner[15] developed a theory for the ortho-para conversion in gaseous hydrogen resulting from collisions with paramagnetic oxygen molecules. This theory is not directly applicable to liquids but it does seem justifiable to use it to calculate the order of magnitude of the relative rates of conversion in liquid hydrogen and deuterium.

For the ortho to para conversion in gaseous hydrogen resulting from collisions with paramagnetic oxygen, the probability, W, of a transition from $J=1$ to $J=0$ is related to the moment of inertia, I_H, of the H_2 molecules, the magnetic moments μ_1 and μ_2 of the oxygen molecule and the proton, and the spin, i, of the proton. We apply this relation to the ortho to para conversion

$$W(J=1\rightarrow J=0) \propto I_H\mu_1^2\mu_2^2((2i+1)/i) \quad (12)$$

resulting from collisions with paramagnetic $o-H_2$ in liquid H_2, substituting for μ_1, the magnetic

[12] Cremer and Polanyi, Zeits. f. physik. Chemie **B12**, 231 (1921).

[13] I. Estermann and O. Stern, Nature **132**, 169 (1933); **133**, 911 (1934); I. I. Rabi, J. M. B. Kellogg and J. R. Zacharias, Phys. Rev. **46**, 157, 163 (1934).

[14] The value 0.42 is based upon the assumption that the rotational moments are proportional to the angular velocities of rotation.

[15] Wigner, Zeits. f. physik. Chemie **B23**, 31 (1933).

moment of $o-H_2$. The velocity constant, K_H, of the ortho to para conversion in liquid hydrogen is proportional to $W(J=1\rightarrow J=0)$. Substituting numerical values for the symbols in Eq. (12), we obtain

$$K_H = CI_H[\tfrac{1}{3}((6.6)^2+(5.9)^2+(5.0)^2)](2.9)^2 4 = 1.2\times 10^3 C'.$$

For the para to ortho conversion in liquid deuterium resulting from the collision of two para molecules

$$W_{p,\,p}(J=1\rightarrow J=0) \propto I_D\mu_1^2\mu_2^2(i+1)(2i+1)/i^2. \quad (13)$$

The different statistics applicable to H and D require different spin factors in Eqs. (12) and (13)

$$K_{p,\,p} = C(2I_H)[\tfrac{1}{3}((1.2)^2+(0.9)^2+(0.3)^2)] \times (0.75)^2 6 = 5.3C'.$$

For the para to ortho conversion resulting from collisions of $o-D_2$ and $p-D_2$ molecules

$$W_{o,\,p}(J=1\rightarrow J=0) \propto (5/6)\times\tfrac{1}{2}I_D\mu_1^2\mu_2^2 \times(i+1)(2i+1)/i^2 \quad (14)$$

and

$$K_{o,\,p} = C\times(5/12)(2I_H)(1.5)^2(0.75)^2 6 = 6.3C'.$$

The factors 5/6 and 1/2 were introduced to take account of the fact that (1) only 5/6 of the $o-D_2$ molecules have a magnetic moment, and (2) the *a priori* probability of a para to ortho conversion for the collision of an ortho and a para molecule is only half of that for the collision of two para molecules.

If $[o-H_2]$ and $[p-D_2]$ are the concentrations of $o-H_2$ and $p-D_2$ in liquid hydrogen and liquid deuterium, respectively

$$d[o-H_2]/dt = K_H[o-H_2]^2 = 1.2\times 10^3 C'[o-H_2]^2$$

and

$$d[p-D_2]/dt = K_{p,\,p}[p-D_2]^2 + K_{o,\,p}(1-[p-D_2])[p-D_2] = \{6.3[p-D_2]-[p-D_2]^2\}C'.$$

The ratio of the rate of $o-H_2\rightarrow p-H_2$ in liquid normal hydrogen, to the rate of $p-D_2\rightarrow o-D_2$ in normal deuterium is

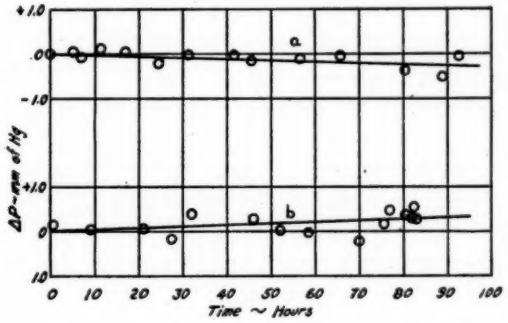

FIG. 3. The uncatalyzed change in the vapor pressure of liquid normal deuterium at 20.4°K.

$$(d[o-H_2]/dt)_{n.H_2}/(d[p-D_2]/dt)_{n.D_2} = 3.4\times 10^2.$$

For the ratio of the rates of change of the vapor pressures we have

$$(dP/dt)_{n.H_2}/(dP/dt)_{n.D_2} = 1\times 10^3.$$

Although this calculation is not to be regarded as rigorous, it shows that the rate of conversion of para to ortho deuterium is approximately proportional to the concentration of $p-D_2$ instead of to the square of the concentration as it is for the corresponding change in liquid hydrogen. It also shows that the rate of the para to ortho conversion in liquid deuterium must be very much smaller than for the ortho to para conversion in liquid hydrogen.

Fig. 3a and b are graphs of observations of the vapor pressure of normal deuterium at 20.38°K plotted against the age of the condensed state. Fig. 3a is a reproduction of previously reported data obtained February 1934. The data of Fig. 3b were observed December 1934 with purer deuterium. ΔP is the difference between the observed vapor pressure and the intercept with the axis of vapor pressures of a line through the observations determined by the method of least squares, with each point given equal weight.[16] These are the lines drawn through the observations in the two figures. The observations of February indicate a slow decrease in vapor pressure with time whereas those of December indicate an increase about equal to the decrease of the February observations. When the two series

[16] We are indebted to W. E. and L. S. Deming of the Bureau of Chemistry and Soils, Department of Agriculture for the statistical analysis of our data.

of observations are thrown together and treated statistically as a single set, the line through the observations, determined by the method of least squares, indicates a decrease in vapor pressure of 0.027 mm of Hg in 100 hours. We conclude that the vapor pressure of liquid normal deuterium over a period of 100 hours is constant to within the accuracy of our measurements. The *estimated probable error* calculated from our observations is ± 0.27 mm at 100 hours.

Rotation in the Condensed States

Although it was surmised that there would be *free* rotation of deuterium molecules in the liquid and solid states just as in the case of hydrogen, we now have definite evidence from the ortho-para vapor pressures that this is so. The latent heats of vaporization of solid and liquid deuterium are 355 and 305 calories per mole, respectively, and the rotational energy ($J=1$) of $p-D_2$ in the vapor phase at liquid hydrogen temperatures is 170 calories per mole.[17] If there were no rotation in the condensed states, the heats of vaporization of $p-D_2$ would be about 170 calories per mole greater than the corresponding values for $o-D_2$. Actually there may be a small difference in the heats of vaporization of $p-D_2$ and $o-D_2$, but it is less than for liquid hydrogen in which the difference is 3 calories per mole. We conclude, therefore, that there is free rotation in condensed states of deuterium just as in the case of hydrogen.

[17] Johnston and Long, J. Chem. Phys. **2**, 389 (1934).

NOVEMBER, 1935 JOURNAL OF CHEMICAL PHYSICS VOLUME

The Infrared Spectrum of Heavy Water

E. F. Barker and W. W. Sleator, *University of Michigan*

(Received August 15, 1935)

Samples of water vapor containing 90 and 40 percent of deuterium have been examined in the infrared, and the absorption bands ν_2 and ν_3 for D_2O and ν_2 and ν_1 for HDO have been located. The position of ν_1 for D_2O is known from Raman scattering. Of the nine fundamental frequencies for the three varieties of water, eight have now been observed. The ninth, ν_3 for HDO, should lie very close to the corresponding band for H_2O and is apparently completely masked. Computed values of these frequencies already available agree very well with the measured ones. A fair degree of resolution is obtained in the bands ν_2. The fine structure observed agrees approximately with that predicted by using the molecular dimensions obtained by Mecke, *viz.*, OH distance $\sim 0.95\times 10^{-8}$ cm and apex angle $\sim 105°$. The magnitude of the interactions is so great, however, that precise determinations of these constants must await a more complete solution of the mechanical problem.

ALL available evidence indicates that the three atoms of the water molecule form an isosceles triangle. Hence there should be three active fundamental vibrations, and the bands should be of two types, involving changes in electric moment parallel to or perpendicular to the bisector of the apex angle. If this angle were smaller than 86.5° two of the fundamental bands should have zero branches and the other should not since the moment of inertia (B) about an axis bisecting the apex angle would then be less than the one (A) about a perpendicular axis lying in the plane. A larger angle ($A<B$) would require one band with and two without zero branches. Only two fundamental bands have been identified however, and one is of each type. The fact that the one of lower frequency at 6.26μ (ν_2) has no zero branch strongly suggests the obtuse form. The fundamental ν_1 has not been observed in the infrared. It must be weak, and is apparently masked by ν_3, the intense band at 2.67μ. In this region it would be exceedingly difficult to locate if no zero branch occurs. Its small intensity suggests that the associated motion must be nearly symmetrical (hence the designation ν_1) and consequently that it should yield the strong-

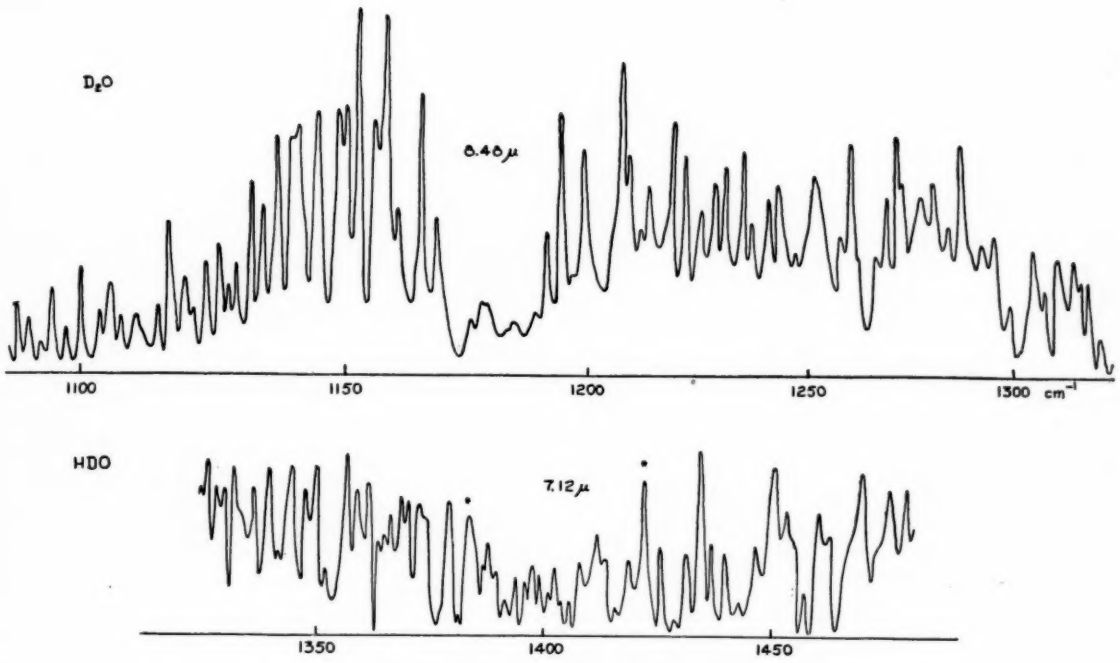

FIG. 1. The absorption bands ν_2 for D_2O and HDO.

est Raman line. This, according to Bender,[1] lies at 3654 cm^{-1}, corresponding to 2.74μ.

The vibration bands have structures which are clearly characteristic of an asymmetrical rotator, but of one in which interactions play a large part. Precise molecular constants can be obtained from any resolved band only after these interactions have been properly evaluated, but adequate formulae for accomplishing this have not yet been developed. Mecke[2] and his associates have obtained a very satisfactory correlation for the many observed bands by assigning "apparent" moments of inertia which vary from band to band in a consistent manner and which, by extrapolation, yield values characterizing the vibrationless state. This approximation indicates an apex angle of about 105° and an OH distance of about 0.95×10^{-8} cm.

The mechanical problem of determining the normal vibrations for H_2O has recently been discussed from two different points of view. Van Vleck and Cross,[3] employing the idea of directed valence, and introducing known atomic wave functions, have computed the fundamental frequencies for H_2O and HDO. Bonner,[4] on the other hand, has evaluated the constants of the potential function for H_2O starting with the observed frequencies and assuming the dimensions indicated by Mecke. This makes possible a prediction of the fundamental frequencies for D_2O. A test of these hypotheses and of Mecke's conclusions, is provided by the observations presented below.

We have examined the absorption spectrum of heavy water vapor with the prism grating spectrometer, using a cell 24 cm long with windows of rocksalt, which has a heating coil wound on its outer surface. The water, with a deuterium content of about 90 percent, was placed in a glass reservoir projecting outward from the bottom of the cell far enough so that its temperature is not raised appreciably by the heater. The temperature of the cell and windows was maintained at about 10° above that of the room, and the salt windows have remained for months unclouded. With a high concentration of D_2O the bands ν_2 and ν_3 for that molecule are

[1] Bender, Phys. Rev. **47**, 252 (1935).
[2] Mecke, Zeits. f. Physik **81**, 313 (1933).
[3] Van Vleck and Cross, J. Chem. Phys. **1**, 357 (1933).
[4] Bonner, Phys. Rev. **46**, 458 (1934).

TABLE I. *Wave numbers of prominent lines in the ν_2 bands of D_2O and HDO.*

D_2O			HDO		
Positive branch	Transition	Negative branch	Positive branch	Transition	Negative branch
1190.7	$1_{-1}\rightarrow1_{+1}$	1168.0	1412.0	$2_{-2}\rightarrow2_0$	1387.5
1193.5	$2_{-2}\rightarrow2_0$	1165.0	1422.0*	$1_{-1}\rightarrow1_{+1}$	1383.7*
1199.0	$0_0\rightarrow1_0$	1160.0	1425.8	$1_{+1}\rightarrow2_{-1}$	1379.0
1206.4	$2_0\rightarrow2_{+2}$	1156.8	1431.5	$1_0\rightarrow2_0$	1373.8
1207.4	$1_0\rightarrow2_0$	1155.2	1434.8	$0_0\rightarrow1_0$	1372.8
1211.4	$2_{+2}\rightarrow3_0$	1153.0	1437.0		1369.0
1218.5		1149.3	1440.0		1366.0
1221.3		1148.0	1447.5		1361.0
1225.5		1144.5	1451.0		1359.0
1228.0		1140.0	1453.5		1356.0
1230.5		1139.0	1460.5		1350.0
1234.5		1135.5	1463.0		1347.6
1251.5		1131.5	1470.0		1344.5
1259.5		1116.3	1476.0		1339.6
1270.0		1100.0	1480.0		1332.0
1284.5		1095.5			

readily identified, both being shifted from the corresponding bands of H_2O. No indication of ν_1 could be obtained although its position as determined by Raman scattering is not unfavorable for observation. Rank, Larsen and Bordner[5] place it at 2666 cm^{-1}, corresponding to 3.75μ.

The absorption curve for D_2O vapor in the neighborhood of 8.5μ (ν_2) appears in Fig. 1. There is a very transparent region extending some 10 cm^{-1} each way from the band center at 1179.1 cm^{-1}, with strong narrow lines occuring on either side in a somewhat symmetrical fashion. The two lines nearest the center are separated by 22.7 cm^{-1} and have low intensities, while the next pair are strong. In H_2O the central gap is 40.3 cm^{-1} wide, the first lines being strong, and the second ones weak. This reversal in relative intensities indicates the change in statistics when deuterons replace protons. In Table I the wave numbers are given for the more prominent absorption maxima.

The second strong absorption band of D_2O (ν_3) occurs at 2784 cm^{-1} (3.59μ), and is represented in the upper curve of Fig. 2. The resolution obtained is far from complete, but the pattern has a striking resemblance to that of the corresponding H_2O band when the latter is about equally resolved. The zero branch is rather broad, and the positive branch is strong and closely packed indicating considerable convergence. The negative side appears weaker, being more spread out,

[5] Rank, Larsen and Bordner, J. Chem. Phys. **2**, 464 (1934).

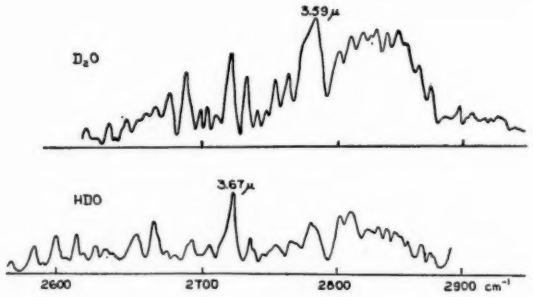

FIG. 2. The absorption bands ν_3 for D_2O and ν_1 for HDO.

and although it shows several intense peaks they are probably not single lines.

When only one of the hydrogen atoms in a water molecule is replaced by deuterium the vibrations lose all symmetry, and the principal axes are inclined to the bisector of the apex angle. The vibration ν_1, which is principally a motion of the H and D atoms toward and away from one another, involves a change in electric moment having a considerable component along the axis A. In contrast to the case of H_2O this gives rise to a band with a well-developed zero branch. It lies very near to the pair of bands ν_1 and ν_3 of D_2O, and is shown in the lower curve of Fig. 2. No corrections have been made here for D_2O absorption, since it should be relatively weak with the vapor used. The rather intense maximum appearing in both curves at 2720 cm^{-1} indicates the band center.

The fundamental vibration ν_2 is one in which the motion of the H and D atoms is almost normal to the line connecting them. The resulting change in electric moment has a very small component along the axis A, and the zero branch is scarcely at all developed. This band lies at 1403 cm^{-1} (7.12μ), and is shown in the lower curve of Fig. 1. Since both H_2O and D_2O absorb strongly in this region the minor details of the curve cannot be considered as significant; the strong lines are unmistakable, however. The graph does not present the absorption as observed, but is corrected to eliminate the effect of H_2O. No attempt has been made to eliminate D_2O absorption, since the corrections are approximate at best. The positions of some of the important lines are given in Table I.

We have been unable to find any trace of the fundamental ν_3 for HDO, although in H_2O and

TABLE II.

	A	B	C	A/B	$\Delta\nu$ comp.	$\Delta\nu$ obs.
H_2O	1.03	2.07	3.10	0.49	35.6	40.3
HDO	1.18	3.74	4.92	0.32	35.4	38.3
D_2O	1.86	4.14	6.00	0.45	20.8	22.8

D_2O it yields strong bands with prominent zero branches. Its predicted position lies very close to that of the band center for H_2O at 2.67μ. A detailed examination of the whole region occupied by this band with samples of water vapor containing 25 and 40 percent of deuterium shows no observable differences from the corresponding H_2O pattern.

If we adopt tentatively the molecular dimensions indicated by Mecke for the vibrationless state of H_2O, and compute moments of inertia without making allowances for the effects of interaction, the values shown in Table II are obtained (the unit is 10^{-40} g cm^2). A simple test of this configuration is to compute the wave number interval between the first lines on either side of the band center. For H_2O these are a pair of strong lines and for D_2O they are weak, but in either case they are easily recognized. The predicted value of this interval, $\Delta\nu=(1/A-1/C)h4\pi^2c$, is compared in the table with that observed for each molecule, the agreement being fairly satisfactory. It is clear that by changing the molecular dimensions slightly a better check could be obtained, but this procedure would hardly be justified since the differences are in large part due to interactions as yet not evaluated. If the "apparent" moments of inertia appropriate to this band are computed by Mecke's formulae, and $\Delta\nu$ determined, the situation is not appreciably improved. The result is 44.2 cm^{-1} for H_2O.

In the case of HDO the observed displacement of the innermost lines from the band center is very much less than the predicted value, and there is no alternating intensity to assure a correct assignment. As indicated in the curve, the first strong maxima on either side form a group of three or more closely spaced lines, and these are followed by several strong single lines. The interval between the first pair of such single lines (indicated by an asterisk in Fig. 1 and in Table I) is the $\Delta\nu$ shown above. The origin of the group of lines lying within this interval may be explained by reference to a figure given by Dennison.[6] The ordinates are values of $\rho=A/B$. Both H_2O and D_2O fall in the middle section, but for HDO this ratio is only about 0.32, at which value a group of lines originating in states with $J>1$ lies inside those for which the transition is $1_{-1}\rightarrow1_{+1}$. An example is $2_{-2}\rightarrow2_0$. The adjacent figure (19) in the same paper indicates how a central zero branch would develop if there were any appreciable component of the change in electric moment along the axis of A. A few of the rotation pairs in these bands may be identified, and transitions assigned with some confidence. These are listed in Table I. In the present status of the problem it does not seem wise to attempt to extend these assignments much further, since the various lines are affected quite differently by interactions.

TABLE III. *Fundamental frequencies of the three water molecules.*

Raman spectra in *italics*. Computed values in parentheses.

	ν_1	ν_2	ν_3
H_2O	*3654*[1, 5]	1596	3756
HDO	2720	1403	
	2718[5]	(1400)[3]	(3750)[3]
D_2O	*2666*[5]	1179	2784
	(2656)[4]	(1180)[4]	(2789)[4]

A summary of the observed and computed values for the various fundamental frequencies is presented in Table III. For the two symmetrical molecules ν_1 has been observed only by Raman scattering, and ν_2 and ν_3 only in the infrared. It should be added that several of the infrared bands have also been observed with a prism spectrograph by Bartholomé and Clusius.[7] Their precision is not as great as that obtained when the bands are resolved, but the agreement is reasonably good.

We are indebted to Professors Anderson, Bates and Halford of the Chemistry Department for samples of heavy water, and to the Faculty Research Fund for the purchase of other samples.

[6] Dennison, Rev. Mod. Phys. 3, 280 (1931), Fig. 20, p. 327.

[7] Bartholomé and Clusius, Zeits. f. Elektrochemie 40, 529 (1934).

The Infrared Absorption of Cyanides and Thiocyanates

WALTER GORDY AND DUDLEY WILLIAMS, *Physics Department, University of North Carolina*

(Received July 30, 1935)

Aqueous solutions of seven inorganic cyanides, two thiocyanates, and one cyanate were studied in the region from 1.2μ to 7.5μ. Two organic cyanides and an organic thiocyanate were studied in the same region. In all the materials a characteristic absorption band was observed in the region from 4.38μ to 4.90μ. The exact position of the band was found to be different for the various substances. This characteristic absorption was attributed to changes in the vibrational energy of the bound CN group. An additional band appearing only in the highly ionized cyanide solutions was attributed to the free CN ions. In the cyanate solution a double band appeared in the region of 7μ which was not characteristic of the cyanide or thiocyanate solutions. Hydrolysis and solvation effects were observed in some of the solutions.

PREVIOUS work has been done on the infrared absorption of organic cyanides and thiocyanates by Coblentz.[1] In other studies[2] Coblentz also gives infrared data for the potassium ferrocyanide crystal. Choi and Barker[3] have made a careful investigation of gaseous HCN and have recorded a number of bands in the region 3μ to 15μ. Recent studies[4, 5] of the infrared absorption spectra of solutions of certain hydroxides have revealed intense bands in the region 3μ to 6μ. These bands were attributed to changes in the energy levels of the hydroxide molecules attached to the molecules of the solvent. A strong band[6] has also been observed in aqueous solutions of alkaline hydroxides at 2.3μ and has been attributed to changes in the vibrational energy of the OH ions. The present study was undertaken to ascertain whether similar hydration and dissociation effects could be observed in the case of cyanides and thiocyanates. In addition to these compounds, one cyanate solution was studied, and, for more accurate determination of the position of the bands, some of the earlier measurements of Coblentz on organic cyanides and thiocyanates were repeated.

A Hilger infrared spectrometer was used as a resolving instrument. A fluorite prism was employed for the entire region studied and the cell windows were likewise of fluorite. In any particular region the cell thickness was maintained constant for all the materials studied, thicknesses being 0.11 mm for the range 1.2μ to 2.5μ and 0.03 mm for the range 2.5μ to 7.5μ. Washers of these thicknesses were made of mica, the same washers being used for all the materials. Concentrations for the various solutions are given in Table I.

In Fig. 1 are shown the results obtained with the solutions in the region from 2.5μ to 7.5μ. No absorption which might be attributed to cyanides or thiocyanates was detected in the region from 1.2μ to 2.5μ, and this part of the spectrum is omitted from the figure. As may be readily seen from this set of curves, all the solutions are strongly absorbing in the region 4.6μ to 4.9μ, the position of maximum absorption varying with the solution. The curve for the NaCN solution is typical of the other cyanides listed in Table I, which are not shown in Fig. 1, in all

TABLE I. *Location of observed bands.*

SUBSTANCE	CHEMICAL FORMULA	MOLAR CONCENTRATION	CHARACTERISTIC BAND*	ADDITIONAL BANDS*
Hydrocyanic acid	HCN	0.8	4.75	
Sodium cyanide	NaCN	5.0	4.78	5.20
				4.44
Potassium cyanide	KCN	5.0	4.80	5.20
				4.44
Barium cyanide	$Ba(CN)_2$	2.5	4.78	
Potassium silver cyanide	$KAg(CN)_2$	1.0	4.66	5.20
Sodium ferrocyanide	$Na_4Fe(CN)_6$	0.5	4.90	5.20
Potassium ferricyanide	$K_3Fe(CN)_6$	1.0	4.70	5.20
Potassium thiocyanate	KCNS	7.0	4.84	
Ammonium thiocyanate	NH_4CNS	7.0	4.84	3.46
				6.94
Potassium cyanate	KCNO	5.0	4.62	7.10
				7.40
Methyl cyanide	CH_3CN	Pure liquid	4.38	3.24
Benzyl cyanide	$C_6H_5CH_2CN$	Pure liquid	4.40	3.24
Methyl thiocyanate	CH_3CNS	Pure liquid	4.62	3.32

* Wave-lengths are given in microns.

[1] W. W. Coblentz, *Investigations of Infrared Spectra*, p. 60, Carnegie Institution of Washington, 35 (1905).
[2] W. W. Coblentz, *Investigations of Infrared Spectra*, p. 26, Carnegie Institution of Washington, 65 (1900).
[3] K. N. Choi and E. F. Barker, Phys. Rev. **42**, 777 (1932).
[4] E. K. Plyler and W. Gordy, J. Chem. Phys. **2**, 420 (1934).
[5] E. K. Plyler and F. D. Williams, J. Chem. Phys. **2**, 565 (1934).
[6] Walter Gordy, J. Chem. Phys. **2**, 621 (1934).

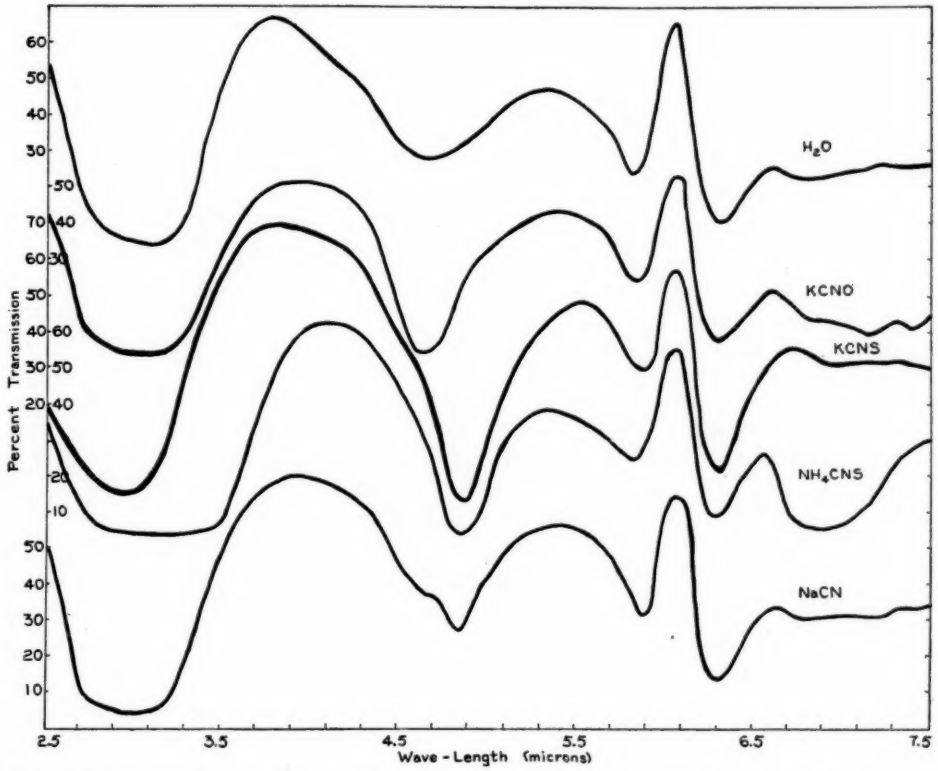

FIG. 1. The percent transmission of typical cyanides, cyanates, and thiocyanates in aqueous solution in the region from 2.5μ to 7.5μ.

parts of the spectrum except 4.6μ and 4.9μ. Their transmissions in this region are given in a different figure. In the case of the thiocyanates the 3μ water band seems to be definitely shifted to shorter wave-lengths. Since this shift was not observed in any of the other compounds studied, it is probably due to a solvation effect in which the linkage is between the sulphur and the water. Another evidence of solvation is the marked increase in the transmission of water in certain regions, which is evident from the figure. This solvation effect is somewhat masked in the case of ammonium thiocyanate by the absorption of the NH_4 group. Reinkober[7] in a study of aqueous solutions of ammonium salts has recorded absorption bands in the regions from 3.09μ to 3.57μ, 4.66μ to 4.85μ, and 6.90μ to 7.12μ. Ammonium thiocyanate was not investigated by Reinkober. Our data reveal the position of the NH_4 bands for this salt to be 3.46μ and 6.94μ. Other bands occurring in the region from 4.6μ to 4.9μ prevented an exact determination of the position of the third NH_4 band.

The transmission curve for potassium cyanate shows absorption in the region of 7μ, which is not characteristic of the other potassium salts nor of the other cyanides and thiocyanate solutions. Plotting the ratio of the absorption of this solution to that of water in this region reveals a broad double band with absorption maxima at 7.1μ and 7.4μ. No similar absorption occurs for the other salts, and these bands are to be attributed to the cyanate radical. Nitrate crystals[8] show characteristic bands near 7.2μ and carbonate crystals[9] at 6.9μ. Since the double band observed in the case of the cyanates is not a characteristic cyanide vibration, it is possible that the components of the band at 7.1μ and 7.4μ are due to other

[7] O. Reinkober, Zeits. f. Physik **35**, 179 (1925).

[8] C. Schaeffer and M. Schubert, Ann. d. Physik **50**, 283 (1916).

[9] C. Schaeffer, C. Bormuth and F. Matossi, Zeits. f. Physik **39**, 648 (1926).

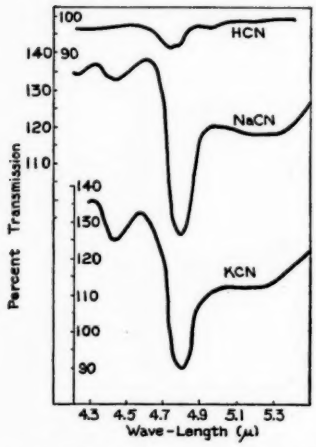

FIG. 2. The ratio of the transmission of HCN, NaCN, and KCN solution to that of water from 4.1μ to 5.5μ.

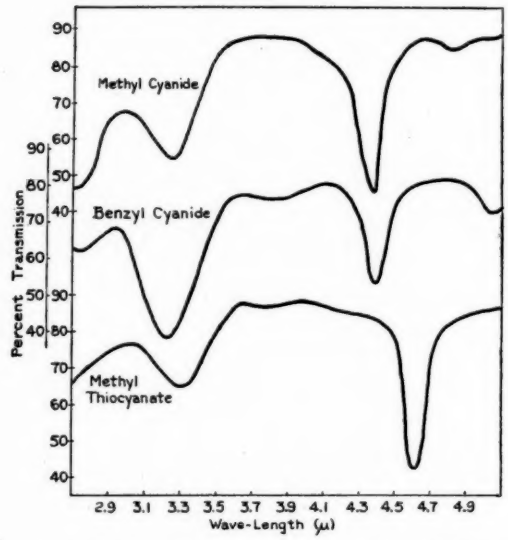

FIG. 3. The percent transmission of two organic cyanides and one organic thiocyanate in the region 2.7μ to 5.1μ.

fundamental frequencies of the CNO group in which a CO vibration and an NO vibration are active.

The HCN, NaCN, and KCN solutions were found to have bands at 4.75μ, 4.78μ, and 4.80μ, respectively, while NaCN and KCN showed less intense bands at 4.44μ and 5.20μ, as may be seen from Figs. 2 and 3. Methyl cyanide shows an intense band at 4.38μ, and benzyl cyanide at 4.40μ. These are shown in Fig. 3. Since this absorption is not characteristic of the organic groups,[10] it is to be attributed to the CN group. There is a striking dissimilarity between the absorption of the KCN and NaCN solutions and that of other substances containing the CN group in that they show three well resolved bands. The absorption at 5.20μ is doubtless due to NaOH and KOH formed by hydrolysis, a band at this position having been previously reported by Plyler and Gordy.[4] The presence of the band at 4.44μ can be attributed to the CN ion liberated by these highly ionized salts. No band was observed at 4.44μ in the HCN solution. The absence of this band is explained by the extremely low degree of ionization of hydrocyanic acid. The bands at 4.75μ, 4.78μ, and 4.80μ in the HCN, NaCN, and KCN, respectively, are due to vibrational energy changes of the CN group in the molecule. The shift between the bands in KCN and NaCN is not as great as would be expected from considerations of atomic weights. In this case the shift to be expected from the differences in atomic weight is probably counteracted by a change in the binding force produced by the two metals.

The transmission of the complex cyanides as compared to water is given in Fig. 4. The Ba $(CN)_2$ curve shows an absorption band with maximum absorption at 4.78μ. The low intensity of this band is accounted for by the slight solubility of this salt. The double salt $KAg(CN)_2$ has maximum absorption at 4.66μ. The additional absorption at 5.20μ reveals either hydrolysis effects or the presence of an impurity. In this case there is no band which can be attributed to the CN ion, a result in accord with chemical data which show that $KAg(CN)_2$ would give on hydrolysis potassium ions and argenti-cyanide ions ($Ag(CN)_2^-$) instead of simple K^+, Ag^+, and CN^-. The position of the band in the barium salt at the longer wave-length is to be expected from a comparison of the atomic weights of barium and silver. A comparison of the absorption of the complex cyanides $Na_4Fe(CN)_6$ and $K_3Fe(CN)_6$ shows a marked difference of band position. From chemical data it is known that there is a high degree of ionization, the solutions yielding ions of the type $Fe(CN)_6^{----}$ and $Fe(CN)_6^{---}$, respectively. Since the atomic weight of the metallic constituent is the same for both ions, the shift

[10] E. K. Plyler and T. Burdine, Phys. Rev. 35, 605 (1929).

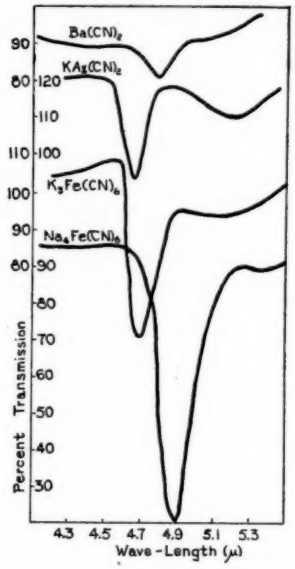

FIG. 4. The percent transmission of solutions of complex cyanides compared to water from 4.1μ to 5.5μ.

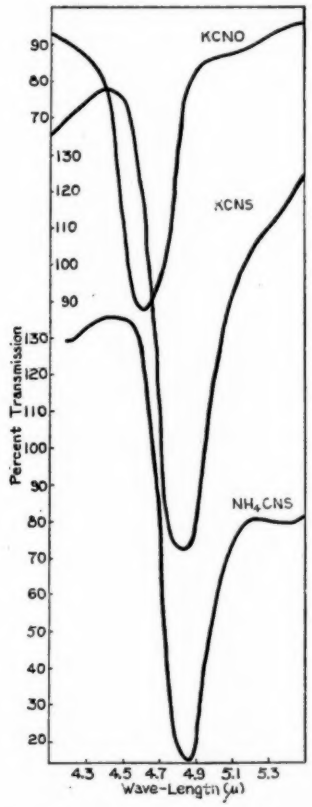

FIG. 5. The ratio of the transmission of some thiocyanate and cyanate solutions to that of water in the region from 4.1μ to 5.5μ.

can be due only to the variations in the CN binding produced by the difference in valence of the ferrous and ferric iron.

Fig. 5 shows the ratio of the transmission of KCNO, KCNS, and NH_4CNS to that of water in the region 4.1μ to 5.5μ. The strong band appearing in this region is again to be attributed to the CN vibration. The band in KCNO appears at a much shorter wave-length than in KCNS. Since the cation is the same in both cases, this shift is produced by the variation of the atom associated with the CN group in the anion. The shift of the KCNS band from the band attributed to the CN ion is approximately twice that of the KCNO, a fact which is in approximate agreement with the differences in the atomic weights of sulphur and oxygen. This direct dependence upon atomic weight indicates similar binding in the CNO and CNS groups. There is no appreciable shift between the NH_4CNS and KCNS bands at 4.84μ, a result indicating either that the absorption is due to the CNS ion or that the binding force between the metal and the CNS group is extremely weak.

In the case of the organic thiocyanate the characteristic band is at a definitely shorter wave-length than in the inorganic thiocyanates. The reason for this seems to be that the sulphur atom is associated with the organic group as CH_3S. Other evidence of this association lies in the marked shifts of the methyl band near 3.3μ to a longer wave-length, as will be observed in a comparison of the first and last curves of Fig. 3. In the curves for the organic cyanides the CN band appears at a shorter wave-length than in the inorganic compounds, a fact indicating closer CN binding in these compounds.

From a consideration of the variation of the maxima of the bands occurring near 4.8μ in HCN, KCN, and NaCN, we have concluded that these bands are due to the CN group in the molecule rather than to the CN ion. The appearance of the absorption of the CNS group so near to that of these molecules indicates similar binding in the CNS group and in the simple cyanide molecules.

The authors are indebted to Professor E. K. Plyler of this department for his helpful discussion of the manuscript.

The Infrared Absorption Spectrum of Methyl Deuteride

NATHAN GINSBURG AND E. F. BARKER, *University of Michigan*

(Received August 15, 1935)

The six fundamental vibrational frequencies of methyl deuteride were observed and the fine structure of the bands resolved. The frequencies are $\nu_6=1156.3$, $\nu_5=1306.8$, $\nu_4=1477.1$, $\nu_3=2205.25$, $\nu_1=2983.0$, $\nu_2=3031.0$. From the fine structure of the bands, the moments of inertia are found to be

$$I_A=7.166\times10^{-40}\text{ g cm}^2,\quad I_C=5.298\times10^{-40}\text{ g cm}^2$$

and the internuclear distances are

$$\text{C}-\text{H}=1.093\times10^{-8}\text{ cm},\qquad \text{H}-\text{H}=1.785\times10^{-8}\text{ cm}.$$

From the four previously known frequencies of methane and each of the frequencies of this molecule, the values of the five potential constants are computed. Three of the sets are consistent and agree well with the values found by Dennison and Johnston, but the other three sets have either negative or imaginary values. The frequencies from which these are calculated are the ones which take part in a resonance interaction which was not included in the theory. From the observed spacings of the zero branches of the perpendicular bands, extreme ranges of the rotation-vibration interaction factors are computed. An overtone, $2\nu_4=2923$, was also observed as were three frequencies of the molecule CH_2D_2, at 1036.0, 1090.5, and 1235.5 cm^{-1}.

INTRODUCTION

THE infrared absorption spectrum of methane was first investigated by Ångström[1] and later by Coblentz,[2] who corrected Ångström's work. He reported bands at 2.35μ, 3.31μ, and 7.7μ. Cooley[3] resolved the two longer wavelength bands into their fine structure obtaining separations of 5.4 and 9.7 wave numbers. This gave two different values for the moment of inertia when only one was expected. Neither Dennison,[4] assuming a regular tetrahedral structure, nor Guilleman,[5] assuming a pyramidal structure for the molecule, could give a satisfactory explanation of this.

With the discovery of the heavy isotope of hydrogen, it was possible to replace one of the H atoms of methane by a D atom and thus remove part of the degeneracy of the vibrational levels. This also introduces a preferred axis for rotation, the moment of inertia about it being the same as for normal methane.

Rosenthal[6] was able to obtain expressions for all of the frequencies of the various isotopic methanes in terms of five potential constants and certain mass factors. The four vibrational frequencies of methane (shown in Table I) uniquely determine two of the constants, while two more are given in terms of the fifth. Thus, one of the frequencies of any of the isotopic methanes determines these three constants so that all of the other frequencies can be calculated. Dennison and Johnston[7] were able to obtain values for these constants from consideration of the rotation-vibration interaction of normal methane. These computed constants, together with Rosenthal's equations, enabled them to calculate all the vibrational frequencies. The observed values will be compared with their computed ones later.

TABLE I. *The frequencies have been numbered according to the methyl halide system.* α—Dennison and Johnston's computed values. β—This frequency is inactive and can be obtained only from combination bands. γ—This frequency appears in the Raman effect.

Methane		Methyl deuteride		Observed	Calculated[α]
ν_4	1307	B	ν_6	1156.3	1151
		A	ν_5	1306.8	1300
ν_2	(1520)[β]	D	ν_4	1477.1	1460
		C	ν_3	2205.25	2183
		E	$2\nu_4$	2923	
ν_1	(2915)[γ]	F	ν_1	2983.0	2944
ν_3	3012	G	ν_2	3031.0	3013

EXPERIMENTAL

Apparatus and procedure

Two different grating spectrometers with rock-salt fore prism were used in this investigation.

[1] Ångström, Ofversigt af Kongl. Vetenskaps-Akad. Forh. **47**, 331 (1890).
[2] Coblentz, *Investigations of Infrared Spectra*, p. 43 and Diagram 12.
[3] J. P. Cooley, Astrophys. J. **62**, 73 (1925).
[4] D. M. Dennison, Astrophys. J. **62**, 84 (1925).
[5] V. Guilleman, Ann. d. Physik **81**, 173 (1926).
[6] J. Rosenthal, Phys. Rev. **45**, 538 (1934).
[7] Dennison and Johnston, Phys. Rev. **47**, 93 (1935).

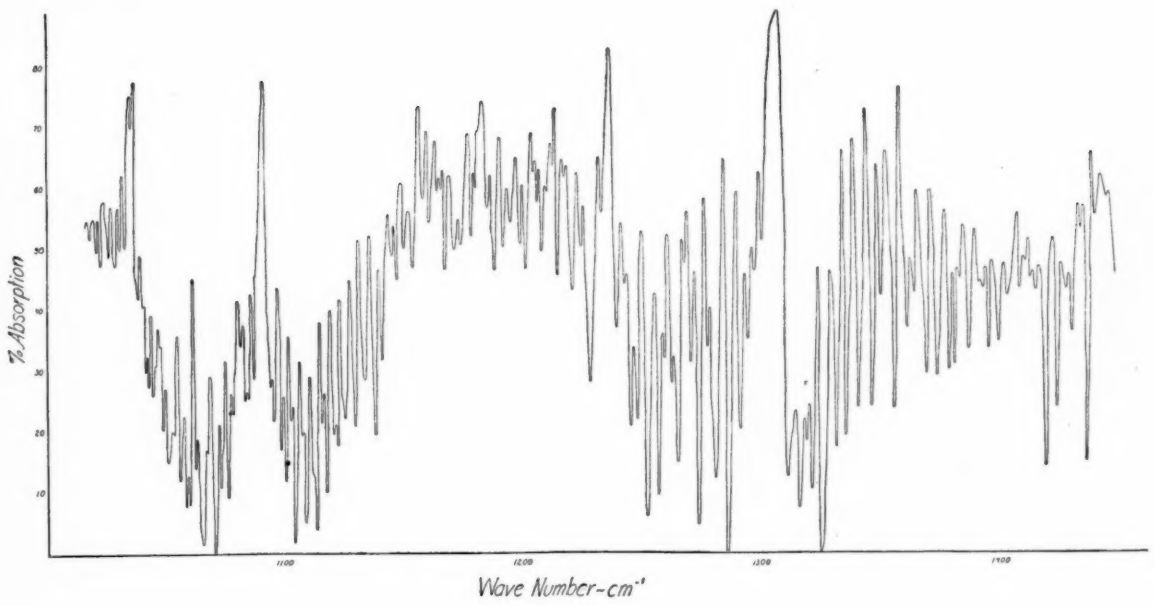

FIG. 1.

The one built and described by Barker and Meyer[8] was used with a Moll-Burger relay, the galvanometer being read at a distance of four meters; the second was built by Hardy[9] with a Pfund thermoelectric amplifier, the galvanometer being read at a distance of three meters. Two gratings were used, a 2400-line per inch grating in the 6 to 10μ region, and a 4800-line per inch grating in the 3 to 5μ region. A ten-cm glass cell, in the shape of two elliptical cones placed apex to apex, was used in order to get maximum absorption with the small amount of gas available. After more gas was made, a twenty-five cm elliptical glass cell with rocksalt windows was used. The source of the continuous radiation was a Nernst glower.

The procedure is as follows: With the cell in the beam, the slit widths are adjusted to give maximum deflection with good resolution. The grating is set at equal intervals throughout the spectral region under examination. Readings are taken with the cell in the beam and out of it, at least three being taken at each setting of the grating. Then the percent absorption is plotted against the frequency as determined from the grating relation $1/\nu = k \sin\theta$, where θ is the angle from the central image and k is the spectrometer constant. The position of the central image is determined at the beginning and end of each run. The spectrometer constants were known from previous work, but were rechecked. Each band was mapped at least twice, the results being in very good agreement.

Exploratory measurements

A sample of gas was obtained from W. A. Webb which contained a mixture of methyl deuterides, mostly CH_3D. With the 10-cm cell, the absorption spectrum was mapped in the regions from 6μ to 10μ and from 3μ to 3.5μ. Five very prominent bands were found in the long wave region (Fig. 1) with centers at 1036.0, 1090.5, 1156.5, 1235.5 and 1306.7 cm^{-1}. In the 3.3μ region, only one band was found, its center being at 3013 wave numbers. This, and the one at 1306.7 cm^{-1}, were identified as ν_3 and ν_4 of normal methane since the spacings of the fine structure are the same as those found by Cooley. The 1036 and 1235 cm^{-1} bands were identified as belonging to the CH_2D_2 molecule because of their irregular fine structure, which would be expected from an asymmetric rotator. The other

[8] Barker and Meyer, Trans. Faraday Soc. **25**, 913 (1929).
[9] J. Hardy, Phys. Rev. **38**, 2162 (1931).

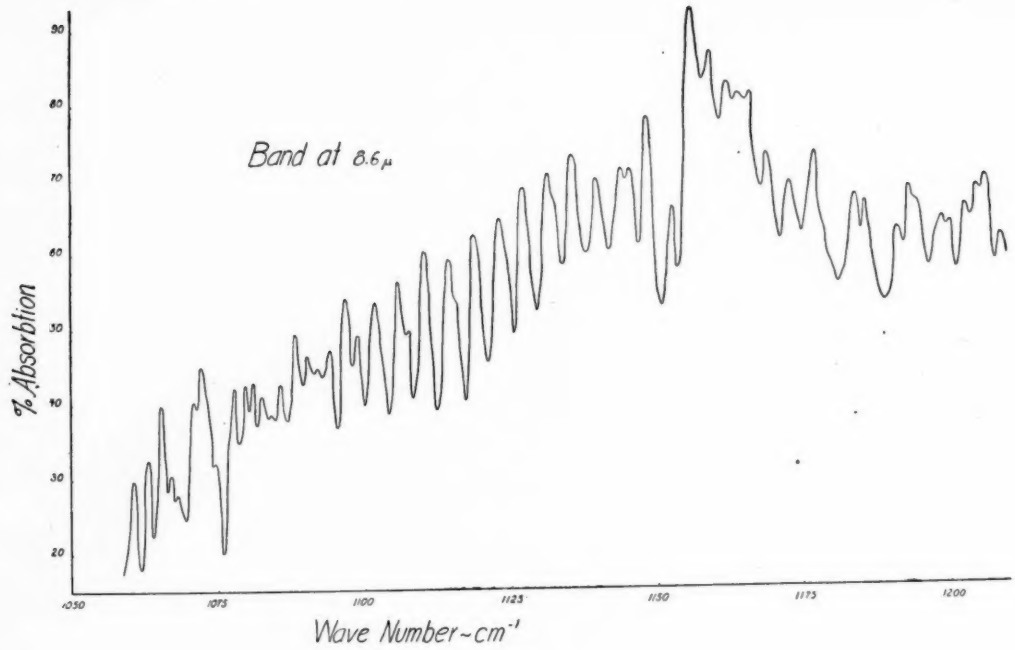

FIG. 2.

two bands were temporarily identified as ν_5, a parallel band,[10] and ν_6, a perpendicular band, of CH_3D. Calculations were then made with $\nu_5=1090$ to obtain the fifth potential constant which is required to solve the equations for the other vibrational frequencies. None of the frequencies so computed could be identified with the observed bands. Because of this ambiguity in the identification of the bands of the various methanes present in the mixture, it was necessary to prepare a new sample of gas by a method which gives methyl deuteride in a much higher concentration.

Preparation of the gas

A new supply of gas was prepared by means of the Grignard process, using heavy water.

$$CH_3I+Mg=CH_3MgI$$
$$CH_3MgI+D_2O=CH_3D+MgI(OD).$$

Dibutyl ether, rather than ethyl ether, was used as the solvent for the Grignard reagent because it is less volatile. In order to remove the small amount of ether vapor that came over in spite of all precautions, the gas was collected over concentrated sulphuric acid.

On spectroscopic examination of this gas, the bands of CH_2D_2 were again observed but with so much smaller intensity that they did not prove annoying. The band at 1090 cm^{-1} was also very weak and consequently was identified as belonging to the CH_2D_2 molecule. There was a small percentage of normal methane present too.

Results

Six fundamental frequencies are expected for the CH_3D molecule. Three of these will be parallel and single, and three will be perpendicular and double. Each of the triple frequencies of normal methane splits up into a parallel and a perpendicular band, just as in the case of the methyl halides. However, the methyl halides have as their lowest frequency a parallel vibration and then alternating perpendicular and parallel bands, while this molecule has as its lowest frequency band a perpendicular vibration. All six of the bands were observed, together with their fine structure. Their frequencies are given in Table I and are compared with Dennison and

[10] Barker and Ginsburg, J. Chem. Phys. **2**, 299 (1934).

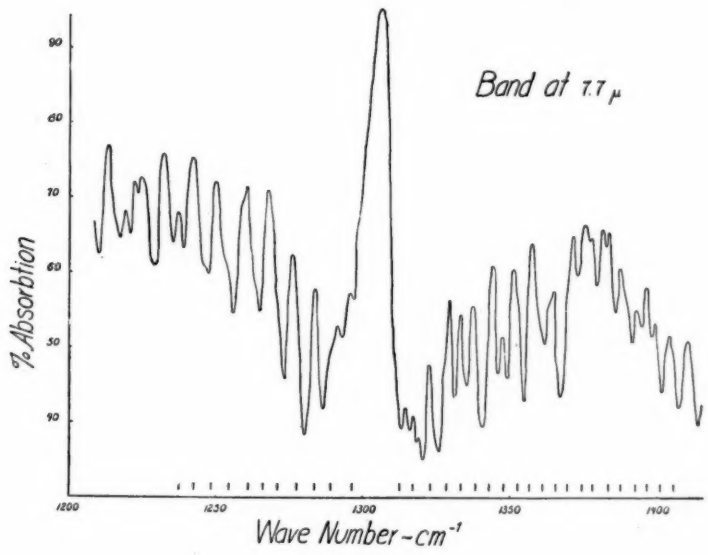

FIG. 3.

Johnston's calculated values. The location of the overtone is somewhat doubtful.

The lowest frequency band is ν_6, with the maximum at 1156.3 wave numbers (Fig. 2). The fine structure has a very regular spacing, with separations ranging from 3.8 to 4.5 wave numbers (Table II). An unusual feature of this band is the "hole" on the low frequency side of the center. Measurements were not extended to higher frequencies because of the overlapping of the 1307 cm^{-1} band.

The parallel band, $\nu_5 = 1306.8$ cm^{-1}, has almost the same frequency as ν_4 of normal methane, consequently there is some overlapping. The positions of the methane lines are marked on the absorption curve (Fig. 3) and correspond exactly to some of the observed lines (Table III). The separation between lines near the center of the band, where the overlapping is less marked, is about 7.7 cm^{-1}.

A second perpendicular band, ν_4, appears just on the high frequency side of the parallel band. It is not as intense as the others and lies

TABLE II. *The fine structure lines of the perpendicular band* ν_6. The irregularity in the positive branch is due to the overlapping of ν_5.

POSITIVE BRANCH	NEGATIVE BRANCH
1156.3	1156.3
1159.4	1152.7
1162.3	1148.6
1164.0	1145.4
1166.1	1144.0
1168.9	1139.6
1172.8	1135.5
1176.8	1131.4
1184.0	1127.3
1185.6	1123.1
1191.2	1118.9
1193.1	1114.6
1198.7	1110.3
1200.2	1105.7
1202.6	1101.8

TABLE III. *The fine structure of* ν_5 *showing the overlapping of the normal methane band,* ν_4.

POSITIVE BRANCH		NEGATIVE BRANCH	
CH_3D	CH_4	CH_3D	CH_4
1314.2		1295.4	1295.5
1317.0	1317.2	1291.1	
1319.0		1283.3	1283.5
1322.1		1275.6	
1329.2		1267.3	
1333.1	1333.2	1259.7	
1337.2		1249.6	
1343.6		1241.9	
1347.3	1347.5	1236.9	
1351.1		1231.8	
1357.0	1356.7	1224.1	
1364.5		1222.0	
1371.0		1218.8	
1375.1	1375.0	1213.0	
1377.5			
1381.0			
1383.0	1383.2		
1386.8			
1392.7	1392.6		
1396.3	1396.4		
1398.8			
1403.6			
1410.0			

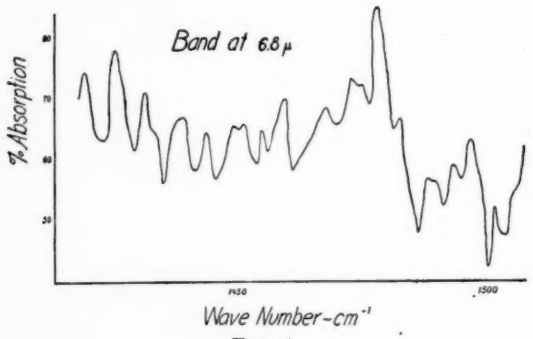

FIG. 4.

in the midst of the 6μ water vapor absorption region, making it very difficult to measure. It, too, has a "hole" near the center of the band, but on the high frequency side (Fig. 4). The spacing is somewhat irregular, varying between five and six wave numbers.

The second parallel band, ν_3, has its center at 2205.25 cm^{-1} (Fig. 5). Since this region is free of other bands, it could be very accurately measured. The fine structure lines are very regularly spaced, so that the formula

$$\nu_m = 2202.25 + 7.714m - 0.0434m^2$$

could be fitted to them. The observed frequencies of these lines together with their differences from the calculated values are given in Table IV. The increased absorption on the high frequency side is due to the CO_2 of the atmosphere.

TABLE IV. *The frequencies of the parallel band, ν_3.*

m	Positive branch Observed	Positive branch Δ	Negative branch Observed	Negative branch Δ
1	2212.0	−0.91	2196.75	−0.75
2	2220.4	−0.10	2190.1	+0.43
3	2227.6	−0.42	2181.7	−0.03
4	2235.4	−0.02	2173.4	−0.29
5	2242.65	−0.07	2165.5	−0.08
6	2249.9	−0.07	2157.4	0.00
7	2257.4	+0.24	2148.95	−0.17
8	2264.65	+0.41	2140.85	+0.13
9	2271.7	+0.52	2132.3	−0.01
10	2278.3	+0.23	2123.6	+0.09
11	2285.1	+0.23	2115.1	−0.04
12	2291.6	+0.04	2106.5	+0.07
13	2298.3	+0.10	2097.9	+0.23
14	2305.05	+0.31	2088.9	+0.11

In the 3.3μ region, there are two fundamentals, an overtone, and a band of normal methane, the latter appearing with small intensity. The parallel band, ν_1, has its center at 2983.0 cm^{-1}, no fine structure being observed because of the overlapping. The perpendicular band, ν_2, at 3031.0 cm^{-1}, has a very strong narrow center as if all the zero branches fall close together. The overtone, $2\nu_4$, is at 2923 wave numbers, being displaced and intensified by resonance interaction with ν_1. Measurements were taken at three pressures (Fig. 6) as given in Table V.

An attempt was made to locate some of the overtone and combination bands but due to the small amount of gas available, none were observed.

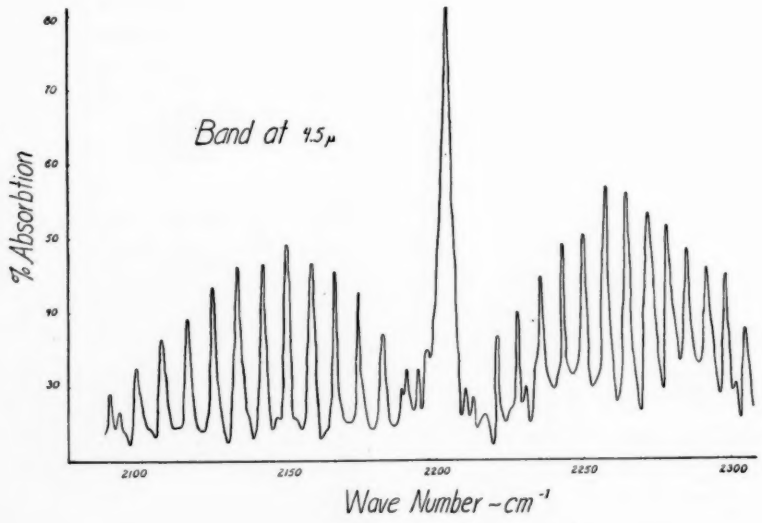

FIG. 5.

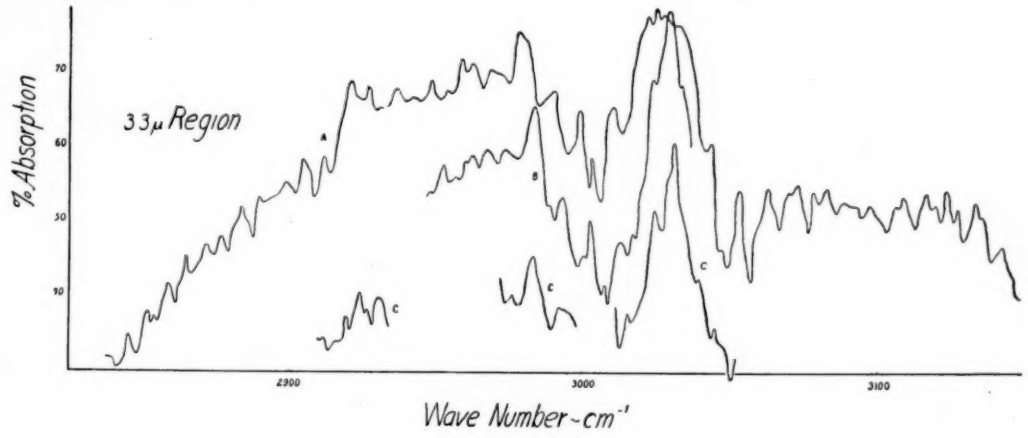

FIG. 6.

TABLE V. *Experimental data for the various bands.*

BAND	CELL	PRESSURE (mm Hg)	SLIT WIDTH (cm^{-1})	INTERVAL BETWEEN READINGS (cm^{-1})
Exploring Run	Short	700	0.7 to 1.5	0.55 to 1.4
ν_6	Long	180	0.65 to 0.9	0.6 to 0.8
ν_5	Long	180	0.9 to 1.3	0.85 to 1.05
ν_4	Long	700	1.0 to 1.05	1.2 to 1.3
ν_3	Long	180	0.8 to 0.95	0.6 to 0.75
3.3μ Region				
A	Long	180	0.7 to 0.85	1.2 to 1.45
B	Long	80	"	"
C	Short	50	"	"

TABLE VI.

FREQUENCY	COMPUTED CONSTANTS (10^5 dynes/cm) D	A	B	C	E
1156	1.323	7.485	0.4377	0.34047	0.3130
1307	1.328	7.281	0.4292	0.34047	0.3130
1477	Imag.	—	—	0.34047	0.3130
2205	1.328	7.304	0.4302	0.34047	0.3130
2983	−0.051	3.026	0.6714	0.34047	0.3130
3031	Imag.	—	—	0.3405	0.3130
Dennison and Johnston	1.278	7.670	0.476	0.341	0.313

INTERPRETATION OF RESULTS

From the frequencies of normal methane, it is possible to obtain two of the potential constants uniquely,[11]

$$C/4\pi^2 = m\omega_2^2/4; \quad E/4\pi^2 = m\omega_1^2/16$$

and two in terms of a third.

$$A/4\pi^2 = 2m\mu\{\omega_3^2+\omega_4^2 \pm[(\omega_3^2-\omega_4^2)^2-(8/\mu m^2)(D/4\pi^2)^2]^{\frac{1}{2}}\},$$

$$B/4\pi^2 = \tfrac{1}{16}m\{\omega_3^2+\omega_4^2 \mp[(\omega_3^2-\omega_4^2)^2-(8/\mu m^2)(D/4\pi^2)^2]^{\frac{1}{2}}\}.$$

By substituting any one of the observed frequencies into the equations for methyl deuteride,[6] it is possible to determine the fifth. The results of this calculation are given in Table VI. The constant D is very sensitive to the value of the selected frequency as can be seen by recomputing the frequencies from any one of the three closely agreeing sets of constants. The results do not differ from the observed values by more than twenty wave numbers, yet the observed frequencies give negative or imaginary values. The three frequencies which do not give acceptable values for the constants are those which take part in a resonance interaction which would be expected to shift them somewhat.

The coefficient of the linear term in the empirical equation for the rotation lines of a parallel band is

$$B = h/4\pi^2 cI_A.$$

For the 2205 cm^{-1} band, this was 7.714. Thus the moment of inertia about an axis perpendicular to the symmetry axis is

$$I_A = 7.166\times10^{-40} \text{ g cm}^2.$$

[11] J. Rosenthal, Phys. Rev. **46**, 730 (1934).

Assuming the regular tetrahedral structure, this gives

$$\text{H}-\text{H distance}=1.785\times10^{-8}\text{ cm}$$
$$\text{and}\quad \text{C}-\text{H distance}=1.093\times10^{-8}\text{ cm}.$$

From this, the moment of inertia about the symmetry axis (which is the same as for normal methane) is computed to be

$$I_C=5.298\times10^{-40}\text{ g cm}^2$$

as compared to

$$I_C=5.47\times10^{-40}\text{ g. cm}^2$$

found by Dennison and Johnston.[7]

Teller[12] has shown that for an axially symmetric molecule, the rotational energy has the form

$$W=J(J+1)\frac{h^2}{8\pi^2A}+\left(\frac{1-\zeta}{C}-\frac{1}{A}\right)\frac{K^2h^2}{8\pi^2},$$

where ζ is the angular momentum due to the vibratory motion alone. Thus the spacing of the zero branches for a perpendicular band is given by

$$\Delta\nu=(h/4\pi^2)((1-\zeta)/C-1/A).$$

Since the moments of inertia have been calculated and the spacing observed, the values of the interaction factors can be computed. It has also been proved that the sum of the factors for all three of the bands is independent of the force constants, and for this case should be one-half the ratio of the moments of inertia.

$$\Sigma\zeta_i=I_C/2I_A=0.370.$$

No possible combination of the ζ's gives this sum, the best selection being

$$\zeta_6=0.625\text{ to }0.692,$$
$$\zeta_4=-0.218\text{ to }-0.312,$$
$$\zeta_2=0.261\text{ to }0.213,$$

giving the sum

$$\Sigma\zeta_i=0.668\text{ to }0.593.$$

The resonance interaction between $2\nu_4$ and ν_2 would probably affect the values of these constants somewhat but would not be expected to produce such a large change.

Conclusion

Having observed the fundamental vibration frequencies of methyl deuteride, as well as the rotational structure of some of the bands, it was possible to compute the moments of inertia and internuclear distances and to obtain the range of values of the rotation-vibration interaction factors. Also the potential constants were evaluated.

Such complete results are possible only for this molecule or similar ones, where the determination of one moment of inertia makes it possible to calculate the other one. The differences between observation and theoretical predictions can be traced to a resonance interaction which has not been taken into account in the theoretical calculations.

We wish to thank Dr. Dennison and Mr. Johnston for conveying to us the results of their calculations which greatly facilitated the correct identification of the bands. The materials for this investigation were purchased from a grant of the Faculty Research Fund of the University of Michigan.

[12] Teller, *Hand- und Jahrbuch des Chem. Physik* (1934), Vol. 9, p. 125.

The Raman Spectra of Oxalic Acid

JAMES H. HIBBEN, *Geophysical Laboratory, Carnegie Institution of Washington*

(Received July 17, 1935)

The Raman spectra of anhydrous oxalic acid, its aqueous and alcoholic solutions, and oxalic acid dihydrate were determined. The spectra from the aqueous solution and anhydrous oxalic acid show that the two carboxyl groups do not behave identically. Peculiarities in the spectrum of the dihydrate are indicated. In the alcoholic solution both carboxyl groups behave similarly. The magnitude of the force constants in the carbonyl groups are consistent with the strength of this acid. Various explanations of these anomalies are discussed briefly.

OXALIC acid is one of the strongest organic acids. From the point of view of classical organic chemistry the simple structural formula

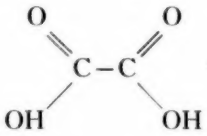

does not explain all its properties. It has been suggested[1] that a tautomeric rearrangement of the acid is possible in conformity with the scheme

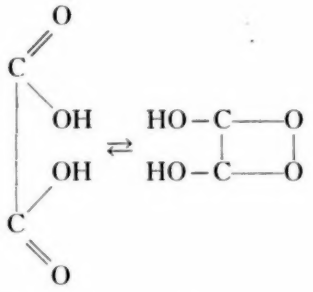

or

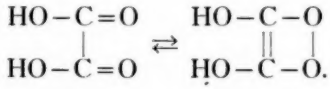

It is further supposed that the crystal hydrate might exist as the poly-hydroxy compound[2]

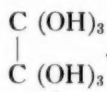

The Raman spectra of the anhydrous acid, the crystal hydrate, and the aqueous and alcoholic solutions of the acid were therefore determined in order to define more clearly the constitution of the molecule, and as illustrative of the method.

[1] Tschitschibabin, J. Prakt. Chem. (2) **120**, 214 (1928).
[2] Noyes, *Organic Chemistry* (Henry Holt & Co., second edition).

TABLE I. *Raman spectra of oxalic acid.*

$(COOH)_2$ in CH_3OH Hibben	$(COOH)_2 \cdot 2H_2O$ Hibben	Aqueous Solution $(COOH)_2$ Rao	Aqueous Solution $(COOH)_2$ Hibben	$(COOH)_2$ Rao	$(COOH)_2$ Hibben
		248 (?)			
403_m			395_m		
			453_m		
		480_m		473_m	
		673 (?)			
850_s	847	845_s	842_s	851_s	848_s
			1310_w		
	1365	1430_{wd}*			1370_d
	1471		1460_d		
				1506_w	
		1656_d	1645_d	1640_d	1651_m
1755_s		1744_s	1740_m	1758_w	1740 (?)

s (strong), w (weak), d (diffuse), m (medium) * ±30

Krishnamurti[3] observed one frequency shift for the hydrate, $\Delta\tilde{\nu}$ (cm^{-1}) 855. Recently Siva Rao[4] examined oxalic acid and its aqueous solution. The results were in partial agreement with those obtained by the author. There are, however, some pertinent points of disagreement. Table I summarizes these results.

So far as the solution is concerned, the difference lies in the two lower frequency shifts and the shift between $\Delta\tilde{\nu}$ 1310 and $\Delta\tilde{\nu}$ 1460. In Fig. 1

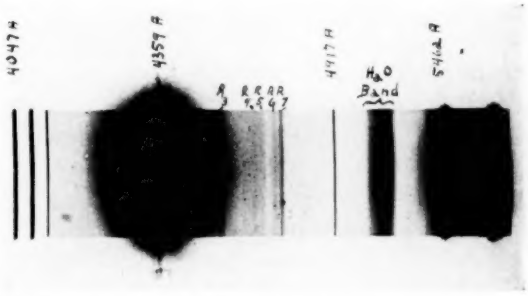

FIG. 1. Raman spectra of oxalic acid in aqueous solution.

[3] Krishnamurti, Ind. J. Phys. **6**, 309 (1931).
[4] Rao, Zeits. f. Physik **94**, 546 (1935).

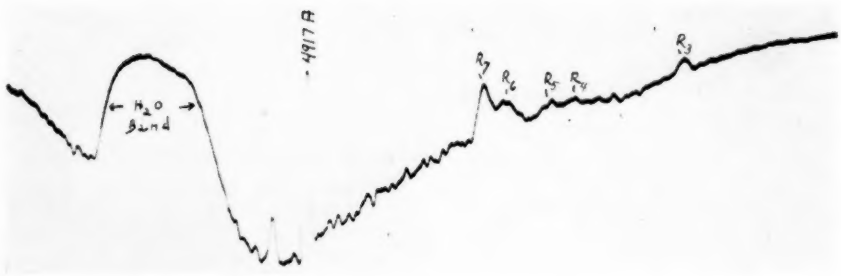

FIG. 2. Microphotometer tracing of the Raman spectra of aqueous oxalic acid.

is shown the positive spectrogram of the aqueous solution with the 4359A mercury line as a source of excitation with $NaNO_2$ and $Co(SCN)_2$ solutions as filters. The two lower shifts are hidden in the print behind the general scattering. The $\Delta\tilde{\nu}$ 1460 and 1310 shifts, however, are clearly apparent. Fig. 2 is a microphotometer tracing of the same plate. Fig. 3 is a similar tracing of a positive contact plate made from the same spectrum. The frequencies $\Delta\tilde{\nu}$ 395 and 453 are thus easily made discernible. The frequency $\Delta\tilde{\nu}$ 248 is too close to the exciting line for its existence to be at all certain. It is possible that the frequency designated as $\Delta\tilde{\nu}$ 480 by Rao is the same as $\Delta\tilde{\nu}$ 453. The discrepancy of 27 wave numbers is greater, however, than the accuracy of measurement. The questionable frequency at $\Delta\tilde{\nu}$ 673 is apparently nonexistent.

For the anhydrous acid the principal frequencies near $\Delta\tilde{\nu}$ 850 and $\Delta\tilde{\nu}$ 1650 are in reasonable agreement with Rao's results, but his lines corresponding to $\Delta\tilde{\nu}$ 1506 and $\Delta\tilde{\nu}$ 473 were not recorded and $\Delta\tilde{\nu}$ 1370 not observed by him was clearly readable. The shift at $\Delta\tilde{\nu}$ 1740 is very difficult to estimate correctly using the unfiltered mercury spectrum employed by Rao. This nearly overlaps the mercury line at 4730A.

In the crystal hydrate the principal shift $\Delta\tilde{\nu}$ 847 is accompanied by $\Delta\tilde{\nu}$ 1365 analogous to the anhydrous acid but with the addition of a weaker shift at $\Delta\tilde{\nu}$ 1471. No shifts corresponding to those at approximately $\Delta\tilde{\nu}$ 1650 and $\Delta\tilde{\nu}$ 1750 of the anhydrous acid were observed in the hydrate. This does not preclude the possibility that they may be extant but if so they are very much weaker than the same shifts in the dehydrated acid. The water band which extends from $\Delta\tilde{\nu}$ 3415 to $\Delta\tilde{\nu}$ 3531 in the hydrate is much sharper than the corresponding water band in aqueous solution which is nearly four times as broad.

It is to be admitted that the exact measurements of diffuse and weak lines is difficult against the strong background scattering of the exciting radiation. This is particularly true of the Raman spectra from small crystals.

In Fig. 4 is given the microphotometer tracing of the alcoholic solution of oxalic acid in comparison with alcohol in which the upper curve represents methyl alcohol. The results are independent of the amount of water which may be present up to 10 percent. The lower frequency shift $\Delta\tilde{\nu}$ 403 is not discernible in the tracing. Nevertheless it is easily measurable on the original plate. There is no evidence of a shift corresponding to approximately $\Delta\tilde{\nu}$ 1650, which is one of the characteristic lines in the aqueous solution of the acid. The frequency at $\Delta\tilde{\nu}$ 1740 in water solution becomes $\Delta\tilde{\nu}$ 1755.

The above are all the experimental observations so far obtained. There appear, however, from these results certain salient facts that are beyond any experimental rationalization, namely, there are apparently two definite frequencies in the aqueous solution of oxalic acid which are normally attributed to the C=O oscillation and which become a single frequency in the alcoholic solution, and these same frequencies are radically diminished in intensity, if not extinct, in the hydrated crystal. The interpretation of these observations is a matter of opinion. A consideration of the Raman spectra of some other organic compounds containing carbonyl groups would be of value in arriving at any conclusion.

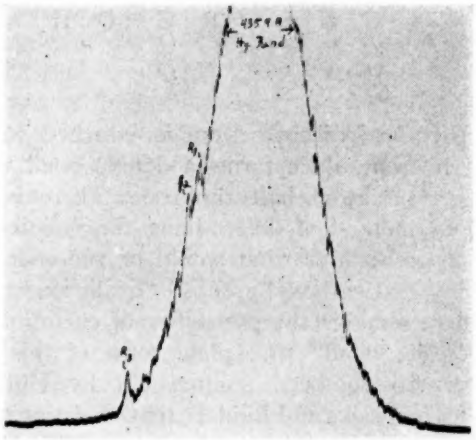

FIG. 3. Microphotometer tracing indicating Raman shifts 395 and 453 in aqueous oxalic acid.

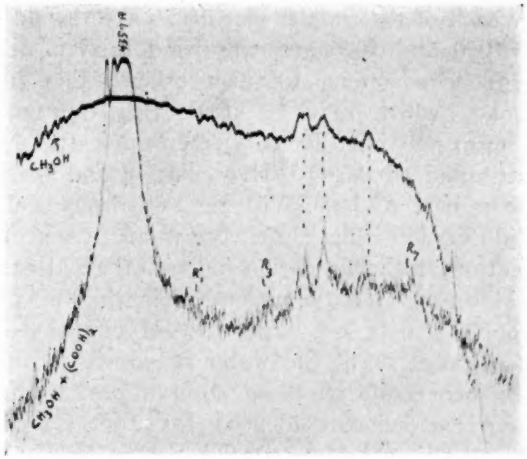

FIG. 4. The Raman spectra of oxalic acid dissolved in CH_3OH and the spectra of CH_3OH. The upper curve represents the pure alcohol.

Siva Rao correctly points out that, in the aliphatic series, C=O frequencies between $\Delta\tilde{\nu}$ 1712 and 1760 are confined to the higher homologues of the esters and the aldehyde and ketone derivatives of the aliphatic hydrocarbons. Ordinarily the acid derivatives of the simple hydrocarbons have a shift which falls within the region $\Delta\tilde{\nu}$ 1640 and 1660. This would account for the frequency shift in the region of $\Delta\tilde{\nu}$ 1650 observed in the aqueous solution of oxalic acid and with the powdered anhydrous acid.

Only one other saturated dicarboxylic acid has been studied. This is malonic acid.[5] The observed shifts were $\Delta\tilde{\nu}$ 908; 960; 1737; 2935. The only other acid which shows a comparable displacement is pyruvic acid[6, 7] yielding $\Delta\tilde{\nu}$ 1735 with a very weak component at $\Delta\tilde{\nu}$ 1769. Pyruvic acid, like oxalic acid, has two carbonyl groups in juxtaposition. From this meager evidence it is impossible, however, to extrapolate with definiteness as to the expected characteristic frequency shift of the carbonyl groups in a saturated dicarboxylic acid.

Siva Rao has suggested that the frequency shift $\Delta\tilde{\nu}$ 1430 is characteristic of the OH group—presumably present in oxalic acid—on the ground that other organic hydroxy compounds (containing CH_2 groups) have such a displacement. This precise designation does not seem to be tenable. In the first place the frequency is measured by him only to within ±30 wave numbers. On the assumption that this is correct, it is to be noted that the frequency falls within the region of frequency shifts observed with all the saturated aliphatic hydrocarbons from ethane to decane. This has been ordinarily ascribed by Kohlrausch[8, 9] and Andrews[10] to the bending moment of the hydrogen in the CH_2 groups. With oxalic acid, however, this assignment is impossible because of the complete lack of CH_2 groups. Nevertheless, $\Delta\tilde{\nu}$ 1430±30 cannot be used as evidence of the OH grouping when CH_2 groups are present. On the contrary, possibly the most characteristic frequency of C↔O is in the region of $\Delta\tilde{\nu}$ 1015 to 1050. This is present in methylene glycol and ethylene glycol. Venkateswaran and Bhagavantam[11] attribute, in addition to the approximate $\Delta\tilde{\nu}$ 1025, also $\Delta\tilde{\nu}$ 1225 and 1365, to the C−OH grouping. This is supported by the work of Bolla,[12, 13] who records 56 lines

[5] Ghosh and Kar, J. Phys. Chem. **35**, 1735 (1931).
[6] Dadieu and Kohlrausch, Monatsh. **55**, 379 (1930).
[7] Dadieu and Kohlrausch, Sitzber. Akad. Wiss. Wien, (IIa) **139**, 77 (1930).

[8] Kohlrausch, *Der Smekal Raman Effekt* (Julius Springer, Berlin, 1931), p. 304.
[9] Kohlrausch, Naturwiss. **22**, 161 (1934).
[10] Andrews, Phys. Rev. **34**, 1626 (1929).
[11] Venkateswaran and Bhagavantam, Ind. J. Phys. **5**, 129 (1930).
[12] Bolla, Zeits. f. Physik **89**, 513 (1934).
[13] Bolla, Zeits. f. Physik **90**, 607 (1934).

for each of the simpler alcohols. Those between $\Delta\tilde{\nu}$ 1050 and 1090 are considered fundamental frequencies among fourteen others. The frequency which may be used with the most certainty to identify an OH group is the one attributed to the O↔H oscillation and which occurs near $\Delta\tilde{\nu}$ 3400. With the anhydrous oxalic acid this shift is not clearly apparent. In aqueous solution, alcoholic solution and with the hydrated acid any O↔H vibration originating in the organic acid is lost in the O↔H vibration of the solvent or of the water of crystallization. The net result of these observations is that there is no definite evidence in favor of a C−OH linkage although its presence is not precluded.*

These considerations together with the experimental data lead to the conclusion that the tautomeric form of oxalic acid as suggested by Tschitschibabin is not present. There are no lines which could be ascribed to C=C or to a true ring structure. The poly-hydroxy form of the hydrated acid is not clearly demonstrated although the lack of C=O frequencies in the hydrate would indicate at least a profound modification in the normal structure. In aqueous solution one carboxyl group behaves normally but the interaction between two closely situated carbonyl groups results in one carbonyl group having more nearly the characteristics of an aldehyde ketone or ester carbonyl than that of the usual acid. In alcoholic solution both carbonyl groups behave abnormally. In any case, in solution the influence of one carboxyl group on the other is to increase the force constant between the carbon and oxygen atoms of at least one carbonyl group. This is similar to the action of any other negative substituent group and is direct evidence for the classical explanation of the strength of this acid.

There are two other hypotheses which may be considered in connection with the structure of oxalic acid. Pauling[14] has suggested that organic acids owe their acidity to carboxyl groups which may exist in resonance in two forms, namely,

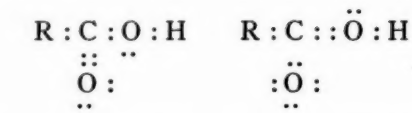

so that the hydrogen atom is attached to an oxygen atom which forms a double bond with the carbon atom half the time. There is no obvious method of determining the validity of this hypothesis or what would be the effect of the adjacent carboxyl groups in oxalic acid.

There remains the possibility of chelation or "hydrogen bond" to explain some of this behavior. It has been pointed out by Hilbert, Wulf, Hendricks and Liddel[15] that chelation may exist between some organic compounds of the type postulated by Sidgwick.[16] In this type of compound a stable ring may be formed between a donor and a possible acceptor. The case of complex ions containing anions of dibasic acids possibly belongs to a rare but existing species. For compounds consisting of larger rings it is assumed that the enolic form of aceto-acetic ester may exist, thus,

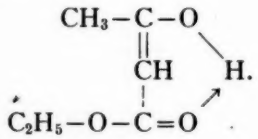

It has been shown[15] that in some more complicated aromatic organic compounds possessing both an O−H and a C=O group in the ortho position the O−H group is not present as such but rather the hydrogen of the OH is chelated with the C=O. Other results, however, indicate that the C=O in normally chelated compounds such as methyl salicylate is unaffected.[17] From the chelate point of view crystalline oxalic acid possibly would have the partial structure

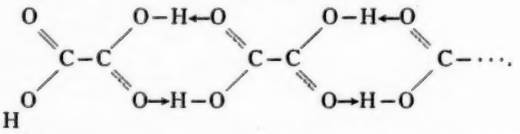

If these chains were relatively short and incomplete this might account for the presence of

* An exciting frequency of 4359A does not yield a frequency shift corresponding to $\Delta\tilde{\nu}$ 3500 as readily as an exciting frequency in the ultraviolet. Strong absorption in the ultraviolet prevents the use of high frequency radiation as a source of excitation.

[14] Pauling, Proc. Nat. Acad. Sci. **18**, 293 (1932).

[15] Hilbert, Wulf, Hendricks and Liddel, Nature **135**, 148 (1935).

[16] Sidgwick, *The Electronic Theory of Valency* (Oxford University Press, 1929), p. 240.

[17] Unpublished results.

the weak C=O frequency and the absence of a normally strong O↔H vibration. The hydrated oxalic acid would have larger aggregates interspersed with normal water of crystallization. It is not inconsistent to suppose that on solution these loose chelate structures would break down into individual molecules showing some residual abnormality

It can be generally stated that while the evidence is not conclusive that the crystal hydrate contains no C=O oscillations, such shifts if present are certainly far weaker than to be expected in comparison with the anhydrous form or the aqueous solution.

Whatever may be the explanation of the behavior of anhydrous oxalic acid, aqueous oxalic acid solutions or solutions in methyl alcohol, it is quite evident that the two carboxyl groups do not behave the same except in organic solvents. The abnormality of oxalic acid is amply confirmed by spectroscopic measurements.

Finally, it may be mentioned that experiments with sodium salts of oxalic acid lead to very weak or no shifts characteristic of the C=O. This is in accordance with the observation of Krishnamurti[3] with ammonium oxalate and of Ghosh and Kar[5] with sodium formate, sodium acetate and sodium malonate. This work is being continued.

NOVEMBER, 1935 JOURNAL OF CHEMICAL PHYSICS VOLUME 3

The Reaction Rate of Acetic Anhydride and Water

E. K. PLYLER AND E. S. BARR, *Department of Physics, University of North Carolina*

(Received September 13, 1935)

The infrared absorption of acetic acid and acetic anhydride has been measured from 1μ to 6.5μ. A number of bands were observed below 5μ which were similar for the two substances, and were attributed to CH bonds. An intense band was found in acetic anhydride at 5.45μ and in acetic acid at 5.75μ. By measuring the intensity of these bands at different times, the reaction velocities of equivalent amounts of anhydride and water were determined. This method offers a new and independent means of determining reaction velocities and related constants. The reaction was approximately unimolecular for any concentration. The reaction constant decreased as the time increased. A different value of the constant was obtained when different concentrations were used. The reaction constant was also determined for three different temperatures. The values of the reaction constant and other constants are tabulated. The error is estimated to be 10 percent.

THE infrared absorption spectra of acetic acid have been measured by Coblentz[1] and its Raman spectra determined by Gansean and Venkateswaran.[2] In the region from 1μ to 5μ the bands are similar to those found in other CH compounds. Acetic anhydride also had the characteristic spectra of CH compounds to 5μ. In order to find bands for the anhydride, which were due to the difference in structure from the acid, it was necessary to work in the 6μ region. Good resolution was obtained by using a fluorite prism, the effective slit width being 0.02μ at 6μ. The method of measurement was similar to that used by Plyler and Barr[3] in a previous paper. In Fig. 1 is shown a comparison of the spectra of acetic acid, acetic anhydride and a mixture of the two substances. The acetic acid had absorption bands at 1.1, 2.25, 2.5, 2.8, 3.35, 3.9 and 5.75μ. These bands are similar to the bands found by Coblentz except those in the region below 3.4μ, where thicker cells than those used by him are necessary to bring out the bands. In the Raman spectra other bands were found at longer wave-lengths than the upper limit of this

[1] Coblentz, *Investigations of Infrared Spectra* (Carnegie Institution of Washington, 1905).

[2] Gansean and Venkateswaran, Ind. J. Phys. **4**, 195 (1929).

[3] Plyler and Barr, J. Chem. Phys. **2**, 306 (1934).

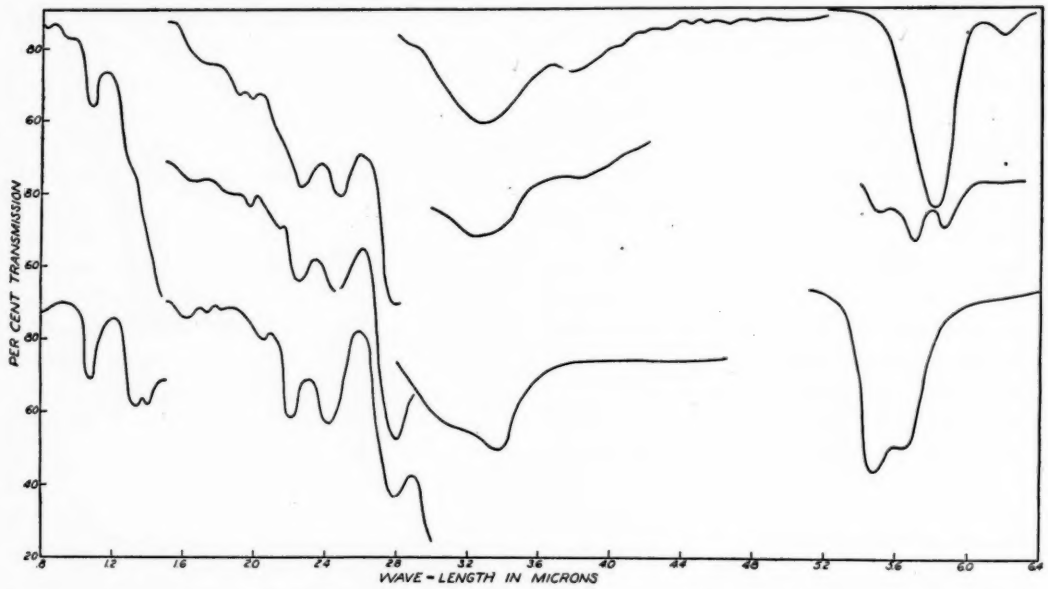

FIG. 1. Upper curves acetic acid, middle curves 70 percent acetic acid and 30 percent acetic anhydride, lower curves acetic anhydride. Cell thickness from 0.8 to 1.5μ was 1.0 cm, from 1.5μ to 2.8μ 0.1 mm, from 2.8μ to 6.4μ approximately 0.01 mm.

study. An examination of Fig. 1 shows that there is an intense band due to the anhydride at 5.45μ and to the acetic acid at 5.75μ. This region was studied further and the effects of different concentrations of anhydride, water and acetic acid were found. The results are shown in Fig. 2. The 5.45μ band varies in intensity with the amount of anhydride present and the 5.75μ band varies with the amount of acetic acid in solution. The band at 6.15μ is due to the presence of water. When the acetic acid spectrum was obtained under high resolution as shown in Fig. 2, the 5.75μ band shown in Fig. 1 is seen to consist of two bands at 5.7 and 5.85μ, the first of these being the band of hydration[3] and the second due to the acid proper.

When the concentration of the water was small, it was found that the reaction had not reached equilibrium in 24 hours. This showed that the reaction velocity was sufficiently slow so that the change could be observed by measuring the intensity of the bands at different times. Equivalent amounts of acetic anhydride and water were mixed and kept at a constant temperature. The concentration was about 8.9 moles per liter. At intervals of time a sample was taken and put into the absorption cell. When the observations did not extend over 6 or 8 hours, the reaction was allowed to take place in the absorption cell itself. In Fig. 3 the results are shown for a set of observations made when the temperature was 50°C. The band at 5.45μ decreased in intensity as the time increased, until it was practically zero. The reaction continued, of course, until equilibrium was attained, so a small amount of the reacting substances remained in solution at all times. Two more sets of observations were made at temperatures of 25° and 70°C. It was found that the intensity of the anhydride band decreased more rapidly in a given time when the reaction was allowed to take place at a higher temperature.

In order to calculate the reaction constant, the relative intensities of the bands had to be known. The expression $\int \rho d\nu$, which is the measure of the intensity of a band, was determined by plotting the absorption curves on graph paper and counting the squares within the enclosed area. Since the band due to the anhydride and the acetic acid band partially overlapped, it was necessary to include only the area below the acetic acid curve. This was done by superimposing an acetic acid curve on the mixture curve.

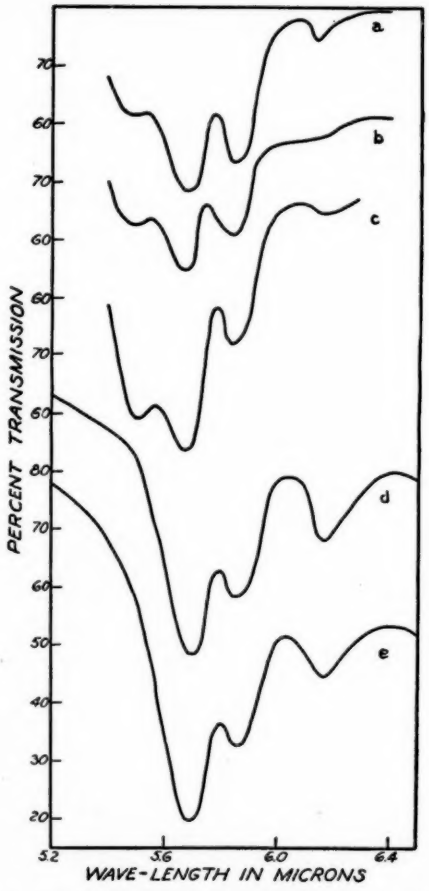

FIG. 2. The absorption of mixtures of acetic acid and acetic anhydride (a) 20 percent anhydride and 80 percent acid, (b) 30 percent anhydride and 70 percent acid, (c) 50 percent anhydride and 50 percent acid, (d) and (e) glacial acetic acid.

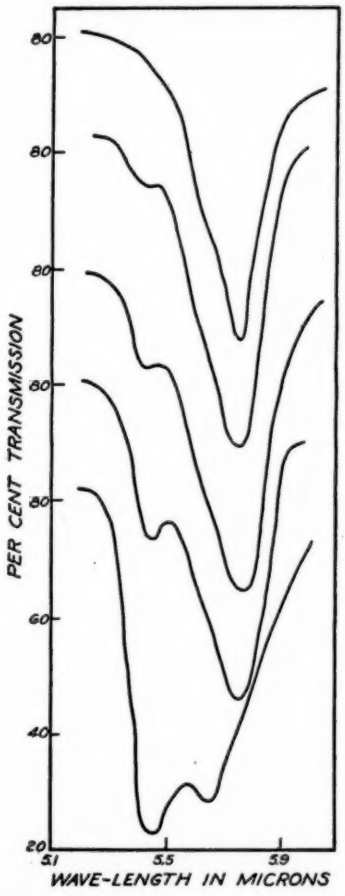

FIG. 3. The change in absorption of acetic anhydride and water with time, the temperature being 50°C. The lowest curve was observed in first time interval after mixing.

After the relative intensities of the bands were found, their values were plotted as a function of time. The results for one set of values are shown in Fig. 4. The curve was extrapolated to zero time and the relative intensity was found to be 1000 in this case. In order to find the concentration of the anhydride for any time, the relative intensity at the given time was divided by 1000 and then multiplied by 8.9, which was the original concentration of the anhydride in moles per liter. In general

$$C=8.9\ R/1000, \tag{1}$$

where C is the concentration at time t and R is the relative intensity at time t. These values of C were then used for $a-x$ in the unimolecular formula

$$k=(1/t)\ \log\ (a/(a-x)), \tag{2}$$

where a is the original concentration of the anhydride, t the time in seconds, and k the reaction constant.

The greatest error in the calculation of the reaction constant is due to extrapolating the curve in Fig. 4 to zero time, because the rate of reaction is greatest at the beginning. Also there is some uncertainty as to the correct position in superimposing the acetic acid curve upon the anhydride curve in obtaining the relative intensity of the bands. This error is the greatest for the small intensities. It is estimated that about 10 percent error is produced in the value of the reaction constant by these two effects.

It was found that more consistent values could be obtained for the reaction constant if the

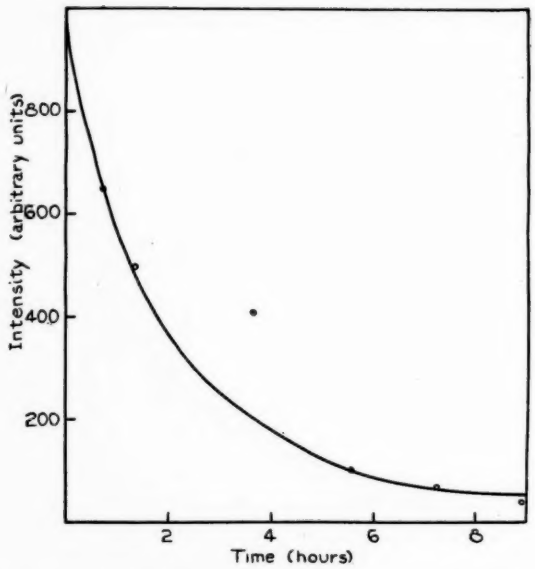

FIG. 4. The relative intensity of the acetic anhydride bands as a function of time.

reaction was treated as unimolecular instead of bimolecular. Benrath,[4] who attempted to measure this reaction velocity by means of change in density of solution, found that with even equivalent amounts the reaction was roughly unimolecular. Lumière and Barbier[5] and Rivett and Sidgwick[6] also found the reaction unimolecular, but that the reaction constant decreased with the increase of acetic acid in solution. Rivett and Sidgwick used the conductivity of the solution as a measure of the amount of acetic acid present. From these measurements they calculated the reaction velocity constant for 29 different concentrations which varied from 0.02 to 1.07 normal.

In Table I are given the results obtained in the present work for temperatures of 25°, 50°, and 70°C. The value of k decreases as the time increases. This result is in accordance with that

[4] Benrath, Zeits. f. physik. Chemie **67**, 501 (1909).
[5] Lumière and Barbier, Bull. soc. chim. **35**, 625 (1906).
[6] Rivett and Sidgwick, J. Chem. Soc. **97**, 732 (1910).

TABLE I. *Reaction constant k for acetic anhydride at 25°, 50° and 70°C.*

T°C	TIME (sec.)	$k\times10^5$	T°C	TIME (sec.)	$k\times10^5$
70	1800	92		9600	22
	2700	85		15120	19.5
	4500	75	25	6360	6.6
	6300	69		10140	6.5
50	1200	23		40080	5.1
	5880	25		64200	5.0

TABLE II. *The value of the activation constant E for different temperature changes.*

$k_1\times10^5$	$k_2\times10^5$	T_1	T_2	E
5.6	22	298	323	11,760
5.6	85	298	343	12,200
22	85	323	343	14,800

of previous observers. The hydration of some of the water with the acetic acid formed probably keeps the water from having a part in the reaction and the presence of the acetic acid also decreases the number of collisions in a given time between the anhydride and the water molecules.

The effect of temperature was checked by the equation

$$E=(T_1T_2/(T_2-T_1))\log(k_2/k_1)R. \qquad (3)$$

In Table II are given the values of E for the different changes in temperature. The check is satisfactory and indicates that the relative values of the different k's are approximately correct.

Further work by the infrared method may make it possible to obtain a greater accuracy in determining reaction rates. However, the results given in this paper show that the reaction is approximately unimolecular. The value of k is dependent on the amount of water, and tends to decrease as the reaction progresses. Some measurements on three parts water to one part anhydride indicated that the reaction rate was greatly increased with an increase in the amount of water present.

The Linear Thermal Expansion of Sodium Tungstate Between 20° and 600°

J. B. AUSTIN AND R. H. H. PIERCE, JR., *Research Laboratory, United States Steel Corporation, Kearny, New Jersey*

(Received September 5, 1935)

(1) The linear thermal expansion of anhydrous sodium tungstate has been determined between 20° and 600°C by means of an interferometer, with results given by the following equations:

$$v = v_{20}[1 + 53.194(t-20)10^{-6} + 41.5(t-20)^2 10^{-9}],$$
$$\Delta l/l_{20} = 17.73(t-20)10^{-6} + 13.83(t-20)^2 10^{-9},$$
$$\alpha_m = 17.73 \times 10^{-6} + 13.83(t-20)10^{-9},$$
$$\alpha_t = 17.73 \times 10^{-6} + 27.66(t-20)10^{-9}.$$

(2) The results show that at atmospheric pressure the salt is trimorphous. Modification III is stable on heating up to 585° at which temperature it transforms to II with an increase in volume of 17.4 percent. Form II is stable over a very short temperature interval, whose exact extent could not be determined, and then transforms to Na_2WO_4 I with a decrease in volume of 0.12 percent.

IN the course of an investigation of the linear thermal expansion of tridymite prepared by heating powdered quartz with Na_2WO_4 it became desirable to know the expansion of the flux alone. Since such information is not available in the literature we have determined the dilatation of Na_2WO_4 between 20° and 600°C by means of an interferometer previously described.[1] In addition to providing values of the expansion coefficient, the results confirm the phase relations in this system as recently reported by Goranson and Kracek.[2] Thus, it is shown that at atmospheric pressure, anhydrous Na_2WO_4 exists in three crystalline forms which, following Goranson and Kracek, are designated III, II and I in the order of their stability range with increasing temperature. Na_2WO_4 III, is stable up to 585°C, at which temperature it transforms to Na_2WO_4 II with an increase in volume of approximately 17 percent. Na_2WO_4 II then changes to modification I a few degrees above the transition III→II, but in this case there is a decrease in volume of 0.12 percent. These transitions lie so close together that on heating under our experimental conditions the second one was always masked by the large change of volume accompanying the first. It was, on the other hand possible to separate them on cooling because of their different tendencies to undercool. Thus, on cooling from 600°C, Na_2WO_4 I transforms to Na_2WO_4 II at approximately 580°C, the exact temperature depending on the rate of cooling; modification II then persists in metastable equilibrium to some lower temperature which again depends on the rate of cooling. At a rate of 3°C per min. the transition II→III was observed to take place close to 525°C, or 60°C below the equilibrium temperature. This behavior provides another convincing example of the error which may be introduced into a determination of phase equilibria in solids by approaching the equilibrium from one side only, particularly if this approach is by cooling, as is often the case.

MATERIAL

A good grade of commercial Na_2WO_4, further purified by recrystallization from water, was fused in gold and was allowed to solidify into a block from which three specimens, approximately 3 mm in height and 3 mm in diameter, could easily be cut. No measurements were made on single crystals because we were not able to prepare suitable ones; Na_2WO_4 could not be made to form well-defined anhydrous crystals of satisfactory size from aqueous solution, and all attempts to grow a single crystal from the melt failed because a crystal formed on cooling was invariably shattered on cooling through the inversion II→III.

RESULTS. THERMAL EXPANSION BELOW 585°C

Up to approximately 400° the salt showed a normal reversible thermal expansion (see Fig. 1) but just above 400° the expansion coefficient

[1] Austin and Pierce, J. Am. Chem. Soc. **55**, 661 (1933). For a complete description of the method see Merritt, Bur. Standards J. Research **10**, 159 (1933).

[2] Goranson and Kracek, J. Chem. Phys. **3**, 87 (1935).

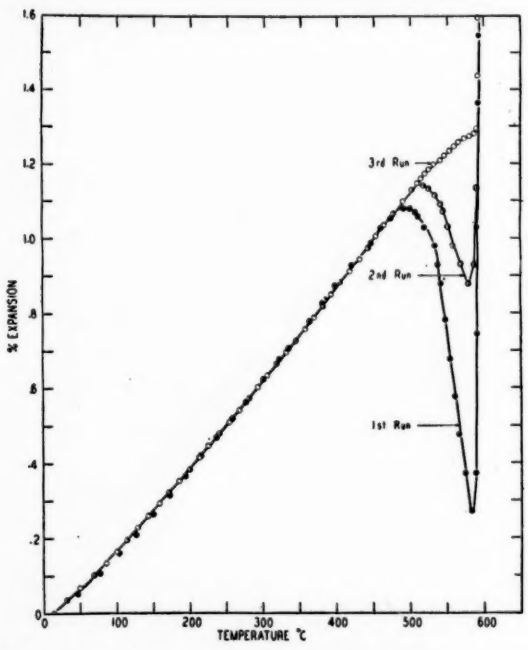

FIG. 1. The linear thermal expansion of Na_2WO_4 up to 585° as determined on three successive runs on the same sample under a load of 63 grams.

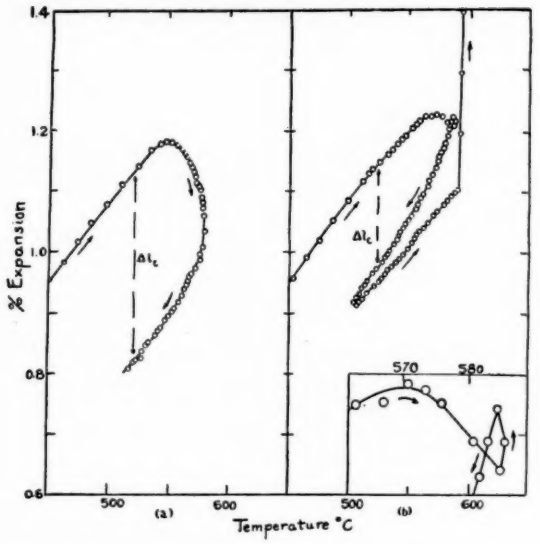

FIG. 2. Curves showing the linear thermal expansion of two samples of Na_2WO_4 in the neighborhood of the III→II inversion.

appeared to pass through a maximum and began to decrease, the rate of decrease varying considerably with the experimental conditions. In many cases an actual contraction of the specimens was observed as indicated by the typical curves given in Figs. 1 and 2. The latter gives the length—temperature curves for two sets of measurements in which the specimens were under the load of the upper interferometer plate alone (6 grams). Fig. 2a shows the results for a run in which heating was stopped just short of the inversion and indicates that there was a permanent contraction represented by the length Δl_c, which correspond to 0.30 percent of the length at 20°. In the run shown in Fig. 2b, however, the heating was stopped just as the inversion started (see inset); after cooling to 500° the temperature was again raised to that of the inversion. In this case the apparent irreversible shrinkage was 0.20 percent of the length at 20°.

Although there was little doubt that these permanent changes in length were due to softening or shifting of crystallites in the aggregate it seemed desirable to demonstrate it beyond question, and at the same time to determine whether or not the shrinkage could be reduced or eliminated, by observing the expansion of the same specimens during successive heatings under load. Accordingly, a brass ring weighing 57 grams was placed on the upper plate of the interferometer, bringing the total load to 63 grams. The results for three successive runs, given in Fig. 1, show that on first heating the contraction between 500° and the inversion was very nearly as large as the total increase in length between 20° and 500°; and that on the succeeding runs the shrinkage was much less, as was expected. Since it was not possible to obtain reproducible data from 450° to the inversion point, an extrapolation was made from 400°C to 585°C based on a quadratic equation representing the points below 400°C.

Although the data below 400° showed a reasonable consistency, a careful examination of the individual runs revealed that in every case the length-temperature curve was not strictly a smooth curve but showed an irregular waviness which was not reproducible and which was greater in some cases than in others. In order to eliminate the effect of these undulations all the observations were plotted on a large scale and averaged graphically by drawing a smooth curve through them. That this correction was a very slight one is evident from Fig. 1 which shows how nearly the experimental points fall on the curve below 400°C.

Values of the expansion taken from this smooth curve were used by Goranson and Kracek[2] to derive a least-square quadratic for the volume as a function of temperature on the assumption that the specimens were aggregates of randomly-oriented grains. Their equation is:

$$v-v_{20}=v_{20}[53.194(t-20)10^{-6}+41.5(t-20)^2 10^{-9}].$$

(The equation as printed in their paper erroneously gives the coefficient of the term containing $(t-20)^2$ as 41.5×10^{-8} instead of 10^{-9}.) The corresponding equations for α_m, the mean linear expansion coefficient between 20° and $t°$, for α_t the instantaneous linear expansion coefficient at $t°$, and for $\Delta l/l_{20}$ the increase in length per unit length at 20° are, respectively:

$$\alpha_m=17.73\times10^{-6}+13.83(t-20)\times10^{-9},$$
$$\alpha_t=17.73\times10^{-6}+27.66(t-20)\times10^{-9},$$
$$\Delta l/l_{20}=17.73(t-20)\times10^{-6}+13.83(t-20)^2\times10^{-9}.$$

As a further check on the values of the instantaneous coefficient, the slope of the several length-temperature curves at several temperatures was determined by means of an optical "tangent-meter." Considering the difficulty involved in obtaining high precision with this instrument on a slightly wavy curve the results are in satisfactory agreement with those given by the equation. In two runs, however, the coefficients were slightly greater than in the others although the variation with temperature was substantially the same in all cases. A similar displacement has been observed in crystalline aggregates of substances which have a highly anisotropic expansion, such as polycrystalline zinc, which suggests that the thermal expansion of single-crystal Na_2WO_4 may vary considerably in different orientations.

Crystal Inversions

The transition from III to II at 585° is accompanied by such an extraordinarily large change in volume, and therefore in length, that in most cases the relative height of the specimens was altered to an extent which spoiled the fringes and prevented further observation. This difficulty was in some measure overcome by cutting down the size of the specimens or by loading the upper plate as previously described, so that three runs were finally obtained in which it was possible to follow the expansion above the inversion, and two of these were carried through it again on cooling. A curve showing the linear expansion *versus* temperature for one of these runs is given in Fig. 3.

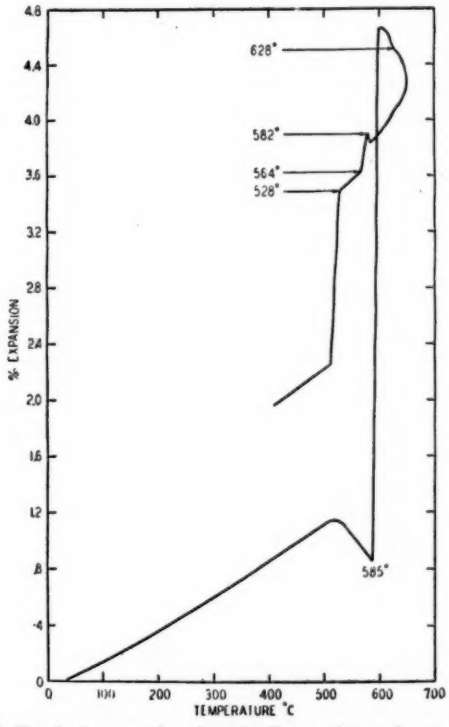

FIG. 3. Typical curve showing the linear thermal expansion of Na_2WO_4 on heating and on cooling.

The temperature at which the III to II inversion starts, as determined from all the observations which were carried to this point, is 585°±2°C, which is in good agreement with the value 587.6° observed by Goranson and Kracek. The transition II to I found at 588.8° by Goranson and Kracek was not detected on heating because it is masked by the transformation III to II, which at the rate of heating of 3°C per minute, is still going on. In one run, however, the rate of passage of the fringes was appreciably less at 590° than either above or below this temperature, which may be an indication of the occurrence of the transformation II→I. The cooling curve, which is discussed below, indicates, however, that both transformations must have occurred.

In every case the specimens contracted after the transformation had apparently been com-

pleted (see Fig. 3) but this shrinkage was irreversible and was probably due to a softening or settling of the aggregate after the disturbance during the inversion. In the three cases in which heating was carried above the transitions the maximum temperature did not exceed 635° because it was considered inadvisable to carry the samples too close to their melting point (695.5°). In two cases a faint but definite irregularity was found at 628°. Since this temperature coincides with that of the eutectic in the system $Na_2WO_4 - Na_2W_2O_7$ as reported by Hoermann[3] it is likely that the "dip" is associated with the presence of a trace of excess WO_3.

In the two runs from which satisfactory cooling curves were obtained a small but definite expansion characterizing the transition I to II was observed close to 582°. This temperature is lower than that found by Goranson and Kracek for equilibrium and indicates that with a rate of cooling of 3° to 4°C per minute the transformation undercools approximately 6°.

On further cooling, there is a rather rapid shrinkage followed by a contraction which is presumably that of the reversible expansion of Na_2WO_4 II. Unfortunately the results in this range are not very reproducible and are not suitable for deriving a precise coefficient. About all that can be said is that α_l for Na_2WO_4 II in the neighborhood of 550°C appears to be much larger, perhaps almost twice as large as α_l for Na_2WO_4 III in the same temperature range. The transformation II to III did not occur until the specimens had cooled to approximately 525°, indicating that at a rate of cooling of 3°C per minute this transition undercools by 60°C. In no case was the total contraction on cooling as great as the expansion at 585° on heating, but this behavior is generally observed in crystalline aggregates of anisotropic materials.[4]

Length and Volume Change at the Inversions

Three measurements were made of $\Delta l/l_{20}$ at the III to II inversion on heating, namely, 3.75, 4.30 and 5.63 percent. Of these the last is believed to be the best for two reasons: (1) This run was the last of the three in which the brass ring was used to weight the upper plate and the specimens seemed to be the most compact of any examined; (2) in counting a large number of fringes passing the reference mark rapidly the observer is more likely to miss a few than to count too many, hence the highest value of $\Delta l/l_{20}$ is the most trustworthy. We have accordingly selected 5.63 as the best value, keeping in mind that even this may be somewhat low. The corresponding volume increase is 17.4 percent, which, so far as we are aware is the largest increase yet reported at a solid transition. By using Goranson and Kracek's value of 0.194 cm³ per gram for the specific volume of Na_2WO_4 III at 20°, the increase in volume at the inversion is 0.034 cm³ per gram, which is in satisfactory agreement with the value of 0.035 cm³ per gram calculated by Goranson and Kracek from the effect of pressure on the transition temperature.

Both measurements of $\Delta l/l_{20}$ accompanying the transformation I to II on cooling, showed an increase of 0.04 percent, which, assuming random orientation of the grains, corresponds to a volume change of 0.12 percent or 0.00023 cm³ per gram. Combining this result with the heat of transition obtained by Goranson and Kracek, the change in transition temperature with pressure calculated by means of the Clausius-Clapeyron equation is approximately -0.0014 degree per bar. This appears to be close to the limit of error of Goranson and Kracek's measurements and explains why they observed no change in the inversion temperature with pressure.

The relatively large undercooling of the transition II to III at a rate of 3° per min. suggested that rapid cooling might preserve form II to room temperature and thus make possible a determination of its optical properties. An attempt to do this has been made by the usual method of quenching into mercury. One procedure employed was to heat the tungstate above its melting point, cool it in the furnace at a rate of approximately 3° per min. to 570°C, and then quench; another was to quench the salt directly from the melt. In each case the optical properties of the quenched samples, for the determination of which we are indebted to Dr. O. Andersen, corresponded to those given by Goranson and Kracek for Na_2WO_4 III, indicating that the usual quenching technique does not provide sufficiently rapid cooling.

[3] Hoermann, Zeits. f. anorg. allgem. Chemie **177**, 145 (1928).

[4] See, for example, Sosman, *The Properties of Silica* (Chemical Catalog Co., New York, 1927), p. 388.

Products and Processes of Ionization in Methyl Chloride as Determined by a Mass Spectrometer

S. H. BAUER* AND T. R. HOGNESS, *George Herbert Jones Laboratory, University of Chicago*

(Received August 30, 1935)

The following ions were found to be produced in methyl chloride as primary products: CH_3Cl^+, CH_3^+, CCl^+, CH_2^+, Cl^+, HCl^+, CH^+ and C^+—listed in order of decreasing intensity. Small concentrations of the H^+ ion were also detected. This latter peak was not investigated completely. The appearance potentials for the CH_3Cl^+, CH_3^+ and Cl^+ ions are 11.0, 14.7 and 26 volts, respectively.

I.

MASS spectrographic studies of organic compounds in which the ions were generated by electrons of known energy, have not been very extensive. From among the gases thus far studied,[1] the appearance potentials for the ions formed in acetylene[2] and methane[3] only have been determined. Since under most circumstances of ionization many different kinds of fragments appear as a result of primary processes, it is evident that unless these potentials are known, the mechanisms of dissociation and ionization must remain uninterpreted. The work reported in this paper was initiated with the hope that the results obtained would be of some value in giving an estimate for the heat of reaction of

$$CH_3Cl = CH_3 + Cl.$$

Such an estimate could only be obtained from a knowledge of the energy necessary for the reaction

$$CH_3Cl = CH_3 + Cl^+ + e^-.$$

This process does not occur to any appreciable extent when methyl chloride is bombarded by electrons.

II.

The apparatus constructed was of the Dempster type as modified by Hogness and Lunn and somewhat further in the present investigation.[4] A section is shown in Fig. 1. A flow system, regulated by means of a low pressure variable gas leak, was set up through the ionization chamber while the pressures in the other compartments were maintained at a low value by means of high speed mercury diffusion pumps.[5] The following details may be of interest.

(1) The radius of curvature of the path of the ions in the magnetic field was 6.35 cm. The collimating slits S_2 and S_3 as well as the receiving slit in front of the collecting plate (not shown) were all 0.025 cm. Further, the pressures in the chambers 3 and 4 were very low (about 10^{-5} and 10^{-6}, respectively) and the refocusing fairly good. Hence, the resolution was such as to permit easily the detection of differences of mass of the order $\Delta m/m = 0.006$. This can be ascertained from Fig. 2 which is a plot of one of the earlier runs.[6]

(2) A Compton electrometer (sensitivity 40,000 to 2000 deflections per volt), whose insulated quadrants were grounded through an "iodine in benzene" resistance[7] of 4×10^{11} ohms, was used as the current measuring device.

(3) The slit S_1 had the dimensions 0.2×0.6 cm. This size was found necessary in order that a

---

* Present address: Gates Chemical Laboratory, California Institute of Technology.

[1] R. Conrad and co-workers, Trans. Faraday Soc. **30**, 215 (1934); E. G. Linder and A. P. Davis, J. Phys. Chem. **35**, 3649 (1931). The above authors used an electric discharge for their ion source. In the following work controlled electron excitation was employed: H. R. Stewart and A. R. Olson, J. Am. Chem. Soc. **53**, 1236 (1931), studied propane and butane; E. G. Linder, Phys. Rev. **41**, 149 (1932), benzene; J. Chem. Phys. **1**, 129 (1933), octane.

[2] J. T. Tate, P. T. Smith and A. L. Vaughan, Phys. Rev. **43**, 1054A (1933); Phys. Rev. **48**, 525 (1935).

[3] T. R. Hogness and H. M. Kvalnes, Phys. Rev. **32**, 942 (1928); J. H. Hipple and W. Bleakney, Phys. Rev. **47**, 802A (1935).

[4] T. R. Hogness and E. G. Lunn, Phys. Rev. **26**, 44 (1925) and subsequent work. The following authors used analyzers modified along lines similar to the present apparatus: H. Kallmann and B. Rosen, Zeits. f. Physik **64**, 806 (1930); O. Luhr, Phys. Rev. **44**, 459 (1933).

[5] Following the design of T. E. Phipps, private communication.

[6] The peaks at 40 : 32 : 29.4, 28 : 18 and 16 are due, respectively, to A^+ : O_2^+ : N_2^+ : H_2O^+ and O^+ which were present in the apparatus before the methyl chloride was put in.

[7] Rollefson, Science **60**, 226 (1924).

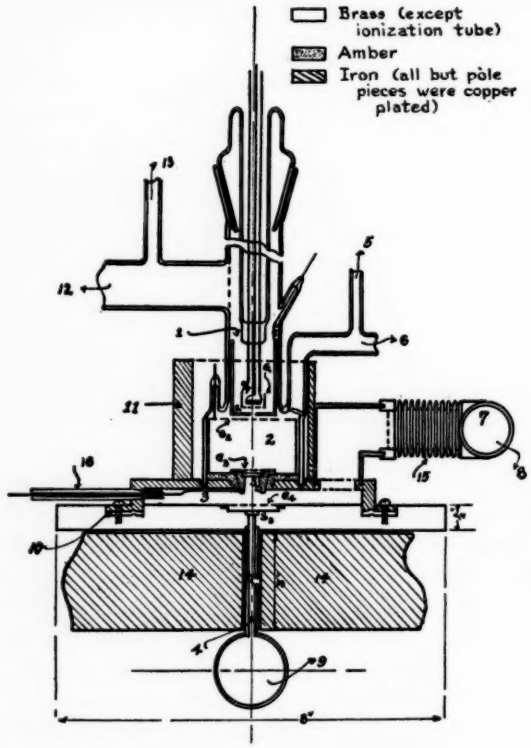

FIG. 1. Side view of the apparatus.

(1) Filament chamber
(2) Ionization chamber
(4) Deflection chamber
(5) To leak No. 1
(6), (8), (9), (13) To valves and McLeod gauge
(7) Metal to glass ground joint
(8) To leak No. 2; also to pump No. 2
(9) To charcoal trap and pump No. 3
(10) Rubber gasket
(11) Laminated shielding
(12) To pump No. 1
(14) Pole pieces
(15) Bendix
(16) Pyrex

sufficient number of electrons would be permitted to enter compartment 2. Nevertheless, because of an efficient pumping system, the pressure in the filament chamber (1) was maintained at 1/20 of that in the ionization chamber. Since by experiment it was determined that the identical peaks were obtained with and without such a differential pumping arrangement in spite of the fact that dissociation on the surface of the filament was found in the latter case, this differential pressure was deemed sufficient.

(4) The performance of the apparatus was satisfactory except for one feature—the presence of ghost peaks at 0.04 to 0.05 mass unit above the primary ones, as shown by 54, 29.4 and 15.7 in Fig. 2 and by 2.1 in Fig. 3. This was very troublesome at first, when both peaks appeared to have about the same intensity. After a series of modifications in the slit system the magnitude of the ghost was reduced to a small value (but could not be eliminated entirely) so that only the large peaks exhibit this structure. The doubling may have been caused either by the peculiar electric field around S_2 or by reflection of the ion beam on some part of the walls of the deflection chamber (4). Since the ghost peaks did not interfere with the experiments while the elimination of both these possibilities would have necessitated the reconstruction of the entire apparatus, no further alterations were made at this time.

III.

From Figs. 2 and 3 it is evident that all the possible positive ions which may result from the dissociation of methyl chloride, except CH_2Cl^+ and $CHCl^+$, appeared. These may have been present in such small quantities as to be entirely obscured by the large peaks at 52 and 50. The H^+ peak due to methyl chloride (Fig. 3) was obtained with 45 v electrons at a pressure of 2×10^{-3} mm of Hg in the ionization chamber. Because of its small intensity and the difficulty of working in this mass range when all the rest of the ions were in an entirely different portion of the scale, this peak was investigated no further. There is no doubt that its appearance potential is quite high (perhaps around 30 v).[8] All the other ions were generated as primary products, as is indicated by the curves in Fig. 4. Their relative intensities depended to some extent on the pressure; roughly in the manner given in Table I. Since none of the curves in Fig. 4 extrapolate to zero intensity for zero pressure, these ions are the results of primary dissociations by electron impact. Multiply charged ions were not observed and would hardly have been expected at low voltages used (33.0−45.0) for the bombarding electrons.

TABLE I.

Ion	(0.08–6.5) $\times10^{-3}$ mm	Ion	(0.08–6.5) $\times10^{-3}$ mm
CH_3Cl^+	56.0−31.0	Cl^+	4.0−8.0
CH_3^+	24.0−45.0	HCl^+	3.0−3.0
CCl^+	5.5− 6.0	CH^+	2.2−2.0
CH_2^+	4.2− 4.3	C^+	1.0−0.6

[8] In methane, Hipple and Bleakney (reference 3) give for the appearance potentials of CH_4^+, CH_3^+, CH_2^+, CH^+, C^+, and H^+ the values 13.7, 14.7, 15.7, 23, 27 and 31, respectively. In methyl chloride one would expect quite similar potentials for the last four ions.

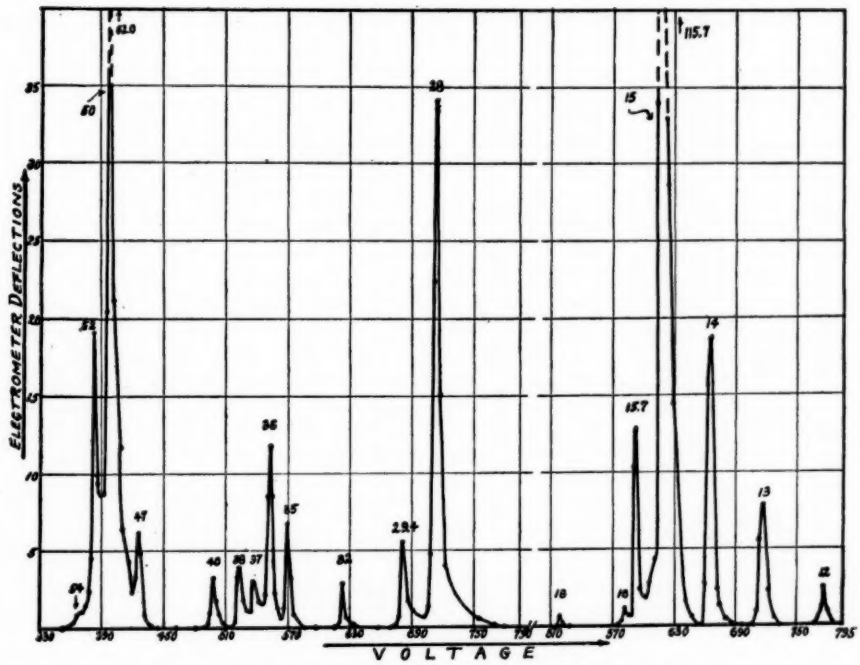

FIG. 2. Mass spectrum of methyl chloride plus residual air.

The appearance potentials for three of the ions were determined. They are: CH_3Cl^+ 11.0±0.5; CH_3^+ 14.7±0.3; Cl^+ 26.5±1. The value obtained for the ionization potential of methyl chloride may be compared with the one given by T. N. Jewitt[9] (10.7 v) who used molecular ray technique with a Kingdon cage arrangement for the determination, and with the spectroscopic values of W. C. Price[10] (11.17 and 11.25±0.01 v) who found for methyl chloride two electronic series of absorption bands in the far ultraviolet, going respectively to the above limits. The series conformed closely to a Rydberg formula.

Particular efforts were extended to obtain an accurate estimate of the appearance potential of the CH_3^+. The value quoted above is the mean of seven determinations carried out under various conditions. The critical voltages for the others were not considered significant enough to warrant the trouble of the determination since the processes of their formation is complicated and the fragments come off with considerable excitational energy. Thus, one can predict these potentials to be relatively high.[11]

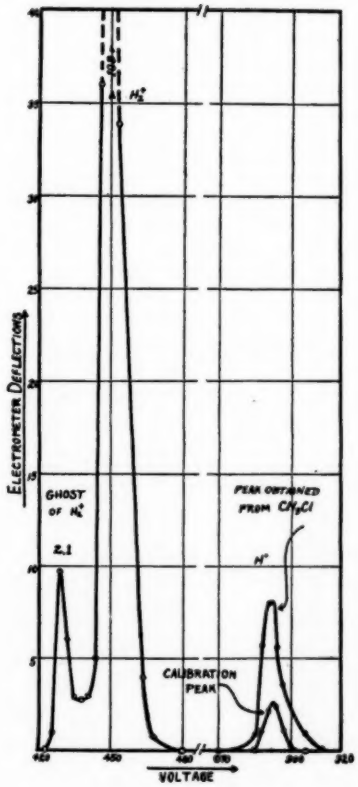

FIG. 3. The H^+ peak of methyl chloride. Hydrogen is used as a calibrating gas.

[9] T. N. Jewitt, Phys. Rev. 46, 616 (1934).
[10] W. C. Price, Phys. Rev. 47, 510L (1935).
[11] See Note 8. In general, for a single substance, a rough idea of the relative magnitude of the appearance potentials

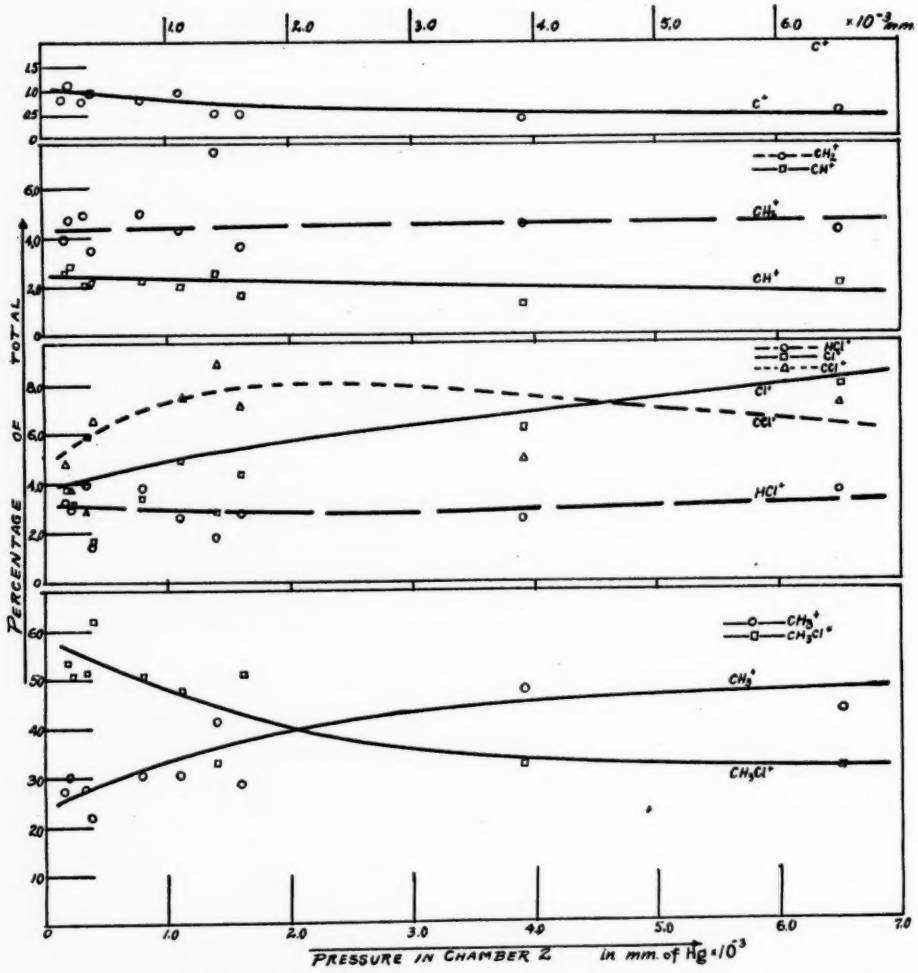

FIG. 4. Variation of the relative intensities of the ion peaks with the pressure. Note change in scale in the three upper sections of the plot.

Details of the experimental procedure

(1) The methyl chloride used was condensed from a tank (Ohio Chemical Company specifications give it as 99.5 percent pure) by liquid air. The sample was then kept at its melting point while pumping from it continued until its volume was reduced to about 3/4 of its original value thus insuring removal of any contaminating hydrogen chloride and other gases of low boiling point. The remainder was then fractionally distilled in vacuum. Only the middle fraction was used.

(2) In the determinations of the variation of intensity with the pressure the necessary integrations were accomplished by tracing all the curves plotted on the same scale on a uniform heavy grade of drawing paper, cutting out the individual peaks and weighing them. A large error is inherent in any form of integration of individual narrow, overlapping peaks, particularly when they are unsymmetrical so that their resolution is very uncertain. Hence the data check as well as can be expected. When these runs were made the electron emission and voltage were kept constant at 4.0 ma and 45.0 v, respectively.

(3) Before or after each appearance potential determination, a calibration of the apparatus was made using argon as the calibrating gas. The relative pressures of the two gases were adjusted so that under the identical conditions the argon

for the different ions can be obtained from the relative intensities of the peaks when the gas is bombarded with electrons whose velocities are well above the highest of the potentials.

peak and the one being investigated had the same height (±5 percent) when the incident electrons were accelerated to 45 volts. This potential was then decreased and the extrapolation made in the usual manner.

IV.

The ionization reaction requiring the minimum energy may be written

$$CH_3Cl = CH_3Cl^+ + e^- + 11.2 \text{ ev}$$

and interpreted, according to R. S. Mulliken,[12] as involving the removal of one of four $3p\pi_{Cl}$ electrons (nonbonding), leaving the molecule in a ^2E state. This explains the presence of two Rydberg series limits in the work of W. C. Price[10] corresponding to the doublet of levels of the final configuration. Obviously the mass spectrograph is too crude an instrument to distinguish the difference between the two.

As was intimated in the introduction, it had been hoped that the products of the reaction

$$CH_3Cl = CH_3 + Cl^+ + e^-$$

should be produced without involving considerable excitational energy. If that were so, the bonding energy of C−Cl could be determined since the ionization potential of Cl is known (12.96 v). This would require the appearance potential of Cl to be in the vicinity of 18 volts.[13] The experimental value 26.5 v indicates that not only was the hope far from being realized but that the reaction yielding Cl^+ does not proceed unless enough energy is supplied to be sufficient to produce other fragments.

In the paper referred to above, Mulliken estimated the energy of removal of one of the bonding $[\sigma a_1]$ electrons in methyl iodide to be somewhat less than 14.4 ev. The corresponding value for methyl chloride would not differ much; it would presumably be little above that for the iodide. It is clear that such a removal may lead to the dissociation

$$CH_3Cl = CH_3^+ + Cl + e^- \quad (+ \text{ excitational or kinetic energy}). \quad (c)$$

We shall therefore assume that the experimental appearance potential of 14.7 ev for the CH_3^+ ion is the energy necessary for the above reaction.

The ionization process in methane[14] resulting in the formation of CH_3^+ has been interpreted by Mulliken.[15] The revised appearance potential value of Hipple and Bleakney[8] indicates that the reaction

$$CH_4 = CH_3^+ + H + e^- \quad (d)$$

may be brought about by electron bombardment without imparting to the fragments more than about 0.5 ev excitational or kinetic energy. This appears reasonable in view of the estimated ionization potential of CH_3[16] and the value chosen for the energy of breaking the initial C−H bond. On the other hand, our results indicate (if the value chosen for the C−Cl bond is correct)

[12] R. S. Mulliken, Phys. Rev. **47**, 413 (1935).

[13] The available data on the heats of combustion of methane and methyl chloride gave the values for the bonding energies of C−H and C−Cl as 4.11 and 3.14 e.v., respectively. The sources are: *Landolt-Börnstein Tables*, fifth edition, original volume. W. Jevons, *Report on Band-Spectra of Diatomic Molecules* (Cambridge, 1932); G. B. Kistiakowsky and H. Gershinowitz, J. Chem. Phys. **1**, 432 (1933). The corresponding estimates given by L. Pauling, J. Am. Chem. Soc. **54**, 3570 (1930); L. Pauling and J. Sherman, J. Chem. Phys. **1**, 606 (1933) are consistently approximately 0.25 ev higher per bond due to the fact that these authors arbitrarily added one volt to the experimental heat of sublimation of carbon to allow for the difference between the ground ^3P state and the excited ^5S state (plus others) which take part in bond formation.

The assumption of equal bonding energies for all C−H bonds in methane or methyl chloride may be misleading if applied to reactions such as

$$CH_4 = CH_3 + H \quad \text{or} \quad CH_3Cl = CH_3 + Cl.$$

The energy of reaction for these may be far different from the average bond energy. According to Mulliken, this assumption may hold fairly well for

$$CH_{4(\text{normal state})} = CH_{3(\text{"valence state"})} + H \quad (a)$$

$$CH_{3(\text{"valence state"})} = CH_{2(\text{"valence state"})} + H, \text{ etc.} \cdots \quad (b)$$

where "valence state" (i.e., tetravalent) is perhaps 7 or 8 volts above the normal state of C atom. Since it is probable that the normal state of CH_3 is nearly the same as the valence state necessary for the reaction $CH_3 + H = CH_4$, the process (a) which would require about 6 volts, may be nearly identical with

$$CH_{4(\text{normal state})} = CH_{3(\text{normal state})} + H.$$

We shall therefore take for the energy of breaking the initial C−H bond at 6 volts and for the C−Cl bond, one electron volt less.

[14] Hogness and Kvalnes, reference 3.

[15] R. S. Mulliken, J. Chem. Phys. **1**, 492 (1933).

[16] 8.0 to 8.5 ev as given R. S. Mulliken, reference 15; also, J. Chem. Phys. **3**, 521 (1935). This estimate is based on the following consideration. One can write for the configurations of

NH_2: $1s^2[sa_1]^2[\pi e]^4[\sigma a_1]^2$, $^1A_1$ I.P. of $[\sigma a_1] = 11.1$ ev
CH_3: $1s^2[sa_1]^2[\pi e]^4[\sigma a_1]$, $^2A_1$.

In the latter case, the ionization potential for the same type of electron should be 2.5 to 3 ev less than the former due to the smaller nuclear charge.

that the excitational energy in the corresponding reaction (c) amounts to as much as 1.5 ev.

Further comparison with thermal data may be made. A simple calculation[17] will show that the energy for the process

$$CH_4+Cl=CH_3Cl+H \text{ is } 0.97 \text{ ev.}$$

From the mass spectrometer experiments on methane and methyl chloride one can write:

For Eq. (d)

$$\Delta E=\begin{cases}15.5 \text{ ev (Hogness and Kvalnes)}\\ 14.7 \text{ ev (Hipple and Bleakney)}\end{cases}$$

For Eq. (c)

$$\Delta E=14.7 \text{ ev (Bauer and Hogness)}$$

[17] See reference 13 for sources of data. The energy of this reaction, which involves a difference between the energies of formation of methane and methyl chloride is independent of the value chosen for the heat of sublimation of carbon or of any assumptions regarding the relative values of bonding energies, and hence is much more reliable than any of the calculations referred to in 13.

resulting in

$$CH_4+Cl=CH_3Cl+H \qquad 0.8 \text{ or } 0.0 \text{ ev} \quad (e)$$

depending on the value chosen for the energy of reaction (d).

The obvious conclusions are: (1) If the reactions (c) and (d) *are analogous* (it is not essential that they be as simple as written; it is only necessary that the same amount of excitational energy occur in both), the Eq. (e) may rightfully be deduced. Then, it is clear, either the second value of (d) or the one given for (c) is incorrect. Or, as was suggested in the preceding paragraph, (2) the first value of (d) may be too high and the reactions are not entirely analogous. There is then no justification for (e) since the products in (c) are excited to an extent of approximately one volt more than in (d).

The authors wish to thank Professor Mulliken for a number of helpful discussions pertaining to questions presented in section IV.

NOVEMBER, 1935 JOURNAL OF CHEMICAL PHYSICS VOLUME 3

Monomolecular Films of Molecules Which Lie Flat on the Surface of Water

I. Surface Pressures and Potentials of Films of Long Molecules: Polymers of ω-Hydroxy Decanoic Acid

WILLIAM D. HARKINS, EVERETT F. CARMAN AND HERMAN E. RIES, JR., *University of Chicago*

(Received September 3, 1935)

Film pressures and surface potentials have been measured for a series of linear polymers of ω-hydroxy decanoic acid, ranging in molecular weight from 780 to 25,200. The molecules are oriented parallel to the surface. An improved form of the apparatus of Harkins and Fischer was used. The chief modification in the procedure was the use of two radioactive polonium electrodes over the film. The pressure-area relations show that the area per molecule in the condensed films is nearly proportional to the molecular weight and that the compressibility of the films is large. The film density is found to be lowest for the polymers of smallest molecular weight. The films are not very sensitive to changes in hydrogen ion concentration, but on changing from an acid to an alkaline substrate the films in the expanded state give higher molecular areas at given pressures, and the pressures for film collapse are considerably higher. Dimensions of the molecules are calculated and a complete table of mean values is included. The vertical cross section of the molecules varies between 19.4 and 19.9 sq. A or is nearly the same as the horizontal cross section (20.5) of vertically oriented molecules such as stearic acid. Some differences between films with perpendicular orientation to the surface and those with parallel orientation are tabulated. The surface potentials of the polymer films rise to between 400 and 450 mv, although the surface density of the polar groups is only 1/3 to 2/5 that of stearic acid type films, which also give potentials of about 400 mv. The contribution of each polar group is, therefore, considerably greater than that of the dipole of the vertically oriented stearic acid molecule. The surface potential of a condensed film was found to increase about 13 percent less rapidly than the surface density of the dipoles.

I. Introduction

WHILE extensive researches have been carried out with substances whose molecules when in a film on water exhibit an orientation perpendicular, or nearly perpendicular, to the plane of the surface, very little work has been done with molecules which give an orientation parallel to the surface. For this to occur it is only necessary, as pointed out in 1916 by Harkins, Davies and Clark[1] that the polar groups in an organic molecule have a proper symmetrical distribution in the molecule. The best distribution is that of the type exhibited by the linear polymers of ω-hydroxy decanoic acid of the formula $HO[(CH_2)_9COO]_xH$ as supplied to us by Drs. W. H. Carothers, E. O. Kraemer and F. J. van Natta.[2] These polymers, of molecular weights from 780 to 25,200, and values of x from approximately 4 to 148, consist of unbranched chains, and with a polar group at every tenth carbon atom.

It was, therefore, assumed, before the experimental work was begun, that these molecules would lie flat on the surface, and the data obtained in the investigation show that this is true.

II. Filmometer

The apparatus used for this work was an improved form of that of Harkins and Fischer.[3] The changes in the apparatus that seemed to contribute to greater accuracy in the work were chiefly as follows:

(1) Two independent radioactive polonium electrodes were used in such a way as to allow movement in any direction. This made it possible to determine almost simultaneously the potential at two different locations. The second electrode was originally designed to test for leakage past the float, but it was found to be of value when used over the film with the first electrode, since it gives a definite indication of the homogeneity or nonhomogeneity of the film. At the same time it serves as a valuable check on the potential measurements after the film has become uniform.

(2) A suspended carrier was used to raise the entire film balance above the trough, as in the work of Gorter. This arrangement permits sweeping the full length of the tray. If the float is raised and lowered several times during this full length sweeping, the operation amounts to a final washing of the float immediately before the experiment is begun.

(3) Special barriers were constructed for use in sweeping close to the float of the balance. These barriers are so shaped that they may be brought into very close proximity to the float and its delicate gold foils. They are used after the float apparatus has been lowered into place and clamped in position.

(4) The float apparatus is clamped securely to the beveled sides of the trough with a wedge-screw device.

(5) Brass weights or compression springs are used on the glass barrier during the compression of the film to insure a firm contact between the paraffined surfaces of the barrier and the edges of the trough.

Redistilled chloroform was used as the solvent in preparing dilute solutions of the polymers.

III. Pressure-Area Relations

The pressure-area relations of nine linear polymers are given in Fig. 1.

The films are of the "expanded" type at pressures below about 1.3 dynes, and condensed at higher pressures.

The area (a) per molecule in the condensed films is found to be nearly proportional to the molecular weight at any given film pressure. Fig. 2 shows that this is true for the areas extrapolated to zero pressure.

The compressibility of the condensed films is very large, since the value of $[(a_0-a_1)/a_0]/(f_1-f_0)$ lies between 0.040 and 0.053, and is almost independent of molecular size. Similar values for vertically oriented molecules are in general only one-tenth to one-sixtieth as large.

Because of this high compressibility, the accuracy and reproducibility of the work on these films is not expected to be as high as for those which exhibit the other type of orientation,

[1] Harkins, Davies and Clark, J. Am. Chem. Soc. **39**, 584 (1917).
[2] Kraemer and van Natta, J. Phys. Chem. **36**, 3175 (1932). Carothers and van Natta, J. Am. Chem. Soc. **55**, 4714 (1933).
[3] Harkins and Fischer, J. Chem. Phys. **1**, 852 (1933).

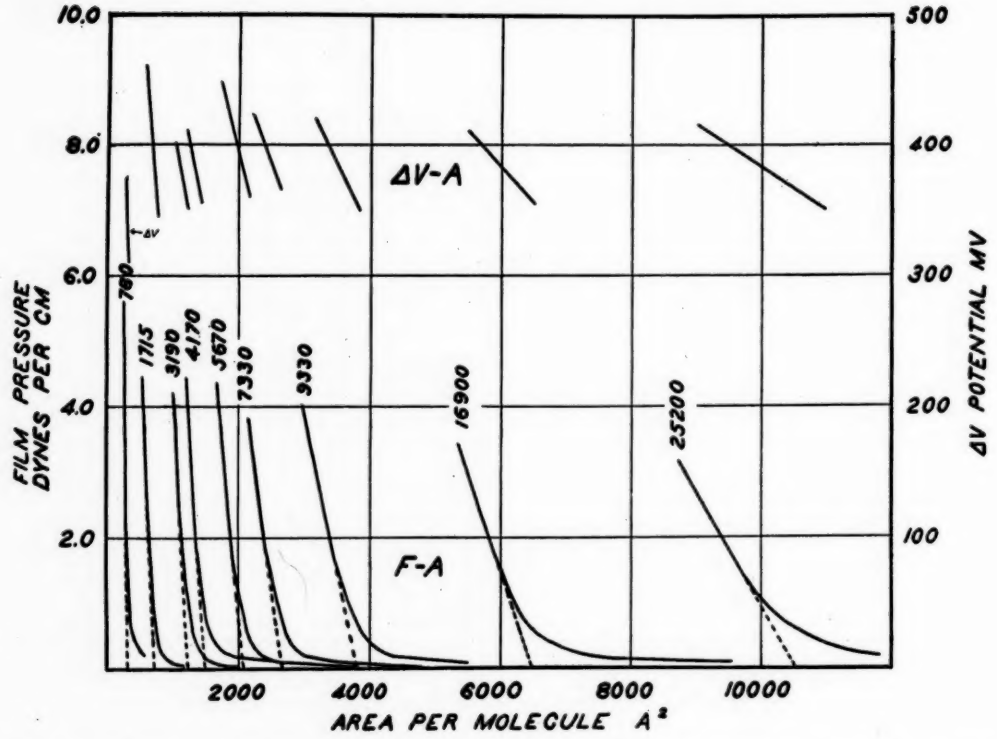

FIG. 1. Exhibits the fundamental relations of films of molecules which lie flat on the surface of water. Film pressure (f) and surface potential relations of linear polymers of molecular weights from 780 to 25,200.

as commonly investigated. However, Figs. 3 to 8, which represent the data, show that when the conditions are identical, a considerable degree of accuracy is attained. It should be noted that the areas are affected by the pH of the solution, especially at low pressures.

While the concentration of material in the film is at any given pressure not highly dependent on molecular size, the lowest density is found for the smallest molecules, those of molecular weight 780, and the highest film density for those of intermediate size (7330). This is shown in Table I.

TABLE I. *Density of films in units of 10^{-8} gram per sq. cm.*

MOLECULAR WEIGHT	DENSITY AT 3 DYNES PER CM PRESSURE	MOLECULAR WEIGHT	DENSITY AT 3 DYNES PER CM PRESSURE
780	4.5	16900	5.1
1715	4.6	5670	5.2
25200	4.7	4170	5.3
9330	4.8	7330	5.4
3190	4.9		

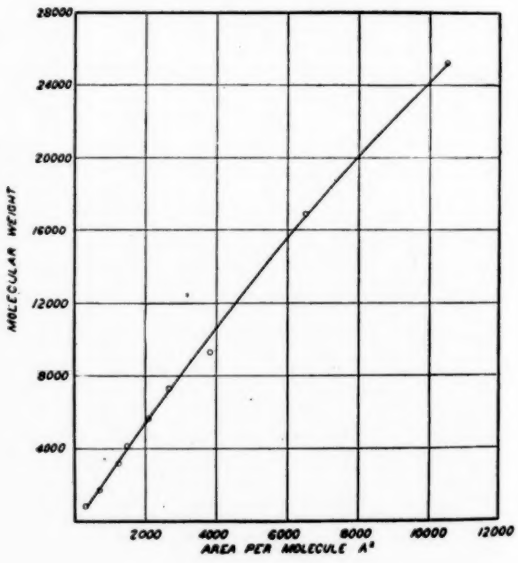

FIG. 2. Exhibits the nearly linear relation between molecular area at zero pressure and the molecular weight of a linear polymer.

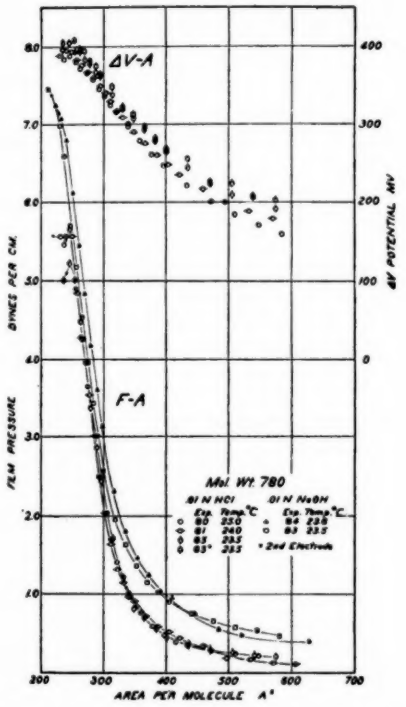

FIG. 3. Film pressure and surface potential relations of the polymer of molecular weight 780 on 0.01 N aqueous solutions of acid and base.

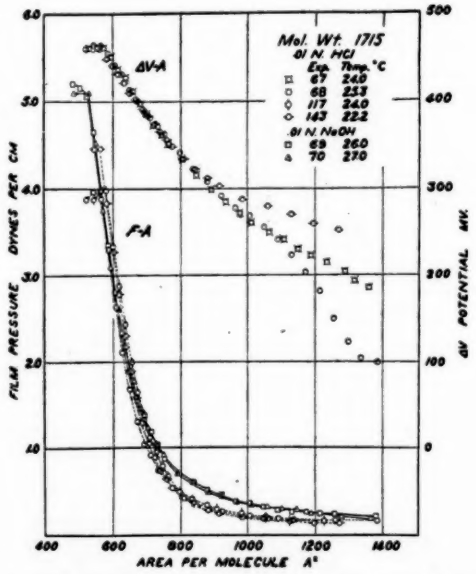

FIG. 4. Film pressure and potential for the polymer of molecular weight 1715.

It may be noted that the pressure-density curves for the condensed films are linear and nearly parallel (Fig. 9).

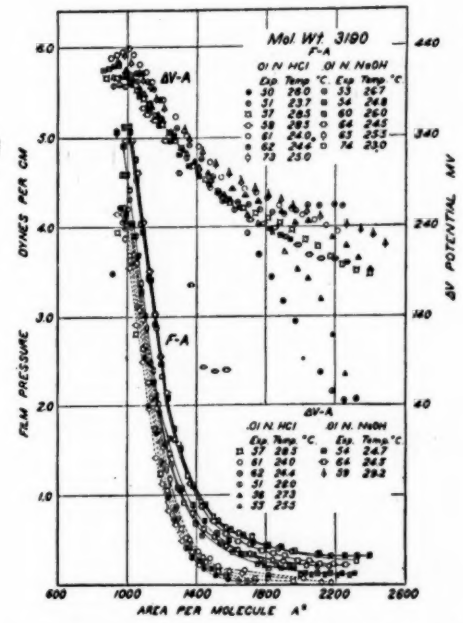

FIG. 5. Polymer of molecular weight 3190. Islands are prominent in the films at areas above 1800 sq. A.

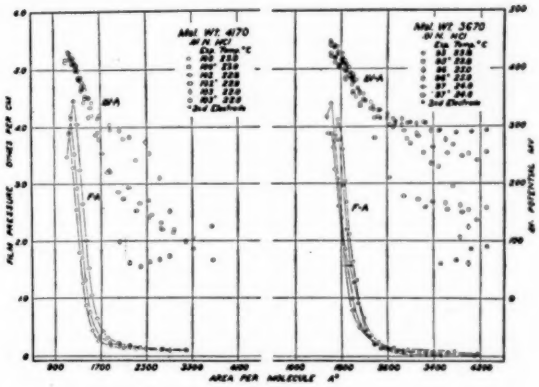

FIG. 6. Polymers of molecular weights 4170 and 5670. Exhibit a marked island effect at higher areas.

IV. EFFECTS OF ACIDS AND BASES

While these films are not extremely sensitive to a variation of the hydrogen ion concentration, two important differences are found.

The molecular area for the expanded film is higher for any given pressure when the aqueous substrate is alkaline with 0.01 molal sodium hydroxide than when acid with 0.01 molal hydrogen chloride.

The pressure of collapse is *much* higher on the alkaline than on the acid solutions: e.g., 7.5 dynes per cm as compared with 5.5 for the

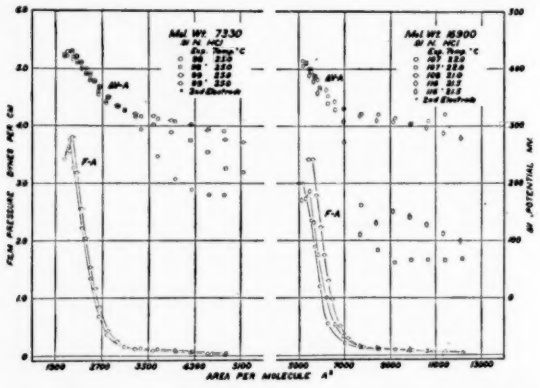

FIG. 7. Polymers of molecular weights 7330 and 16,900. For the latter the potential relations show the island effect at areas above 7000 sq. A.

polymer of M.W. 780; 5 as compared with 4 for M.W. 1715 and 3190; 4 as compared with 3 for M.W. 9330.

V. MOLECULAR DIMENSIONS

The volume of the molecule, as given in Table II, is obtained from the density. The length of the molecule is calculated from the atomic spacing in linear hydrocarbon derivatives as obtained from x-ray investigations. The apparent thickness of the film, columns 9, 10, and 11, is calculated on the basis of a layer of the same density as that of the solid compound. The area per molecule (cols. 5, 6, and 7) is obtained from the experimental values and Avogadro's number.

The width of the molecular space (cols. 12, 13, and 14) is of interest. At the maximum pressure, the film may be slightly folded, so the values at 3 dynes per cm will be considered. At this pressure, the width of the molecular space varies from 4.0 to 4.8A, with a mean value of 4.3. This distance agrees well with that found between linear hydrocarbons in crystals, or with the spacing in liquids, as revealed by x-rays.

If it be assumed that on compressing the film beyond zero extrapolated pressure, the distance between the chains remains constant, the actual distance between carboxyl groups in the same chain will decrease. At zero extrapolated area the average length per chain is 14.7A; at a pressure of three dynes the average distance between carboxyl groups is 12.6A, which amounts to a decrease of 2.1A. This decrease would cause the chain to bow since it is anchored to the surface at both ends by carboxyl groups. However, it is probable that the decrease in distance between adjacent chains is a more major effect than this type of buckling of the molecule.

The most prominent characteristics may be

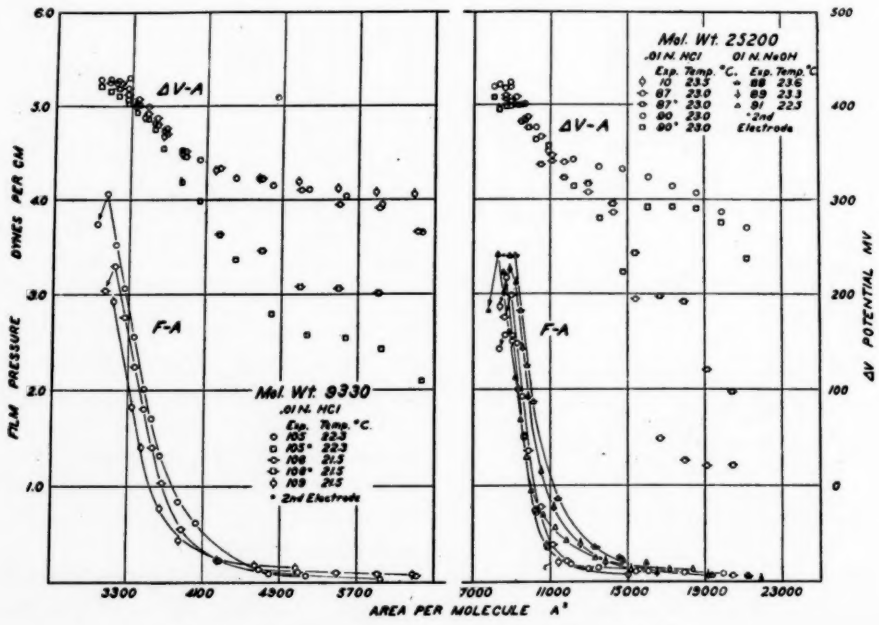

FIG. 8. Polymers of molecular weights 9330 and 25,200.

TABLE II. *Films of polymers of ω-hydroxy decanoic acid on water.*
Mean values at temperatures from 21.5 to 26.0°. Concentration of hydrogen chloride in the water 0.01 *M*
Columns 2 and 3 are taken mostly from the paper of Carothers and van Natta.

1	2	3	4	5	6	7	8	9	10	11	12	13	14	15	16
MOL. WT.	DENSITY d^{25}_4	LENGTH OF MOLECULE (A)	VOL. OF MOLECULE (cu. A)	AREA PER MOLECULE AT A FILM PRESSURE $f=0$	$f=3$	$f=$max.	MAXIMUM FORCE f_m	t=THICKNESS OF FILM AT A FILM PRESSURE $f=0$	$f=3.0$	$f=$ max.	d=WIDTH OF MOLECULAR SPACE AT $f=0$	$f=3.0$	$f=$ max.	$t\times d$ MOLECULAR CROSS SECT. AT 3 DYNES (sq. A)	COMPRESSIBILITY AT $f=0$
780	1.0957	60	1170	330	290	246	5.7	3.6	4.0	4.8	5.5	4.8	4.1	19.5	0.040
1715	1.0935	133	2590	700	604	556	4.5	3.7	4.3	4.7	5.3	4.5	4.2	19.4	.046
3190	1.0877	248	4840	1260	1080	970	4.2	3.9	4.5	5.0	5.1	4.4	3.9	19.6	.048
4170	1.0814	324	6360	1490	1300	1130	4.5	4.3	4.9	5.6	4.6	4.0	3.5	19.6	.043
5670	1.0751	440	8700	2050	1800	1688	4.4	4.2	4.8	5.2	4.7	4.1	3.8	19.7	.041
7330	1.0715	570	11330	2670	2277	2180	3.8	4.2	5.0	5.2	4.7	4.0	3.8	19.9	.049
9330	1.0668	730	14450	3800	3200	3000	4.0	3.8	4.5	4.8	5.2	4.4	4.1	19.8	.053
16900	1.0627	1320	26200	6440	5510	5270	3.4	4.1	4.8	5.0	4.9	4.2	4.0	19.9	.048
25200	1.0621	1970	39100	10430	8800	8700	3.2	3.8	4.4	4.5	5.3	4.5	4.4	19.9	.052

listed for a pressure of 3 dynes per cm unless otherwise stated,

Thickness of films from 4.0 to 5.0A.

Distance between centers of adjacent chains 4.0 to 4.8A. Apparent vertical cross section of molecule 19.4 to 19.9 sq. A, or nearly the same as the horizontal cross section (20.5) of molecules, such as stearic acid, oriented vertically. The area (a) per molecule in condensed films is nearly proportional to the molecular weight at any given film pressure (f).

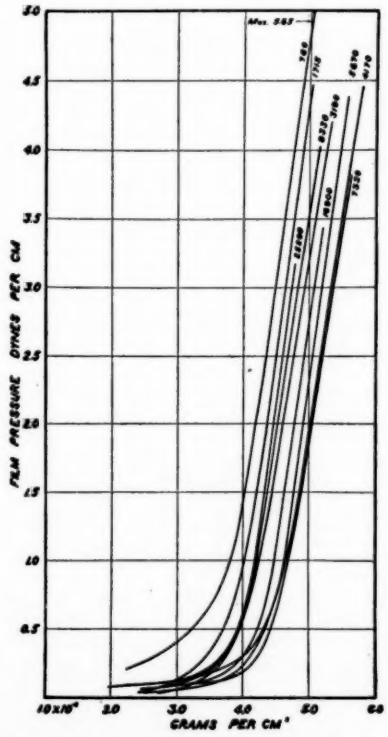

FIG. 9. Density of the films in grams per sq. cm$\times 10^{-8}$ as a function of the molecular weight and of the film pressure.

The molecular area of the compound of molecular weight 25,200 is 10,400 sq. A for zero pressure, or 8800 sq. A at 3 dynes per cm pressure. This is the largest area thus far found for any molecule.

At a pressure of 3 dynes per cm, the area per group of 10 carbon atoms $(CH_2)_9COO$ is a maximum of 65 for M.W. 780, a minimum of 53 for M.W. 4170 and 7330, and rises to 59 for 25,200 (Fig. 10).

VI. ORIENTATION OF THE MOLECULES

That the molecules in these films are oriented parallel to the plane of the surface is shown by the thinness of the condensed films, by the fact that the molecular area is proportional very

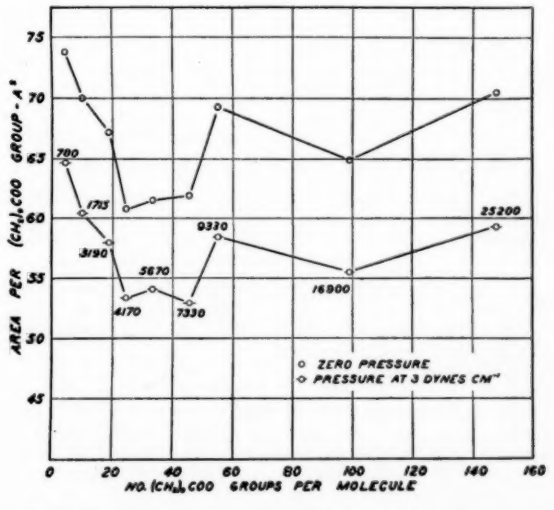

FIG. 10. Area per unit group $[(CH_2)_9COO]$ as a function of the number of unit groups in the molecule at a pressure of 3 dynes per cm and of zero dynes (extrapolated value).

TABLE III. *Properties of films with different orientations of the molecule.*

LONG AXIS VERTICAL	LONG AXIS HORIZONTAL
Molecular area independent of length	Molecular area increases with length
Withstand high pressures (to the order of 50 dynes per cm)	Collapse at low pressures (2 to 10 dynes)
Surface potential increases with length of molecules up to 18 carbon atoms	Surface potentials of the same order for long and short molecules
Compressibility decreases with increasing length of chain	Compressibility high and independent of length of molecules

nearly to the molecular weight, by the independence of the surface potential and the molecular weight, and by the agreement between the width of the molecular space, calculated on the hypothesis that the molecules lie flat and the molecular distances derived from x-ray measurements.

The differences in the properties exhibited by films with perpendicular and parallel orientations to the plane of the surface, are listed in Table III.

VII. SURFACE CONTACT POTENTIALS*

The Righi-Kelvin method for the determination of contact potentials of metals was found by Guyot and by Frumkin to give a contact potential between a metal and the surface of an aqueous solution. While this method did not give consistent results, it was suggested to Frumkin by Harkins that the difficulty did not lie in the method for the determination of the potential, but to variations in the film itself. The use of a combined film pressure apparatus and movable polonium coated electrodes has, as used by various investigators, shown this to be true.

Although the condensed films of the polymers of ω-hydroxy decanoic acid are very thin (*ca.* 4.5A) the surface potentials rise to between 400 and 450 mv, which is as high as for a very thick film of an acid of the type of stearic acid. Stearic acid itself gives about 400 mv.

The surface potential is practically independent of the length of the molecule, while with a perpendicular orientation it increases with the length of the molecule.

The surface potential (ΔV) of any one of the condensed films increases about 13 percent less rapidly than the surface density of the film. Thus the surface potential seems to increase with and nearly as the number of polar groups per unit area. However, the mutual effect of the dipoles is such as to decrease the potential.

At low pressures the expanded films become nonhomogeneous, since the surface potential varies with the location on the surface. This island effect is much more prominent for polymers of high than for those of low molecular weight.

While the number of dipoles in the surface is for the highly compressed film only 1/3 to 2/5 as great as for condensed films of stearic or palmitic acid, the surface potential is as high as that for stearic acid and higher than that for palmitic acid.

It is, therefore, obvious that the surface potential is not proportional to the number of dipoles. At the water surface the COO group might have a higher moment than the COOH group, but it is not improbable that the explanation lies in the dipoles of the water molecules.

However, since considerable work on the problem of the surface potential is in progress in this and in other laboratories, a more general discussion of the factors involved will be left to a later paper.

This work was begun by Dr. Earl K. Fischer under a grant from the Chemical Foundation.

* *Fundamental Papers on Contact Potentials and Papers on Surface Potentials*

1. Sir Wm. Thomson, Lord Kelvin, *Mathematical and Physical Papers*, Vol. VI, *Contact Electricity of Metals* (Cambridge Press, 1911), pp. 110 to 145. See also Righi, J. de Physique (2) **7**, 153 (1888).
2. Bichat and Blondlot, J. de Physique (2) **11**, 548 (1883).
3. Kenrick, Zeits. f. physik. Chemie **19**, 625 (1896); Guyot, Ann. de Physique (10) **2**, 506 (1924); Frumkin, Zeits. f. physik. Chemie **111**, 190 (1924); **116**, 485 (1925); Garrison, J. Phys. Chem. **29**, 1517 (1925); Buhl, Ann. d. Physik (4) **84**, 211 (1927); (4) **87**, 877 (1928).
4. Williams and Vigfusson, J. Phys. Chem. **35**, 348 (1931).
5. Guyot, Ann. de Physique (10) **2**, 506 (1924). Frumkin, Zeits. f. physik. Chemie **116**, 485 (1925).
6. Frumkin and Williams, Proc. Nat. Acad. Sci. **5**, 400 (1929).
7. Schulman and Rideal, Proc. Roy. Soc. **A130**, 259, 270, 284 (1930).
8. Adam and Harding, Proc. Roy. Soc. **A138**, 411 (1932). See also Schulman and Hughes, ibid. **430** (1932), and Fosbinder and Lessig, J. Frank. Inst. **215**, 425 (1933).
9. Whalley and Rideal, Proc. Roy. Soc. **A140**, 484, 489, 497 (1933).
10. Zisman, Rev. Sci. Inst. **3**, 7 (1932).
11. Zisman and Yamins, Physics **4**, 7 (1933).
12. Yamins and Zisman, J. Chem. Phys. **1**, 656 (1933).
13. Harkins and Fischer, J. Chem. Phys. **1**, 852 (1933).

Electron Diffraction by Gases

L. R. MAXWELL, S. B. HENDRICKS AND V. M. MOSLEY, *Bureau of Chemistry and Soils, Washington, D. C.*

(Received August 25, 1925)

The method of electron diffraction is used for determining the C−O−C valence angle (α) in 4,4′ diiododiphenyl ether [$(C_6H_4I)_2O$] and the molecular structures of phosphorus (P_4) and arsenic (As_4). The electron diffraction photographs were analyzed by four different methods as follows: (1) Visual measurements, (2) measurements of densitometer records, (3) conversion of densitometer records into relative intensity curves, (4) comparison of transformed intensity curves obtained by multiplying the intensity of scattering by $[(1/\lambda)\sin\theta/2]^2$ which produces prominent maxima for measurement. The valence angle α was found to be 118±3° for 4,4′ diiododiphenyl ether, definitely greater than the oxygen valence angle found for simpler types of molecules. Phosphorus and arsenic molecules were found to have a regular tetrahedral structure within the limits of experimental error, the atomic separations being 2.21A and 2.44A, respectively, [methods (1) and (2) were used for the case of arsenic]. The minimum atomic distances as found by crystal structure analysis for phosphorus and arsenic are approximately the same as the atomic separations obtained for the gas molecules, showing in addition that these distances do not change greatly when the bond angle decreases from 100° to 60°.

VALENCE ANGLE OF OXYGEN IN 4,4′ DIIODODIPHENYL ETHER

IT IS a matter of considerable theoretical importance to ascertain the value and the possible constancy of the valence angle of oxygen. This can be accomplished directly by electron diffraction methods and has already been carried out for several molecules.[1] The compound 4,4′ diiododiphenyl ether is unusually well adapted for this purpose on account of the predominant scattering of electrons by the iodine atoms. As a first approximation it can be considered as a triatomic molecule I−O−I, with an I−O distance of 6.26A.[2] The geometry of the complete molecule can, with considerable confidence, be taken as that shown in Fig. 1 which has two perpendicular planes of symmetry. Deviation from this model by rotation about the C−O bond would bring the carbon atoms of separate benzene rings into juxtaposition for values of α less than 150°. Actually the analysis is not sensitive even to this alternative since rotation of the groups would not materially change the intensity expressions. The theoretical intensity of electron scattering for the model assumed in Fig. 1 can be expressed as follows:

$$I(x_{cc}) = I_{II} + I_{IC} + I'_{IC} + I_{IO} + I_{CO} + I_{CC} + I_{inc},$$

where

$I_{II} = 2\psi_I^2(1+(\sin px_{cc})/px_{cc})$ ..... coherent scattering between iodine atoms

$I_{IC} = 4\psi_C\psi_I\left(\frac{\sin 1.48x_{cc}}{1.48x_{cc}} + 2\frac{\sin 2.14x_{cc}}{2.14x_{cc}} + 2\frac{\sin 3.1x_{cc}}{3.1x_{cc}} + 2\frac{\sin 3.48x_{cc}}{3.48x_{cc}}\right)$ .. iodine to carbon cross product terms, independent of valence angle

$I'_{IC} = 4\psi_C\psi_I\left(\frac{\sin qx_{cc}}{qx_{cc}} + 2\frac{\sin rx_{cc}}{rx_{cc}} + 2\frac{\sin sx_{cc}}{sx_{cc}} + \frac{\sin tx_{cc}}{tx_{cc}}\right)$ ..... iodine to carbon cross product terms dependent on valence angle

$I_{IO} = 4\psi_C\psi_I\left(\frac{\sin 4.41x_{cc}}{4.41x_{cc}}\right)$ ..... iodine to oxygen scattering ψ_O replaced by ψ_C

$I_{CO} = 4\psi_C\psi_C\left(\frac{\sin x_{cc}}{x_{cc}} + 2\sin\frac{3\frac{1}{2}x_{cc}}{3\frac{1}{2}x_{cc}} + 2\frac{\sin 2.64x_{cc}}{2.64x_{cc}} + \frac{\sin 3x_{cc}}{3x_{cc}}\right)$ ..... carbon to oxygen cross product terms independent of valence angle; ψ_O is replaced by ψ_C

[1] L. E. Sutton and L. O. Brockway, J. Am. Chem. Soc. 57, 473 (1935); H. Boersch, Monat. f. Chemie 65, 311 (1935).

[2] This value can be obtained from the I−C distance 2.00A as found by electron diffraction results from para diiodobenzene (see reference 4), the known C−C distances in the benzene molecule and from the assumed C−O separation of 1.42 (theoretical value for the single bond C−O separation).

$$I_{CC}=12\psi_C\psi_C\left(1+\frac{2\sin x_{cc}}{x_{cc}}+\frac{\sin 2x_{cc}}{2x_{cc}}+\frac{2\sin 3\frac{1}{2}x_{cc}}{3\frac{1}{2}x_{cc}}\right)$$ ..... total coherent scattering from two independent benzene rings with cross product terms between them omitted

$$I_{ine}=\frac{1}{\left(\frac{\sin\theta/2}{\lambda}\right)^4}[106\,S(\nu_I)+72S(\nu_C)+8S(\nu_O)]$$ ..... incoherent scattering from all the atoms in the molecule (hydrogen atoms omitted)

where

$$x_{cc}=4\pi l_{cc}\left(\frac{\sin\theta/2}{\lambda}\right), \qquad l_{cc}=\text{C}-\text{C distance}=1.42\text{A}$$

$$\psi_i=(Z_i-F_i)\Big/\left(\frac{\sin\theta/2}{\lambda}\right)^2, \quad \nu_i=4\pi b_i\frac{(\sin\theta/2)}{\lambda}$$

Z_i = atomic number, $\qquad b_i=0.176/Z_i^{\frac{1}{2}}$

F_i = atomic scattering factor.*

Electron scattering from the hydrogen atoms has been omitted as also has the C−C scattering between atoms of different benzene rings. Although the relatively large value of ψ_I causes the I_{II} term to be the most important, the other terms considered cannot be omitted since they give an intensity that has pronounced maxima and minima. Results of calculations for various valence angles, C−O−C, are shown in Fig. 2.

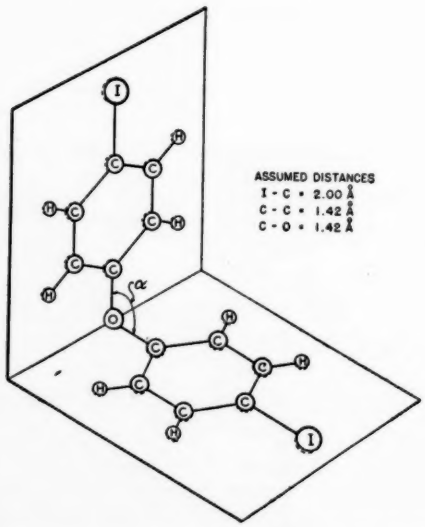

FIG. 1. Diagram of molecular model of 4,4′ diiododiphenyl ether.

* Obtained from calculated values of R. W. James and G. W. Brindley, Phil. Mag. **12**, 81 (1931).

TABLE I. *Data on parameters used in calculating electron scattering from 4,4′ diiododiphenyl ether.*

OXYGEN VALENCE ANGLE	p	q	r	s	t
180°	8.82	5.41	5.96	6.96	7.40
120°	7.63	4.99	5.32	6.05	6.45
110°	7.22	4.85	5.11	5.75	6.12
90°	6.24	4.51	4.58	5.06	5.33

Data on the parameters used in these calculations are given in Table I. These curves show only prominences or points of inflection. However, if $I(x_{cc})((\sin\theta/2)/\lambda)^2$ is plotted with respect to x_{cc} or x_{II}, as in Figs. 3 and 4, these prominences are accentuated in such a manner as to give actual maxima that permit unambiguous comparison with the experimental data. Positions of the maxima of the curves shown in Fig. 4 are listed in Table II.

The above calculations are to be compared with the experimental results[3] obtained. Four methods, as given below, have been used in making this comparison. The apparatus used has been described elsewhere.[4]

(1) *Visual measurements.* The photographs were characterized by one very prominent ring appearing at $(1/\lambda)\sin\theta/2=0.24$ with two inner rings that were considerably weaker but easily

[3] We are indebted to Professor R. Q. Brewster of the University of Kansas for a liberal supply of the 4,4′ diiododiphenyl ether which was used in this work.

[4] S. B. Hendricks, *et. al.*, J. Chem. Phys. **1**, 549 (1933).

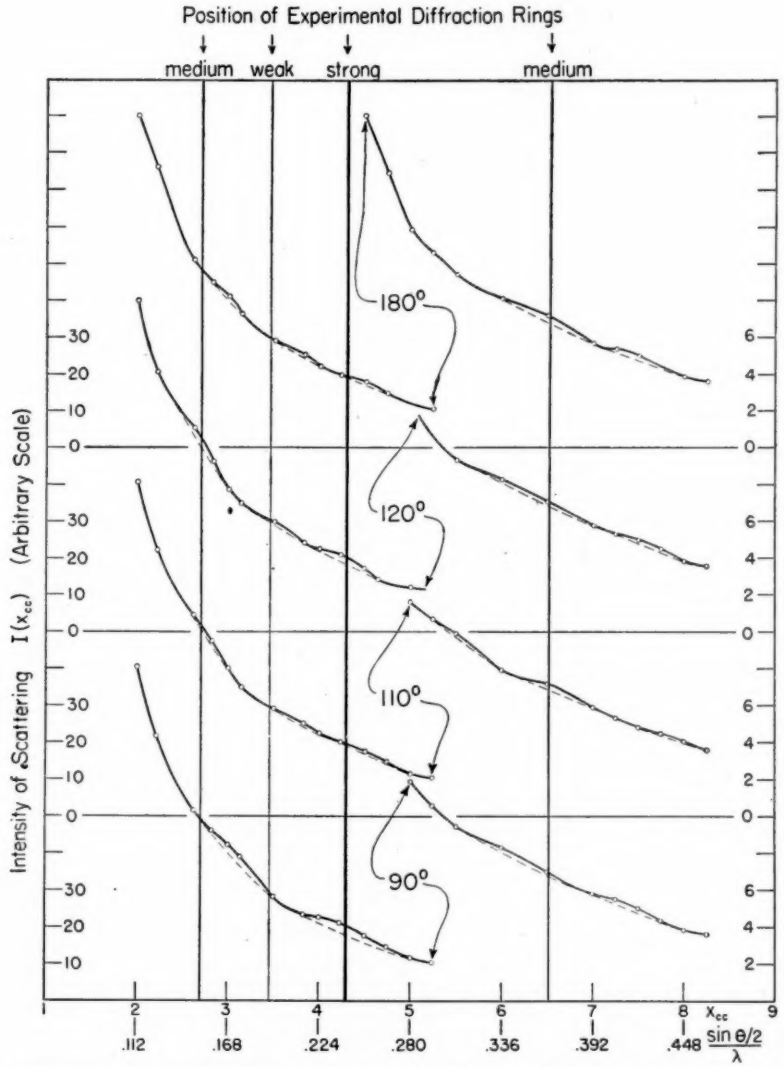

FIG. 2. Theoretical electron scattering curves $I(x_{cc})$ for 4,4′ diiododiphenyl ether. Position of experimental diffraction rings as measured visually are indicated for comparison. The circles represent points calculated in this instance and also for subsequent curves. (Figs. 3, 4, 7, 8, and 9.)

detectable on several photographs. Positions of apparent diffraction maxima as visually measured are shown on Fig. 1 and are listed in Table III. Although this method is possibly open to a psychological error occasioned by the rapidly varying background[5] it is sufficiently accurate to indicate that the valence angle, C−O−C, is probably in the region about 110° or 120°.

(2) *Densitometer measurements.* Results obtained from densitometer records are recorded in Table IV and are illustrated by the typical record shown in Fig. 5a. The position of the single prominent ring, the third maxima of Table IV, is determined by first constructing as a base line a smooth continuation of the densitometer curve through the region in which the prominence occurs and then bisecting the area between these two curves by a vertical line. A similar method is applied to the theoretical intensity curve and values so obtained are also listed in Table IV. These data are useful in

[5] For the discussion of the possible psychological errors arising in locating visually the position of electron diffraction rings see, for instance, Linus Pauling and L. O. Brockway, J. Chem. Phys. 2, 867 (1934).

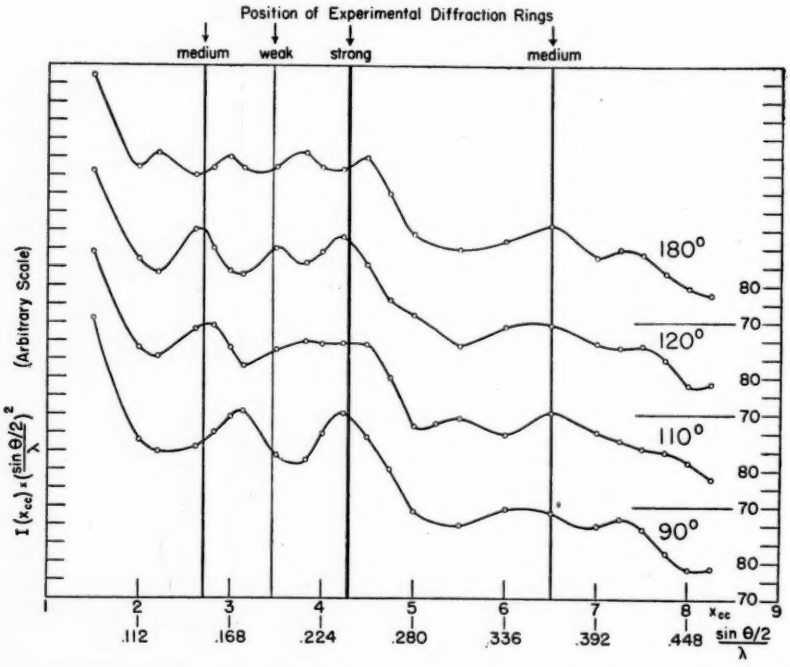

FIG. 3. Theoretical electron scattering curves $I(x_{cc})[(\sin\theta/2)/\lambda]^2$ for 4,4′ diiododiphenyl ether. Position of experimental diffraction rings as measured visually are indicated for comparison.

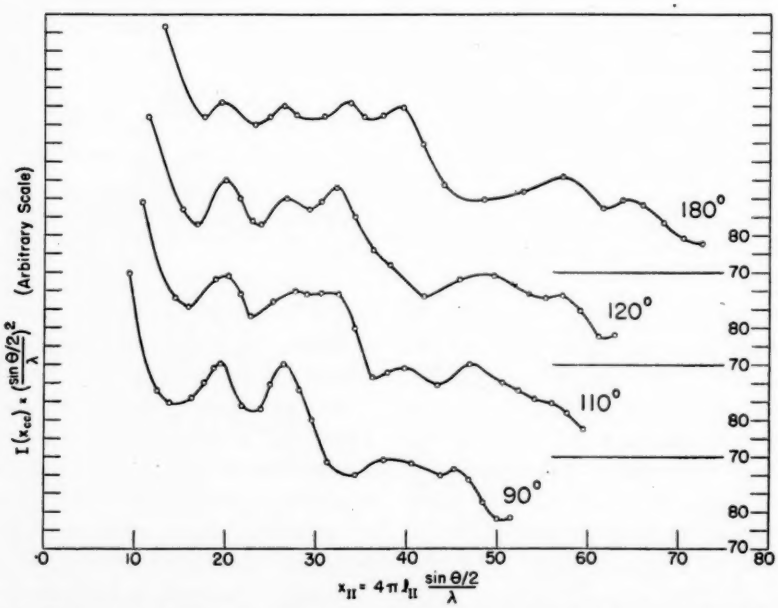

FIG. 4. Theoretical electron scattering curves $I(x_{cc})[(\sin\theta/2)/\lambda]^2$ for 4,4′ diiododiphenyl ether with respect to $x_{II}=4\pi l_{II}[(\sin\theta/2)/\lambda]$ made to illustrate how closely the scattering can be represented by a pure diatomic iodine structure.

TABLE II. *A summary of the position of calculated interference maxima for 4,4′ diiododiphenyl ether expressed in terms of* $x_{II}=4\pi l_{II}(1/\lambda)\sin\theta/2$.

Valence angle	1st maximum C	1st maximum D	2nd maximum C	2nd maximum D	3rd maximum C	3rd maximum D	4th maximum C	4th maximum D
90°	19.6	19.50	27.0	26.5	38.9	38.4	46.30	45.2
110°	20.3	19.8	27.4	27.6	33.2	shoul-der	40.2	39.7
120°	20.4	20.0	27.1	26.8	32.7	32.2	49.0	48.2
180°	—	19.5	26.5	26.4	33.4	33.2	39.9	39.0
For pure I-I scattering maxima would come at approximately	20.37		26.66		32.9		39.2	

C Position of humps located by using complete intensity formula $I(x_{cc})$ including incoherent scattering (method of bisecting areas used).
D Position of maxima located from $I(x_{cc})\times((\sin\theta/2)/\lambda)^2$ curves, real maxima measured in all cases.

TABLE IV. *Results of densitometer measurements on the electron diffraction photographs of 4,4′ diiododiphenyl ether and comparison with theory.*

Plate No.	λ	Position of humps measured by bisecting areas, expressed in units of $(1/\lambda)\sin\theta/2$		
		1st maximum	2nd maximum	3rd maximum
12	0.0770	absent	absent	0.242
13	.0826	absent	absent	.244
14	.0838	absent	absent	.246
15	.0863	absent	absent	.246
Average				0.244 ±.002
Expressed in units of x_{cc}				4.35 ±.004
Theoretical position of corresponding prominence expressed in units of x_{cc}			90°	4.33
			110°	4.60
			120°	4.29
			180°	4.55

differentiating between "α" (Fig. 1) equal to 110° and 12 since the 90° and 180° cases are eliminated by the visual measurements. The experimental value, $x_{cc}=4.35$, is in good agreement with the theoretical value, 4.28, for $\alpha=120°$, and in definite disagreement with the 110° model whose $x_{cc}=4.60$.

(3) *Relative intensity measurements.* Since the above method involved the questionable comparison of an intensity curve with a densitometer record it was considered feasible to obtain experimental values for the relative intensity of scattering. This required the determination of the relationship between the photographic density and the intensity of the electrons, which was obtained by means of plate calibrations.[6] Fig. 5b shows a relative intensity distribution obtained in this manner from the densitometer record shown in Fig. 5a. The method of bisecting areas as described above was applied to this curve and leads to a value of $x_{cc}=4.35$ for the prominent ring, which is the same as that obtained from the densitometer records. This corresponds to $\alpha=120°$.

(4) $I(\theta)\times[(1/\lambda)\sin\theta/2]^2$. It has been shown above that it is possible to obtain theoretical curves with true maxima by multiplying the intensity of scattering $I(x_{cc})$ by $[(1/\lambda)\sin\theta/2]^2$. We can obtain equivalent experimental curves

TABLE III. *Visual measurements on the electron diffraction photographs of 4,4′ diiododiphenyl ether* (position of maxima)

Plate No.	λ	1st maximum sin θ/2 / λ	1st maximum description	2nd maximum sin θ/2 / λ	2nd maximum description	3rd maximum sin θ/2 / λ	3rd maximum description	4th maximum sin θ/2 / λ	4th maximum description
1	0.0577					0.232	strong	present	
2	.0598					.239	strong	0.368	
3	.0650					.249	strong	present	
4	.0662					.238	strong	present	
5	.0662	0.152	medium	0.187	weak	.238	strong		
6	.0662	.152	medium	.194	weak	.238	strong		
7	.0680	.153	medium	.194	weak	.239	strong		
8	.0686	.150	medium	.195	very weak	.251	strong	.362	
9	.0700					.238	strong		
10	.0700					.232	strong		
11	.0765	.153	weak	.200	weak	.249	strong	.368	
12	.0780					.235	strong		
13	.0830					.247	strong		
14	.0838					.238	strong		
15	.0863	present	weak			.242	strong		
Average value		0.152 ±.006		0.194 ±.01		0.240 ±.005		0.366	
Expressed in units of x_{cc}		2.71±.107		3.46±.18		4.29±.089		6.53	

[6] Plate calibrations were made for the type of emulsion used (Eastman lantern slide slow emulsion) by exposing different portions of the calibration plate to the electron beam for different times of exposure. Since the reciprocity law is known to hold accurately at these voltages (A. Becker and E. Kipphan, Ann. d. Physik **10**, 15 (1931)) the calibrations could be obtained. Separate plates were used for the calibration. They were developed with the electron diffraction plates so that both received exactly the same development.

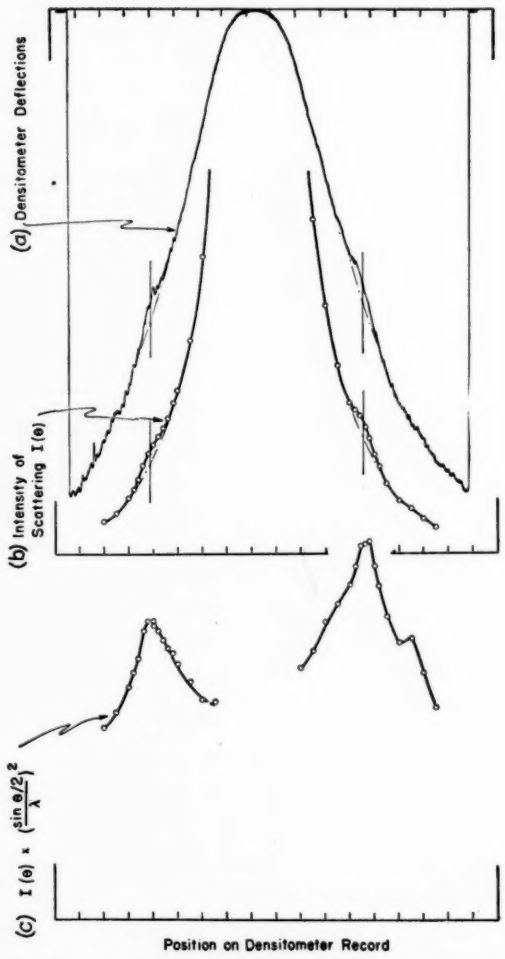

FIG. 5. (a) Densitometer record of the prominent interference ring of 4,4′ diiododiphenyl ether at approx. $(1/\lambda)\sin\theta/2=0.24$. (b) Experimental relative intensity curve made from (a) after plate calibrations. Vertical line through hump shows how area under curve is bisected. (c) Transformed electron scattering curve constructed from (b) in order to produce real maxima for measurement.

by the same method, as illustrated for the molecule 4,4′ diiododiphenyl ether in Fig. 5c.[9] This results in the production of a maximum at $x_{cc}=4.32$ which is in approximate agreement with the corresponding theoretical value of 4.20 for $\alpha=120°$ and again eliminates the model with $\alpha=110°$ since in that case only a broad maxima is obtained.

A less exact theoretical treatment has been used by Wierl[7] and later workers[8] who have compared their experimental results with calculated electron scattering curves in which ψ_i is replaced by Z_i and the incoherent scattering is omitted. This was done in order to simplify the calculation and also to produce true maxima in the calculated curves. While it is apparently satisfactory, particularly for large values of $(1/\lambda)\sin\theta/2$, it must be used in all instances with considerable caution. The approximate treatment does not give the true relative intensity of scattering. In many cases considerable additional information can be obtained if the correct theoretical intensity of scattering is known.

An alternative method for determining the valence angle.

More direct advantage can be taken of the predominance of the I_{II} scattering term than is apparent in the above analysis. In doing this it is most convenient to consider x_{II} as the variable so that maxima given by I_{II} will not be a function of α. From Fig. 4 and Table II it can be seen that the position of the first prominence is approximately independent of α and closer analysis shows that this must be caused by the prominent I_{II} term. Given the geometry of

TABLE V. *Determination of the I–I separation and valence angle of oxygen in 4,4′ diiododiphenyl ether.*

Method of measurement	1st maximum		2nd maximum		3rd maximum	
	$\frac{\sin\theta/2}{\lambda}$	l_{II}(A) for $x_{II}=20.4$	$\frac{\sin\theta/2}{\lambda}$	l_{II}(A) for $x_{II}=27.1$	$\frac{\sin\theta/2}{\lambda}$	l_{II}(A)
Visual	0.152±0.006 (5)	10.68±0.40	0.194±0.01 (5)	11.12±0.50	0.240±0.005 (15)	10.84±0.20 for $x_{II}=32.7$
b.a. dens. rec'd					0.244±.002 (4)	10.66± .09 for $x_{II}=32.7$
b.a. rel. int. curve					0.242 (1)	10.75 for $x_{II}=32.7$
$I(\theta)\times((\sin\theta/2)/\lambda)^2$					0.242 (1)	10.59 for $x_{II}=32.2$

b.a. means bisecting area.
Number in parentheses represents number of measurements made. Most probable I−I distance, 10.75±0.20A. Most probable valence angle, 118±3°.

[7] R. Wierl, Ann. d. Physik **13**, 453 (1932).
[8] See references listed by Louis R. Maxwell, *et al.*, J. Chem. Phys. **2**, 331 (1934).

[9] A feature of this treatment lies in the fact that it does not require the accurate location of the origin of the angle of scattering on the densitometer record but instead it

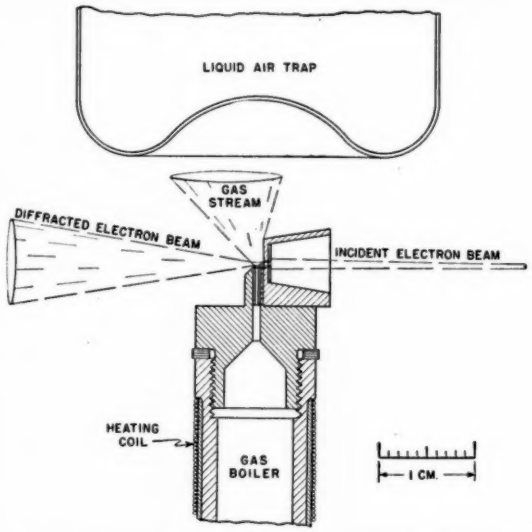

FIG. 6. Improved form of gas boiler containing the electron diaphragm as an integral unit.

Fig. 1 this leads to 118° as the value of α corresponding to an I−I distance of 10.70A. With this approximate limitation of α the method is also found to be applicable to the second and to the more accurately measured third prominence. Combination of these results, as shown in Table V, lead to a valence angle, C−O−C, of 118±3°.

Discussion

The analysis of the rotation vibration spectrum of the water molecule by Mecke and coworkers[10] leads to 104°–106° as the valence angle of oxygen. This angle has been determined in several other compounds from analysis of electron diffraction patterns. Thus Sutton and Brockway[11] found 105±5°, 111±2°, and 111±4° for the oxygen valence angle in F_2O, Cl_2O, and $(CH_3)_2O$, respectively, while Boersch[12] found $\alpha=100\pm3°$ in F_2O. These values are all definitely lower than that found above for 4,4′ diiododiphenyl ether.

It is also possible to calculate the valence angle of oxygen from measurements of electric moments although such a method involves several questionable assumptions. This method has been applied to 4,4′ dibromodiphenyl ether, 4,4′ dibromobenzene, and diphenyl ether, by Hampson, Farmer, and Sutton.[13] They found $\alpha=142°$ but a similar analysis by Pai[14] gave a value of 126.9°. More recently Sutton and Hampson* have revised their value of α to 128±4° which is closer to the electron diffraction results. Hare and Mack[15] obtain $\alpha=107°$ from viscosity determinations of diphenyl ether by the use of shadow areas obtained from various molecular models. This procedure does not possess the accuracy of electron diffraction methods so therefore it can be considered only as substantiating the electron diffraction value of 118°.

Molecular Structure of Phosphorus and Arsenic

These two elements are of particular interest in that they form homonuclear molecules of high symmetry in the vapor phase and extended homopolar nets in some of their crystalline forms. The opportunity is thus present for comparing the internuclear separations and valence angles occurring in these different forms. Vapor density measurements indicate that the molecules are predominantly tetratomic under the experimental conditions described below.

In order to obtain the requisite vapor pressures it was necessary to heat phosphorus to about 200°C and arsenic to *ca.* 500°C. This was conveniently accomplished in a boiler of the type shown in Fig. 6. A diaphragm for restricting the electron beam was attached to the boiler in such a manner as to insure electron collisions with the molecular beam issuing from the boiler. The entire unit was maintained at a sufficiently high temperature to prevent any condensation of the scattering substance on the electron diaphragm. The cross section of the electron beam incident on the diaphragm was large enough to accommodate any expansion or displacement of the boiler unit. Each substance required a some-

can be shown that an arbitrary origin differing as much as 10 percent in position from the true origin can be used for obtaining the position of the experimental maxima without introducing any detectable error.

[10] See for instance H. A. Stuart, *Molekulstruktur*, p. 313 (1934).

[11] Reference 1.

[12] Reference 1.

[13] G. C. Hampson, R. H. Farmer and L. E. Sutton, Proc. Roy. Soc. **A143**, 147 (1934). See also Stuart's *Molekulstruktur*, p. 142.

[14] N. Gopala Pai, Ind. J. Phys. **9**, 121 (1934).

* L. E. Sutton and G. C. Hampson, Trans. Faraday Soc. **31**, 945 (1935).

[15] Weston A. Hare and Edward Mack, Jr., J. Am. Chem. Soc. **54**, 4272 (1932).

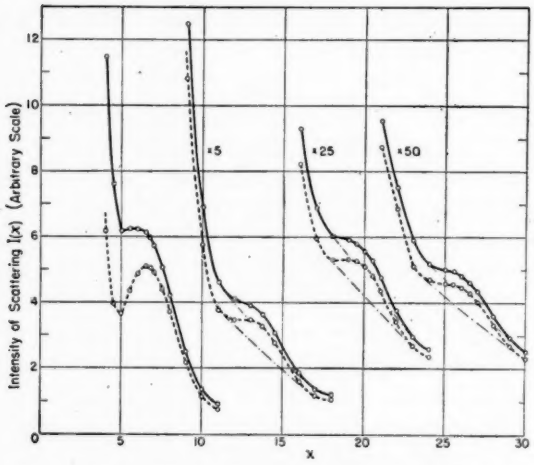

FIG. 7. Theoretical electron scattering curves of phosphorus (P_4) for a regular tetrahedral model. The dotted curve represents the coherent scattering while the full curve gives the total intensity (incoherent and coherent).

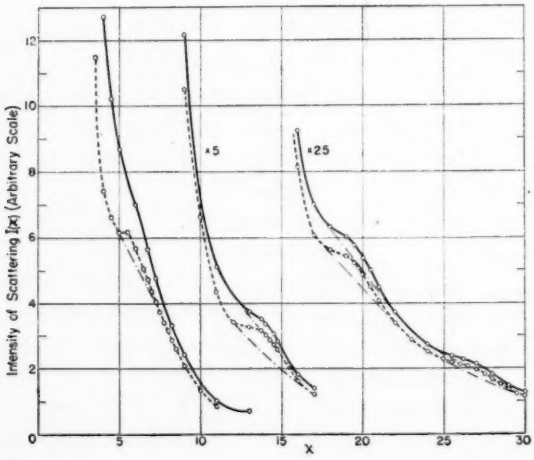

FIG. 8. Calculations for P_4 similar to Fig. 7 except for a square model.

what special technique owing to the fire hazard from phosphorus and the readiness with which arsenic alloys with hot metals. Carefully purified phosphorus was distilled in an inert atmosphere into a glass cup and then covered with a small amount of water. This cup was then introduced into the furnace shown in Fig. 6 and the water evaporated. Fire hazards were eliminated by condensing CCl_4 vapor on the exposed phosphorus surfaces at the end of the exposures. Arsenic was purified from the oxide by heating, in nitrogen, to about 600°C. It then was introduced into a quartz furnace similar to the metal one shown in Fig. 6. Electron diffraction photographs from phosphorus were taken with plate distances of 26.2 cm and 10 cm while only the shorter distance was used for arsenic.

Complete electron scattering curves for phosphorus are shown for a regular tetrahedral model in Fig. 7 and for a square model in Fig. 8. $I(x)\times((\sin\theta/2)/\lambda)^2$ is plotted as a function of x for these two cases in Fig. 9.[16] The intensity equations used in calculating these curves are for a regular tetrahedron:

$$I(x)\dagger = 4\psi_p^2\left(1+3\frac{\sin x}{x}\right)+I_{inc}$$

and for a square array:

$$I(x)=4\psi_p^2\left(1+2\frac{\sin x}{x}+\frac{\sin\sqrt{2}x}{\sqrt{2}x}\right)+I_{inc},$$

where

$$\psi_p=\frac{Z_p-F_p}{\left(\frac{\sin\theta/2}{\lambda}\right)^2},\quad I_{inc}=\frac{60\times S(\nu_p)}{\left(\frac{\sin\theta/2}{\lambda}\right)^4},$$

$$x=4\pi l_{p-p}\frac{\sin\theta/2}{\lambda},\quad l_{p-p}=\text{P}-\text{P separation}.$$

Positions of theoretical interference maxima for the two models as obtained by the approximate and rigorous methods of calculations are listed in Table VI. The approximate methods lead to important differences particularly in the case of the first maximum.[17] This maximum shows the greatest variance for the two models being prominent in the tetrahedral case and almost absent for the square model (compare Figs. 7 and 8). These calculations also can be used for the arsenic molecule without introducing any appreciable error since the only difference between the two cases arises in the magnitude of the ψ factors and the incoherent scattering. These changes would not materially alter the position of the outer prominences.

[16] It is necessary to assume at least an approximate value of $l_{P-P}=2.30$A in order to obtain the ψ functions. Although this value was also used here for obtaining the $I(x)\times((\sin\theta/2)/\lambda)^2$ functions it was not required because it can be shown that the position of these theoretical maxima are independent of l_{P-P}, in fact the expression $I(x)\times x^2$ could be used for locating the maxima.

† In these equations and the foregoing the constant factor is omitted.

[17] The value of intensity relationships has been previously described (Louis R. Maxwell, *et al.*, reference 8).

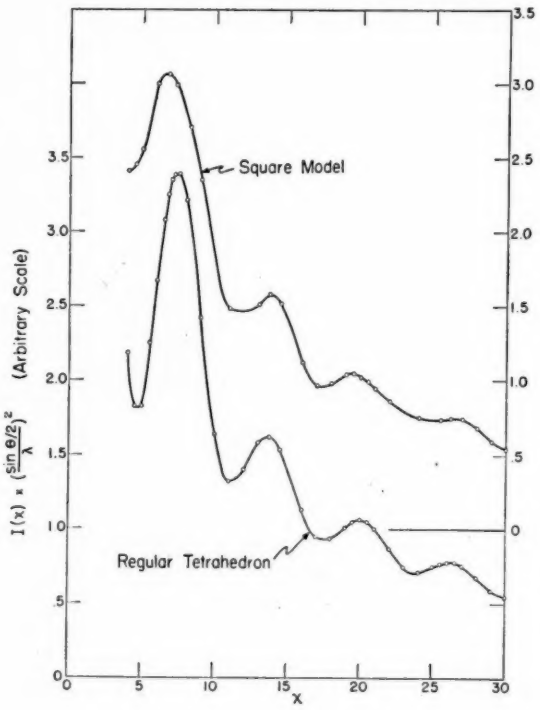

FIG. 9. Transformed theoretical electron scattering curves for P_4 obtained from the total scattering curves shown in Fig. 7 and Fig. 8.

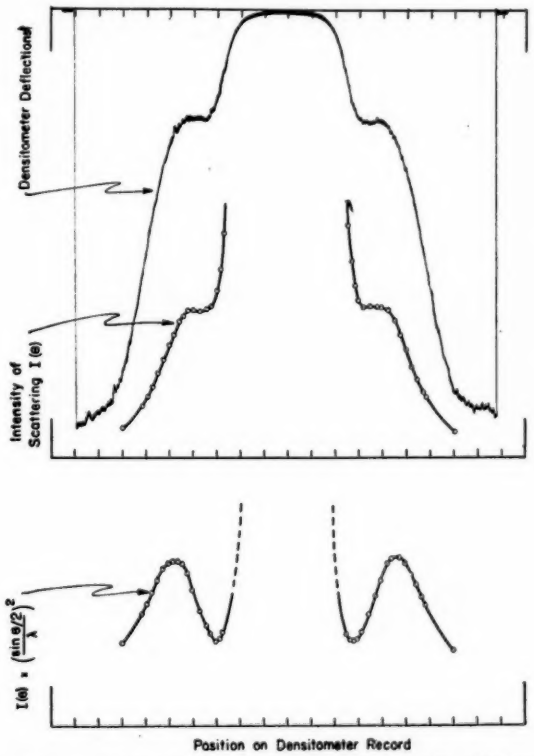

FIG. 10. Illustration of experimental results obtained for the first maximum of P_4. Method of treatment same as described in Fig. 5.

TABLE VI. *Theoretical positions of interference maxima for phosphorus.*

Model	1st maximum				2nd maximum				3rd maximum				4th maximum			
	A	*B*	*C*	*D*	*A*	*B*	*C*	*D*	*A*	*B*	*C*	*D*	*A*	*B*	*C*	*D*
Regular Tetrahedron	7.72	6.50	6.00	7.3	14.06	13.9	13.9	13.6	20.37	20.2	20.2	20.0	26.66	26.5	26.5	26.3
Plane Square	7.75	shoulder	very slight hump	6.6	14.25	14.20	14.30	13.80	19.80	19.80	19.8	19.5	27.0	27.1	27.1	26.6

A. Position of maxima located by using approximate solution in which ψ_i are replaced by Z_i (real maxima measured).
B. Position of maxima located by using complete intensity formula without incoherent scattering (method of bisecting areas used except for first maxima where a real maximum was observed).
C. Position for maxima located by using complete intensity formula incoherent scattering included (method of bisecting areas used except for first maxima where a real maximum was observed).
D. Position of maxima located from $I(x) \times((\sin\theta/2)/\lambda)^3$ curves, real maxima measured in all cases.

TABLE VII. *Average values obtained for $(1/\lambda)\sin\theta/2$ from (A) visual and (B) densitometer measurements of electron diffraction photographs of phosphorus (P_4).*

	$(1/\lambda)\sin\theta/2$									
	2nd maximum		3rd maximum		4th maximum		5th maximum		6th maximum	
	A	*B*	*A*	*B*	*A*	*B*	*A*	*B*	*A*	*B*
Wave-length range 0.055 to 0.077A	0.494±0.011	0.497±0.003	0.732±0.007	0.725±0.004	0.954±0.008		1.188±0.005		1.412±0.002	
*	(13)	(4)	(16)	(2)	(9)		(4)		(2)	
$I_{P-P}(A)$ for regular tetrahedron	2.24		2.20		2.21		2.21		2.21	
	(x=13.9)		(x=20.2)		(x=26.5)		(x=32.95)		(x=39.24)	
$I_{P-P}(A)$ for square model	2.30		2.15		2 26		2.19		2.24	
	(x=14.3)		(x=19.8)		(x=27.1)		(x=32.75)		(x=39.7)	

* No. of measurements made given by number in parentheses.

TABLE VIII. *Summary of measurements of the P–P distance (A) in phosphorus (P_4).*

METHOD OF OBSERVATION	1ST MAXIMUM	2ND MAXIMUM	3RD MAXIMUM	4TH MAXIMUM	5TH MAXIMUM	6TH MAXIMUM
Visual		2.24 (13)	2.20 (16)	2.21 (9)	2.21 (4)	2.21 (2)
*b. a. dens. rec'd		2.22 (4)	2.22 (2)			
*b. a. rel. int. curve $I(\theta)$		2.21 (1)				
$I(\theta)\times\left(\frac{\sin\theta/2}{\lambda}\right)^2$	2.25 (1)	2.21 (1)				

No. of measurements made given by number in parentheses.
Most probable structure—regular tetrahedron with P−P distance of 2.21±0.02A.
* b. a. means bisecting area.

TABLE IX. *Experimental results obtained from the electron diffraction photographs of arsenic (As_4).*

	2ND MAXIMUM	3RD MAXIMUM	4TH MAXIMUM	5TH MAXIMUM	6TH MAXIMUM
$(1/\lambda)\sin\theta/2$					
visual measurements	0.448±0.005 (10)*	0.654±0.005 (9)	0.861±0.003 (7)	1.068±0.007 (4)	1.268 (1)
l_{As-As}	2.47	2.46	2.45	2.45	2.46
regular tetrahedron	($x=13.90$)	($x=20.20$)	($x=26.50$)	($x=32.95$)	($x=39.24$)
l_{As-As}	2.54	2.41	2.50	2.44	2.49
square model	($x=14.30$)	($x=19.80$)	($x=27.10$)	($x=32.75$)	($x=39.70$)
$(1/\lambda)\sin\theta/2$					
b. a. dens. rec'd	0.455±0.003 (3)	0.663±0.006 (6)	0.871±0.005 (4)		
l_{As-As}	2.43	2.42	2.42		
regular tetrahedron	($x=13.90$)	($x=20.20$)	($x=26.50$)		

* No. of measurements made given by number in parentheses.
b. a. means bisecting area.
de Broglie wave-length range 0.0586–0.0708A.
Most probable structure regular tetrahedron with As−As distance 2.44±0.03A.

Experimental intensity curves for the first two rings of the electron diffraction pattern of phosphorus are shown in Figs. 10 and 11. The particular record illustrated in Fig. 10 for the first maximum was an average record. Considerable variation in the shape of this maximum was found so that its exact distribution was not obtained. The character of these relative intensity curves should be compared with the theoretical curves given in Figs. 7 and 8. The prominence of the first maximum serves adequately to eliminate the square model. All the details of the pattern are found to be in substantial agreement with the requirements of a regular tetrahedral molecule. A summary of the experimental data is given in Table VII. Measurements of the P−P distance according to the four methods used above for phosphorus are summarized in Table VIII. Visual measurements on the first maximum are omitted since the errors in locating its theoretical and experimental positions are considerable. The combined data show that the molecule has the form of a regular tetrahedron with a P−P distance of 2.21±0.02A.

The electron diffraction pattern of arsenic is very similar to that of phosphorus and in particular the prominence of the first ring is such as again to eliminate the square model. Results of visual and densitometer measurements are listed in Table IX, while in Fig. 12 is shown a reproduction of a typical photograph obtained. The theoretical positions of the maxima calculated for the phosphorus molecule were used here in comparison with the experimental results for arsenic. We conclude from these data that the arsenic molecule is similar to the P_4 molecule in shape, having a regular tetrahedral structure but with a somewhat greater nuclear separation of 2.44±0.03A.

Discussion

Crystal structure information is available for some of the forms of phosphorus and arsenic. In black phosphorus each atom has three nearest neighbors at a distance of 2.18A[18] with bond angles near 102°. Fourier analysis of the diffraction pattern of red phosphorus[18] indicates that the immediate surrounding of a phosphorus atom is similar to that of the black variety, although the experimental value, 2.28A, for the atomic separation is somewhat greater. Black phosphorus contains molecular nets and it is

[18] Ralph Hultgren, N. S. Gingrich and B. E. Warren, J. Chem. Phys. 3, 351 (1935).

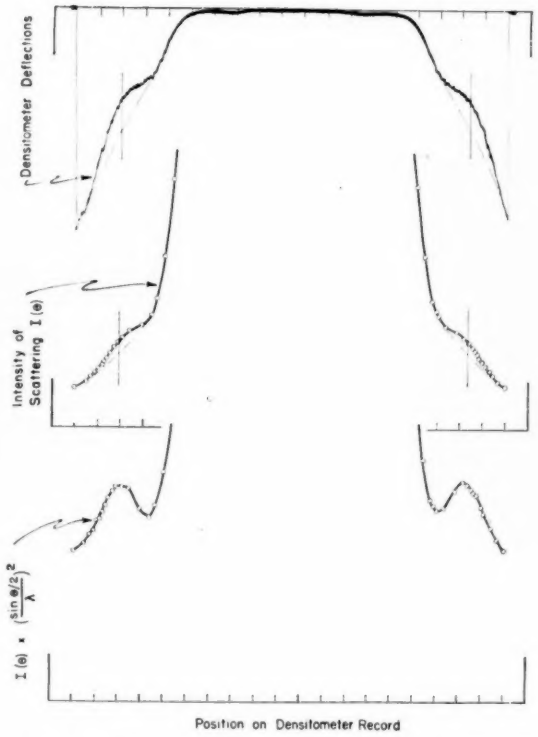

FIG. 11. Illustration of experimental results obtained for the second maximum of P_4. Method of treatment same as described in Fig. 5. Vertical line through prominence shows how area is bisected.

probable that the red modification forms either nets or a spatial array. Crystalline yellow phosphorus on the other hand possibly has a lattice formed from P_4 molecules of the type found in the vapor by the electron diffraction results and on account of their high symmetry they might be expected to be rotating at room temperature.

Arsenic crystallizes into a metallic rhombohedral form and in a supposedly cubic nonmetallic form that can be maintained only in darkness at low temperatures. Crystal structure analysis of the metallic modification[19] indicates that the closest distance of approach of the

[19] A. J. Bradley, Phil. Mag. **47**, 657 (1924); S. V. Olshausen, Zeits f. Krist. **61**, 463 (1935).

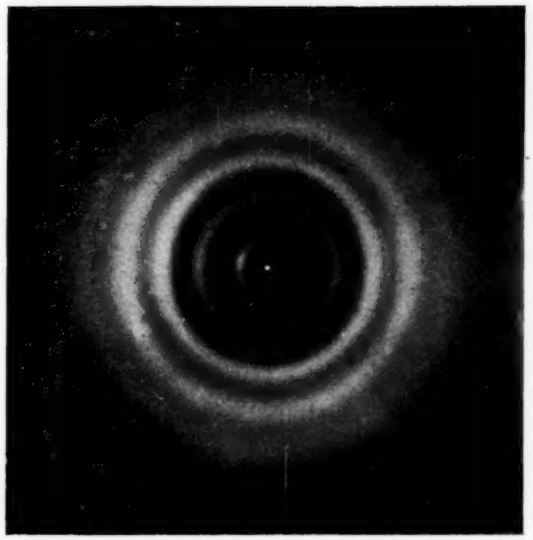

FIG. 12. Reproduction of electron diffraction photograph obtained from arsenic vapor (As_4). de Broglie wavelength 0.0617A, plate distance 10 cm. Magnified 2×.

arsenic atoms is very near to 2.51A and that the bond angles are approximately 97°. The yellow modification is formed when arsenic vapor is condensed at low temperatures. This condition of formation suggests that the lattice consists of As_4 molecules that might be expected to have the configuration found from electron diffraction.

The minimum atomic separations, which are the covalent bond distances, as found by crystal structure analysis for phosphorus and arsenic, are nearly the same as those found in the present work for the gas molecules. This is of particular interest since the bond angle for the tetrahedral vapor molecules is but 60° while the values in the crystalline forms are near 100°. The P−P separation of 2.21A found in this work is in close agreement with the value 2.20A suggested by Pauling.[20] His As−As value, 2.42A, agrees with the value 2.44 ± 0.03A as found from electron scattering while it is slightly lower than 2.51A from x-ray diffraction.

[20] Linus Pauling, Proc. Nat. Acad. Sci. **18**, 293 (1932).

The Relation Between the Internuclear Distances and Force Constants of Molecules and Its Application to Polyatomic Molecules

RICHARD M. BADGER, *Gates Chemical Laboratory, California Institute of Technology*

(Received August 10, 1935)

The relation between the internuclear distances and force constants found for diatomic molecules is discussed, and is shown to carry over to polyatomic molecules. It is shown that internuclear distances of polyatomic molecules can be predicted from vibrational data alone, with considerable accuracy.

ONE would expect, on theoretical grounds, that there should be a relation between the internuclear distances and the constants of the potential function of a molecule. Though the complete relation must necessarily be very complex the writer observed several years ago, in the case of diatomic molecules, that the equilibrium internuclear distance, r_e, can be expressed with fair accuracy as a function only of d^2V/dr^2, at the equilibrium separation, and of the positions in the periodic system of the atoms composing the molecules. The fact that such a simple relation can be found is apparently due to the fact that the several factors on which r_e depends do not vary in an arbitrary and independent fashion through a set of molecules, but change in a more or less parallel manner.

It is to some extent a matter of taste as to how one may best express the relation between r_e and $(d^2V/dr^2)_{r_e}$ or k_e, which may be called the "bond force constant," as the relation is not perfectly exact. The writer believes that an equation which he proposed some time ago,[1] and which, with a slight modification described below, may be written in the following manner:

$$r_e = (C_{ij}/k_e)^{\frac{1}{3}} + d_{ij}, \qquad \text{Relation I}$$

is of the most satisfactory form, since with the proper choice of constants it fits very accurately the various electronic states of a given molecule, with the exception of a few abnormal states.

Two other rules have been more recently proposed,[2,3] which for comparison with Relation I may be rewritten as follows:

$$r_e^2 = C_{ij}'(\mu/nk_e)^{\frac{1}{3}}. \qquad \text{Clark rule.}$$

$$r_e^2 = C_{ij}''/k_e^{\frac{1}{3}}. \qquad \text{Allen, Longair rule.}$$

These rules fit quite well within a certain range but they do not appear to be of as satisfactory a form as Relation I for fitting the various excited states of a given molecule, and have not the latitude of the two constant formulas necessary for getting a good fit for the heavy molecules.

All the relations mentioned are at best a compromise, and attempt to fit a considerable amount of data with the smallest possible number of arbitrary constants. As was mentioned, Relation I has a suitable form for fitting most states of a given molecule with a single pair of constants, but to get an accurate fit C and d must be given values considerably different from those which give the best average fit for a group of molecules. It might seem reasonable that C and d could be expressed as functions of the atomic numbers of the atoms composing the molecule, which might have an effect similar to that of the parameter n in the Clark equation. This might be possible for the symmetrical molecules for which the constants appear to vary in a systematic manner, but for unsymmetrical molecules they behave in an erratic fashion. This fact, together with the occurrence of some abnormal states which deviate from any simple rule, indicates that any more refined rule must take into account the type of binding present in each state.

The writer has had considerable success in adding to his relation a correction in $\mu\omega_e x_e$ but so far has not found a rule which makes more accurate predictions than Relation I and gives a *unique* answer unless the type of bond in question is known, which is often not the case.

[1] R. M. Badger, J. Chem. Phys. **2**, 128 (1934).
[2] C. H. Douglas Clark, Phil. Mag. **18**, 459 (1934).
[3] H. S. Allen and A. K. Longair, Nature **135**, 764 (1935).

However, Relation I can be improved somewhat, still keeping C and d constant through a group of molecules, if C is allowed to vary with d from group to group, instead of taking a universal value as was previously done. This necessitates taking slightly different values for d_{ij}, as given in Table I.

TABLE I.

TYPE OF MOLECULE Atom i an element in row	Atom j an element in row	Example	$(C_{ij})^{\frac{1}{3}}$	$d_{ij}(A)$
1	1	NO, O_2, NO	0.571	0.68
1	2	SO, PN, CS	0.535	0.94
1	3	TiO	(0.500)	(1.06)
1	4	SnO	(0.490)	(1.18)
1	5	PbO	(0.490)	(1.26)
2	2	Cl_2, S_2, P_2	0.490	1.25
2	4	ICl	(0.505)	(1.48)
3	3	Br_2, K_2	0.505	1.48
4	4	I_2	(0.49)	(1.76)

Parentheses indicate that constants were determined from data on only one molecule except in the case of SnO where the values were estimated with the assistance of the author's Relation II.[4] The dimensions and units of C are such as to give r_e in Angstrom units when k_e is given in *megadynes* per centimeter.

APPLICATION TO POLYATOMIC MOLECULES

The relation between k_e and r_e which has been found to exist for diatomic molecules has proved to be useful in a number of ways. It is the purpose of this paper to enquire whether this relation carries over, in general, to the polyatomic molecules. The number of cases in which all, or even any of the internuclear distances in polyatomic molecules can be exactly evaluated from the analysis of the rotational structure of their bands is definitely limited, for obvious reasons. On the other hand, a great deal of information about the vibrational structure of the spectra of such molecules has already accumulated and if it can be made available for determining internuclear distances several interesting possibilities will be opened up.

These vibrational data have already been used, in the cases of several typical molecules, in evaluating the constants of simple potential functions. With one or two exceptions one has been content with potential functions containing not higher than quadratic terms, but it is the coefficients of certain of these quadratic terms which interest us at present, as we wish to study their relation to the internuclear distances.

In making an examination of this sort one is confronted with several difficulties. In the first place there are few cases where one knows exact internuclear distances and at the same time has complete vibrational data available. To make even the ordinary normal coordinate treatment of a molecule, to obtain the second derivatives of the potential energy with respect to the various coordinates, one should employ the normal frequencies of vibration for infinitesimal amplitude. These are obtained through an extrapolation from the observed frequencies which it is usually not possible to make on account of the incompleteness of the data. However, it seems improbable that the approximation introduced in making use directly of the observed frequencies of the fundamental bands and Raman lines will lead to serious error in the important force constants except in the case of light molecules, particularly the hydrogen-containing molecules.

But now we are faced with another difficulty in regard to the form of potential function which we shall attempt to apply to molecules. It would of course be desirable to start with the most general function containing all possible quadratic terms. But usually, even for rather simple molecules, we should find that we have insufficient data to evaluate all the constants. Furthermore, even the most general function can usually be written in several different forms which are equivalent, but which suggest different physical interpretations of the molecule.

Now in the study of many properties of molecules it has been found that they may be regarded as the sum of several individual parts which to a good approximation may be regarded as independent. So also it is convenient to regard the potential energy as made up of a sum of various rather independent parts, and one criterion for selecting a suitable form of function would be that it should be suggestive of the concept of a molecule which has been developed from other experimental information. If this concept is sufficiently well developed we should expect it to be a good guide in deciding which of the constants of the potential function are small and may be ignored and which we shall

[4] R. M. Badger, Phys. Rev. **48**, 284 (1935).

attempt to determine from the limited data available.

These expectations appear to be justified. For a number of different types of molecules so far investigated there appears to be one *general* method of setting up the potential function which is preferable to other methods. The potential energy is regarded as made up of three main parts, as far as concerns the quadratic terms. **Part I,** and the most important, is regarded as dependent only on the distances between the atoms which are directly bonded to each other. For small displacements from the equilibrium position the change in energy is given by:

$$2V_r = \Sigma k_{e_i}(\Delta r_i)^2.$$

For larger extensions or compressions of a bond there is some evidence that a Morse function may be applied.

In the case of certain molecules which we shall discuss first, where the bonds are not under appreciable tension, we may designate the coefficients of the terms of Part I as "bond force constants," represented again by the symbol k_e, rather than k_e, and may compare them directly with these constants for diatomic molecules.

Part II of the energy is dependent on the angles between chemical bonds, and **Part III,** which must be added to complete the function so that it will fit the vibrational data, contains terms which may be interpreted as arising from interactions between atoms not directly bonded to each other. When the potential function is written as described these interaction terms are usually rather small and sometimes may be ignored. However, it is occasionally important how they are written, owing to the effect on the magnitude of the k_e's. From the data so far available it appears that the interactions mentioned result mainly from the repulsions of nonbonded atoms and the interaction terms should be written so as to suggest this fact.

Now in writing the potential energy as described we shall frequently introduce a redundancy of coordinates, in which case we expect linear terms also to appear in the complete expression. These will not concern us immediately though indirectly they are of importance.

The fact which is now of interest is that in a potential function written as above described the k_e's do appear to have the same relation to the r_e's as was found for diatomic molecules. This fact will now be illustrated by a number of cases.

Molecules with Bonds Under Little Tension

In the first cases considered as exact a test as possible will be made and instead of employing Relation I with the constants given in Table I, a plot of $(1/k_e)^{\frac{1}{3}}$ against r_e will be given for the atom pairs: O−H, C−O, C−S, and S−O, both when found as a diatomic molecule[5] and when constituting part of a polyatomic molecule. It will be seen that for a given atom pair all points fall very close to a straight line.

The most satisfactory tests are for O−H and C−O, since for both H_2O and CO_2 rather complete vibrational analyses have been made,[6] and internuclear distances are accurately known.[7] In the case of H_2O the interaction terms are small and the value of k_e (OH in H_2O) will not be materially affected by how they are introduced. The fit of the H_2O point with those for the O−H molecule will be seen in Fig. 1 to be practically perfect.

In the case of CO_2 or CS_2 we might write the potential function in the two equivalent forms:

$$2V = k_e(\Delta r_1^2 + \Delta r_2^2) + k_{12}(\Delta r_1 + \Delta r_2)^2 + \cdots,$$

$$2V = k_e'(\Delta r_1^2 + \Delta r_2^2) + 2k_{12}(\Delta r_1 \times \Delta r_2) + \cdots.$$

Now k_e and k_e' differ by k_{12}, which is appreciable both for CO_2 and CS_2, but there seems to be no doubt but that the former is the one which we should compare with the data on CO and CS, respectively, since the vibrational analysis of CO_2 by Adel and Dennison shows that the interaction term arises mainly from a repulsion of the oxygen atoms, indicating that the former

[5] The data for diatomic molecules have been taken from the report of Jevons (Physical Society) except where more recent work is available.

[6] (H_2O) L. G. Bonner, Phys. Rev. **46**, 458 (1935); (CO_2) Adel and Dennison, Phys. Rev. **44**, 99 (1933).

[7] (H_2O) Freudenberg and Mecke, Zeits. f. Physik **81**, 465 (1933); (CO_2) Barker and Adel, Phys. Rev. **44**, 185 (1933).

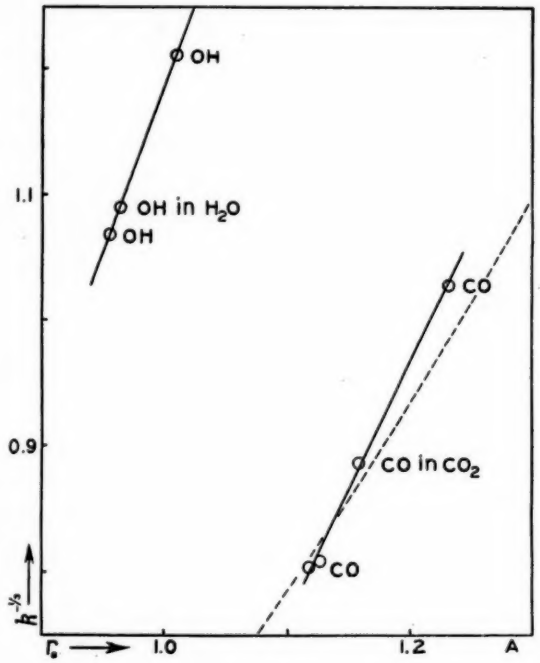

FIG. 1. A plot of $(1/k_e)^{\frac{1}{2}}$ against r_e for the atom pairs: O−H and C−O, when found as diatomic molecules or in the H_2O and CO_2 molecules, respectively. The units of k_e are megadynes per cm. The dotted line shows the locus of points for the CO molecule predicted by the C. H. Douglas Clark rule.

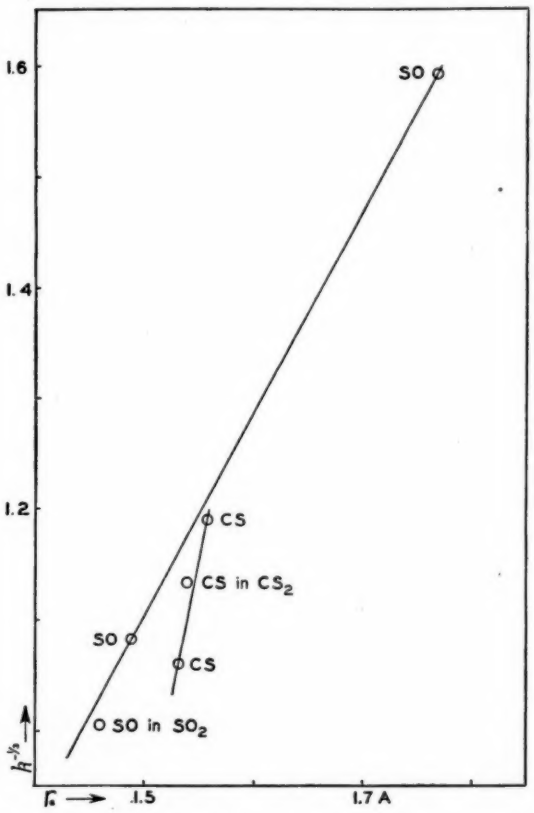

FIG. 2. A plot of $(1/k_e)^{\frac{1}{2}}$ against r_e for the atom pairs C−S and S−O.

expression of the potential function is to be preferred. For CO_2 the fit with the data on the diatomic molecule is again seen to be very good if k_e is used, as in Fig. 1, but with k_e' the point deviates about 0.015A from the line as drawn. In the case of CS_2 and also SO_2 we must be content with a less accurate test, as we are obliged to use internuclear distances determined by electron diffraction methods,[8] in which the error may be as large as 0.02A, and in the normal coordinate treatment the observed fundamentals have been employed rather than the frequencies for infinitesimal amplitude. In SO_2 [9] the interaction between the oxygen atoms has been ignored, which may lead to some error. In spite of these approximations the fit for CS_2 and SO_2 is still quite satisfactory, as seen in Fig. 2, as the deviation from the straight line is of the order of the uncertainty of the measurement of the distance.

MOLECULES WITH BONDS UNDER TENSION

We shall now consider some molecules of a somewhat different type, those with the general formulas: MX_4 and MX_6, for example CCl_4 and SF_6, in which one central atom is surrounded by several relatively large halogen atoms. A satisfactory treatment of these molecules by normal coordinate methods has only recently been made[10, 11] and has shown that the halogen atoms appear to be compressed considerably so that the mutual repulsions result in a stretching of the bonds between the halogen atoms and central atom.

[8] Private communication from Dr. L. O. Brockway.
[9] For the force constants of SO_2 the author is indebted to Dr. Paul C. Cross who has made a normal coordinate treatment of this molecule.

[10] Jenny E. Rosenthal, Phys. Rev. **46**, 730 (1934).
[11] Sachse and Bartholomé, Zeits. f. physik. Chemie **B28**, 257 (1935).

The vibrational analyses have yielded values for both d^2V_r/dr^2 and dV_r/dr for the molecules in the equilibrium position,[12] at which we may call the distance from central to outer atom r_ϵ. If we assume that a Morse function applies to V_r we can calculate the difference between r_ϵ and r_e, the distance at which $dV_r/dr=0$, or in other words the amount of stretching of the bond. To do this, however, we must assume some value for the constant a, appearing in the exponent of the Morse function. The author has found that for a single bond the a may be sufficiently well estimated by the relation:*

$$a=1.15/(r_e-d_{ij}).$$

Values of $r_\epsilon-r_e$ calculated in this manner for several molecules appear in Table II.

TABLE II.

MOLECULE	k_ϵ (megadynes/cm)	$(dV_r/dr)_{r_\epsilon}$ (megadynes $\times 10^5$)	$r-r_e$(A)	r (calc.)	r_ϵ(obs.)
CCl_4	0.178	0.066	0.19	1.76	1.76
$SiCl_4$	0.255	0.0464	0.12	1.98	2.02
$SnCl_4$	0.227	0.0343	0.11	2.27	2.29
SF_6	0.344	0.196	0.19	1.56	1.58
SeF_6	0.368	0.141	0.17	1.67	1.70
TeF_6	0.395	0.112	0.15	1.80	1.84

These results are very interesting since we observe that when one or more of the halogen atoms, say in CCl_4, are replaced by the small hydrogen atom, allowing the remainder to separate somewhat and to take up a new and more "comfortable" position, they do not actually shrink in appreciably. The C−Cl distance is, within experimental error, the same in CCl_4 and CH_3Cl. It appears then that the same Morse function cannot be applied to the C−Cl bond in the two cases, and the constancy of the C−Cl distance seems to be a somewhat accidental affair arising from certain compensations.

Now we shall proceed to apply Relation I to molecules of the type just discussed. Evidently we cannot expect to do this directly since the experimental data give us values of r_ϵ and k_ϵ or d^2V_r/dr^2 at r_ϵ, and the expression relates r_e and k_e. However, we may apply the Morse function again to correct k_ϵ to k_e, then calculate r_e by Relation I, and correct it back to r_ϵ.

In this way, by using the constants in Table I, r_ϵ has been calculated for several molecules and in Table II is compared with the experimental value obtained from electron diffraction measurements.[13] In only two cases does the deviation greatly exceed the possible error in the electron diffraction measurements. The error in the calculated value seems to increase with the weight of the central atom which suggests that the method of calculation might be further improved.

CONCLUSION

The above tests exhaust the suitable data at present available, but for the types of molecule discussed they do appear to justify the division of the potential energy into the parts previously mentioned and show that the relation between $(d^2V_r/dr^2)_{r_e}$ and r_e found for diatomic molecules persists in the polyatomic molecules. This fact should be of considerable use since it provides a method of calculating internuclear distances in these molecules from vibrational data alone, with sufficient accuracy for many purposes.

[12] For the hexafluorides the constants in columns II of the table of Sachse and Bartholomé have been used.

* *Note added in proof:* This is an empirical rule which appears to serve fairly well in the comparison of similar molecules. The constant varies from one type of molecule to another and in the case of the fluorides 1.05 was used in the calculations though a still smaller value would have given better agreement with experiment.

[13] Pauling and Brockway, J. Chem. Phys. **2**, 867 (1934); Brockway and Wall, J. Am. Chem. Soc. **56**, 2373 (1934); Pauling and Brockway, Proc. Nat. Acad. Sci. **19**, 68 (1933).

A Generalized Thermodynamic Notation

H. A. C. McKay, *Balliol College, Oxford*

(Received July 24, 1935)

It has recently been shown by Koenig that, as a result of the symmetry of the fundamental relations of thermodynamics, thermodynamic equations can be grouped into families. In the present paper a generalized notation is described which leads to an elegant method of writing down from one generalized equation all the members of a family; in particular, the signs of the various terms are very easily manipulated. The question of the number of members of a family is considered, and a method is given for obtaining the generalized equation when any one member of a family is known. Finally the extension of the method to problems of capillarity, magnetization, etc., is shown to be very readily carried out.

Derivation of Generalized Formulae

A ONE-PHASE system containing $n-2$ chemical components has n degrees of freedom, provided gravitational, electrical, magnetic, and capillary effects can be neglected. At least one of these degrees of freedom must be extensive.[1]

The thermodynamic properties of such a system may, then, be described by means of n extensive variables:

$$X_1X_2\cdots X_n.$$

Two of these are S and $-V$, S being the entropy and V the volume; we take $-V$ rather than V purely for convenience in generalizing our equations. For the rest we may take the numbers of moles, the N's, of any set of $n-2$ independent chemical species.

The internal energy, E, of the system is a function of the X's, and its partial differential coefficients with respect to each X in turn are the intensive variables of the system:

$$x_r=\partial E/\partial X_r, \tag{1}$$

$$dE=\sum_{r=1}^{n} x_r dX_r. \tag{2}$$

(2) is usually met with in the form:

$$dE=TdS-PdV+\sum\mu dN,$$

where T is the temperature, P the pressure, and the μ's are chemical potentials.

Any pair of variables X_r, x_r related by (1) is known as a conjugate pair of variables. A set of variables containing one member from each conjugate pair is known as a canonical set. Corresponding to the general canonical set of variables:

$$x_1x_2\cdots x_p,\ X_{p+1}\cdots X_n$$

we may define a characteristic function Φ, such that

$$\Phi=E-\sum_{r=1}^{p} x_rX_r. \tag{3}$$

Differentiating and combining with (2) we get:

$$d\Phi=-\sum_{r=1}^{p} X_r dx_r+\sum_{r=p+1}^{n} x_r dX_r. \tag{4}$$

E is the characteristic function corresponding to the canonical set consisting of all the X's.

Let us take in general a canonical set:

$$Y_1Y_2\cdots Y_n$$

and let:

$$y_1y_2\cdots y_n$$

be the corresponding conjugate quantities. Then in virtue of (4):

$$d\Phi=\sum_{r=1}^{n} y_r d|Y_r|. \tag{5}$$

The symbol $|Y_r|$ indicates that Y_r is to be taken with a positive sign when Y_r is an extensive variable and with a negative sign when Y_r is intensive. From (5) we get

$$\partial\Phi/\partial|Y_r|=y_r, \tag{6}$$

where r takes all values from one to n in turn. The next differential coefficients give rise to the generalized form of the Maxwell relations:

$$\frac{\partial^2\Phi}{\partial|Y_r|\partial|Y_s|}=\frac{\partial y_r}{\partial|Y_s|}=\frac{\partial y_s}{\partial|Y_r|}, \tag{7}$$

[1] Craxford, Gatty and Philpot, Phil. Mag. [7] **16**, 849 (1933).

where r and s assume all values from 1 to n subject to the restriction $r \neq s$.

We may next consider relations arising from the use of two characteristic functions simultaneously. Let these be Φ_1 corresponding to the same canonical set as before, and Φ_2 corresponding to the set:

$$Y_1 Y_2 \cdots Y_p, \quad y_{p+1} \cdots y_n,$$

where of course $1 \leq p < n$. It follows at once from the definition of the Φ's in Eq. (3) that

$$\Phi_2 = \Phi_1 - \sum_{r=p+1}^{n} y_r |Y_r|. \tag{8}$$

By combination of (8) with (6) we get a generalized relation of the type of the Gibbs-Helmholtz equation:

$$\Phi_2 = \Phi_1 - \sum_{r=p+1}^{n} |Y_r| \partial \Phi_1 / \partial |Y_r|.$$

Since the $|Y_r|$'s occur in pairs we can write this simply as

$$\Phi_2 = \Phi_1 - \sum_{r=p+1}^{n} Y_r \partial \Phi_1 / \partial Y_r \tag{9}$$

or in Jacobian notation as

$$\Phi_2 \Phi_1^{n-p-1} = (-1)^{n-p} \prod_{r=p+1}^{n} Y_r^2 \frac{\partial(\Phi_1/Y_{p+1}, \Phi_1/Y_{p+2}, \cdots \Phi_1/Y_n)}{\partial(Y_{p+1}, Y_{p+2}, \cdots Y_n)}. \tag{9a}$$

When $p = n-1$, this reduces to

$$\Phi_2 = -Y_n^2 (\partial/\partial Y_n)(\Phi_1/Y_n).$$

By differentiation of (8) with respect to $|Y_s|$ at constant all the other Y's, we can find the partial derivatives of a Φ when the set of variables taken as independent is not its own set. When $1 \leq s \leq p$, we get

$$\frac{\partial \Phi_2}{\partial |Y_s|} = \frac{\partial \Phi_1}{\partial |Y_s|} - \sum_{r=p+1}^{n} |Y_r| \frac{\partial y_r}{\partial |Y_s|}$$

$$= y_s - \sum_{r=p+1}^{n} Y_r \frac{\partial y_s}{\partial Y_r}, \tag{10}$$

using (6) and (7). This result also might be expressed in Jacobian form, for it is of the same form as (9). When $p < s \leq n$, there is only one case of interest, namely, when $p = n-1$ and $r = s = n$. We get

$$\partial \Phi_2 / \partial |Y_n| = \partial \Phi_1 / \partial |Y_n| - y_n - |Y_n| \partial y_n / \partial |Y_n|$$

$$= -Y_n \partial y_n / \partial Y_n. \tag{11}$$

We might introduce more than two Φ's into the problem simultaneously; but the equations obtained would be mostly of small importance and would be very complicated to deal with except in special cases. There is however one important type of formula in which four different canonical sets of variables are involved; the formula for the difference between constant pressure and constant volume specific heats is included in this type.

We start from the familiar mathematical identity

$$\left(\frac{\partial y_r}{\partial Y_r}\right)_2 - \left(\frac{\partial y_r}{\partial Y_r}\right)_1 = \left(\frac{\partial y_r}{\partial Y_n}\right)_1 \left(\frac{\partial Y_n}{\partial Y_r}\right)_2.$$

Here the suffix 1 implies that the set of variables corresponding to Φ_1 are to be taken as independent in forming the differential coefficient in question, and 2 implies that the set corresponding to Φ_2 are to be taken as independent. We have assumed too that $p = n-1$. Multiply both sides of this equation by Y_r and use (7); this yields

$$Y_r \left(\frac{\partial y_r}{\partial Y_r}\right)_2 - Y_r \left(\frac{\partial y_r}{\partial Y_r}\right)_1 = Y_r \left(\frac{\partial y_n}{\partial |Y_r|}\right)_1 \left(\frac{\partial |Y_n|}{\partial Y_r}\right)_2.$$

The two terms on the left-hand side can now be dealt with by means of (11), so that we get finally

$$\left(\frac{\partial \Phi_3}{\partial Y_r}\right)_1 - \left(\frac{\partial \Phi_4}{\partial Y_r}\right)_2 = Y_r \left(\frac{\partial y_n}{\partial Y_r}\right)_1 \left(\frac{\partial |Y_n|}{\partial Y_r}\right)_2. \tag{12}$$

Here the canonical set of variables corresponding to Φ_3 differs from set 1 in that y_r replaces Y_r, and set 4 differs from set 2 in the same way.

There is one other result which may be mentioned. Write the Φ corresponding to the general canonical set as $\Phi^{x_1, x_2, \cdots x_p, X_{p+1}, \cdots X_n}$. Then it follows from (3) that

$$\Phi^A+\Phi^B+\Phi^C+\cdots=\Phi^{A'}+\Phi^{B'}+\Phi^{C'}+\cdots, \quad (13)$$

provided that each variable occurring in the superscripts A, B, C, etc. occurs in the superscripts A', B', C', etc., the same number of times. A particular case will make this clear. Consider the variables S, V, T, and P. Then

$$\Phi^{SV}+\Phi^{PT}=\Phi^{SP}+\Phi^{VT}$$

or in ordinary notation (following Guggenheim's *Modern Thermodynamics*) $E+G=H+F$.

The Application of the Generalized Formulae

Eqs. (5) to (12) contain in epitome most of the important basic results of thermodynamics. To show how to employ them it will be best to take a couple of examples.

Consider first Eq. (7). Put $n=2$ and take S, V, T, and P as variables. We take as our Y's any canonical set chosen from among these four variables, say S and P; then the corresponding y's are T and V, respectively. The Φ corresponding to the choice of S and P as independent variables is the heat content, H. Thus, allowing for the sign change whenever V appears in an equation, (7) becomes

$$\partial^2 H/\partial|S|\partial|P|=\partial T/\partial|P|=-\partial V/\partial|S|;$$

or, remembering our rule about the interpretation of the symbols $|S|$ and $|P|$,

$$\partial^2 H/\partial S\partial P=\partial T/\partial P=\partial V/\partial S.$$

The other three Maxwell relations arise similarly when we take S and V, T and V, and T and P as independent variables. What is particularly to be remarked about this method is the elegant way in which the plus and minus signs are manipulated.

As a second, more complicated, example, we will take Eq. (12). Once again put $n=2$ and take S, V, T, and P as our variables. For the set 1 of variables we will choose T and P with G as the characteristic function; for set 2, T and V with F; for set 3, S and P with H; and for set 4, S and V with E. This choice is in accordance with the requirements of the equation. This gives at once the familiar result for the difference between constant pressure and constant volume specific heats, namely

$$\left(\frac{\partial H}{\partial T}\right)_P-\left(\frac{\partial E}{\partial T}\right)_V=T\left(\frac{\partial V}{\partial T}\right)_P\left(\frac{\partial P}{\partial T}\right)_V.$$

Koenig's f_1^1 Families of Equations

It will be seen that this method affords a very ready way of generating families of thermodynamic equations of the f_1^1 type considered by Koenig.[2] We have only to take the requisite generalized formula and make a fairly obvious sequence of substitutions to obtain all the members of a family. The procedure seems to be considerably neater than that of Koenig, who requires a rather complicated series of arrays of characteristic functions and variables in order to make the necessary sequence of substitutions and to obtain equations with the appropriate signs. Moreover, as will be seen later, the present method is more readily extended to other systems than the type so far considered.

To show that the present method of generating families of thermodynamic equations is in every respect as powerful as Koenig's, we must consider how to deduce the generalized formula when a particular case is given. An obvious method is to recapitulate in generalized notation the proof used for the particular case, but this is usually unnecessary.

Let us take for example the equation

$$\partial^2 H/\partial T\partial P=-T(\partial^2 V/\partial T^2)_P.$$

Here the set of variables is T and P and the corresponding Φ is G. There is also an H in the equation; H is the characteristic function of the set S and P. So we take Y_1 for P, y_1 for V, Y_2 for T, y_2 for S, and Φ_2 for H; we get

$$\partial^2\Phi_2/\partial Y_1\partial Y_2=Y_2(\partial^2 y_1/\partial Y_2^2)_{Y_1},$$

where the sign is still to be adjusted. We now place absolute value signs round every Y and correct the signs of the various terms to agree with the particular case given. We get

$$\partial^2\Phi_2/\partial|Y_1|\partial|Y_2|=-|Y_2|(\partial^2 y_1/\partial|Y_2|^2)_{Y_1}.$$

We can of course omit the absolute value signs when a pair of Y's occur together; this enables us to write more simply

$$\partial^2\Phi_2/\partial|Y_1|\partial Y_2=-Y_2(\partial^2 y_1/\partial Y_2^2)_{Y_1}.$$

[2] Koenig, J. Chem. Phys. 3, 29 (1935).

This is the equation obtained from (11) by setting $n=2$ and differentiating with respect to $|Y_1|$.

The Number of Members of a Family

It is of interest to see how many members each family of equations contains. There are obviously as many equations of type (5) as there are Φ's. Since a canonical set of variables is got by choosing one member from each of the X_r, x_r pairs, and there is a Φ corresponding to each canonical set, there are 2^n Φ's and 2^n equations of this type. Each Φ gives rise to n equations of type (6), so there are in all $n\cdot 2^n$ equations of this type. Similarly, each Φ yields $\frac{1}{2}n(n-1)$ equations of type (7), so there are $n(n-1)\cdot 2^{n-1}$ equations of this type in all.

It is unnecessary to go through each case in detail. The following are the actual results for the rest of the equations:

Eq. (8). $2^{n-1}(2^n-1)$ equations in all. These can be split into groups according to the value of p, that is, according to the number of terms the equation contains. There are $2^{n-1}n!/(p!n-p!)$ equations in each of these groups.

Eq. (9). $2^n(2^n-1)$ equations in all; $2^n n!/(p!n-p!)$ in each group.

Eq. (10). $n\cdot 2^{2n-1}$ equations in all; $2^n n!/(p-1!\,n-p!)$ in each group.

Eq. (11). $n\cdot 2^n$ equations.

Eq. (12). $n(n-1)\cdot 2^{n-1}$ equations.

For a "closed" system, a system at constant composition, we have $n=2$. Most of the families of equations considered by Koenig are closed-system equations: it is easily verified that inserting $n=2$ into the expressions just given for the number of members of a family leads in each case to the number given by Koenig. Thus there are four Maxwell relations from (7), and eight Gibbs-Helmholtz equations from (9) with $p=n-1$.

For a one-component system, $n=3$. Koenig ignores in his investigation equations in which the μ's appear as independent variables, so we cannot simply insert $n=3$ in our expressions for the number of members of a family. There are in fact no new equations of type (5). Type (6) yields one new equation for each Φ, so we get the four-membered family

$$\mu=\left(\frac{\partial E}{\partial N}\right)_{SV}=\left(\frac{\partial H}{\partial N}\right)_{SP}=\left(\frac{\partial F}{\partial N}\right)_{TV}=\left(\frac{\partial G}{\partial N}\right)_{TP}.$$

Likewise Eq. (7) yields an eight-membered family.

Most of the equations for systems for which $n>3$ represent nothing more than unnecessary duplication of equations already obtained. Thus for $n=4$ we should get the pair of equations

$$\mu_1=(\partial E/\partial N_1)_{SVN_2},\quad \mu_2=(\partial E/\partial N_2)_{SVN_1}.$$

There are, however, relations like

$$(\partial\mu_1/\partial N_2)_{N_1}=(\partial\mu_2/\partial N_1)_{N_2},$$

which are of interest; Koenig's treatment would require a special extension to include such equations.

Extension of Systems of Other Types

We have so far considered a system for which such things as capillary and electrical work terms can be neglected. But the method can be extended immediately to any system for which there holds an equation of the form of (2).

Thus, for a closed system containing an approximately plane interface

$$dE^s=TdS^s-pdV^s+\gamma dA,$$

where E^s, S^s, and V^s are the surface energy, entropy, and volume, γ is the surface tension, and A is the surface area.[3] This equation is of the form of (2), so the generalized Eqs. (5)–(11) are immediately applicable. By way of illustration, let us take the canonical set of variables P, T, and A; then (7) gives

$$(\partial\gamma/\partial T)_{PA}=-(\partial S^s/\partial A)_{PT};$$

$$(\partial\gamma/\partial P)_{TA}=(\partial V^s/\partial A)_{PT}.$$

Or again, the electrocapillary equation[4]

$$dG=\gamma dA+\Delta\varphi dq$$

(at constant p, T) where $\Delta\varphi$ is the electrical potential difference and q is the quantity of electricity flowing round the external circuit, gives at once

$$(\partial\gamma/\partial\Delta\varphi)_A=-(\partial q/\partial A)_{\Delta\varphi},$$

the Lippmann-Helmholtz equation.

[3] Butler, *Chemical Thermodynamics, Part II* (London, 1934).

[4] Craxford, Phil. Mag. [7] **16**, 66 (1933).

As a third example, let us take the equation for closed one-phase systems in a magnetic field

$$dE=TdS-pdV+HdM,$$

where H is the magnetic field and M the magnetic moment.[5] Typical results which follow from the generalized equations are

$$(\partial T/\partial M)_{SV}=(\partial H/\partial S)_{MV},$$

$$(\partial E/\partial M)_{TV}=H-T(\partial H/\partial T)_{MV},$$

$$(\partial\Phi_3/\partial T)_{PM}-(\partial\Phi_4/\partial T)_{PH}=T(\partial H/\partial T)_{PM}(\partial M/\partial T)_{PH}$$

(where $\Phi_3=E+PV$ and $\Phi_4=E+PV-HM$). The third equation here is the formula for the difference between the constant moment and constant field specific heats, both at constant pressure.

The Internal Energy as a Homogeneous Linear Function of the Extensive Variables of the System

Up to the present we have made no use of the fact that E is a homogeneous function of the first degree in the X's. From Euler's theorem we get

$$E=\sum_{r=1}^{n} X_r\partial E/\partial X_r=\sum_{r=1}^{n} x_rX_r. \tag{14}$$

Differentiating this and using (2) we get the generalized Gibbs-Duhem formula

$$\sum_{r=1}^{n} X_r dx_r=0. \tag{15}$$

(15) shows that the canonical set consisting of all the x's is not an independent set. To give a complete description of the system it is necessary to include at least one X, in order to define the extent of the system.

The Φ corresponding to the canonical set of all the x's is identically zero, for it is equal to $E-\sum_{r=1}^{n}x_rX_r$. This Φ might perhaps be excluded from consideration in the earlier part of this paper. But we should not on these grounds exclude $G(=E-TS+PV)$ in the case of a closed system. We must remember that the physical process involved in deriving (14) from (2) is that of increasing the quantity without altering the state of the system; this is not a possible process for a system at constant all the N's (i.e., a closed system). In fact the simplest case to which (14) applies is that of a one-component system, with $n=3$.

The formulae obtained with the aid of (14) cannot be treated by the Y notation hitherto adopted, because the distinction between intensive and extensive variables is now of importance in other respects than that of determining the signs of the terms. The results are thus necessarily less elegant, and the families of equations (the f_2^1 families of Koenig) more restricted. In practice (15) is by far the most important equation of the f_2^1 class, so we shall not develop the matter very far.

From (3) and (14) we get

$$\Phi=\sum_{r=p+1}^{n} x_rX_r. \tag{16}$$

The partial derivatives of Φ in the corresponding canonical set are thus given by

$$\partial\Phi/\partial x_s=\sum_{r=p+1}^{n} X_r\partial x_r/\partial x_s \quad (1\leq s\leq p),$$

$$\partial\Phi/\partial X_s=x_s+\sum_{r=p+1}^{n} X_r\partial x_r/\partial X_s \quad (p<s\leq n).$$

Comparing these expressions with (6) we find that

$$X_s+\sum_{r=p+1}^{n} X_r\partial x_r/\partial x_s=0, \tag{17}$$

$$\sum_{r=p+1}^{n} X_r\partial x_r/\partial X_s=0. \tag{18}$$

These can be converted further by using (7). We find

$$X_s=\sum_{r=p+1}^{n} X_r\partial X_s/\partial X_r, \tag{19}$$

$$\sum_{r=p+1}^{n} X_r\partial x_s/\partial X_r=0. \tag{20}$$

In (17) and (19), s ranges from 1 to p, and in (18) and (20), from $p+1$ to n. Eq. (18) is of considerable importance, for it is the form in which the Gibbs-Duhem relation is usually applied.

[5] Stoner, Phil. Mag. [7] **19**, 565 (1935).

Electronic Structures of Molecules

XIV. Linear Triatomic Molecules, Especially Carbon Dioxide

ROBERT S. MULLIKEN, *Ryerson Physical Laboratory, University of Chicago*

(Received August 20, 1935)

Electron configurations of the triatomic linear molecules CO_2, BO_2^-, N_2O, CS_2, COS, NO_2^+, N_3^-, NCO^-, NCS^-, BeF_2, $HgCl_2$, ClCN, ClBO, etc. are given. The electron configurations probably of all of these are formally analogous, or formally identical in the case of isoelectronic molecules, such as CO_2, N_2O, BeF_2, etc. The BeH_2 type is also touched on. The relations of the electron configurations to ordinary valence conceptions are discussed, and the importance in practice of cases intermediate between those represented by simple valence formulas is emphasized. The usefulness of the present method in giving a simple description of intermediate cases of all sorts (between double-bonded A=B=C and single-bonded A−B−C, between homopolar A−B−C, etc., and heteropolar $A^-B^{++}C^-$, etc., between A−B≡C and $A^+=B=C^-$, etc.) is brought out. The ionization potentials of CO_2, CS_2, N_2O, $HgCl_2$ are interpreted in relation to their electron configurations. The minimum potentials of CO_2, of CS_2, and of $HgCl_2$, respectively, correspond to removal of a nearly nonbonding $p\pi$ electron of the O, S, or Cl atom. It is shown that the ultraviolet emission bands of CO_2 probably represent transitions among four electron states of CO_2^+ which correspond to the four lowest ionization potentials of CO_2; if this interpretation of the bands is correct, the CO_2^+ molecule has a linear form in these states. According to this interpretation, the four lowest potentials of CO_2 are probably 13.72, 17.09, 18.00, and about 21.5 volts (or perhaps 14.63, 18.00, 18.91, and about 22.4 volts). These values are based on identification of the CO_2 Rydberg absorption series limit at 18.00 volts with one of the potentials. The minimum potential above obtained (13.72 or perhaps 14.63 volts) differs considerably from the accepted value 14.3 or 14.4 volts based on electron impact. Radicals N_3, NCO, NCS, and molecules NO_2 and others are also touched on. A reason for the triangular form of NO_2 is found in the fact that linear NO_2^+ (like CO_2 or N_2 or NO^+) is composed of a stable system of closed shells, while the final electron added to make neutral linear NO_2 would have to go into a probably fairly high energy antibonding orbital (as in NO). Evidently the actual NO_2 avoids this by being triangular. Ultraviolet absorption spectra of CO_2, CS_2, and COS are also considered.

1. NORMAL STATE OF CO_2

IN X of this series,[1] various molecules containing the C=O and C=S double bond in compounds $\begin{matrix}\diagdown\\ C=O\\ \diagup\end{matrix}$ and $\begin{matrix}\diagdown\\ C=S\\ \diagup\end{matrix}$ were considered. In the present paper, O=C=O and various other linear triatomic molecules and ions whose structures are more or less the same (N_2O, BO_2^-, N_3^-, NO_2^+, NCO^-) or analogous (CS_2, COS, NCS^-, etc.) are considered. On comparison with the results of X, it will be found that, although relations can be traced and although here as well as there it is justifiable to speak of C=O and C=S double bonds (essentially two pairs of bonding electrons per C=O or C=S bond), the electronic structures of these bonds are in effect very different here than there. In addition to the double-bonded types, certain other linear triatomic molecules ($HgCl_2$, BeF_2, CNCl, BOCl, and the like) are discussed here, since it is found that their electronic structures are closely related, at least formally, to those of the double-bonded types.

The structure of CO_2 has already been described briefly in I of this series.[2] The structure there indicated for the normal state (symmetry $D_{\infty d}$ like O_2 or H_2) can be written, omitting 1*s* electrons, as

$$(2s)^2(2s)^2(\sigma+s+\sigma,\sigma_g)^2(\sigma+\sigma-\sigma,\sigma_u)^2(\pi+\pi+\pi,\pi_u)^4(\pi-\pi,\pi_g)^4,\ {}^1\Sigma^+_g. \tag{1a}$$

Locn.	O O	O−C−O	O−C−O	O−C−O	O↔O
Pred. $I_{vert.}$	two values <32	>19.1	>14.2	>14.0	<15.23
Obs. I	− −	21.5? (or 22.4?)	18.0 (or 18.9?)	17.1 (or 18.0?)	13.7 (or 14.6?)

[1] R. S. Mulliken, J. Chem. Phys. **3**, 564 (1935): X of this series.

[1a] For a general survey of data and further references on CO_2, N_2O, CS_2, HgX_2, etc., cf. R. de L. Kronig, *The Optical Basis of Chemical Valence*, The Macmillan Co., New York, 1935; and H. Sponer, *Molekülspektren I* (Julius Springer, Berlin, 1935); *Landolt-Börnstein Tabellen*, fifth edition, third Sup. Volume, Part I (J. Springer, 1935): electric moments etc.

[2] R. S. Mulliken, Phys. Rev. **40**, 60 (1932): I.

That configuration (1a), composed of closed shells, is essentially correct will be shown in section 4 to be extremely probable.

In (1a) the four most loosely bound electrons are in a π_g molecular orbital of LCAO type[3] $\alpha(2p\pi_A - 2p\pi_B)$, with $\alpha = 2^{-\frac{1}{2}}$ approximately (A and B refer to the two O atoms). It will be noted that this $(\pi-\pi)$ orbital involves only the two O atoms (cf. section 4 for derivation of this result), and so gives neither bonding nor antibonding between C and O. Technically, it is O$\underline{\leftrightarrow}$O antibonding, but since the two O atoms are relatively far apart, this effect is of little importance, i.e., the orbital is practically nonbonding. Because of the relatively large distance between the O atoms, we have here a case where, unlike the usual case of strongly bonding or antibonding orbitals,[3] the LCAO form must represent a good approximation to the true molecular orbital. Here it is $2^{-\frac{1}{2}}(2p\pi_A - 2p\pi_B)$, with the $2p\pi$ O atom orbitals of about the same size as for neutral O atoms, or better, as for somewhat negatively charged O atoms, because of the C^+O^- polarities within the molecule.

But now since the $(\pi-\pi)$ molecular orbital connects two atoms relatively far apart, should we not get a much better approximation for the total wave function if the four electrons assigned to $(\pi-\pi)$ in (1a) were assigned instead to corresponding atomic orbitals, i.e., to $2p\pi$ O atom orbitals, with two electrons on each O atom? This change would seem to be called for by our usual rule that the use of molecular orbitals gives good approximations only for strongly shared electrons, while atomic orbitals are best for unshared (i.e., nonbonding) electrons. If we make this change, the assignment of the last four electrons is altered so that (1a) is replaced by:

$$\cdots(2p\pi_O{}^2 2p\pi_O{}^2), \quad {}^1\Sigma^+_g. \tag{1}$$

In (1) it must be specifically understood that the actual state corresponds to a ${}^1\Sigma^+_g$ wave function built up approximately from determinants (four in number) in which the m_l and m_s values of the last four (i.e., the $2p\pi_O$) electrons appear in various combinations, but only in such ways that there are two $2p\pi$ electrons on each O atom, and that the sum of the m_l's, and likewise of the m_s's, is zero. The fact that CO_2 is diamagnetic gives assurance that a ${}^1\Sigma$ function, which can then hardly be other than ${}^1\Sigma^+_g$, is needed in (1).

In regard to the relative merits of (1) and (1a), obviously (1a) is neater, and also it correctly indicates the fact that there must be only a single I value corresponding to the four π nonbonding O atom electrons, and that removal of one of them gives a ${}^2\Pi_g$ state of CO_2^+. On the other hand, it would seem that the configuration (1), although rather awkward, should represent a much better approximation according to our usual criteria. It can be shown, however, that when the complete wave functions corresponding to (1) and (1a) are written out, the difference between them is not as great as one might have anticipated.

This is because of certain relations which exist between the $(\pi+\pi+\pi)^4$ and the $(\pi-\pi)^4$ or $(2p\pi_O{}^2 2p\pi_O{}^2)$ shells. If $(\pi+\pi+\pi)$ were to lose entirely its C$-$O bonding properties (i.e., if we had $b''=0$ in (2), below), making it of the type $\beta(2p\pi_A + 2p\pi_B)$, with $\beta = 2^{-\frac{1}{2}}$ nearly, then (1) and (1a), respectively, would become

$$\cdots(2p\pi_A)^4(2p\pi_B)^4 \text{ and } \cdots(\pi+\pi, \pi_u)^4(\pi-\pi, \pi_g)^4.$$

Now it can be shown very easily that in this case, if we use the LCAO approximations for $(\pi+\pi)$ and $(\pi-\pi)$, as would be correct here if $b''=0$, the complete antisymmetrical wave functions corresponding to (1) and (1a) would be *identical*.

The fact that $b''\neq 0$ in (2) of course disturbs the foregoing identity of the (1) and (1a) wave functions, but nevertheless leaves them more nearly alike than one would have at first thought. Hence while (1) is probably better than (1a), still (1a) should not be bad, and has certain advantages as already noted.

Turning now to the other orbitals in (1) or (1a), it will be noted that we have used three whole-molecule orbitals each of which gives bonding between the central C atom and both the O atoms simultaneously. Written out in the form of rough LCAO approximations, these three bonding orbitals are as follows (A and B refer to the O atoms):

[3] R. S. Mulliken, J. Chem. Phys. **3**, 375 (1935): VI.

[4] R. S. Mulliken, J. Chem. Phys. **1**, 492 (1933): V.

$$a(2p\sigma)_A+b(2s)_C+a(2p\sigma)_B,$$
$$a'(2p\sigma)_A+b'(2p\sigma)_C-a'(2p\sigma)_B, \quad (2)$$
and $$a''(2p\pi)_A+b''(2p\pi)_C+a''(2p\pi)_B.$$

The positive end of each $(2p\sigma)_O$ is taken as directed toward the C atom, the positive end of $(2p\sigma)_C$ toward oxygen atom A; with this convention, all O−C interactions in (2) are bonding, since the overlapping atomic orbitals used are of like sign in regions of strong overlap. The construction of the forms given in (2), and others, including $(\pi-\pi)$ of (1a), will be further discussed in section 4.

Rough estimates can be made of the relative values of coefficients a, b, etc., in (2). These depend partly on symmetry, partly on electronegativity of O relative to C, in a manner discussed in XI, XII of this series.[5] As electroaffinities of $2s_C$, $2p_C$, and O (i.e., $2p_O$), it will probably be safe for rough qualitative purposes here to use the usual P scale values (cf. XII), even though these are based on single-bonded compounds while here we have double bonds. These values, relative to P_H, are $P(2s_C)=3.04$, $P_O=1.40$, $P(2p_C)=-0.28$.

If $(2s)_C$ had the same electroaffinity as $(2p\sigma_A+2p\sigma_B)$, then these would appear with equal coefficients in the first line of (2), assuming the forms $2s_C$ and $(2p\sigma_A+2p\sigma_B)$ each first separately normalized (cf. XII, section 2). Neglecting the slight lack of orthogonality between $2p\sigma_A$ and $2p\sigma_B$, we should multiply $(2p\sigma_A+2p\sigma_B)$ by a normalizing factor $2^{-\frac{1}{2}}$, and would thus have $b=2^{\frac{1}{2}}a$ in the first line of (2).

However, since $2s_C$ is actually considerably more electronegative[5] (i.e., higher in effective term value) than $(2p\sigma_A+2p\sigma_B)$,—or what is nearly the same thing, than $2p\sigma_O$,—we must expect b/a to be considerably greater than $2^{\frac{1}{2}}$. In a similar way it can be shown that b'/a' and b''/a'' must each be very considerably less than $2^{\frac{1}{2}}$. We might then proceed further[5] to determine approximate numerical values of b/a, etc., but this will not be attempted here.

It is of interest to note in the foregoing that as a result of the symmetry of the molecule, just as in CH_4 and CX_4,[4] there is no mixing between $2s_C$ and $2p_C$. In other carbon compounds of lower symmetry, however,[6] some mixing occurs, usually of $2s_C$ with $2p\sigma_C$. [In the present case, although mixing of $2s_C$ with $2p\sigma_C$ is absent, mixing of $2s_O$ with $2p\sigma_O$ does occur (see below).]

In addition to the assignments already mentioned, four electrons in (1a) or (1) are assigned to nonbonding O atom $2s$ orbitals. Instead one might assign these electrons to molecular orbitals which may be indicated by $(s+s,\ \sigma_g)$ and $(s-s,\ \sigma_u)$. There would then be more or less mixing between these and $(\sigma+s+\sigma,\ \sigma_g)$ and $(\sigma+\sigma-\sigma,\ \sigma_u)$, respectively. If this mixing were very pronounced, it would definitely be much better to substitute whole-molecule orbitals for $2s_O$ orbitals in the case of the four electrons in question (cf. section 4).

The nature of the valence bonds in CO_2 is related to configuration (1) or (1a) as follows. Essentially, there are just eight bonding electrons (σ_g, σ_u, and π_u in (1)). Since these, on a time average, are distributed in a symmetrical manner, there are two pairs of bonding electrons per C=O bond. The bonding would be pure homopolar if we had $b/a=b'/a'=b''/a''=2^{\frac{1}{2}}$. Actually this is not true, but $b/a>2^{\frac{1}{2}}$ (favoring the C atom), while b'/a' and $b''/a''<2^{\frac{1}{2}}$ (favoring the O atoms), with a net effect decidedly favoring the O atoms, in accordance with their greater electronegativity. That is, the bonding is partially polar with the O atoms decidedly negative.

It may be of interest to give a rough estimate of the relative charges of the C and O atoms in accordance with Eq. (41) of XI of this series,[5] by using the method of calculation of section 1 of XII.[5] The mean effective electronegativity of C is $P=0.55$, that of O is 1.40, hence $P_O-P_C=0.85$, for C−O *single bonds*. It is uncertain how nearly correct this will be for double bonds, but we can try it. Substituting in Eq. (41) of XI, we get $Q_C=+0.27e$, per bond. Since there are four bonds, the calculated total Q_C is $+1.08e$, so that CO_2 may be formulated as $O^{-0.54}C^{+1.08}O^{-0.54}$. This would correspond to a bonding 27 percent heteropolar, 73 percent homopolar in character, which appears not unreasonable, but of course represents only a very rough estimate.

In connection with (1) or (1a), vertical I's have been predicted by the usual methods.[7] The

[5] R. S. Mulliken, J. Chem. Phys. 3, 573, 586 (1935): XI, XII.

[6] R. S. Mulliken, J. Chem. Phys. 3, 517 (1935): IX.

[7] R. S. Mulliken, J. Chem. Phys. 3, 514 (1935): VIII.

predictions are based on the following valence state I's, also obtained in the usual way:[7] C atom I° values, in volts: 21 for $2s$, 11.23 for $2p\sigma$, 10.86 for $2p\pi$; O atom I° values: 17.17 volts for $2p\sigma$ and $2p\pi$; O atom I^* values: 32 volts for $2s$, 15.23 volts for $2p\pi$.

The predicted I's involving inequality signs can be made more definite if we estimate the magnitudes of the inequalities. Comparison with CO is helpful in the case of the π_u orbital (not, however, for the σ orbitals, where complications arise in CO). In CO there is a C−O bonding π orbital similar to π_u of CO_2, with predicted $I>14.0$ just as for the latter. The observed I is known experimentally to be 17.1 volts, assuming the correctness of the electron impact value 14.3 volts for the minimum I of CO.[8] Hence the inequality sign amounts to about 3 volts for π in CO. A similar or perhaps even larger value would appear reasonable for π_u of CO_2; also a comparable value for σ_u of (1).

For the nonbonding $2p\pi_O$ of (1) or $(\pi-\pi, \pi_g)$ of (1a), the inequality sign corresponds mainly to effects of charge-transfer, whereby I should be lessened because of net negative charges on the O atoms. These net charges may be expected to be less than in such a case[1] as H_2O or H_2CO, since the charges on both O atoms must here be drawn entirely from one C atom. Also, the $2p\pi$ or $(\pi-\pi)$ orbital is strongly subjected to the positive field of the neighboring C atom. On the whole, the inequality between I_{obs} and I^* should be considerably less here than in H_2CO or H_2O. —Similar considerations apply to the nonbonding $2s$ orbitals in (1) or (1a).

Experimentally, we may first consider the electron-impact I of CO_2, which is 14.3 volts according to Mackay.[9] There can be no doubt, in view of the foregoing predictions, that this must correspond to the removal of one $2p\pi_O$ from (1) or one $(\pi-\pi)$ from (1a), and that it must give the normal state of CO_2^+, which may be written

$$\begin{aligned} &\cdots(\pi-\pi)^3, \quad {}^2\Pi_g \text{ corresponding to (1a)}, \\ \text{or} \quad &\cdots(2p\pi 2p\pi^2), \ {}^2\Pi_g \text{ corresponding to (1)}. \end{aligned} \tag{3}$$

A second experimental I is obtained from a pair of Rydberg series in the ultraviolet absorption spectrum of CO_2.[10] These both give $I=18.00 \pm 0.03$ volts. This I (unless it should prove spurious, as might be remotely possible) must clearly belong either to π_u or to σ_u of (1) and (1a), more probably to the former, as we shall see below.

2. Ultraviolet CO_2^+ Emission Bands

Further progress can now be attempted by a consideration of the emission band spectrum which is obtained by electrical discharges in CO_2. This spectrum has been shown to contain at least three band systems.[11] There has been much discussion as to whether the spectrum is due to CO_2 or to CO_2^+, but the weight of evidence now seems to favor the latter as emitter of the entire spectrum. In the case of the strong double band near λ2900 the direct experimental evidence for CO_2^+ is nearly conclusive,[12] as is also, independently, the evidence of the band structure.

The λ2900 band is apparently composed of two similar but not identical sub-bands each of complex structure, one centered about λ2883, the other about λ2895. Both sub-bands show marked Zeeman effects.[11] No satisfactory analysis of the rotational structure has been made, but there are evidently several branches in each band, and the existence of perturbations has been established. The almost uniform spacings within the discernible series indicate that the moment of inertia is nearly unchanged from the initial to the final electronic state. This situation, in view of the Franck-Condon principle, also affords a reasonable explanation of the isolated occurrence of one double band: it is presumably mainly a 0,0 band, i.e., one starting and ending on vibrationless levels. The main band, however, is pre-

[8] Cf. R. S. Mulliken, Phys. Rev. **46**, 550 (1934).
[9] C. A. Mackay, Phys. Rev. **24**, 319 (1924).

[10] H. J. Henning, Ann. d. Physik [5] **13**, 599 (1932); G. Rathenau, Zeits. f. Physik **87**, 32 (1933).
[11] H. D. Smyth, Phys. Rev. **38**, 2000 (1931); **39**, 380 (1932). R. F. Schmid, Phys. Rev. **41**, 732 (1932); Zeits. f. Physik **83**, 711; **84**, 732 (1932). R. S. Mulliken, Phys. Rev. **42**, 364 (1932); in this paper the discussion of the κ selection rule (middle p. 365) is in error, the correct rules being $\Delta\kappa=0$ if $\Delta\Lambda=0$, $\Delta\kappa=\pm1$ if $\Delta\Lambda=\pm1$. R. F. Schmid, Zeits. f. Physik **85**, 384 (1933): doublet structures of lines in main band system. R. F. Schmid, Zeits. f. Physik **83**, 711 (1933): λ2900 double band. R. F. Schmid, Zeits. f. Physik **84**, 732 (1933): λ3660 double band.
[11a] P. E. Martin and E. F. Barker, Phys. Rev. **41**, 291 (1932).
[12] A. S. Roy and O. S. Duffendack, Proc. Nat. Acad. Sci. **19**, 497 (1933).

sumably overlain by weaker bands starting from upper vibrating states and ending on lower vibrating states but without change of vibrational quantum numbers.[11]

What is known of the structure appears on the whole to be most consistent with a $^2\Pi \rightarrow {}^2\Sigma$ or a $^2\Sigma \rightarrow {}^2\Pi$ transition in a linear molecule. In view of the strong experimental evidence[12] that the final state is the normal state of CO_2^+, the transition should be $^2\Sigma^+{}_u \rightarrow {}^2\Pi_g$. The two parts of the double band should then correspond to the two components of the $^2\Pi_g$, and the observed doublet width in the band (about 161 cm^{-1}) should be that of the $^2\Pi_g$. This doublet width $\Delta\nu$ should be equal to the spin-orbit coupling coefficient a for a $2p$ electron of the O or O^+ atom, since the $^2\Pi_g$ is obtained by removing a $2p\pi_O$ or $(\pi - \pi, \pi_g)$ electron.[13] The coefficient a is 149 cm^{-1} for neutral O and about 270 cm^{-1} for O^+, and the observed $\Delta\nu$ might be expected to lie between these values. [In this connection, cf. the observed $\Delta\nu = 195$ cm^{-1} for the $^2\Pi_g$ normal state of O_2^+, in which one $(\pi - \pi, \pi_g)$ electron is present.] The observed $\Delta\nu = 161$ cm^{-1} in the λ2900 CO_2^+ band appears to be in reasonable agreement with the prediction.

Although other possible interpretations of the λ2900 band cannot be excluded with certainty until it has been analyzed, the foregoing considerations (together with others too numerous and detailed to give here) make it fairly certain that the band is $^2\Sigma^+{}_u \rightarrow {}^2\Pi_g$. The $^2\Sigma^+{}_u$, which from the frequency of the λ2900 band must be 4.28 volts above the $^2\Pi_{1/2g}$ lowest level of CO_2^+, is then identified as the state expected on removal of one σ_u electron from (1). That is, the transition is identified as being from

$$\cdots(\sigma_u)^{-1}, \quad {}^2\Sigma^+{}_u \tag{4}$$

to the $^2\Pi_g$ of (3).

The interval 4.28 volts checks fairly well with the interval between the minimum I of CO_2 observed at 14.3 volts (electron impact) and the higher I at 18.0 volts (Rydberg series). It will be seen, however, that the agreement is not accurate. Accepting the spectroscopic value as reliable, one finds that the minimum I of CO_2 must be $18.00 - 4.28 = 13.72$ volts ($\pm$ about 0.03). This is about 0.6 volts less than the electron impact value. Such a discrepancy is within the usual range of reliability of electron impact I's determined several years ago, and the direction of the discrepancy is the usual one.

An alternative possibility, however, is that the observed I at 18.00 volts may correspond to removal of a π_u electron from (1) to give

$$\cdots(\pi_u)^{-1}, \quad {}^2\Pi_u, \tag{5}$$

instead of a σ_u to give (4). This possibility will be discussed shortly.

Turning now to the λ3660 doublet band,[11] there is again a large Zeeman effect in both subbands. The structure seems to be simpler than in the λ2900 band. Again there appears to be only an isolated double band, presumably a (0,0) band, although Franck-Condon reasons for this are not evident, since the band structure indicates that the moment of inertia is larger in the upper state. Except for the pronounced Zeeman effects, which tend to favor the interpretation $^2\Sigma \leftrightarrow {}^2\Pi$ again, the structure appears consistent with $^2\Pi \leftrightarrow {}^2\Pi$. The relatively small observed $\Delta\nu$ (about 58 cm^{-1}) cannot readily be explained in terms of expected low energy states of CO_2^+ if we assume $^2\Sigma \leftrightarrow {}^2\Pi$.

Supposing the band is $^2\Pi_u \rightarrow {}^2\Pi_g$, starting from (5) and ending on (3), the observed $\Delta\nu$ can be immediately explained as the difference between a $\Delta\nu = 103$ cm^{-1} of the $^2\Pi_u$ and the value 161 cm^{-1} already found for the $^2\Pi_g$. The bands for a transition $^2\Pi_u \rightarrow {}^2\Pi_g$, both $^2\Pi$'s being case a and inverted, should contain four main series of lines, namely, two P, R sets each giving one strong head.[14] The observed structure, aside from additional weak series and heads which might be due to superposed bands involving vibrating states, looks like this.

A $\Delta\nu = 103$ cm^{-1} is reasonable for the $^2\Pi_u$ state of (5). The π_u orbital from which an electron has been removed to get (5) is in LCAO approximation a mixture of $2p\pi_C$ and $2p\pi_O$ (cf. (2)), and should have a spin-orbit coupling coefficient a intermediate between those of $2p$ of C and O (or tending toward something between those of C^+ and O^+). The coefficient a is 28 cm^{-1} for $2p$ of C and 43 cm^{-1} for C^+. By way of comparison with $\Delta\nu = 103$ cm^{-1} for π_u here, the observed

[13] R. S. Mulliken, Rev. Mod. Phys. **4**, 34–39 (1932).

[14] Cf. R. S. Mulliken, Rev. Mod. Phys. **3**, 90–155 (1931).

value for the rather similar π orbital in CO^+ (again a mixture of $2p\pi_C$ and $2p\pi_O$) is 125 cm^{-1}. The lower value here would tend to indicate a stronger proportion of $2p\pi_C$, less of $2p\pi_O$, which is not unreasonable.

If the foregoing interpretation of the λ3660 band is correct, the $^2\Pi_{1/2u}$ level of (5) is 3.36 volts above the $^2\Pi_{1/2g}$ level of (3), and 0.90 volt below the $^2\Sigma^+_u$ of (4). This is entirely reasonable according to our predicted I's for CO_2. A point supporting this interpretation is that the occurrence of the $^2\Pi_u$ level a little below the $^2\Sigma^+_u$ affords a reasonable possible explanation of the observed occurrence of perturbations in the λ2900 ($^2\Sigma^+_u \rightarrow {}^2\Pi_g$) band.

If we accept 18.00 volts (see above) as the I required to produce $^2\Sigma^+_u$ of (4) from neutral CO_2, we now get the following system of I's: 13.72 volts for π_g, 17.09 for π_u, 18.00 for σ_u. Another possibility is that 18.00 volts belongs to π_u, in which case we get 14.63 volts for π_g, 18.00 for π_u, 18.91 for σ_u. This seems less probable, since it makes the minimum I somewhat greater than the reported electron impact value, and makes the inequality signs in the predictions for σ_u and π_u very large (cf. (1)). In any case, it should be borne in mind that the foregoing conclusions based on the λ3660 band, while reasonable, are still open to some doubt until the rotational structure has been satisfactorily analyzed. Then again, there might perhaps be a slight possibility that the Rydberg series giving the 18.00 volt potential is illusory.

Finally, the remaining extensive system of red-shaded bands, extending from about λ3200 to λ3800 and beyond, can probably also be fitted into the CO_2^+ electron level scheme. The structures of these bands were at first found by Schmid to be of a simple $P-R$ branch type like $^1\Sigma \rightarrow {}^1\Sigma$ of a diatomic or linear molecule, although certain complications indicated $^1\Pi \rightarrow {}^1\Pi$ as more probable.[11] Schmid's later discovery that each band line is a very narrow doublet can, however, be understood most simply if the bands are $^2\Sigma \rightarrow {}^2\Sigma$. In a diatomic molecule composed of light atoms, this explanation of the doublets would be altogether the most probable. In the present case, however, the doublets might conceivably arise as a result of the presence of degenerate vibrations,[15] but the $^2\Sigma \rightarrow {}^2\Sigma$ explanation nevertheless appears on the whole the most probable. If the bands are $^2\Sigma \rightarrow {}^2\Sigma$, they cannot be due to neutral CO_2 but must belong to CO_2^+. Other evidence bearing on the question of CO_2^+ as against CO_2 appears inconclusive, although the regular appearance of these bands with the λ3600 and λ2900 bands supports their assignment to a common carrier; moderate differences observed in excitation behavior as compared with λλ3660, 2900 are obviously explainable by the different initial electronic states.

If the bands are $^2\Sigma \rightarrow {}^2\Sigma$, they can immediately be identified as $^2\Sigma^+_g \rightarrow {}^2\Sigma^+_u$, coming from

$$\cdots(\sigma_g)^{-1}, \quad {}^2\Sigma^+_g \tag{6}$$

in which a σ_g has been removed from (1), and ending on $^2\Sigma^+_u$ of (4). The energy changes corresponding to the observed bands are about 2.6–3.9 volts. The exact energy of the vibrationless transition is unknown, since the vibrational numbering is uncertain. A value of about 3.5 volts may be taken as a reasonable estimate; if correct it makes I about 21.5 volts or 22.4 volts for σ_g of CO_2, the former if $I=18.00$ volts belongs to σ_u, the latter if it belongs to π_u. Such values are in harmony with what is predicted for I of σ_g (cf. (1)).

Mention should be made of the moments of inertia for the various electronic levels of CO_2^+, as indicated by the band structures. In terms of the rotational constant B ($B=h/8\pi^2cJ$, J=moment of inertia), the relations are as follows: B about 0.34 cm^{-1} for $^2\Sigma^+_g(6)$ and about 0.38 cm^{-1} for $^2\Sigma^+_u(4)$, from Schmid's work;[11] B probably about the same for $^2\Pi_g(3)$ as for $^2\Sigma^+_u(4)$, hence about 0.38 cm^{-1} for both; B somewhat less for $^2\Pi_u(5)$ than for $^2\Pi_g(3)$, hence <0.38 cm^{-1}, if the λ3660 band is correctly interpreted above. Finally, for the normal state of neutral CO_2, $B=0.390$ from data on infrared bands.[11a] The above value B about 0.38 for the $^2\Pi_g$ normal state of CO_2^+ is in agreement with expectation, since the electron removed from neutral CO_2 to produce this state is a nearly

[15] In connection with this question, compare the important paper of R. Renner, Zeits. f. Physik **92**, 172 (1934). Renner's work would raise questions particularly in regard to the interpretations given above for the λ2900 and λ3600 bands, but not in such a way as to make these interpretations improbable in view of the evidence favoring them.

nonbonding one. In the case of the other three CO_2^+ states, (4), (5), and (6), the electron removed is a C−O bonding one, so that we would expect a larger J and smaller B than for neutral CO_2 or than for $^2\Pi_g(3)$ of CO_2^+. The differences, however, should not be great, since in each case only one bonding electron is missing out of the eight which are present in (1). The observed results are in agreement with expectation except in the case of $^2\Sigma^+_u(4)$, where the B does not show the expected decrease.

Although the foregoing interpretation of the emission bands obtained in CO_2 must be considered somewhat tentative until the bands have been rather completely analyzed, it seems worth putting forward as being rather probably correct and as furnishing also a guiding scheme for testing by further research. In the latter connection, one notes that a fourth system of CO_2^+ bands, representing the transition $^2\Sigma^+_g(6)\rightarrow{}^2\Pi_u(5)$, should be found in the same neighborhood as the other bands.

An interesting feature of the foregoing interpretation is that all the band systems attributed to CO_2^+ are here ascribed to the jumping of an electron from one inner orbital to another, no excited orbitals being involved. In this respect the spectrum would be like an x-ray spectrum, as are all the known spectra of CO^+, N_2^+, CN, and BO, except one N_2^+ system. Support for CO_2^+ as emitter of the present bands can be found in the absence of any marked predissociation. As in the bands of CO^+, N_2^+, CN, and BO, this can be readily explained by the fact (or probable fact here) that the bands involve mostly electron levels of low energy relative to the normal state of the emitting system.

In the preceding discussion, it has been assumed more or less tacitly that in the various electron states of CO_2^+ considered, the molecule is linear just as in the normal state of CO_2. While the structures of the λ2900 and λ3600 bands cannot yet be conclusively cited as support for this, what is known of them appears to agree with it. In the case of the main system of bands, attributed above to $^2\Sigma^+_g\rightarrow{}^2\Sigma^+_u$, the structure is definitely that of a linear molecule.[11] From the theoretical standpoint, it appears entirely reasonable that the known linear form of neutral CO_2 should be preserved in all the CO_2^+ ion states (3)–(6). In the normal state (3), the absence of a nonbonding electron should not appreciably alter the forces determining the bond angles. In the other states (4)–(6), where one bonding electron is removed, there appears to be no reason why the remaining bonding electrons should not find a linear form still the most stable.

3. Linear Molecules ABC

Langmuir[16] introduced the term isostere to designate molecules having the same number of electrons and believed to have essentially the same electronic structure as judged by their properties. As examples of isosteres Langmuir gave, among others, N_2, CO, CN^-; CO_2, N_2O, N_3^-, NCO^-.

It was shown by the writer and by Hund in 1928 that N_2 and CO (and NO^+ and implicitly CN^-) have very similar electronic structures in terms of molecular orbitals.[17] This gave added justification and a more precise meaning to Langmuir's concept of isosterism.

The nature of the isosterism of CO_2, N_2O, N_3^-, NCO^-, to which may be added NO_2^+ and BO_2^-, can now be made clear. To all of these as well as to the analogous molecules SCN^-, OCS, CS_2 and others, can be assigned electron configurations more or less similar to (1) or (1a) given above for CO_2, with supplementary descriptions of orbitals similar to those in (2). In this group also perhaps come XBO and XCN (X = halogen); for example, ClCN and ClBO are isoelectronic with SCN^-. Even BeF_2, isoelectronic with CO_2 but hardly isosteric, can be described by an at least formally similar configuration, while the other bivalent metal halides MeX_2 have analogous structures (Me = Mg, Ca, Hg, etc.).

The similarities and the differences among the molecules and ions just mentioned can best be understood by a systematic treatment. In each case, we can safely assume that we are dealing with a linear molecule ABC. In most cases linearity has been satisfactorily proved by evidence from band spectrum, electric moment, electron diffraction, or crystal structure data.[18]

[16] I. Langmuir, J. Am. Chem. Soc. **41**, 868, 1543 (1919).
[17] R. S. Mulliken, Phys. Rev. **32**, 186 (1928); F. Hund, Zeits. f. Physik **51**, 759 (1928).

The molecules ABC can be divided into two sets: (*a*) those of type ABA, where atoms A and C are identical, and the symmetry is $D_{\infty d}$; (*b*) those where A and C are different, giving symmetry $C_{\infty v}$. The treatment is simpler for the first type, which will be considered in the next section.

All the molecules ABC of both types are alike in having sixteen outer electrons. These all correspond, if ABC is separated into A+B+C, to *ns* and *np* outer electrons of atoms A, B, and C. For example in O+C+O we have two 2*s* electrons for each atom, and in addition two 2*p* for the C atom and four 2*p* for each O atom. In S+C+S everything is similar except that we have 3*s* and 3*p* instead of 2*s* and 2*p* electrons for the S atoms. When entering into the structure of ABC, *ns* may be labeled $ns\sigma$, while *np* splits up into two types $np\sigma$, $np\pi$.

Our problem now is to find the correct orbitals to which these sixteen electrons should be assigned in the normal states of the various molecules ABC. Matters will prove to be simplified if at first we assign them all to molecular orbitals, and afterwards decide whether and how the approximation can be improved by replacing some of these by corresponding atomic orbitals (cf. the case of CO_2 in section 1). In determining the nature of the molecular orbitals, we shall find it convenient to build them up in LCAO approximation out of the various *ns*, $np\sigma$, and $np\pi$ atomic orbitals.

There are twelve of these, capable, if fully occupied, of holding twenty-four electrons instead of the actual sixteen. They are $ns\sigma_A$, $ns\sigma_B$, $ns\sigma_C$, $np\sigma_A$, $np\sigma_B$, $np\sigma_C$, $np\pi_A$, $np\pi_B$, $np\pi_C$, the last three each embracing two linearly independent forms. Out of these twelve atomic orbitals exactly twelve LCAO molecular orbitals can be constructed (cf. V of this series,[4] sections 2, 4). The latter can be divided into a set of six σ molecular orbitals constructed from the six σ atomic orbitals, and a set of six $(3\times2)\pi$ orbitals constructed from the six $(3\times2)\pi$ atomic orbitals. The σ offer more difficulty than the π molecular orbitals.

4. Symmetrical Linear Molecules ABA

In the case of molecules of symmetry $D_{\infty d}$, the σ and π types of molecular orbitals can be subdivided, giving types σ_g, σ_u, π_u, π_g. In building up such orbitals, we can proceed in two steps. First we make linear combinations of the normalized atomic orbitals of A and C so as to obtain normalized forms conforming to the types σ_g, σ_u, π_u, π_g; then we combine the resulting forms with the normalized orbitals of atom B, which already belong to these types. Adopting the letters *s*, σ, π as shorthand for $ns\sigma$, $np\sigma$, and $np\pi$, we now have the following to work with (the normalization factors $2^{-\frac{1}{2}}$ are only approximate):

$$\begin{aligned}\sigma_g&: 2^{-\frac{1}{2}}(s_A+s_C),\ s_B,\text{ and } 2^{-\frac{1}{2}}(\sigma_A+\sigma_C)\\ \sigma_u&: 2^{-\frac{1}{2}}(s_A-s_C),\ \sigma_B,\text{ and } 2^{-\frac{1}{2}}(\sigma_A-\sigma_C);\end{aligned}\tag{7}$$

$$\begin{aligned}\pi_u&: 2^{-\frac{1}{2}}(\pi_A+\pi_C),\text{ and } \pi_B\\ \pi_g&: 2^{-\frac{1}{2}}(\pi_A-\pi_C).\end{aligned}\tag{8}$$

For each *s* orbital, the outer part is taken as positive in sign; for σ_A and σ_C, the end facing toward the central atom B is taken as positive; for σ_B, the end facing toward atom A is taken as positive.

We now have the problem of finding three new σ_g and three new σ_u forms by making suitable linear combinations of the forms in (7); and similarly of finding two new π_u forms from those in (8). The π_g in (8) is all right as it stands.

The three σ_g molecular orbitals can all be expressed by

$$\sigma_g=a2^{-\frac{1}{2}}(s_A+s_C)+b(s_B)+c2^{-\frac{1}{2}}(\sigma_A+\sigma_C);\tag{9}$$

the three different desired orbitals correspond to three different value-sets *a*, *b*, *c*. Similarly the three desired σ_u orbitals can all be described by

$$\sigma_u=a'2^{-\frac{1}{2}}(s_A-s_C)+c'2^{-\frac{1}{2}}(\sigma_A-\sigma_C)+b'(\sigma_B).\tag{10}$$

Assuming that we knew the forms and term values of the three initial orbitals in each case, each problem could be solved systematically by perturbation theory (cf. e.g., XII,[5] section 2, for a similar problem involving two initial orbitals). We shall not, however, attempt here to do more than to establish certain approximate qualitative relations among the coefficients *a*, *b*, *c* or *a'*, *b'*, *c'* belonging to each solution of (9) or (10).

In attacking either of the two problems, it is well to note certain fixed characteristics of the three initial functions. For definiteness let us first consider (9). Here it is always true that the

initial term value belonging to $2^{-\frac{1}{2}}(s+s)$ is very considerably larger than that of $2^{-\frac{1}{2}}(\sigma+\sigma)$, also that these two functions are approximately orthogonal. Both, however, are very far from being orthogonal to the third function s_B, and the largest perturbation effects occur between the latter and each of the former. Sometimes (e.g., N_3^-) the term value of s_B is somewhat larger than that of $(s+s)$, in other more usual cases (e.g., CO_2) it lies between those of $(s+s)$ and $(\sigma+\sigma)$, while in other cases (e.g., BeF_2 and perhaps BO_2^-) it is smaller than that of $(\sigma+\sigma)$.

In the case of (10), the functions $(s-s)$ and $(\sigma-\sigma)$ are always nearly orthogonal, and $(s-s)$ always has the larger term value. Sometimes (e.g., N_3^-) the term value of σ_B is a little larger than that of $(\sigma-\sigma)$, more usually it is less, or (e.g., BeF_2) very much less.

A qualitative survey of the approximate relative values of the coefficients in (9) and (10) can profitably be made for each of two special cases: (A), term value of s_B nearly equal to that of $(s+s)$, term value of σ_B nearly equal to that of $(\sigma-\sigma)$; (B), term value of s_B equal to that of $(\sigma+\sigma)$, of σ_B much less than that of $(\sigma-\sigma)$. The qualitative results for other cases can then readily be seen by interpolation or extrapolation. In making this survey, we can conveniently proceed as follows. In (9) for case A, we first solve the problem of the resonance between $2^{-\frac{1}{2}}(s+s)$ and s_B, neglecting $2^{-\frac{1}{2}}(\sigma+\sigma)$; then we consider the mutual perturbations between $(\sigma+\sigma)$ and each of the two functions, namely, $\frac{1}{2}\alpha(s+s)+2^{-\frac{1}{2}}\alpha s_B$ and $-\frac{1}{2}\beta(s+s)+2^{-\frac{1}{2}}\beta s_B$, which resulted from the first step. We can treat (9) for case B and (10) for case A in a similar way.

In following the foregoing procedure, we note from the forms of the orbitals that in every case the energy is lowered (term value increased), and a bonding effect is produced, when the sign of b (or b') is the same as that of a or c (or a' or c'). When the sign of b (or b') is opposite to that of a or c (or a' or c') the energy is raised and an antibonding effect is produced. *Maximum* term value and more or less bonding are secured when a, b, c all have the same sign; *minimum* term value and more or less (usually a strong) antibonding effect when b (or b') is opposite in sign to both a and c (or a' and c'). An *intermediate* term value and more or less of a net bonding or sometimes antibonding effect are produced when b is like c, but opposite to a, in sign (it can be shown that the reverse case does not occur here). The three cases just mentioned (maximum, intermediate, and minimum term values) correspond to the three solutions of the problem (9), or (10).

The statements just made as to signs of coefficients and their relation to energy and bonding effects are equally valid for case A or B or intermediate cases, but the relative numerical values of the coefficients, and the bonding properties, for the three solutions, of course differ considerably in cases A and B. This can be seen from the following detailed summary of the results; in each case the three solutions of each type are listed *in order of increasing energy* (decreasing term value):

Case A, σ_g: $(a_1 \approx b_1 > c_1)$;
$(-a_2 \approx b_2 > c_2)$; $(a_3 < -b_3 < c_3)$. (11a)

Case A, σ_u: $(a_1' > b_1' > c_1')$;
$(-a_2' < b_2' \approx c_2')$; $(a_3' < -b_3' \approx c_3')$. (12a)

Case B, σ_g: $(a_1 > b_1 > c_1)$;
$(-a_2 < b_2 \approx c_2)$; $(a_3 < -b_3 \approx c_3)$. (11b)

Case B, σ_u: $(a_1' > b_1' > c_1')$;
$(-a_2' < b_2' < c_2')$; $(a_3' < -b_3' > c_3')$. (12b)

The approximate-equality ($\approx$) or inequality signs refer directly only to the relation between adjacent letters. These approximate-equality signs would become equality signs and simultaneously the third coefficient would vanish, if there were no $s-p\sigma$ hybridization, i.e., no mixing of (s_A+s_C) with $(\sigma_A+\sigma_C)$ and of $(s-s)$ with $(\sigma-\sigma)$. Actually such mixing must occur, but probably always or nearly always only to an extent sufficiently moderate so that the case of no mixing is a better approximation than the case of complete (i.e., 50−50) mixing. As noted earlier, there is never any mixing between s_B and σ_B, for reasons of symmetry. In rare cases, the inequality signs given in (11) and (12), and possibly sometimes the signs of some of the small coefficients in (11) and (12), may be unreliable.

The signs of all the coefficients are (or may be taken as) + or − according as *no* sign, or a minus sign, precedes the coefficient in (11) or (12). [Of course for any given orbital the signs of all coefficients can be reversed simultaneously,

if desired.] Signs and magnitudes of bonding effects for the various cases included in (11), (12) can be read from the relative signs and magnitudes of the coefficients. Likeness of sign between b and a or c gives bonding, unlikeness antibonding; equality of magnitude between b and a or c tends to give maximum strength of bonding (or antibonding). In extreme cases, b (or both a and c) may be nearly zero, and such orbitals are nearly nonbonding. [Throughout this discussion, we have neglected the small and unimportant bonding or antibonding effects between end-atoms A and C, involved in the forms $(s \pm s)$ and $(\sigma \pm \sigma)$.]

To the foregoing results for the σ_g and σ_u orbitals may now be added those for the π_u orbitals. The two π_u orbitals can both be covered by

$$\pi_u = b''(\pi_B) + c''2^{-\frac{1}{2}}(\pi_A + \pi_C). \qquad (13)$$

For the above-discussed cases A and B one finds:

Case A, π_u: $(b_1'' = c_1'')$, $(-b_2'' = c_2'')$. (14a)

Case B, π_u: $(b_1'' < c_1'')$, $(-b_2'' > c_2'')$. (14b)

Finally, for the type π_g, at least if we consider only the original twelve s and p atomic orbitals of the outer shells of the atoms A, B, and C, we have only the single representative $(\pi - \pi)$ given in (8). This, if we neglect the slight A$\leftrightarrow$C antibonding, should be essentially nonbonding.

As noted earlier, we now have twelve molecular orbitals (counting each π orbital double) of which only eight are needed to hold the sixteen available electrons. For the normal state of each molecule, the eight lowest energy orbitals out of (11), (12), (14), and π_g of (8) will be filled up, leaving the four highest energy orbitals as excited orbitals. Examination of the twelve available orbitals indicates without reasonable doubt that the two lowest σ_g, the two lowest σ_u, the lower π_u, and the π_g will be filled, leaving the highest σ_g, the highest σ_u, and the higher π_u as excited orbitals in both the cases A and B and in intermediate cases and in all other, outside, cases which we meet in this paper. Of the filled orbitals, there seems to be no reasonable doubt that the nonbonding π_g should be the most loosely bound (last to be filled) in all the cases. These conclusions show that all the sixteen-outer-electron linear molecules here considered should be at least formally analogous in outer-electron structure.

Of the excited orbitals, it appears that all or most should be high in energy above the last filled (π_g) orbital. The only excited orbital which seems likely ever to come rather low in energy is the excited σ_g in or beyond case A. In this case (cf. (11a)), the excited σ_g is of the form

$$\sigma_g = c_3 2^{-\frac{1}{2}}(\sigma_A + \sigma_C) - b_3(s_B) + \cdots,$$

with $b_3 < c_3$. For $b_3 = 0$, this σ_g would be approximately equal in term value to the filled orbital π_g and so would begin to compete with the latter. Actually b is still probably large enough, however, even in case A and for some distance beyond (in the direction away from case B), to keep the σ_g well above the π_g. In going *toward* case B and on beyond it, the energy of this σ_g should become very considerably higher.

Roughly speaking, the filled orbitals include all the bonding and nonbonding orbitals of (11), (12), (14), and (8), while the excited orbitals include the antibonding orbitals of (11), (12), and (14). This situation shows how it is that the sixteen-outer-electron linear molecules under consideration represent a particularly stable diamagnetic type with properties characteristic of closed-shell electronic structures (cf. the somewhat similar diatomic closed-shell molecules N_2, CO, CN^-, NO^+).

It should be possible to arrange the various molecules under consideration in a series with respect to their relation to the cases A and B discussed above. In this way the differences in their outer-electronic structures can be expressed in terms of variations in the coeffiicents a, b, c, etc., of (11), (12), (14). It is not difficult to see that the series must run about as follows:

$$N_3^-,\ \mathbf{A},\ NO_2^+,\ CS_2,\ CO_2,\ \mathbf{B},\ BO_2^-,\ HgI_2,\ \text{etc.}\cdots BeF_2,\ \cdots RaF_2. \qquad (15)$$

Here N_3^-, NO_2^+, and CS_2 are probably near case A, with N_3^- somewhat to the left of it; CO_2 is probably well between cases A and B, BO_2^- is probably near case B, HgI_2 considerably to the right of B, with other salts MeX_2, especially the fluorides, extending much farther to the right with RaF_2 probably the most extreme case.

Electron configurations for the normal states of typical molecules of the series (15) can now

be given (see (16a)). As already pointed out, these are all identical except for variations in relative values of a, b, and c in the orbitals used. Over the range covered by (15), however, these variations are large, and suffice to account for the change from molecules classed as double-bonded to those classed as single bonded homopolar and finally to single-bonded heteropolar.

In obtaining the orbital symbols used in the configurations (16a), the following procedure was used. In (11), (12), (14), the smallest of the three coefficients, which is usually small enough to be roughly negligible, was first dropped; or in extreme cases, all coefficients but one were dropped as negligible. Referring then to (9), (10), (13), the usual LCAO shorthand symbol, corresponding to the remaining non-negligible coefficients, was written down for each orbital. In deciding which coefficients might properly be neglected, (15) was used. Naturally the results are not exact, but are intended to give a survey of the essential features of the electron configurations in the various cases. A more exact understanding can be obtained by referring back to (11), (12), (14). It should always be borne in mind, in any case, that even the rather complicated LCAO forms represented by (11), (12), (14) constitute only crude approximations to the real forms of the actual best molecular orbitals. Further, the molecular orbital symbols in (16a) and elsewhere, even though given in LCAO shorthand, should always be thought of as really referring fundamentally to the actual best molecular orbitals.[3]

$$\begin{aligned}
&\text{FMeF}: (s+s,\sigma_g)^2(s-s,\sigma_u)^2(\sigma+s+\sigma,\sigma_g)^2(\sigma-\sigma,\sigma_u)^2(\pi+\pi,\pi_u)^4(\pi-\pi,\pi_g)^4\\
&\text{IMeI}: (s+s,\sigma_g)^2(s-s,\sigma_u)^2(\sigma+s+\sigma,\sigma_g)^2(\sigma+\sigma-\sigma,\sigma_u)^2(\pi+\pi,\pi_u)^4(\pi-\pi,\pi_g)^4\\
&\text{OCO}: (s+s+s,\sigma_g)^2(s-s,\sigma_u)^2(\sigma+s+\sigma,\sigma_g)^2(\sigma+\sigma-\sigma,\sigma_u)^2(\pi+\pi+\pi,\pi_u)^4(\pi-\pi,\pi_g)^4\\
&(\text{NNN})^-: (s+s+s,\sigma_g)^2(s+\sigma-s,\sigma_u)^2(s-s+s,\sigma_g)^2(\sigma+\sigma-\sigma,\sigma_u)^2(\pi+\pi+\pi,\pi_u)^4(\pi-\pi,\pi_g)^4\\
&\text{ABA in general}: \sigma_g^2\sigma_u^2\sigma_g^2\sigma_u^2\pi_u^4\pi_g^4, \text{ with forms given by (9), (10), (13), (8).}
\end{aligned} \tag{16a}$$

In all cases the resultant state is of course $^1\Sigma^+_g$. In every case, inner-shell electrons are omitted.

The excited molecular orbitals derivable from (7), (8) and included in (9)–(14) are

$$\begin{aligned}
&\text{MeF}_2: (\sigma-s+\sigma,\sigma_g);\quad (np\sigma_u)_{\text{Me}};\quad (np\pi_u)_{\text{Me}}\\
&\text{MeI}_2: (\sigma-s+\sigma,\sigma_g);\quad (\sigma-\sigma-\sigma,\sigma_u);\quad (np\pi_u)_{\text{Me}}\\
&\text{CO}_2: (\sigma-s+\sigma,\sigma_g);\quad (\sigma-\sigma-\sigma,\sigma_u);\quad (\pi-\pi+\pi,\pi_u)\\
&\text{N}_3^-: (\sigma-s+\sigma,\sigma_g);\quad (\sigma-\sigma-\sigma,\sigma_u);\quad (\pi-\pi+\pi,\pi_u).
\end{aligned} \tag{17}$$

In (16a) and (17), two sizes of type are used to indicate varying relative magnitudes of the coefficients with which the various atomic orbitals appear in each LCAO approximate molecular orbital. In estimating the relative sizes of the coefficients, allowance has been made for the factors $2^{-\frac{1}{2}}$ which appear in (9), (10), and (13). For instance, the N_3^- orbital written as $(s+s+s,\sigma_g)$ in (16a) is obtained by putting $a=b$ and neglecting c in (9),—cf. (11a). The resulting orbital is then approximately of the form

$$\alpha(\tfrac{1}{2}s_A+2^{-\frac{1}{2}}s_B+\tfrac{1}{2}s_C),$$

so that s_B is considerably more prominent than s_A and s_C. In (16a) and (17), wherever just one atomic orbital symbol appears, it belongs to the central atom B (cf. e.g., $np\pi_u$ in (17)). Where two symbols appear, they belong to the end atoms A and C (cf. e.g., $(s+s)$ for MeI_2 in (16)). Where three atomic symbols appear, they refer to atoms A, B, C in that order (cf. e.g., $(s+s+s)$ for N_3^- in (16a)).

Since those orbitals in (16a) which involve only the two end atoms A and C are really practically nonbonding, the approximation may be improved if these orbitals are replaced by corresponding atomic orbitals (cf. discussion of $(\pi-\pi)$ of CO_2 given in section 1 in connection with (1) and (1a)). [Exception: when bonding and corresponding antibonding shells of this type are both filled up, e.g., $(s+s)^2(s-s)^2$ of MeF_2, MeI_2, CO_2, or $(\pi+\pi)^4(\pi-\pi)^4$ of MeF_2 or MeI_2, in (16), then there is no real improvement in the

wave function on substituting atomic orbitals (cf. section 1). Nevertheless the use of the latter perhaps gives a somewhat clearer idea of the nature of the electronic structure.] Making the changes indicated, we have instead of (16a) the following:

$$\begin{aligned}
&MeF_2: \ 2s_F^2 2s_F^2(\sigma+s+\sigma,\sigma_g)^2(2p\sigma_F 2p\sigma_F)2p\pi_F^4 2p\pi_F^4\\
&MeI_2: \ 5s_I^2 5s_I^2(\sigma+s+\sigma,\sigma_g)^2(\sigma+\sigma-\sigma,\sigma_u)^2 5p\pi_I^4 5p\pi_I^4\\
&CO_2: \ (s+s+s,\sigma_g)^2(2s_O 2s_O)(\sigma+s+\sigma,\sigma_g)^2(\sigma+\sigma-\sigma,\sigma_u)^2(\pi+\pi+\pi,\pi_u)^4(2p\pi_O^2 2p\pi_O^2)\\
&N_3^-: \ (s+s+s,\sigma_g)^2(s+\sigma-s,\sigma_u)^2(s-s+s,\sigma_g)^2(\sigma+\sigma-\sigma,\sigma_u)^2(\pi+\pi+\pi,\pi_u)^4(2p\pi_N^2 2p\pi_N^2).
\end{aligned} \tag{16}$$

In arriving at the configurations (16a) and (16), and in interpreting them in relation to ordinary valence theory, a knowledge of the distribution of charge between the three atoms A, B, C would be helpful. For this purpose it is sufficient to determine the net charge on atom B, which can be done if it can be ascertained how many of the sixteen outer electrons belong, on the average, to atom B. Aside from the inherent arbitrariness involved in trying to draw boundaries for "atom B" inside the molecule ABC, this can be done in a fairly sensible way, insofar as the LCAO approximation is valid (cf. XI of this series, section 7).

From a knowledge of the various coefficients a, b, c in (11), (12), (14), it is possible to compute how much of the charge $-2e$ of each electron-pair belongs, on the average, to atom B. By summing over the eight outer-electron pairs, and subtracting this sum from the number of outer (ns, np) electrons in the neutral atom B, the mean charge on atom B is obtained.

For one electron-pair, proceeding in analogy to Eq. (38) of XI, one writes

$$\begin{aligned}
-2e=-2e\int(\phi_{ABC})^2 dv=\\
-2e[a^2+b^2+c^2+2b(aS_{XB}+cS_{YB})],
\end{aligned}$$

where $S_{XB}=\int\phi_X H\phi_B dv$. The final result on the right of the equation is obtained after dropping a term $2ac\int\phi_X\phi_Y dv$ which should be negligibly small. [Note that ϕ_X is of the form $2^{-\frac{1}{2}}(s_A\pm s_C)$ and ϕ_Y is of the form $2^{-\frac{1}{2}}(\sigma_A\pm\sigma_C)$ or $2^{-\frac{1}{2}}(\pi_A+\pi_C)$; also note that $a=0$ in the case of π_u, cf. (14).] Of the total charge $-2e$, the portion

$$-q_B=-2e[b^2+b(aS_{XB}+cS_{YB})] \tag{18}$$

may reasonably be allotted to atom B (cf. XI, section 7 just after Eq. (38)). Making use of the normalization condition implicit in the preceding equation just given above, Eq. (18) can be reduced to

$$n_B=-q_B/e=(1+b^2-a^2-c^2),$$

which will be seen to yield $q_B=-2e$, as it should, if $a=c=0$, $b=1$.

Now summing over the two σ_g, two σ_u, and two π_u electron pairs (the two π_g pairs have $q_B=0$), we have for the (average) number of outer electrons assignable to atom B,

$$\begin{aligned}
N_B=\Sigma n_B=\Sigma(1+b^2-a^2-c^2)\\
=6+\Sigma(b^2-a^2-c^2),
\end{aligned} \tag{19}$$

the summation being taken over all the orbitals appearing in (16a), with coefficients a, b, c as in (11), (12), and (14), and with the π_u orbital taken twice. For the net (mean positive) charge Q_B on atom B, we have

$$Q_B/e=N^\circ_B-N_B, \tag{20}$$

where N°_B is the number of outer electrons on atom B in the free neutral state ($N^\circ_B=5, 4, 3, 2$ for atoms N, C, B, Me, respectively).

The quantity N_B is of course expected to run more or less parallel to N°_B. Now it will be found on examination of (11), (12), (14) in connection with (19) that N_B decreases in the direction from case A to case B, i.e., from left to right in (15). For case A, we find, to the approximation that (11a) and (12a) with equality signs instead of near-equality signs $\approx$ are correct,

$$N_B=6-c_1^2-a_1'^2+b_1'^2-c_1'^2-c_2^2-a_2'^2. \tag{21}$$

In practice, this gives N_B somewhat less than 5. If there were no mixing at all between orbitals of the types ϕ_X and ϕ_Y, nor between σ_B and $(\sigma_A-\sigma_C)$, i.e., no $s-p\sigma$ hybridization, we would have $c_1=b_1'=c_2=a_2'=0$ and $a_1'=1$ in Eq. (21), which would hold exactly, and would then give $N_B=5$.

For case B, N_B is clearly less than for case A. For a case so far to the right that it is a good approximation to put $a_1=a_1'=c''=1$, $b_1=c_1=b_1'=c_1'=b_1''=0$, we get $N_B<2$ (cf. MeI_2, MeF_2 in (16)). For a case $N_B=2$, it is clear that there would be considerable departures from the relations $a_1=a_1'=c''=1$, $b_1=c_1=b_1'=c_1'=b_1''=0$.

The case $N_B=4$, $Q_B=0$ would evidently correspond to the usual chemical conception of an ideal homopolar double-bonded type A=B=A; $N_B=2$, $Q_B=0$ to an ideal homopolar single-bonded type $A-B-A$; and $N_B=0$, $Q_B=+2$ to an ideal heteropolar type $A^-B^{++}A^-$. Actual molecules never conform exactly to these ideal cases. When approximate conformity exists, an approximately valid classification can be made in accordance with ordinary valence theory. In intermediate cases, which are rather common in practice, ordinary valence theory is somewhat at a loss, and arbitrary attempts are often made to force molecules into one of the simple ideal categories. In such cases, disputes have been frequent as to which ideal category is the proper one. It is, however, often but not yet universally realized now that the admission of intermediate or mixed cases affords the only correct way of settling such disputes (cf. especially Pauling's papers on "resonance" of molecules between different valence states).

The present method shows particularly clearly the "naturalness" of the intermediate cases and the relative improbability of the pure ideal cases. It also shows the possibility of a great variety of types of intermediacy, particularly when we consider molecules and ions ABC (see below) as well as ABA. We can illustrate here by a discussion of some of the important examples of the types ABA, as listed in (15) and described in (16) and (16a).

We may well begin with N_3^-, at the extreme left in (15). A structure $N^-=N^+=N^-$ is frequently assigned to this molecule. Such a structure would imply $Q_B/e=+1$, $N_B=4$. As will be shown, however, $N_B=5$ is in all probability much more nearly correct, so that $N^-=N^+=N^-$ is probably a very poor approximation to the real structure.

If (*I*) we knew the exact location of N_3^- in (15), the various a, b, c's would be more or less definitely determined, so that, using (19), N_B would be more or less definitely determined. On the other hand (*II*) if we knew N_B, this would suffice to determine approximately the relative term values of the three N atoms in N_3^- and so to locate N_3^- in (15). The two distinct conditions (*I*) and (*II*), taken jointly, evidently impose a condition of *self-consistency* on N_B. This is similar to the condition of self-consistency met in using the Hartree method for determining the forms of atomic or molecular orbitals.

In seeking to determine the true value of N_B for N_3^-, we may proceed by a trial and error or variation method until consistency is obtained as regards conditions (*I*) and (*II*). As an initial trial assumption, let us suppose that N_3^- in (15) comes just at case A, and let us first apply condition (*I*). N_B is then given, very nearly, by Eq. (21). Although an exact result cannot be obtained without calculation, a survey of the coefficients a, b, c in Eq. (21) shows that N_B is somewhat less than 5, but in all probability nearer 5 than 4. The value $N_B=5$ represents approximately an upper limit, which would hold for the case of no mixing of $(s+s)$ with $(\sigma+\sigma)$ nor of $(s-s)$ or σ_B with $(\sigma-\sigma)$; for this case, $c_1=b_1'=c_1'=c_2=a_2'=0$ and $a_1'=1$, giving $N_B=5$. Since there is actually some mixing, we see that $N_B<5$.

But now if $N_B<5$, it is easily shown, on applying condition (*II*), that N_3^- *cannot* belong to case A, but must lie rather far to the left of A in (15), thus contradicting our initial trial assumption. The proof that, if $N_B<5$, N_3^- must be to the left of case A in (15), is as follows. Suppose we had $N_B=5\frac{1}{3}$ (equal distribution of charge among the three N atoms, which may be formulated $N^{-\frac{1}{3}}N^{-\frac{1}{3}}N^{-\frac{1}{3}}$). In this case, roughly, one might expect corresponding term values of the three atoms to be equal, fulfilling case A. More accurately, however, N_3^- would fall to the left of case A in (15) for $N_B=5\frac{1}{3}$, since for a given orbital, an electron of the central atom B surely would move on the average in regions of lower potential than for the same orbital in one of the outer two atoms; thus B would have somewhat higher term values than the other atoms, so placing the molecule to the left of case A. Now for $N_B<5$, the term values of atom B would be still further increased, placing N_3^- still further

to the left of case A in (15). Hence our initial trial assumption of case A for N_3^- is not consistent with itself, since by (*I*) it requires an N_B which by (*II*) would put N_3^- far to the left of case A.

Hence our initial assumption must be altered considerably, and it is readily seen that, to get self-consistency, N_3^- must actually be located well to the left of case A in (15) and N_B must be considerably greater than is given by the relation $N_B < 5$ required by case A. While the exact value of N_B cannot be determined by this qualitative argument, it becomes very probable that it is in the neighborhood of 5, quite possibly even somewhat greater than 5, and practically certainly much greater than 4. The charge distribution then corresponds in all probability not to $N^-N^+N^-$, but probably much more nearly to $N^{-\frac{1}{2}}NN^{-\frac{1}{2}}$ or possibly even $N^{-\frac{1}{2}}N^{-\frac{1}{2}}N^{-\frac{1}{2}}$. [The whole argument is subject of course to some uncertainty insofar as it depends on the use of LCAO forms for molecular orbitals; but it at least tends to cast very grave doubt on the formulation $N^-=N^+=N^-$.]

The structure thus indicated for N_3^- is one which cannot very well be described by an ordinary chemical formula, at least by no single formula; it is a highly intermediate case. Nevertheless, on examination of (16) and (16a), one sees that the internal electronic structure of N_3^- is very similar to that of CO_2, having, in particular, similar bonding electrons. It is also readily seen that NO_2^+ and CS_2 should be intermediate in these respects between N_3^- and CO_2 (cf. (15)).

In comparing the configurations of N_3^- and CO_2, the most noticeable difference is that there is a partial shift of bonding power from lower- to higher-energy σ orbitals in going from N_3^- to CO_2. In N_3^- the lowest σ_g is strongly bonding, the second one probably mildly antibonding; in CO_2 the first σ_g is weakly bonding, the second strongly bonding; the net total bonding power of the two σ_g may, however, be somewhat the same in the two molecules. In N_3^- the lowest σ_u is weakly bonding, the second one moderately bonding; in CO_2 the lowest σ_u is probably nearly nonbonding, the second one strongly bonding, but the total bonding power of the two σ_u may be somewhat the same in the two molecules.

For the π_u orbitals, we have $b_1''=c_1''$, nearly, in N_3^-, but $c_1''>b_1''$ in CO_2 (cf. (14)). This tends to make the π_u homopolar bonding stronger in N_3^- than in CO_2. Similar differences exist also in the σ orbitals.

In the various molecules N_3^-, NO_2^+, CS_2, CO_2, the bonding may be described as partially heteropolar, partially homopolar, the homopolar part then being described as double-bonded, single-bonded, or some mixture. In CO_2, for instance, it was estimated in section 1 that the charge distribution within the molecule is roughly $O^{-\frac{1}{2}}C^{+1}O^{-\frac{1}{2}}$, i.e., $Q_B/e=+1$, or $N_B=3$. In terms of ordinary chemical bonds, this would correspond to a condition about half-way between O=C=O (neutral atoms, two covalent double bonds) and $O^- - C^{++} - O^-$ (two covalent single bonds, and two ionic bonds like those in $F^-Ba^{++}F^-$). Or one might say that there are two, approximately half polar, double bonds.

In the present method the amount of heteropolar bonding may be judged from the estimated Q_B values, while the amount of homopolar bonding may be qualitatively read out of the signs and magnitudes of the LCAO coefficients a, b, c involved in the molecular orbitals in (16a) or (16). In the present method, there is no very definite way *in general* of expressing the number of chemical bonds, as ordinarily assigned, in terms of *numbers of bonding electrons*. In simple cases, as was pointed out by Herzberg for homopolar diatomic molecules, the number of ordinary chemical bonds is equal to the number of pairs of (strongly) bonding electrons minus the number of pairs of (strongly) antibonding electrons. Roughly, we can say (cf. (16a), (16)) that there are four pairs of bonding electrons in the molecules CO_2, CS_2, NO_2^+, N_3^-; this would agree with ordinary chemical ideas. More accurately, however, it will be seen that the total bonding power is not precisely confined to just eight bonding electrons, but spreads more or less over the other electrons. Strictly speaking, some bonding power (positive or negative) must be attributed to all the electrons, as was pointed out for diatomic molecules in the writer's 1928 paper on the use of electron configurations built from molecular orbitals.

In the present case, it will be seen from the comparison of N_3^- and CO_2 orbitals given above

that eight σ and four π_u electrons participate more or less actively in the bonding, although the total bonding effect is about the same as if only four σ and the four π_u electrons participated strongly, so that we may speak with reasonable justification of the presence of two double bonds. Intermediate cases often arise, however, where it becomes purely arbitrary to decide how many bonding electron pairs there are which are *strongly enough* bonding to be counted as chemical bonds. Since bonding power can vary continuously, no sharp line can be drawn between bonding and nonbonding electrons. As will be seen from (16a) and (16), the bonding power of the two pairs of π_u electrons, which entitles them to be called bonding electrons in CS_2 or CO_2, becomes small enough to be neglected in $HgCl_2$ or MeX_2, so that "double bonds" in CO_2 fade into "single bonds" in $HgCl_2$.

An interesting intermediate case should exist in BO_2^-. One might seek to formulate this chemically either as $O=B^-=O$ like $O=C=O$, with four bonding electron pairs, or as $O^- - B^+ - O^-$ like $Cl-Hg-Cl$, with two bonding electron pairs. Probably the second is the more nearly correct, but a better answer is that we have an intermediate case. BO_2^- can be interpolated between CO_2 and MeI_2 in (15) and (16a). Clearly there are two strongly bonding electron pairs (one σ_g, one σ_u, as in CO_2 and MeI_2) which correspond to the two bonds of the formulation $O^- - B^+ - O^-$. In addition, there can be no doubt that the four π_u electrons have an amount of bonding power which is not negligible, although surely much smaller than for the π_u electrons in CO_2, CS_2, or N_3^-. Thus the two π_u electron pairs are intermediate in character between bonding and nonbonding, although here probably somewhat nearer the latter, if such a description makes sense. They represent the second bonds of two double bonds which are here well on the way toward becoming single bonds.

Digressing for a moment from the discussion of the series of cases in (15), reference may be made to the interpretation of the observed ionization potential I of CS_2 in relation to electron configurations (16), (16a). The observed I is 10.4 ± 0.2 volts by electron-impact methods,[18] while a value of 10.1 volts from Rydberg absorption series is given by Price.[18] These values are in reasonable agreement with the predicted I, i.e., $I^*(3p\pi)$ of the S atom, which has the value 11.13 volts. The fact that the observed I is somewhat less than the predicted suggests the presence of some net negative charge[7] on the S atoms. This would be contradictory to the fact that sulfur is slightly less electronegative than carbon on Pauling's scale; however, the scale was developed only for single bonds and may not hold very well for double bonds.

Turning to $(NNN)^-$, it will be noted that the minimum I (belonging to the $2p\pi_N$ orbital, according to (16)) represents the *electron affinity* of linear N_3. It can be estimated that this electron affinity is fairly large,—comparable with that of CN or Cl,—since the structure of N_3^- consists of a set of very stable closed shells rather like those of CN^-, which resembles Cl^-.

The molecules MeX_2 (e.g., BeF_2, CaF_2, $CaBr_2$, HgF_2, HgI_2) are of course very different from the others in (16), being intermediate between $X^-Me^{++}X^-$ and $X-Me-X$ in character, with hardly any tendency toward $X^+=Me^{=}=X^+$. A linear structure is fairly well assured for most if not all these molecules in the vapor state. In the most nearly homopolar types HgX_2, this is evident from the zero dipole moment.[1a] In the more heteropolar types it is to be expected because of the electrostatic repulsion between the two X^- ions, taking into account also the absence of any considerable polarizability of the central Me^{++} ion which might make possible (cf. H_2O) a triangular form.

The electron configurations of these molecules are then describable as in (16a) or as in (16). The formulations (16a) show that the structures may be regarded as formally like those of CO_2 and the other $A=B=C$ types. However, the π_u orbitals which give two of the homopolar bonds in the latter now lose nearly all homopolar bonding power because $np\pi$ of X is so much more electronegative than $np\pi$ of Me. Hence ($np\pi - np\pi$, π_u) of X+X and $np\pi_u$ of Me occur nearly unmixed, the former in (16a), the latter as an excited orbital in (17). In MeF_2 a similar situation exists also for the σ_u orbitals, where nearly unmixed ($np\sigma - np\sigma$, σ_u) of F+F occurs in (16a) and $mp\sigma_u$ of Me in (17). In MeI_2, how-

[18] H. D. Smyth and J. P. Blewett, Phys. Rev. **46**, 276 (1934). W. C. Price, unpublished work, kindly communicated to the writer.

ever (except for the most electropositive Me atoms like Ca), it appears very probable that the σ_u in (16a) gives rather strong I−Me−I homopolar bonding, and so should be formulated $(\sigma+\sigma-\sigma, \sigma_u)$.

The foregoing conclusions are based on considerations of relative electronegativity and of overlapping. By using the writer's electroaffinity scale (M scale),[5] estimates of M values have here been made for the $2s$ and $2p$ orbitals of Be and the $6s$, $6p$ orbitals of Hg. The difference in M between iodine ($5p$) and np of Be (about 1.92) or of Hg (about 2.12) is found to be about the same as the difference (2.05) between F ($2p$) and H ($1s$), so that, with comparable overlapping, the degree of homopolar bonding might be comparable. Now in HF the bonding orbital, which in LCAO approximation is $a(2p\sigma_F)+b(1s_H)$, has b/a very considerably less than 1, but large enough to correspond to a very considerable amount of homopolar bonding. A somewhat similar relation may then reasonably be expected for the σ_u orbitals of MeI_2, given in LCAO approximation essentially by

$$2^{-\frac{1}{2}}c_2'(5p\sigma_I)+b_2'(mp\sigma_{Me})-2^{-\frac{1}{2}}c_2'(5p\sigma_I),$$

since there should be strong overlapping of $(mp\sigma_u)_{Me}$ with each $5p\sigma_I$. For the π_u orbitals of MeI_2 in (16a), however, the overlapping is so much less, hence H_{AB} so much less,[5] that the ratio b_2'/c_2' is probably negligibly small.[5] In MeF_2, the electronegativity difference between fluorine ($2p$) and mp_{Me} is much larger than between iodine ($5p$) and mp_{Me}, so that the ratios b/c are probably negligible even for σ_u and certainly for π_u. Various intermediate cases should occur for molecules $MeCl_2$ and $MeBr_2$, although both of these types (in agreement with experimental data) should resemble the iodides more closely than the fluorides.

In the case of the σ_g orbital in (16a) which is built up in LCAO approximation mainly from ms_{Me} and $np\sigma_X$, there can be no doubt that there is a considerable X−Me−X homopolar bonding except perhaps in the most extreme heteropolar cases like CaF_2. In the least heteropolar case (probably HgI_2), the ratio b_2/c_2 in

$$[2^{-\frac{1}{2}}c_2(5p\sigma_I)+b_2(6s)_{Hg}+2^{-\frac{1}{2}}c_2(5p\sigma_I)],\ \sigma_g$$

is probably close to unity, since the s (i.e., $6s$) electroaffinity of Hg is estimated to be $M=+0.19$, nearly the same as the ($5p$) electroaffinity $M=+0.41$ of iodine.

Summarizing, we find for the molecules MeX_2 a range of types from the most nearly heteropolar cases like CaF_2 in which one σ_g pair of electrons gives a little homopolar bonding, to the most nearly homopolar cases like HgI_2 where the σ_g pair gives essentially homopolar bonding while a second, σ_u, pair gives bonding which is partially (perhaps half) homopolar. The net total bonding may be described as perhaps nearly pure heteropolar in the one extreme and perhaps about three-fourths homopolar in the other. (The meaning of the present discussion will be made clearer by comparison with the more detailed considerations concerning molecules MA_4 in XII of this series.) The present discussion illustrates well the possibility in the present method of describing the electronic structures of molecules of varying polarity from a single standpoint in a way which is hardly possible in terms of ordinary chemical valence concepts.

The descriptions (16) and excited orbitals (17) should be of value in interpreting the electronic bands of molecules MeX_2, which are especially well known in the case of the HgX_2 absorption spectra.[1a] This subject will not be entered upon here. Mention may be made, however, of the observed electron-impact ionization potentials[1a] of $ZnCl_2$ (12.9 volts) and $HgCl_2$ (12.1 volts). According to (16), modified to fit $MeCl_2$, each of these observed potentials should correspond to removal of a nonbonding $3p\pi_{Cl}$ electron from the molecule. The predicted I for this process, according to VIII of this series,[7] is <13.62 volts, the inequality sign representing 1 or 2 volts and corresponding to the effect of the net negative charge on the Cl atoms. The observed potentials for $HgCl_2$ and $ZnCl_2$, especially the former, are in excellent agreement with this prediction. The higher value for $ZnCl_2$ than for $HgCl_2$ is very likely due to experimental error: since the net negative charge on the Cl atoms should be larger in $ZnCl_2$ than in $HgCl_2$, the I ought to be somewhat less.

The structures and low excited orbitals of molecules MeH_2 should be essentially similar to those of MeI_2 in (16) and (17) if one omits all

ns_X and $np\pi_X$ electrons from (16) and (17), and replaces $\pm np\sigma_X$ by $1s_H$ in the LCAO forms. The normal state of BeH_2 has already been formulated in V of this series,[4] Table I.

5. Unsymmetrical Linear Molecules ABC

In the unsymmetrical molecules NNO, OCS, $(NCO)^-$, $(NCS)^-$, also NCCl, OBCl, etc., the $_g$, $_u$ classification of the states and orbitals is lost and as a result the LCAO forms become less simple. Roughly speaking, the configurations are like (16) or (16a) but with mixing between σ types corresponding to σ_g, σ_u and again between π types corresponding to π_u, π_g of (16a). Or in other words, instead of having four distinct and relatively simple secular problems as in (7), (8), we have two more complicated problems, one for the six σ molecular orbitals, one for the 3×2 π orbitals. Under these circumstances, a qualitative treatment becomes more difficult than before. Somewhat helpful in the case of NNO is the fact that it forms a sort of mean between $(ONO)^+$ and $(NNN)^-$, which are both rather near to but on opposite sides of case A (cf. (15)). Similarly, OCS is a sort of mean between OCO and SCS; and ClBO between OCO and ClBeCl.

The following represents a very tentative description of the electron configuration of N_2O using molecular orbitals for the sixteen outer electrons:

$$\underset{N-N-O}{(s+s+s,\ \sigma)^2}\underset{N-N\leftrightarrow O}{(s+\sigma-s,\ \sigma)^2}\underset{N\leftrightarrow N\leftrightarrow O}{(s-s+s,\ \sigma)^2}\underset{N-N-O}{(\sigma+\sigma-\sigma,\ \sigma)^2}\underset{N-N-O}{(\pi+\pi+\pi,\ \pi)^4}\underset{N-N\leftrightarrow O.}{(\pi+\pi-\pi,\ \pi)^4},\quad {}^1\Sigma^+ \tag{22a}$$

Here bonding and antibonding effects between atoms are indicated by $-$ and $\leftrightarrow$, respectively; the antibonding effects in (22a) are probably all relatively weak. In each LCAO molecular orbital, the coefficients of the three atomic orbitals used are more or less unequal, as roughly indicated by the sizes of the type used. The minimum I should be that of the very likely nearly nonbonding orbital denoted $(\pi+\pi-\pi)$. The I of $(\pi+\pi-\pi)$ may reasonably be compared with $I^*(2p\pi)$ of N or O, probably more nearly of N. The observed I of N_2O is given as about 12.9 volts (electron-impact[19]), which may be compared with $I^*=12.7$ or 15.23 volts for $2p\pi$ of N or O.

The structure of N_2O (cf. discussion of N_3^- in section 3) is probably not very close to $N^-=N^+=O$, but may be intermediate between this and various other structures such as $N\equiv N^+-O^-$, $-N=N-O-$, etc.[19a]

The structures of OCS, OCN^-, and SCN^- are doubtless intermediate between the structures $O=C=S$, $O=C=N^-$, $S=C=N^-$ and other structures analogous to those just mentioned for N_2O. Especially for SCN^-, there might be a considerable tendency toward $S^-C\equiv N$, but chemical evidence, and the fact that normally N is considerably more electronegative than S, indicate that this tendency is not predominant. The linear molecule NCCl, however, although isoelectronic with NCS^-, doubtless has a structure which is predominantly $N\equiv C-Cl$, but with appreciable tendencies toward $N^-=C=Cl^+$.

If the structure of CNCl is predominantly $C\equiv N-Cl$, it might be described tentatively more or less as follows:

$$(s_{Cl},\sigma)^2(s_N+s_C,\sigma)^2(s_C-s_N,\sigma)^2(\sigma_{Cl}+\sigma_C,\sigma)^2(\pi_N+\pi_C,\pi)^4(\pi_{Cl})^4,\quad {}^1\Sigma^+. \tag{23}$$

Here we have more or less arbitrarily used orbitals localized within the Cl atom and the CN radical. Only one orbital, $(\sigma_{Cl}+\sigma_C)$, has been used to represent bonding between the Cl and the CN. Such localization is, at least to a large extent, allowable in the sense that the corresponding wave function should represent a good approximation.

The relation of (23) to (22a) and others in this paper is made clearer by giving up this localization and using whole-molecule orbitals; it can be shown that the corresponding wave function is

[19] H. D. Smyth and E. C. G. Stueckelberg, Phys. Rev. **36**, 478 (1930).

[19a] L. Pauling, Proc. Nat. Acad. Sci. **18**, 498 (1932) considers that the structure of N_2O is a mixture of $N^-=N^+=O$ and $N\equiv -O^-$.

not very much altered thereby. We then have, very tentatively,

$$(s+s+s,\sigma)^2(s+s-s,\sigma)^2(s-s+s,\sigma)^2(\sigma+\sigma-\sigma,\sigma)^2(\pi+\pi+\pi,\pi)^4(\pi-\pi-\pi,\pi)^4, \quad {}^1\Sigma^+. \tag{24}$$
$$Cl-C-N \quad Cl-C\leftrightarrow N \quad Cl\leftrightarrow C\leftrightarrow N \quad Cl-C-N \quad Cl-C-N \quad Cl\leftrightarrow C-N$$

The formulas (23) and (24), although very tentative, illustrate the possibility of getting a net bonding effect equivalent to the structure $Cl-C\equiv N$, even though using an electron configuration which, if the LCAO coefficients were properly readjusted, would correspond to $Cl^+=C=N^-$. This is another illustration (cf. the cases of BO_2^- and MeX_2 in section 3) of how formal analogies of chemically quite dissimilar molecules are revealed by the present method, and of how molecules belonging to types intermediate between the orthodox chemical bond types can be simply described and understood.

Another interesting case is that of BOCl. According to ordinary valence theory, this would have a structure intermediate between the homopolar form $O=B-Cl$ and the heteropolar form $O^-B^{+++}Cl^-$ or perhaps $O^- - B^{++}Cl^-$. According to the present method, the structure would be similar to that of CNCl as given by (23) or (24). [It will be recalled that the electronic structure and low excited levels of BO according to the present method are very similar to those of CN.] The LCAO coefficients would, however, be considerably altered, in such a way as to give, on the whole, increased weight to the O and decreased weight to the B atom, as compared with the respective corresponding atoms N and C in NCCl.

In the molecules SCN^- and OCN^-, like NNN^-, the electron affinity should be fairly large (cf. CN^-), since the electron removed is from a stable group of closed shells. It would appear also from the foregoing electron configurations that each of the free radicals SCN, OCN, and NNN should be a fairly stable physical structure, rather like CN, and like the latter should have some low energy x-ray-like excited states obtained by shifting the missing electron from one to another of the orbitals in (16a) or (22a). Another similar radical would be OBO.

6. NO_2 and Other Molecules. Ultraviolet Absorption of CO_2, COS, CS_2 and N_2O

In the various molecules $A=B=C$ just considered, the electronic structure of the normal state consists in a set of firmly bound closed shells of electrons, giving a chemically saturated structure. The orbitals represented are of two kinds (*a*) types which give strong bonding between the central atom B and one or both of the two outer atoms; (*b*) types which are essentially nonbonding. No types with pronounced net antibonding properties are present, or at most one, of high I. This situation is closely similar to that which is met in the diatomic molecules N_2, CO, CN^-, NO^+, etc. The situation is evidently responsible for the resemblance of the neutral molecules of these various types (N_2, CO, CO_2, N_2O) to rare gases (most closely to argon), and of the negative and positive ions to atom-ions with rare gas shells (most closely to Cl^- and perhaps K^+).

Our knowledge of these types forms an interesting point of departure for the study of other molecular types having more or fewer electrons. Types having one less electron are physically stable but chemically unsaturated free radicals (CN, BO, OCN, SCN, NNN) or positive ions (N_2^+, CO^+, CO_2^+, N_2O^+, etc.) possessing various low energy electron levels permitting the ready occurrence of easily observable band spectra. Types with two less electrons, e.g., C_2, also occur and give band spectra.

Types having one or more additional electrons form a quite different class of molecules (NO, NO_2, OO_2 or SO_2, ClO_2, etc.) or ions (O_2^+, SO_2^+, etc.). The case of NO is typical for the diatomic examples. Since all the available low energy bonding (and nonbonding) orbitals are filled up with NO^+, the last electron has to go into a strongly antibonding and relatively high energy orbital.[20]

Now it appears very probable that an analogous situation exists in linear NO_2. Linear NO_2^+ is a stable closed-shell arrangement like CO_2 (cf. (16)), but if another electron is added, the lowest energy available orbital is of one of the three types given by (17). From their forms, it is evident that these give an antibonding action between the central atom and the two outer

[20] Cf. R. S. Mulliken, Rev. Mod. Phys. **4**, 1 (1932).

atoms. Moreover, what is more important, it is probable that these three orbitals of (17) are all of high energy. This is immediately evident in the cases of σ_u and π_u of (17), but in the case of σ_g of (17),—cf. second paragraph preceding (15), —it is less clear. We may, however, reasonably postulate that the σ_g of (17) is of at least moderately high energy for linear NO_2. Empirical evidence in support of this postulate is to be found in the absence of evidence for low energy excited electron levels in CO_2, COS, and CS_2 (see below).

Now NO_2 differs from NO in that it has a means of avoiding acceptance for its last electron of a loosely bound antibonding orbital; namely, by an alteration in the shape of the molecule, the forms, energies, and properties of the various orbitals of (16) and (17) may be radically altered. From the fact that NO_2 is empirically known to have a triangular shape, we may fairly safely conclude empirically that the high energy of the last electron of linear NO_2 is actually lowered, and more than enough to make up for any net increase in the energies of the other electrons, when the molecule takes on a triangular form. The observed minimum ionization potential I_{min} of NO_2 (11 volts)[1a] presumably corresponds to removal of an electron from what would be the σ_g orbital of (17) if NO_2 were linear. It will be noted that this I, in spite of the fact that it is presumably considerably larger, according to the foregoing argument, than if NO_2 were linear, is still about 3 volts less than I_{min} of CO_2.

Similar considerations apply to O_3, SO_2, ClO_2, and others. A detailed consideration, showing how the observed spectra and other properties of such molecules, including NO_2, can be understood along these lines, will be reserved for another paper.

We may next consider the ultraviolet absorption spectra of CO_2 and CS_2. Experimentally,[21] CO_2 is practically transparent to below λ1800, and shows a very weak system of red-degraded bands from about λ1712. The maximum intensity for this system is near λ1600 or below. At shorter wave-lengths, other stronger band systems occur.[10] Very roughly, we may take λ1600 or even less as corresponding to the vertical excitation energy of the first CO_2 absorption system. This then amounts to about 8 volts. Subtracting from the observed I of CO_2 (about 14 volts), we get about 6 volts, or perhaps less, as the I of the excited orbital involved.

This may be identified with one of the three orbitals σ_g, σ_u, π_u of (17). Since the electron excited surely comes out of π_g of (1), the transition is then from (1) to one or more of the states

$$(\pi_g)^{-1}\sigma_g,\ ^{1,3}\Pi_g \quad \text{or} \quad (\pi_g)^{-1}(\sigma_u),\ ^{1,3}\Pi_u \quad \text{or} \quad (\pi_g)^{-1}(\pi_u),\ ^{1,3}\Sigma^+_u,\ \Sigma^-_u,\ \Delta_u. \qquad (25)$$

Although theoretical considerations indicate (cf. second paragraph preceding (15)) that the $^{1,3}\Pi_g$ should be lowest in energy of the states of (25), identification of the $^1\Pi_g$ as the upper level of the observed bands is rendered somewhat doubtful by the fact that transitions from the normal state to it are forbidden by the electronic selection rules for symmetry $D_{\infty d}$ (linear molecule). Low intensity violations of these rules are possible,[22] however, if suitable allowed transitions occur in the neighborhood, as seems to be the case here (occurrence of stronger bands at shorter wave-lengths). Another factor which might help here in allowing otherwise forbidden bands to occur weakly is that the equilibrium form of the molecule in the upper level of the observed bands might be triangular. For since a triangular form minimizes the energy of NO_2, the same might well be true of the excited states of CO_2 given by (25). Although the Franck-Condon principle would still preclude the occurrence of any *strong* transitions violating the selection rules characteristic of the symmetry $D_{\infty d}$ of the initial state, nevertheless *weak* transitions could occur if allowed, as would be true in the present case, by the selection rules for a triangular molecule (symmetry C_{2v}). On the whole, it seems very likely that the observed weak system of bands with which the CO_2 absorption begins does represent transitions to the $(\pi_g)^{-1}\sigma_g$, $^1\Pi_g$ state (accompanied by much fainter transitions to the $^3\Pi_g$). This would make I about 6 volts for the σ_g excited orbital in CO_2. In case, however, the observed bands involve a π_u or σ_u excited orbital, then the I of σ_g may be less or greater than 6 volts. the former is unlikely, while the latter

[21] S. W. Leifson, Astrophys. J. **63**, 73 (1926).

[22] G. Herzberg and E. Teller, Zeits. f. physik. Chemie **B21**, 410 (1933); cf. also discussion in reference 1.

(i.e., $I>6$ volts) would be possible only in case the electronic selection rules operate so rigorously that transitions to the $^1\Pi_g$ of (25) have an intensity too weak to have been observed. Further work will be needed to clear up this question with certainty, but it seems fairly probable, especially in view of the evidence from CS_2 and COS now to be presented, that the result I=about 6 volts for the excited σ_g is correct.

The first, moderately intense, electronic absorption band system[23] of CS_2, occurring at λλ2900–3800, with maximum intensity near λ3200 (3.9 volts), shows a large number of more or less sharp bands. Some of these are reported by Jenkins to show indications of having a simple structure like that for a linear molecule. The complicated and irregular arrangement of the bands, however, suggests that the equilibrium form of the molecule may be triangular for the upper electron level; but without more complete analysis, this must be considered uncertain. The vertical I of the excited orbital involved in the CS_2 bands is found to be about $10.2-3.9=6.3$ volts, nearly the same as for the lowest excited orbital in CO_2.

In seeking to determine the nature of the excited orbital involved in the CS_2 bands, we have the same kinds of possibilities as in CO_2. As compared with CO_2, however, the bands are apparently more intense, also they are apparently more widely separated from the next ultraviolet system, so that it is rather hard to believe that they can represent a transition forbidden by the selection rules of $D_{\infty d}$, unless it be that the equilibrium form of the molecule in the upper electron level is triangular. It should be noted that the I of the excited orbital here in CS_2, although nearly the same as that from the first bands of CO_2, is *relatively* considerably higher than in CO_2. In CO_2, I=about 6 volts for the excited orbital, about 14 for the π_g, giving a ratio of $6/14=0.43$; in CS_2, I=about 6.3 volts for the excited orbital, about 10.2 for the π_g, giving a ratio of 0.62, much higher than in CO_2. This behavior is what would be expected if the excited orbital is σ_g (cf. second paragraph preceding (15)), but is not so readily explained if it is σ_u or π_u. On the whole, considering also the evidence from COS given below, it appears rather probable that the excited orbital involved in the CS_2 bands near λ3200 is the σ_g orbital.

The absorption spectrum of COS is continuous,[24] beginning near λ2550. The absence of longer wave-length absorption indicates that the three excited orbitals analogous to those in (17) here definitely are all of high energy, since in COS there is no $_g$, $_u$ electronic selection rule to restrain transitions to any of the three. This result for COS leaves little doubt that the three excited orbitals (17) are all of fairly high energy also in CO_2 and CS_2, and probably in NO_2, thus furnishing a reasonable basis for the explanation given above for the instability of linear NO_2. To be sure, the excited σ_g (probably; or possibly it is the π_u or σ_u) is only 3.9 volts above the π_g in CS_2, and may be no higher in NO_2 (cf. second paragraph preceding (15)), so that it would seem that the instability of linear NO_2 relative to triangular NO_2 may be not so very pronounced.

The electronic absorption spectrum of N_2O begins with continuous absorption near λ2000.[21, 25] Taking into consideration the probably somewhat lower $I_{min.}$ for N_2O than for CO_2,[19] this indicates that the lowest excited orbital has an I about the same as in the case of CO_2.

[23] E. D. Wilson, Astrophys. J. **69**, 34 (1929); F. A. Jenkins, Astrophys. J. **70**, 191 (1929); V. Henri, Leipziger Vorträge, 1931; W. W. Watson and A. E. Parker, Phys. Rev. **37**, 1013A (1931); R. K. Asundi and R. Samuel, Proc. Acad. Sci. U.P., India **4**, 203 (1934).

[24] W. Lochte-Holtgreven and C. E. H. Baun, Trans. Faraday Soc. **28**, 698 (1932).

[25] G. Herzberg, Zeits. f. physik. Chemie **B17**, 68 (1932): CO_2 and N_2O, including a discussion of dissociation products and predissociation. O. R. Wulf and E. H. Melvin, Phys. Rev. **39**, 180 (1932): N_2O absorption.

The Crystal Structure of Hexagonal Silver Iodide

LINDSAY HELMHOLZ,* *Gates Chemical Laboratory, California Institute of Technology*

(Received August 31, 1935)

On the basis of oscillation data a structure has been assigned to hexagonal silver iodide at room temperature in which the silver atoms are distributed at random among four positions tetrahedrally surrounding the ideal position in the wurtzite structure. Previous work is discussed and evidence supporting the preference of this structure is presented. At liquid-air temperatures the structure is found to approximate closely that of wurtzite with the ideal parameter value of 1/8. Physical characteristics of silver iodide are discussed in relation to the proposed structure.

INTRODUCTION

THE anomalous physical properties of crystalline silver iodide which in the main are still unexplained have led us to undertake a redetermination of the crystal structure of this substance in spite of the seemingly satisfactory state of our present knowledge of it.[1] Since the beginning of this work a structure has been found for the high temperature (above 146°C) form which can be correlated nicely with its physical character.[2] Also a reinvestigation of the low temperature hexagonal form by the powder method has been reported to show that it has essentially the wurtzite structure with a parameter slightly larger than the ideal value, one-eighth.[3] The agreement between calculated and experimental intensities is certainly not good, the differences being attributed by the authors to preferred orientations in the sample. In addition, high orders where such a small difference in the parameter would become effective were not or could not be used in the powder analysis. The unusually high temperature factor introduces another complication. In view of these facts it seems doubtful that any great weight can be attached to the apparent (but very slight) deviation from the ideal structure.

In this investigation powder, Laue, and oscillation methods were used and the oscillation diffraction pictures found to be the most conclusive and satisfactory. Photographs were taken over a 300-degree temperature range. The low temperature data indicate that at −180°C the structure is essentially that of wurtzite with the ideal parameter value. On the basis of the room temperature pictures a structure has been assigned in which the silver atoms are distributed at random among four positions tetrahedrally surrounding the ideal position. A gradual transition (with rising temperature) is postulated between these two arrangements. The attempt has been made to explain some of the peculiarities of silver iodide on the basis of these structures.

PROCEDURE

Single crystals of silver iodide were prepared by a slight modification of the method of Zepharovich.[4] Concentrated hydrogen iodide solution was saturated with silver iodide and a thin layer of absolute alcohol spread over the heavy liquid. The hydrogen iodide diffusing into the upper layer and reacting with the alcohol removed iodide ions slowly enough to permit good crystals of the salt to form. It was also found that placing silver in the saturated solution was effective in making crystals and somewhat simpler, the reaction of hydrogen iodide with metallic silver being sufficiently slow to allow the formation of small crystals. By the first method hexagonal plates of silver iodide with edges 5 mm in length were obtained. Hexagonal crystals, usually hexagonal pyramids, were formed exclusively by these procedures. No trace of a cubic modification was found in any case.

Laue photographs were taken along the hexagonal axis perpendicular to the thin plates. The

* National Research Fellow.

[1] R. B. Wilsey, Phil. Mag. **46**, 487 (1923).

[2] Lester Strock, Zeits. f. physik. Chemie **B25**, 441 (1934).

[3] N. W. Kolkmeijer and J. W. A. van Hengel, Zeits. f. Krist. **88**, 317 (1934).

[4] V. von Zepharovich, Zeits. f. Krist. **4**, 119 (1880).

pictures checked those of Aminoff,[5] allowing for the difference in wave-length range used, and the data were found to be consistent with the space group C^4_{6v} and with a structure approximating that of wurtzite. For the determination of the parameter value, however, the data were too meager. The Laue pictures were so poor in first order reflections that the best that could be done was to limit the range of the parameter between 0.625 and 0.700. Unsymmetrical pictures taken in an effort to increase the amount of data indicated that for no value of the parameter could the intensities be fitted, but the absorption in the case of these pictures was so large as to invalidate the results or at least to make them questionable. With a ten-day exposure no reflections requiring a larger unit were observed.

Powder pictures were taken of samples prepared according to the directions of Bloch and Muller[6]—the photographs obtained matched those of Kolkmeijer and van Hengel. No attempt was made to determine the structure from these pictures.

Oscillation pictures were taken with Mo $K\alpha$ radiation on two different spectrographs. Most of them were taken from the (00·1) cleavage face of the crystal. Three types of crystals were tried in an attempt to find the most satisfactory. First, a very small thin plate was used, with which it was hoped completely to avoid absorption effects, but a plate of the smallest practical dimensions, $0.2\times0.2\times0.05$ mm, was found to give too much absorption to permit the use of this technique. A small thick crystal totally included in the beam was used next. In this case the calculated intensities were multiplied by a factor $\sin\theta$ to take into account the fraction of the beam striking the prepared face of the crystal. The large absorbing crystal intercepting the entire beam was found most satisfactory because of the greater reflected intensity and the fact that the factor $\sin\theta$ was not necessary. Also absorption could be more easily taken into account for this case. The last two types of crystals gave concordant results. The cleavage faces were ground and no differences observed in the reflected intensities from ground and freshly cleaved faces.

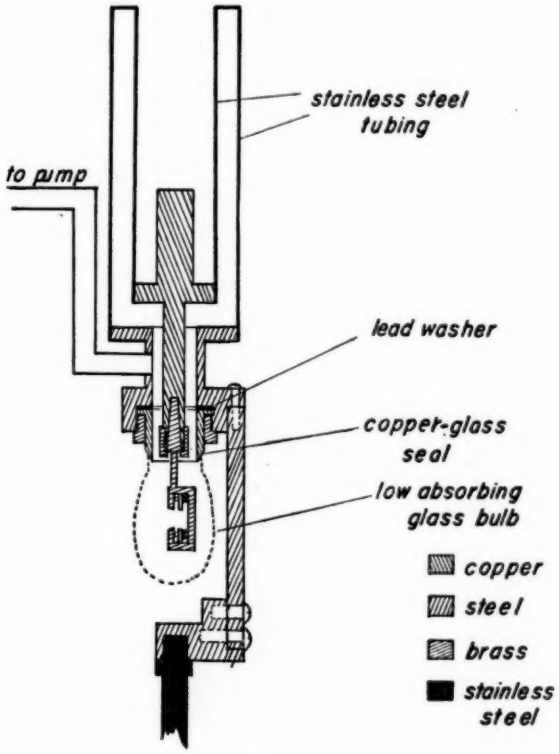

FIG. 1.

The large temperature factor, as will be seen later, plays an important role in an attempt to fit the experimental intensities. To obtain a value for this factor and to obtain more data an apparatus was constructed for taking oscillation pictures at temperatures down to that of liquid air. It was also desired later to investigate the anomalous contraction of silver iodide with rising temperature. This apparatus consists of a metal Dewar supported on a stand and open at the bottom, with the crystal support attached to the inside of the Dewar and extending out through the opening (Fig. 1). The Dewar is closed by means of a thin glass bulb which surrounds the crystal which is cooled by conduction down the supporting rod. It was assumed that with a good vacuum the temperature of the crystal was the same as that of the support after a period of one hour. The whole apparatus was oscillated in the x-ray beam, the connection to a diffusion pump being through rubber tubing. The agreement between experimental intensities and those

[5] G. Aminoff, Geol. Foren. Stockholm Forh. **44**, 444 (1922).
[6] R. Bloch and H. Muller, Zeits. f. physik. Chemie **A152**, 245 (1931).

calculated for different temperatures with the factor $e^{-2\beta(\sin\theta/\lambda)^2}$ indicates that within the errors of the intensity measurements the temperature of the liquid in the Dewar and the crystal were the same.

With the unit cell and the space group already known the intensities were of greatest interest for this work. For room temperature estimates, comparison pictures were taken. Three sets of five exposures differing in length by convenient multiples were obtained. Comparison of lines of equal intensity on photographs of different exposures gave fairly reliable estimates of relative intensity. Because of the difficulty of taking the low temperature pictures, this procedure was not possible and the relative intensities were measured by means of a calibrated scale. These two methods were checked one against the other for the room temperature case and the agreement was within the error of the comparison method. The estimates of intensity are probably reliable to 20 percent.

Results

The size of the unit and the space group were found to be the same as previously reported in the literature: hexagonal unit with two molecules in the cell, $a=4.59$A, $c=7.52$A ($c/a=1.64$), and the space group C^4_{6v}. The atomic positions for the wurtzite structure:

$$\text{Ag}\quad 00u,\ \tfrac{1}{3},\tfrac{2}{3},u+\tfrac{1}{2};\quad \text{I}\quad 000,\ \tfrac{1}{3},\tfrac{2}{3},\tfrac{1}{2}.$$

The parameter is taken here in accordance with the first work of Aminoff and is equal to $1-u'$, where u' is the value given by Kolkmeijer and van Hengel.

At liquid-air temperatures the size of the unit was found to be $a=4.57$A, $c=7.48$A with $c/a=1.63$. The data are given in Table I. These measurements cannot be considered as very accurate since the two crystals used at low temperatures gave broad diffuse lines, good for intensity estimates, but difficult to measure accurately, and layer line measurements are in themselves not very accurate.

The interest of the investigation lay in placing the silver atoms by plotting calculated intensities against the parameter u, and finding a value of u for which the calculated intensities match the experimental. The intensities were calculated according to the formula:

Table I.

Reflecting plane	Line	Sin θ	$d_{(00.1)}$
(00·4)	Mo $K\alpha$	0.1896	7.48A
(00·6)		.2854	7.46
(00·8)		.3798	7.47
(00·10)		.4735	7.48
(00·12)		.5664	7.49
(00·14)		.6621	7.49
(00·16)		.7580	7.48
		Average:	7.48

From the layer line measurements, Layer line	Sin θ	$d_{(10.0)}$
1	0.1568	4.57A
2	.3080	4.60
3	.4658	4.57
	Average:	4.58

$$I=C\frac{1+\cos^2\theta}{2\sin 2\theta}|S|^2e^{-\beta(\sin\theta/\lambda)^2}A,$$

where $|S|^2$ is the familiar absolute value of the structure factor squared. The values for f_I and f_{Ag}, the atomic scattering factors, were taken from the tables of Pauling and Sherman[7] and plotted against $\sin\theta$. For convenience these values were multiplied by $e^{-\beta(\sin\theta/\lambda)^2}((1+\cos^2\theta)/2\sin 2\theta)^{\frac{1}{2}}$. Account was taken of the fact that in using Mo $K\alpha$ radiation the K electrons of silver and iodine do not contribute to the diffraction. The f values were decreased by two units over the range of $\sin\theta$ used here. Correction was also made for absorption by means of a formula easily derived if one neglects secondary extinction. The ratio A gives the factor by which the calculated intensity must be multiplied in order to take account of absorption:

$$A=2\Big/\left(1+\frac{\sin\alpha}{\sin(\varphi-\alpha)}\frac{1}{\cos\chi}\right),$$

where φ is the azimuthal angle of the reflection, α is the angle through which the crystal has been turned when reflection takes place (this can be easily found from the reciprocal lattice), and χ

[7] Linus Pauling and J. Sherman, Zeits. f. Krist. **81**, 1 (1932).

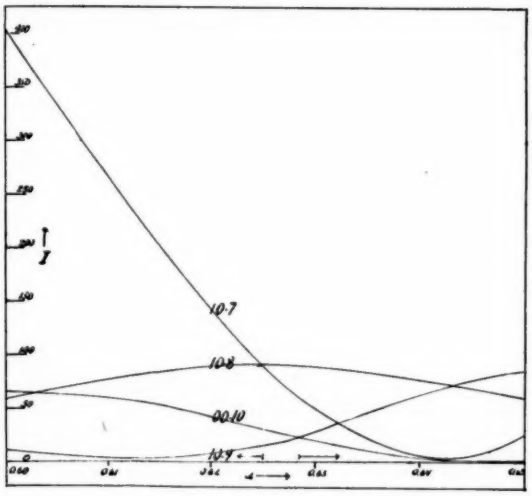

FIG. 2.

is the layer line angle. This relation could be checked semiquantitatively in cases where lines of the same form reflected at different α. The agreement was good enough so that it was though well worth while to use this correction factor. Naturally it holds only for the case of the large absorbing crystal where the limits for the calculation are well defined. A factor was also included in the calculations to take care of the relative time of exposure of the different lines. This factor, multiplying the calculated intensity, is $1/(1-(h\lambda/d \sin 2\theta)^2)^{\frac{1}{2}}$, where h is the index of the layer line, and d the identity distance in the vertical direction.

It was soon found in trying to fit the intensities that, with reasonable values of β, the agreement was fairly good for the wurtzite structure with $u=0.63$ (compare with 0.629 of Kolkmeijer and van Hengel) except for two qualitative comparisons which ruled the structure out altogether as shown in Fig. 2. $(10\cdot7)$ is observed stronger than $(10\cdot8)$ forcing the parameter to lie below 0.625, and $(10\cdot9)$ is observed stronger than $(00\cdot10)$ giving 0.629 as the lowest possible value by this comparison. This is indicated by the two arrows at the bottom of the plot. The use of larger values of u solves the $(10\cdot9)\geqq(00\cdot10)$ difficulty and aggravates the $(10\cdot7)\geqq(10\cdot8)$ discrepancy. The region in which no value of u is permitted is narrowed down considerably by increasing β but with $\beta=6$ the dilemma is still unresolved and the quantitative relationships of other lines are thrown out by a factor of two or more. There is the additional objection to increasing β that at a value of five the qualitative agreement in the prism reflections, which are independent of u, is upset, $(10\cdot0)$ becoming stronger than $(30\cdot0)$ while actually the reverse is observed. From specific heat data one obtains a value of 3.0 for β assuming that the crystal behaves as a simple cubic lattice and that it is still in the temperature range where these formulae are valid. It was assumed from these considerations that no solution was to be reached by using β as an additional parameter.

Believing that wurtzite had been ruled out, we investigated numerous combinations of structures or alternating structures with fractional atoms at positions consistent with the space group. Combinations of the special positions for wurtzite with those of niccolite or sphalerite were tried but gave no agreement at all, so that, although it is probable that all combinations were not tried, we feel confident that nothing of this nature would represent the state of the crystal. As an example of this sort of procedure: the atom positions were taken Ag/2: $\frac{1}{3}, \frac{2}{3}, p+\frac{1}{2}$; $\frac{2}{3}, \frac{1}{3}, p+\frac{1}{2}$; 2 at $0, 0, p$. I: $\frac{1}{3}, \frac{2}{3}, \frac{1}{2}$; $\frac{2}{3}, \frac{1}{3}, \frac{1}{2}$; 2 at $0, 0, 0$. This variation is one of the simplest and gave no possibility of fitting the layer line intensities. However it shows the sort of attempts that were made. The failure of this procedure led us to believe that whatever the structure was it could not be very different from wurtzite itself.

Next we attempted to place the silver atoms at random among four positions at points extended tetrahedrally from the ideal wurtzite position $(u=0.625)$ toward the faces of the tetrahedra formed by the surrounding iodine atoms. This treatment uses two wurtzite positions and six more equivalent positions belonging to C_6^4. The atomic positions for the structure are:

I: $0, 0, 0$; $\frac{1}{3}, \frac{2}{3}, \frac{1}{2}$

Ag/4: $\frac{1}{3}, \frac{2}{3}, \frac{1}{8}-\frac{3p}{4}$; $\frac{1}{3}+\frac{p}{\sqrt{6}}, \frac{2}{3}-\frac{p}{\sqrt{6}}, \frac{1}{8}+\frac{p}{4}$;

$\frac{1}{3}-\frac{2p}{\sqrt{6}}, \frac{2}{3}-\frac{p}{\sqrt{6}}, \frac{1}{8}+\frac{p}{4}$; $\frac{1}{3}+\frac{p}{\sqrt{6}}, \frac{2}{3}+\frac{2p}{\sqrt{6}}$,

$\frac{1}{8}+\frac{p}{4}$; $0, 0, \frac{5}{8}-\frac{3p}{4}$; $-\frac{p}{\sqrt{6}}+\frac{p}{\sqrt{6}}, \frac{5}{8}+\frac{p}{4}$;

$\frac{2p}{\sqrt{6}}, \frac{p}{\sqrt{6}}, \frac{5}{8}+\frac{p}{4}$; $\frac{p}{\sqrt{6}}, \frac{-2p}{\sqrt{6}}, \frac{5}{8}+\frac{p}{4}$

where p, the parameter here is the altitude of the tetrahedron at the corners of which the silver atoms are located. Reasons for choosing this structure will be discussed later; certainly it was the only one found that would resolve the difficulties enumerated above. That this is not just a subterfuge to decrease the f value of the silver atom is shown by the fact that if the silver atoms are spread out toward the corners of the iodine tetrahedron (rather than the faces), the agreement is considerably worse than for wurtzite itself. The intensity comparisons are found in Table II, the third column giving calculated intensities from the tetrahedral silver structure and the fourth those from wurtzite. The amount of data is not imposing but it may be mentioned that the intensity relationships in the fourth layer line follow very closely those in the second as is borne out by the calculations. With the axis 11·0 vertical the odd layer lines are greatly influenced by absorption and have not been considered in the room temperature pictures. $(2\bar{1}\cdot 6)$ and $(2\bar{1}\cdot 8)$ were observed on pictures taken with the axis 10·0 vertical. The $(20\cdot 7)\cong(20\cdot 8)$ difficulty in the fourth layer line is more acute than the corresponding case in the second layer line since the f values for these reflections are more nearly equal. Also the difference in intensity is more marked.

TABLE II.

$(hk\cdot l)$	I_{obs}	I_{calc} TETRAHEDRAL Ag $\beta=3.5$	I_{calc} WURTZITE $\beta=4.0$
(00·2)	whole beam not intercepted		
(00·4)	1.2	1.2	1.0
(00·6)	10.0	8.0	10.0
(00·8)	3.6	3.0	3.2
(00·10)	0.25	0.20	0.15
Second layer line			
(10·5)	16.0	14.5	17.5
(10·6)	1.6	1.7	1.9
(10·7)	0.70	0.62	0.38
(10·8)	.60	.53	.68
(10·9)	.30	.25	.19
(10·10)	.00	.05	.05
(10·11)	.15	.13	.13
Third layer line			
$(2\bar{1}\cdot 6)$	4.1	3.8	4.6
$(2\bar{1}\cdot 8)$	1.6	1.4	2.0
Fourth layer line			
(20·7)	0.60	0.60	0.26
(20·8)	.30	.26	.55
Prism reflections†			
(10·0)	60.0	56.0	
(20·0)	23.0	23.0	
(30·0)	28.0	29.5	
(40·0)	2.8	2.2	
(50·0)	0.70	0.65	
(60·0)	0.0	0.50	

† The calculated and observed intensities for the prism planes bear no relation to the preceding values.

TABLE III.

$(hk\cdot l)$	I_{obs}	I_{calc}	$(hk\cdot l)$	I_{obs}	I_{calc}
(00·4)	0.60	0.65	(01·8)	6.5	7.1
(00·6)	20.0	19.7	(01·9)	2.7	1.9
(00·8)	15.0	15.0	(01·10)	1.4	1.5
(00·10)	3.5	3.1	(01·11)	4.5	4.1
(00·12)	0.10	0.01	(01·12)	0.0	0.00
(00·14)	.60	1.0	(01·13)	1.75	1.85
(00·16)	.30	.50			
(03·16)	.20	.20	$(2\bar{1}\cdot 6)$	12.0	9.0
			$(2\bar{1}\cdot 8)$	10.0	7.0
(01·6)	1.9	1.75	$(2\bar{1}\cdot 10)$	1.7	2.0
(01·7)	1.5	1.3			

The best agreement for the tetrahedral arrangement of silver atoms was obtained at $p=0.0425$, giving the distance of the atoms from the center of the tetrahedron as 0.23A. For this value of p the bonded silver iodine distance is 2.74A and the "nonbonded" distance 3.05A.

The low temperature exposures gave much the same pictures with no indication of a radical change in structure or parameter value, but with greatly enhanced intensities and more orders. Whereas at room temperature (00·10) had been barely visible after long exposure, even the much more complicated reflection (03·16) was quite strong at liquid air temperatures. At this temperature the intensities are accounted for satisfactorally by assuming the ideal wurtzite structure ($p=0$), with the exception of the line (00·12) which is too strong experimentally. This reflection appears on only one photograph and may be explained without too great difficulty. The data are given in Table III. The factor multiplying the calculated intensities to bring them to agreement with the arbitrary experimental standard is here the same as for the room temperature case so that the check indicates that the change of intensity with temperature is given fairly well by the factor $e^{-2B(\sin\theta/\lambda)^2}$.

The first thing that was noticed in the low temperature pictures is that (00·4) becomes decidedly weaker in absolute intensity at −180°C.

The intensity of this line depends essentially on $(f_I - f_{Ag})^2$, so that this behavior is contrary to what one would expect and can only be interpreted as meaning that the silver atom has lost mobility or has become less spread out in going from the higher to the lower temperatures as these are the only means by which f_{Ag} can be increased. This is, of course, true only in the absence of some structural change, but would be true if with decreasing temperature silver iodide changed from the postulated room-temperature structure to ideal wurtzite. As can be seen, this fits the x-ray data nicely.

This result opened up another line of attack on the room-temperature intensities. Rigorously one should use an individual β for each type of atom in the crystal, and it was thought possible that by giving the silver atoms a larger temperature factor than the iodine the anomalous behavior of $(00\cdot4)$ could be explained as well as the $(10\cdot7) \geqq (10\cdot8)$ and $(10\cdot9) \geqq (00\cdot10)$ difficulties. By using $\beta_I = 3.00$ and $\beta_{Ag} = 5.00$ this can be done in a measure, but then $(00\cdot4)$ becomes approximately three times too large in relative intensity. The value of u again lies close to 0.63. The attempt to fit intensities in this way was abandoned because of $(00\cdot4)$ and because so large a difference in the temperature factors appears unsound.

In another attempt to account for the data, the scattering matter of each silver atom was distributed over the surface of a sphere about the ideal position of the atom; the radius of this sphere being used as the parameter. This was done on the assumption that the greater mobility of the silver was causing the troublesome intensity relationships, or that the silver existed in the crystal with different coordination numbers, causing it to oscillate among several positions approximately on the surface of a sphere. The calculations were carried out by multiplying the f values by $\sin x/x$, and making a set of curves for each value of the parameter. x here $= 4\pi r \sin\theta/\lambda$ θ and λ having the usual meaning, and r being the radius of the sphere. At $r = 0.25$A, the difficulties still persisted, and in reality this procedure amounts to little more than giving one atom a larger β value than the other at one particular temperature. To explain the behavior of $(00\cdot4)$ one would have to assume a gradually decreasing radius for the sphere with decreasing temperature. Also the distance of closest approach of the silver and iodine seemed rather small on this picture so the attempt was abandoned in favor of the structure with the tetrahedrally distributed silver atoms.

With the introduction of three new positions for each silver atom reflections of the type $(n0\cdot l)$ $n = 3$ mod. 3 and l odd, absent in wurtzite, should appear. In no case were these lines observed but the calculated intensities show them to be vanishingly small due to the symmetrical distribution of silver atoms around the ideal position. The calculated intensities were always smaller than those of allowed lines not observed in the photographs.

Discussion

It will be seen from Table II that the agreement between experimental and calculated intensities is almost as good for wurtzite with $u = 0.63$ as for the postulated random distribution of silver atoms. The decision between the two structures rests on three main points. (1) The very small change from the ideal position seems improbable for two reasons. If, as this structure would indicate, the crystal is composed of silver iodide molecules one would think a larger difference should exist between the bonded and nonbonded Ag–I separations which are here 2.77A and 2.835A, respectively. Then, too, for this arrangement an axial ratio corresponding so closely to hexagonal close packing would hardly be anticipated. (2) If the crystal is of a homopolar nature with covalent bonds running throughout the structure, it seems hardly likely that the silver atoms can have a temperature factor enough larger than the iodine atoms to explain the results since the two types of atoms are so intimately connected. It is seen too in this connection that when the intensities in general are accounted for by the use of differing β values, $(00\cdot4)$ becomes much too strong. It is true that the intensity of this line is very sensitive to small errors in the f values, but even the allowance of a five percent error in each curve will not account for the discrepancy. (3) The impossibility of fitting the intensity relationships $(10\cdot7) \geqq (10\cdot8)$ and $(10\cdot9) \geqq (00\cdot10)$ seems to eliminate the wurtzite structure entirely. In thirty oscillation

where p, the parameter here is the altitude of the tetrahedron at the corners of which the silver atoms are located. Reasons for choosing this structure will be discussed later; certainly it was the only one found that would resolve the difficulties enumerated above. That this is not just a subterfuge to decrease the f value of the silver atom is shown by the fact that if the silver atoms are spread out toward the corners of the iodine tetrahedron (rather than the faces), the agreement is considerably worse than for wurtzite itself. The intensity comparisons are found in Table II, the third column giving calculated intensities from the tetrahedral silver structure and the fourth those from wurtzite. The amount of data is not imposing but it may be mentioned that the intensity relationships in the fourth layer line follow very closely those in the second as is borne out by the calculations. With the axis 11·0 vertical the odd layer lines are greatly influenced by absorption and have not been considered in the room temperature pictures. $(2\bar{1}\cdot 6)$ and $(2\bar{1}\cdot 8)$ were observed on pictures taken with the axis 10·0 vertical. The $(20\cdot 7)\cong(20\cdot 8)$ difficulty in the fourth layer line is more acute than the corresponding case in the second layer line since the f values for these reflections are more nearly equal. Also the difference in intensity is more marked.

TABLE II.

$(hk\cdot l)$	I_{obs}	I_{calc} TETRAHEDRAL Ag $\beta=3.5$	I_{calc} WURTZITE $\beta=4.0$
(00·2)	whole beam not intercepted		
(00·4)	1.2	1.2	1.0
(00·6)	10.0	8.0	10.0
(00·8)	3.6	3.0	3.2
(00·10)	0.25	0.20	0.15
Second layer line			
(10·5)	16.0	14.5	17.5
(10·6)	1.6	1.7	1.9
(10·7)	0.70	0.62	0.38
(10·8)	.60	.53	.68
(10·9)	.30	.25	.19
(10·10)	.00	.05	.05
(10·11)	.15	.13	.13
Third layer line			
$(2\bar{1}\cdot 6)$	4.1	3.8	4.6
$(2\bar{1}\cdot 8)$	1.6	1.4	2.0
Fourth layer line			
(20·7)	0.60	0.60	0.26
(20·8)	.30	.26	.55
Prism reflections†			
(10·0)	60.0	56.0	
(20·0)	23.0	23.0	
(30·0)	28.0	29.5	
(40·0)	2.8	2.2	
(50·0)	0.70	0.65	
(60·0)	0.0	0.50	

† The calculated and observed intensities for the prism planes bear no relation to the preceding values.

TABLE III.

$(hk\cdot l)$	I_{obs}	I_{calc}	$(hk\cdot l)$	I_{obs}	I_{calc}
(00·4)	0.60	0.65	(01·8)	6.5	7.1
(00·6)	20.0	19.7	(01·9)	2.7	1.9
(00·8)	15.0	15.0	(01·10)	1.4	1.5
(00·10)	3.5	3.1	(01·11)	4.5	4.1
(00·12)	0.10	0.01	(01·12)	0.0	0.00
(00·14)	.60	1.0	(01·13)	1.75	1.85
(00·16)	.30	.50			
(03·16)	.20	.20	$(2\bar{1}\cdot 6)$	12.0	9.0
			$(2\bar{1}\cdot 8)$	10.0	7.0
(01·6)	1.9	1.75	$(2\bar{1}\cdot 10)$	1.7	2.0
(01·7)	1.5	1.3			

The best agreement for the tetrahedral arrangement of silver atoms was obtained at $p=0.0425$, giving the distance of the atoms from the center of the tetrahedron as 0.23A. For this value of p the bonded silver iodine distance is 2.74A and the "nonbonded" distance 3.05A.

The low temperature exposures gave much the same pictures with no indication of a radical change in structure or parameter value, but with greatly enhanced intensities and more orders. Whereas at room temperature (00·10) had been barely visible after long exposure, even the much more complicated reflection (03·16) was quite strong at liquid air temperatures. At this temperature the intensities are accounted for satisfactorally by assuming the ideal wurtzite structure ($p=0$), with the exception of the line (00·12) which is too strong experimentally. This reflection appears on only one photograph and may be explained without too great difficulty. The data are given in Table III. The factor multiplying the calculated intensities to bring them to agreement with the arbitrary experimental standard is here the same as for the room temperature case so that the check indicates that the change of intensity with temperature is given fairly well by the factor $e^{-2\beta(\sin\theta/\lambda)^2}$.

The first thing that was noticed in the low temperature pictures is that (00·4) becomes decidedly weaker in absolute intensity at −180°C.

The intensity of this line depends essentially on $(f_I - f_{Ag})^2$, so that this behavior is contrary to what one would expect and can only be interpreted as meaning that the silver atom has lost mobility or has become less spread out in going from the higher to the lower temperatures as these are the only means by which f_{Ag} can be increased. This is, of course, true only in the absence of some structural change, but would be true if with decreasing temperature silver iodide changed from the postulated room-temperature structure to ideal wurtzite. As can be seen, this fits the x-ray data nicely.

This result opened up another line of attack on the room-temperature intensities. Rigorously one should use an individual β for each type of atom in the crystal, and it was thought possible that by giving the silver atoms a larger temperature factor than the iodine the anomalous behavior of $(00\cdot4)$ could be explained as well as the $(10\cdot7) \geqq (10\cdot8)$ and $(10\cdot9) \geqq (00\cdot10)$ difficulties. By using $\beta_I = 3.00$ and $\beta_{Ag} = 5.00$ this can be done in a measure, but then $(00\cdot4)$ becomes approximately three times too large in relative intensity. The value of u again lies close to 0.63. The attempt to fit intensities in this way was abandoned because of $(00\cdot4)$ and because so large a difference in the temperature factors appears unsound.

In another attempt to account for the data, the scattering matter of each silver atom was distributed over the surface of a sphere about the ideal position of the atom; the radius of this sphere being used as the parameter. This was done on the assumption that the greater mobility of the silver was causing the troublesome intensity relationships, or that the silver existed in the crystal with different coordination numbers, causing it to oscillate among several positions approximately on the surface of a sphere. The calculations were carried out by multiplying the f values by $\sin x/x$, and making a set of curves for each value of the parameter. x here $= 4\pi r \sin\theta/\lambda$ θ and λ having the usual meaning, and r being the radius of the sphere. At $r = 0.25$A, the difficulties still persisted, and in reality this procedure amounts to little more than giving one atom a larger β value than the other at one particular temperature. To explain the behavior of $(00\cdot4)$ one would have to assume a gradually decreasing radius for the sphere with decreasing temperature. Also the distance of closest approach of the silver and iodine seemed rather small on this picture so the attempt was abandoned in favor of the structure with the tetrahedrally distributed silver atoms.

With the introduction of three new positions for each silver atom reflections of the type $(n0\cdot l)$ $n = 3$ mod. 3 and l odd, absent in wurtzite, should appear. In no case were these lines observed but the calculated intensities show them to be vanishingly small due to the symmetrical distribution of silver atoms around the ideal position. The calculated intensities were always smaller than those of allowed lines not observed in the photographs.

Discussion

It will be seen from Table II that the agreement between experimental and calculated intensities is almost as good for wurtzite with $u = 0.63$ as for the postulated random distribution of silver atoms. The decision between the two structures rests on three main points. (1) The very small change from the ideal position seems improbable for two reasons. If, as this structure would indicate, the crystal is composed of silver iodide molecules one would think a larger difference should exist between the bonded and nonbonded Ag–I separations which are here 2.77A and 2.835A, respectively. Then, too, for this arrangement an axial ratio corresponding so closely to hexagonal close packing would hardly be anticipated. (2) If the crystal is of a homopolar nature with covalent bonds running throughout the structure, it seems hardly likely that the silver atoms can have a temperature factor enough larger than the iodine atoms to explain the results since the two types of atoms are so intimately connected. It is seen too in this connection that when the intensities in general are accounted for by the use of differing β values, $(00\cdot4)$ becomes much too strong. It is true that the intensity of this line is very sensitive to small errors in the f values, but even the allowance of a five percent error in each curve will not account for the discrepancy. (3) The impossibility of fitting the intensity relationships $(10\cdot7) \geqq (10\cdot8)$ and $(10\cdot9) \geqq (00\cdot10)$ seems to eliminate the wurtzite structure entirely. In thirty oscillation

pictures taken from (00·1) of ten different crystals these intensity relations are observed and in no case the opposite. The comparison (10·9) against (00·10) may not be as good as could be desired since the lines are somewhat diffuse but we feel that in making the intensities equal adequate allowance has been made for the uncertainties involved in qualitative comparison.

The anomalies of the physical behavior of AgI are well known. It was hoped at the outset to explain the pronounced basal cleavage by reference to the crystal structure. This cannot be done rigorously but suggestions can be made. Wurtzite (hexagonal ZnS) itself has good prismatic cleavage and poor basal cleavage. The explanation presumably lies in the fact that basal cleavage with the breaking of one bond per unit cell leaves the two halves oppositely charged while breaking the same number of bonds in cleaving along (10·0) leaves both halves neutral. In order to leave both cleaved basal planes neutral it would be necessary to break two bonds per unit cell. For the case of the structure here suggested for silver iodide, however, only an average of 1.25 bonds must be broken to produce the observed cleavage if we assume that the long Ag–I distance is nonbonded. At room temperature the mean thermal displacement of the atoms from the equilibrium positions is of the order of magnitude of the distance between the four equivalent silver positions indicating that there is probably continual movement of the silver atoms between these potential minima. This shifting of bonds would be such as further to weaken the basal plane binding relative to that of the prism planes. These considerations show how basal cleavage (poor in wurtzite) may become more pronounced in silver iodide, but they cannot be said to give a thoroughly reliable explanation of the cleavage.

The movement of the silver atoms from place to place in the lattice is familiar in the explanation of the electrolytic cation conductivity of the high temperature form.[2] Somewhat similar motion is shown here with the difference that in the low temperature structure it is impossible for the silver atoms to escape from their tetrahedra of surrounding iodine atoms so that they cannot contribute to the conductivity.

No exact explanation has been obtained about the volume contraction with rising temperature found over a 150° range up to 146°C;[8] however, it might be suggested that the increased movement of the silver atoms among the tetrahedral positions may be responsible for this effect. Pictures of sufficient accuracy to give a microscopic substantiation of this phenomenon have not yet been obtained.

The low temperature pictures indicate that the structure is that of ideal wurtzite. The data are probably not as good as for the room temperature case, since the intensity estimates are not good to more than 30 percent and the method of applying the absorption correction is not exact. Two discrepancies are observed: (00·12) is stronger than would be expected for the ideal structure and (10·9) is noticeably weaker. These two difficulties may be explained if one assumes that all of the silver atoms have not yet given up the tetrahedral positions. Calculation shows that if one-fifth of the atoms are placed in the tetrahedral positions, the intensities of these two lines are brought into agreement with observation and the other lines are practically unaffected.

The fact that silver does not form four strong tetrahedral bonds is indicated by the softness of the crystal and its loose structure. It is one of the few crystals for which the molecular volume is as much as ten percent larger than the sum of the atomic volumes of the components. The three coordinated randomly distributed silver atoms in the proposed structure fit in nicely with the structure found by Strock for the high temperature form, indicating that at 146°C the already randomly arranged silver atoms with large temperature motion can "melt" inside the iodine lattice, allowing the sodium atoms to rearrange and give rise to the high temperature modification.

A possible explanation for the rearrangement of the silver atoms between liquid air and room temperatures is that there are in reality five potential minima within the iodine tetrahedra of nearly the same energy, and that the ideal wurtzite position is of slightly lower energy. Then at low temperatures the crystal would assume essentially the wurtzite structure and at 25°C the distribution would be random among the five positions. With four-fifths of the atoms in the

[8] Rodwell, Proc. Roy. Soc. **25**, 280 (1876); Trans. Roy. Soc. **173**, 1125 (1882).

tetrahedral positions the intensity calculations would be but little different from those given in this paper, although it would probably mean a small increase in the parameter value. The intensity data, however, do not warrant this calculation.

Evidence for three coordinated silver atoms has been found by Dr. Harker of this laboratory in a preliminary investigation of proustite and pyrargyrite where he also finds silver in a flattened pyramidal arrangement with a silver radius of approximately 1.45A. The silver radii from this investigation are: tetrahedral −1.53A, three coordinated −1.46A. The radius of the nonbonded silver is 1.77A.

Thanks are due to Professor Linus Pauling and to Dr. J. H. Sturdivant for valuable assistance with this work.

NOVEMBER, 1935 JOURNAL OF CHEMICAL PHYSICS VOLUME 3

A Study of the Molecular Structure of Diiodoethane

Iodine Bond Resonance and the Molecular Structure of Diiodoethylene. Molecular Packing in Their Crystal Lattices

HAROLD P. KLUG, *University of Idaho, Moscow, Idaho*

(Received August 4, 1935)

Using data from an x-ray study of the crystal structure of *sym*-diiodoethane and *sym*-diiodoethylene (*trans* form) the positions of the iodine atoms in the crystal cells were located. Iodine bond resonance is discussed and a factor of 0.92 of the length of the longer bond proposed for evaluating the interatomic distance for any resonating bond. On the basis of the concepts of tetrahedral carbon bonds, bond resonance, Pauling's normal convalent bond radii, etc., reasonable molecular models for the above substances were predicted. Comparison of these with the x-ray data showed the iodine-iodine distances to be in excellent agreement with certain iodine-iodine distances within the crystal cells, thus locating the molecules within the cells. These models together with Mack's concept of the atomic domain radius of atoms in crystals permitted a consideration of the packing of the molecules in the crystal lattice, thus locating the atomic coordinates of the carbon and hydrogen atoms in the cell. The domain radii found were; iodine =1.97A, and hydrogen=1.23A. The resulting molecular packing is seen to explain and be in excellent agreement with observed physical properties of the two crystals.

INTRODUCTION

AT present our most important methods for investigating molecular structure are based on comparison of experimental data with the results to be expected from a model which we have visualized from our best theoretical and experimental knowledge.

The results of x-ray diffraction studies on crystals give important data for consideration of the structure of the crystal molecule, especially in the case of organic substances. It is often possible to determine important interatomic distances in the molecule from these studies, thus permitting a study of the structure of the molecule, constancy of bond radii, bond angles, bond resonance, etc., by comparison with reasonable molecular models.

In a recent x-ray study[1] of the crystal structures of *sym*-diiodoethane and *sym*-diiodoethylene it was found possible to locate the iodine atoms in the unit cells with considerable accuracy. Using data from this investigation we have made a study of the molecular structures and molecular packing in the crystals of these compounds.

CRYSTAL STRUCTURE DATA

s-diiodoethane was found to possess a two-molecule monoclinic cell with the following dimensions:

$$a_0' = 4.768\text{A}, \quad b_0' = 12.897\text{A},$$
$$c_0' = 4.784\text{A}, \quad \beta' = 105°\ 5'.$$

Its space group is C_{2h}^5. The four-molecule pseudo-

[1] The detailed results of this study are reported in Zeits. f. Krist. 90, 495 (1935).

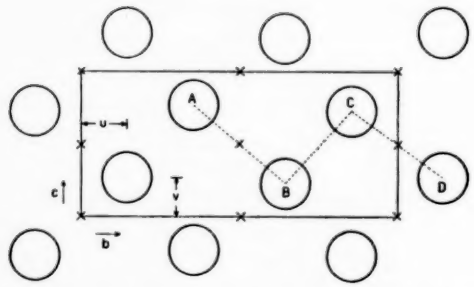

FIG. 1. Section through the cell of diiodoethane in the $(100)_0$ plane showing the location of the iodine atoms in the symmetry plane. The crosses indicate the positions of the symmetry centers. The circles do not indicate the size of the iodine atoms.

orthorhombic unit with

$$a_0=7.582\text{A}, \quad b_0=12.897\text{A},$$
$$c_0=5.810\text{A}, \quad \beta=90°\ 12',$$

is of remarkable interest. In fact the x-ray data from this unit were not observed to show any deviations from perfect orthorhombic symmetry. Treating the crystal as orthorhombic it possesses the space group V_h^{18}, and the eight iodine atoms in the cell are located at the points

$$0uv;\ \tfrac{1}{2},\tfrac{1}{2}-u,v;\ \tfrac{1}{2},u,v+\tfrac{1}{2};\ 0,\tfrac{1}{2}-u,v+\tfrac{1}{2};$$
$$0\bar{u}\bar{v};\ \tfrac{1}{2},u+\tfrac{1}{2},\bar{v};\ \tfrac{1}{2},\bar{u},\tfrac{1}{2}-v;\ 0,u+\tfrac{1}{2},\tfrac{1}{2}-v;$$

with $u=0.145\pm0.005$ and $v=0.27\pm0.01$. Each of the four molecules of this unit must then possess a minimum molecular symmetry of a twofold axis with a plane perpendicular to it. This symmetry plane is parallel to the (100) plane. The molecules will, therefore, have a center of symmetry, and they will be located in the cell on the symmetry planes with their centers at the symmetry centers of the space group.

In Fig. 1 is shown a section of the cell at $(100)_0$. The distances $AB=4.88$A, $BC=3.97$A, and $CD=4.60$A are the closest distances of approach of two iodine atoms in the symmetry plane. Either AB or CD, and not BC, represents the iodine-iodine distance within the molecule, since the midpoint of BC is not a symmetry center.

The x-ray study showed *s*-diiodoethylene (*trans* form) to be isomorphous with *s*-diiodoethane, and to have the following dimensions for its two-molecule monoclinic cell:

$$a_0'=4.58\pm\text{A}, \quad b_0'=13.310\text{A},$$
$$c_0'=4.58\pm\text{A}, \quad \beta'=105°\ 20'\pm.$$

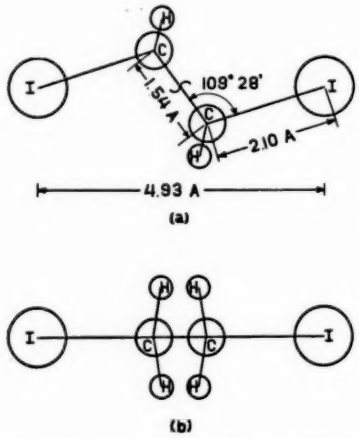

FIG. 2. (a) Projection of the molecule of diiodoethane on the symmetry plane (100). The C−H distance, seen only in projection, is 1.06A. The location of the twofold axis and symmetry center is shown at the center of the C−C bond. The circles do not indicate the relative sizes of the atoms. (b) Projection showing the distribution of the hydrogen atoms on either side of the symmetry plane.

The four-molecule pseudo-orthorhombic cell, whose diffraction effects likewise show no deviations from orthorhombic symmetry, has the dimensions:

$$a_0=7.280\text{A},\ b_0=13.310\text{A},\ c_0=5.553\text{A},\ \beta=90°\pm.$$

The space groups, of course, are the same as for the corresponding cells of diiodoethane. The eight iodine atoms of the orthorhombic cell have the same coordinates and the same identical values of u and v as in diiodoethane. The molecular symmetry of diiodoethylene is, therefore, the same as that of diiodoethane, and the section of its cell at $(100)_0$ is very similar to Fig. 1 except for slight differences in the dimensions. These lead to $AB=4.89$A, $BC=3.94$A, and $CD=4.63$A. As above, the iodine-iodine distance in the molecule must be AB or CD. The remaining considerations of this paper are based on the orthorhombic units described above.

STRUCTURE OF A MOLECULE OF *s*-DIIODOETHANE

The diiodoethane molecules must possess a plane of symmetry with a twofold axis perpendicular to it. The assumption of normal covalent single bonds throughout the molecule, and of tetrahedral bond angles would seem justifiable. The only reasonable configuration satisfying the above considerations is that shown in Fig. 2.

The interatomic distances are those of Pauling's normal covalent bond radii.[2] The iodine-iodine distance is calculated to be 4.93A. This is in excellent agreement with the distance $AB = 4.88$A in the crystal cell, which is to be considered the distance between two iodine atoms of a molecule in the crystal. The possibility that the distance CD in the crystal cell represents the iodine-iodine distance in the individual molecule is not likely in consideration of the poor agreement with our model. To reduce the iodine-iodine distance in our molecular model to $CD = 4.60$A would require considerable change in the bond radii or bond angles, both of which are well established by theory and experiment. For instance it would require reduction of the tetrahedral bond angle to approximately 95°.

Further discussion of the structure of this molecule will be reserved until the discussion of molecular packing.

Iodine Bond Resonance and the Structure of Molecules of *s*-Diiodoethylene

To construct a satisfactory molecular model for diiodoethylene we must consider one of the peculiar valence properties of iodine together with the phenomenon of bond resonance. A number of compounds are known in which certain electronegative elements possess more than four electron-pairs in their valence shell.[3] Iodine is such an element since it apparently has five electron-pairs in its valence shell in certain of its compounds. In fact a satisfactory explanation of the $(ClICl)^-$ ion, the I_3^- ion and of ICl_3 necessitates such an assumption.

Pauling[2] has pointed out that the phenomenon of resonance is to be expected when two or more reasonable Lewis structures can be written for a molecule. This resonance leads to interatomic distances within the molecule nearly as small as the smallest of those for the individual structures. With a few exceptions the values of the interatomic distances for these resonating bonds have never been observed to be as small as the value for the smaller normal bond. The empirically determined factor of 0.92 of the value of the larger bond (Table I) seems to fit the observed data quite well. In considering models of molecules in which resonance occurs it would seem more satisfactory to use the value based on this factor rather than any other values of bond radii.

With iodine's ability to hold five electron-pairs bond resonance is expected to occur where possible. The work of Hendricks and associates[4] on *p*-diiodobenzene clearly demonstrates this bond resonance although they do not point it out. They determined the iodine-iodine distance in the *p*-diiodobenzene molecule to be 6.85 ± 0.10A from electron diffraction in the gaseous state, and 6.85A from x-ray diffraction in the crystals. From these results they pointed out that the carbon-iodine distance was 2.00A instead of 2.10A expected from Pauling's normal covalent bond radii for single bonds.

The following Lewis structures can be written for *p*-diiodobenzene:

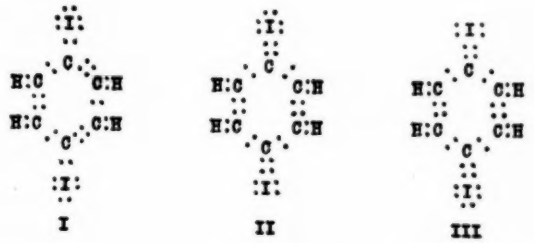

I II III

Now the theoretical iodine-iodine distance to be expected for each of these structures can be calculated for comparison with Hendricks' experimental value. The distance across the *para* positions of the resonating hexagonal benzene ring is quite accurately known from the value, 1.42A, the carbon-carbon distance in benzene and other aromatic structures (Table I). This distance is 2.84A, and will be the same for all of the above structures. The iodine-iodine distance for structure I with two carbon-iodine single bonds is calculated to be 7.04A by using Pauling's bond radii. Structures II and III, which are identical except for the five electron-pairs being on different iodine atoms, will have an iodine-iodine distance of 6.62A as a result of the carbon-iodine double bonds. Comparison of these with Hendricks' value points unquestionably to bond resonance. Considering the carbon-iodine

[2] L. Pauling, Proc. Nat. Acad. Sci. **18**, 293 (1932).
[3] See M. L. Huggins, Chem. Rev. **10**, 427 (1932).
[4] S. B. Hendricks, L. R. Maxwell, V. L. Mosley and M. E. Jefferson, J. Chem. Phys. **1**, 549 (1933).

TABLE I. *Values of resonating bonds.*

BOND	BOND VALUE FROM PAULING'S RADII 1ST BOND	2ND BOND	0.92 OF 1ST BOND	EXP. VALUE OBS.	COMPOUND	NATURE OF OBS.	REFERENCES
C : C⇌C : : C	1.54A	1.38A	1.418A	1.42A	Graphite	C. S.*	Bernal, Proc. Roy. Soc. **A106**, 749 (1924)
				1.42 ±0.03	$C_6(CH_3)_6$	C. S.	Lonsdale, Proc. Roy. Soc. **A123**, 494 (1929)
				1.412	Naphthalene	C. S.	Robertson, Proc. Roy. Soc. **A142**, 674 (1933)
				1.41	Anthracene	C. S.	Robertson, Proc. Roy. Soc. **A140**, 79 (1933)
				1.42	Terphenyl	C. S.	Pickett, Proc. Roy. Soc. **A142**, 333 (1933)
				1.41	Chrysene	C. S.	Iball, Proc. Roy. Soc. **A146**, 140 (1934)
				1.41	Durene	C. S.	Robertson, Proc. Roy. Soc. **A142**, 659 (1933)
				1.43 ±0.03	Diacetylene	E. D.	Brockway, Proc. Nat. Acad. Sci. **19**, 868 (1933)
				1.43 ±0.03	Cyanogen	E. D.	Brockway, Proc. Nat. Acad. Sci. **19**, 868 (1933)
				1.390±0.005	Benzene	E. D.	Pauling and Brockway, J. Chem. Phys. **2**, 867 (1934)
B : N⇌B : : N	1.59	1.43	1.463	1.47 ±0.07	$B_3N_3H_6$	E. D.	Stock and Wierl, Zeits. anal. Chemie **203**, 228 (1931)
				1.45	Boron Nitride	C. S.	Pauling, Proc. Nat. Acad. Sci. **18**, 293 (1932)
N : O⇌N : : O	1.36	1.22	1.251	1.26	NO_3^- ion	C. S.	Wyckoff, *The Structure of Crystals*, 2nd Ed., p. 272
C : O⇌C : : O	1.43	1.28	1.316	1.26	CO_3^- ion	C. S.	Wyckoff, *The Structure of Crystals*, 2nd Ed., p. 272
				1.25 ±0.05	$(COOH)_2 \cdot 2H_2O$	C. S.	Zachariasen, Zeits. f. Krist. **89**, 442 (1934)
				1.29	$Be_4O(C_2H_3O_2)_6$	C. S.	Pauling and Sherman, Proc. Nat. Acad. Sci. **20**, 340 (1934)
				1.25	Urea	C. S.	Wyckoff and Corey, Zeits. f. Krist. **89**, 462 (1934)
				1.29 ±0.02	$(HCOOH)_2$	E. D.	Pauling and Brockway, Proc. Nat. Acad. Sci. **20**, 336 (1934)
C : : O⇌C : : : O	1.28	1.13	1.178	1.15	CO	?	Pauling, Proc. Nat. Acad. Sci. **18**, 293 (1932)
				1.15	CO_2	R. S.	Pauling, Proc. Nat. Acad. Sci. **18**, 293 (1932)
				1.13	CO_2	C. S.	Wyckoff, *Structure of Crystals*, 2nd Ed. Supplement, p. 30
				1.15 ±0.05	NCO^- ion	C. S.	Hendricks and Pauling, J. Am. Chem. Soc. **47**, 2904 (1925)
N : : N⇌N : : : N	1.26	1.10	1.160	1.15 ±0.05	N_3^- ion	C. S.	Hendricks and Pauling, J. Am. Chem. Soc. **47**, 2904 (1925)
C : N⇌C : : N	1.47	1.32	1.353	1.37	Urea	C. S.	Wyckoff and Corey, Zeits. f. Krist. **89**, 462 (1934)
				1.35	Thiourea	C. S.	Wyckoff and Corey, Zeits. f. Krist. **81**, 386 (1932)
C : S⇌C : : S	1.81	1.63	1.665	1.64	Thiourea	C. S.	Wyckoff and Corey, Zeits. f. Krist. **81**, 386 (1932)
N : : C⇌N : : : C	1.32	1.16	1.214	1.15 ±0.05	NCO^- ion	C. S.	Hendricks and Pauling, J. Am. Chem. Soc. **47** 2904 (1925)
				1.16 ±0.02	Cyanogen	E. D.	Brockway, Proc. Nat. Acad. Sci. **19**, 868 (1933)
C : I⇌C : : I	2.10	1.89	1.931	1.96	*trans*-$C_2H_2I_2$	C. S.	Klug, this paper
				2.00	*p*-$C_6H_4I_2$	C. S. and E. D.	Hendricks and Associates, J. Chem. Phys. **1**, 549 (1933)

* C. S. = Crystal Structure, E. D = Electron Diffraction, and R. S. = Raman Spectra.

bond as a resonating bond its value is 0.92 of the single bond value, and the iodine-iodine distance in the molecule becomes 6.70A. This is slightly less than Hendricks' value which is a bit larger than would be expected from these considerations. It has been suggested that the double bonds are somewhat less important in this case than the single bonds, thus requiring a slightly larger factor, 0.93 or 0.94. The factor 0.93 leads to the value 6.76A, which is within the limits of error of Hendricks' data.

Iodine bond resonance is to be expected in the molecule of diiodoethylene, the following Lewis structures being reasonable ones:

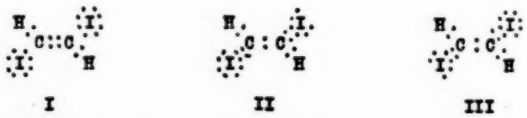

I II III

By using Pauling's bond radii and assuming a tetrahedral angle between the carbon-hydrogen and carbon-iodine bonds, the iodine-iodine distance in the molecule is readily calculated for the above structures with normal bonds, and for a molecule with resonating bonds. The iodine-iodine distance for structure I is found to be 5.13A, while that for structures II and III is 4.83A. The value for a resonating molecule (factor 0.92) is 4.84A.

Since diiodoethylene and diiodoethane are

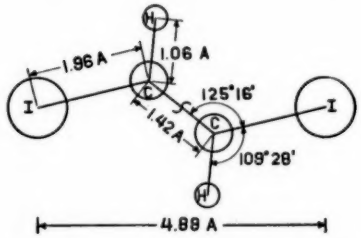

FIG. 3. Projection of the molecule of diiodoethylene on the symmetry plane (100). All atoms of the molecule lie in a plane.

isomorphous the distance $AB=4.89$A in the diiodoethylene cell will be expected to represent the iodine-iodine distance within the molecule of diiodoethylene. The value 4.84A for a resonating diiodoethylene molecule is in quite satisfactory agreement with this. The iodine bond resonance is, thus, very strikingly shown. In fact it might be said that the isomorphism of diiodoethylene with diiodoethane is a result of this bond resonance, since it reduces the iodine-iodine distance within the diiodoethylene molecule to almost exactly that in diiodoethane. The approximate equivalence of this value for the two molecules is a requirement for the isomorphism of the two substances.

Calculating the value of a resonating carbon-iodine bond from the x-ray data ($AB=4.89$A) we have 1.96A as given in Table I. The corresponding factor is 0.93. Fig. 3 is a diagram of the molecule of diiodoethylene in accordance with the above considerations and the molecular symmetry demanded by the x-ray data. Further discussion of its structure is reserved until the discussion of molecular packing.

MOLECULAR PACKING AND THE CRYSTAL-CHEMICAL PROPERTIES

The x-ray data cannot locate the positions of the hydrogen atoms in the molecules and crystal cells of compounds, and in the case of the substances being discussed, even the carbon atoms are not susceptible to location from the x-ray intensities because of the much greater scattering power of the iodine atoms.

Mack[5] has shown that these light atoms can be located in the molecule and in the crystal cell, and a satisfactory stereochemical picture of the crystal lattice explaining many of the observed properties of the crystal obtained, by a study of the spatial packing of molecular models. In the molecular model each atom possesses, in addition to its known values of bond radii and bond angles, an atomic domain which represents its extension in space. This domain is essentially spherical, and for a given kind of atom has a reasonably constant radius from crystal to crystal as long as the conditions remain the same; i.e., same type of binding, no molecular rotation, etc. The domains of separate atoms do not interpenetrate each other except when those atoms are attached to the same atom, as for example, the hydrogens of a methyl group. Atoms on separate molecules will be expected not to interpenetrate each other's domain. Finally, of course, the size and shape of the unit cell as determined by x-ray diffraction are accurately accounted for. The number of positions, satisfying the above conditions, which a given atom can occupy in the molecule or crystal cell is narrowed down in most cases to a single position.

A study of the molecular packing in crystals of these two compounds is of considerable interest. For diiodoethane the molecular model of Fig. 2 has been used, thereby increasing the distance AB (Fig. 1) in the cell to 4.93A. Keeping the angle between AB and the b axis as observed, then $u=0.146$ and $v=0.273$, values well within the limits of the x-ray data. BC then becomes 3.947A and $CD=4.61$A. Fig. 4 (a) shows the packing in the $(100)_0$ plane. The contacts in this plane are across the iodine atoms (represented by large circles). An iodine atom B just kisses an iodine atom C in a neighboring molecule when its domain radius is 1.974A, a value in excellent agreement with the results from other organic compounds containing iodine.[6] The carbon atoms (not shown in Fig. 4) lie in the plane of the iodine atoms, and have the choice of two positions. Indicating the bonds in the molecule by the light lines shown in Fig. 4 (a), position No. 1 is at the intersections P_1. Position No. 2 is at P_2, indicated by the dotted lines on the molecule in the lower left-hand corner. The hydrogen atoms

[5] E. Mack, Jr., J. Am. Chem. Soc. **54**, 2141 (1932).

[6] See S. B. Hendricks, Chem. Rev. **7**, 431 (1930); M. L. Huggins and B. A. Noble, Am. Mineral. **16**, 519 (1931); and H. P. Klug, J. Am. Chem. Soc. **55**, 1430 (1933).

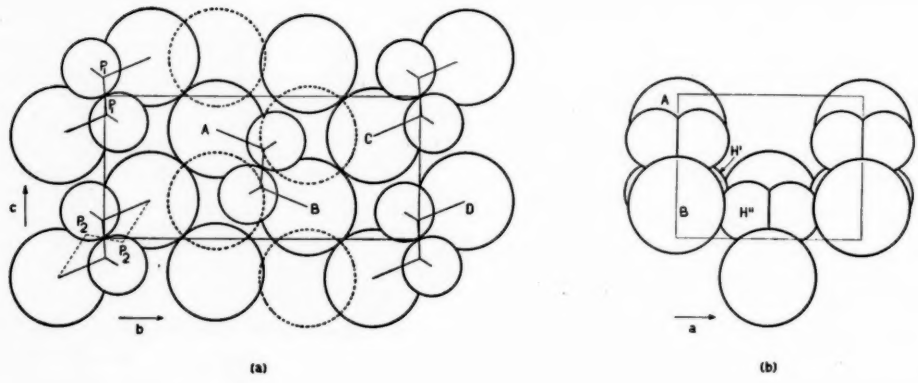

FIG. 4. (a) Section through the cell of diiodoethane in the $(100)_0$ plane showing the packing of the molecules. The large dotted circles locate in projection the iodine atoms of two molecules in the plane $(100)_{a/2}$. (b) Section through the cell in the plane $(010)_{b/2}$.

(small circles in Fig. 4) attached to the carbons by tetrahedral bonds do not lie in the plane of the iodine atoms but at equal distances on each side of it as shown in Figs. 2 (b) and 4 (b). The hydrogen atoms make no contacts with atoms of other molecules in the same plane, but a hydrogen atom H′ just makes contact with the hydrogen atom H″ on a molecule in the $(100)_{a/2}$ plane when its domain radius is 1.23A (Fig. 4 (b)). It is possible that at the same time H″ makes contact with iodine atom *B*, the required hydrogen atom domain radius being 1.246A. A hydrogen domain radius of 1.23A is slightly smaller than 1.29A found by Mack for hexamethylene tetramine. It is, however, in perfect agreement with 1.23A the domain radius just permitting contacts between hydrogen atoms on adjacent carbon atoms of a long chain aliphatic hydrocarbon molecule in the crystal. This considers the carbon atoms of the chain to lie in a plane,[7] the bond angles to be tetrahedral, and Pauling's bond radii throughout. The condition for contacts between hydrogen atoms of adjacent molecules is not essentially different from this case.

Position No. 1 is seen to be the correct position for the carbon chain since position No. 2 would result in hydrogen atoms and iodine atoms approaching each other along the *a* direction so closely as to reduce the hydrogen domain radius to 1.146A. A hydrogen domain radius as small as this is not to be expected except where we have molecular rotation. A calculation shows, however, that complete rotation of the C_2H_4 group about an axis through the two iodine atoms of the molecule would reduce the hydrogen domain radius to approximately 0.95A. This is smaller than Mack[5] observed in crystalline methane in which the occurrence of molecular rotation is well established. The possibility of molecular rotation in diiodoethane seems very unlikely, and position No. 2 is not a possible one. Two attempts, however, were made to locate transitions, indicative of molecular rotation, on its warming curve between liquid air and room temperatures. These somewhat crude preliminary studies by a differential thermocouple method failed to give any evidence of such a transition. The possibility of a slight oscillatory motion about this axis has not been ruled out, but cannot profitably be discussed here.

From the above considerations the carbon atoms are located in another set of the same equivalent positions as the iodine atoms with the calculated values of the parameters as follows: $u_C = -0.0036$ and $v_C = 0.132$. The sixteen hydrogen atoms are in Wyckoff's[8] set of sixteen most generally equivalent positions. Interchanging his *b* and *c* axes to agree with my choice of axes, and moving the origin to the same symmetry center as in the case of the iodine atoms, these positions are as follows:

[7] See A. Müller, Proc. Roy. Soc. **A120**, 437 (1928).

[8] R. W. G. Wyckoff, *The Analytical Expression of the Results of the Theory of Space-Groups* (Carnegie Institution Publication No. 318, Washington, 1922), p. 65.

xyz; $\bar{x}yz$; $x+\frac{1}{2}, y+\frac{1}{2}, \bar{z}$; $x+\frac{1}{2}, \frac{1}{2}-y, z$;
$\bar{x}\bar{y}\bar{z}$; $x\bar{y}\bar{z}$; $\frac{1}{2}-x, \frac{1}{2}-y, z$; $\frac{1}{2}-x, y+\frac{1}{2}, \bar{z}$;
$x+\frac{1}{2}, y, z+\frac{1}{2}$; $x+\frac{1}{2}, \bar{y}, \frac{1}{2}-z$;
$\bar{x}, \frac{1}{2}-y, z+\frac{1}{2}$; $\bar{x}, y+\frac{1}{2}, \frac{1}{2}-z$;
$\frac{1}{2}-x, \bar{y}, \frac{1}{2}-z$; $\frac{1}{2}-x, y, z+\frac{1}{2}$;
$x, y+\frac{1}{2}, \frac{1}{2}-z$; $x, \frac{1}{2}-y, z+\frac{1}{2}$.

The calculated values of the parameters are as follows: $x=0.114$, $y=-0.044$, and $z=0.188$.

By using the molecular model of Fig. 3, the molecular packing in the case of diiodoethylene in the $(100)_0$ plane is very similar to that for diiodoethane with contacts across iodine atoms and also between a hydrogen of one molecule and an iodine of an adjacent molecule along the c axis. The one hydrogen atom on each carbon atom lies in the plane of the carbon and iodine atoms. No molecular rotation is possible because of the double bonds resulting from the bond resonance. There are, therefore, no contacts between atoms in the a direction. The sheets of atoms perpendicular to the a direction are held together by extremely weak binding forces as in graphite perpendicular to the rings. The iodine atom domain radius is 1.97A and that of the hydrogen is 1.21A in quite satisfactory agreement with the values for diiodoethane. The carbon and hydrogen atoms occupy other sets of the same equivalent positions as the iodine atoms with the calculated values of the parameters as follows: $u_C=0.0533$, $v_C=-0.0079$, $u_H=0.095$, and $v_H=-0.17$.

The molecular packing and atom contacts as just discussed are in excellent accord with the cleavage properties, hardness, and melting points of the crystals. Diiodoethane[9] is reported to show perfect cleavage along (100) and (010). On Fig. 4 (a) it is very evident that excellent cleavage parallel to (010) is to be expected at the points $b/4$ and $3b/4$. The cleavage parallel to (100) is equally evident from Fig. 4 (b). From the molecular packing the same cleavage would be expected for diiodoethylene as for diiodoethane. That none has been reported is probably due to the extreme softness and plasticity of diiodoethylene. Jaeger[9] reports that the crystals are "incredibly plastic and bend corkscrew-like at the least touch." This extreme softness and plasticity is readily explained by the very weak binding forces along the a direction. The sheets of molecules in the (100) plane, held together by somewhat stronger forces, are tough but can slip over each other with extreme ease, hence corkscrew-like deformation occurs so readily. The melting points of both crystals are low, but, as would be expected, diiodoethylene with much weaker binding forces along the a direction melts at the lower temperature, 73°C, while the melting point of diiodoethane is 82°C. Thermal motions of the molecules would be expected to overcome the crystalline forces at a lower temperature in the case of the former.

No optical properties of the crystals are available in the literature, and their softness and extreme solubility in the usual refractive index liquids makes the determination of such properties very difficult. A brief optical study of diiodoethane was made with the following results: Acute bisectrix is a, obtuse bisectrix is b, optic normal c of the orthorhombic unit. Minimum refractive index is for light vibrating parallel to the a axis and is approximately 1.65. This is α, and B_{xa} is X, thus the crystal is negative. Wooster[10] has attempted to correlate the structures of inorganic crystals with their optical properties. He pointed out that layer type lattices are negative with B_{xa} perpendicular to the layers. The same undoubtedly holds for organic crystals,[11] and the structure of diiodoethane is seen to be in accord with its optical properties. It was not found possible to obtain optical data on diiodoethylene, however, it is predicted that they will be in keeping with its structure.

The author wishes to express his indebtedness to Dr. Linus Pauling of the California Institute of Technology who first pointed out to him the possibility of iodine bond resonance. Thanks are also due Dr. A. L. Anderson and Mr. Vernon Scheid of this University for the use of the equipment for the optical studies.

[9] F. M. Jaeger, Zeits. f. Krist. **45**, 546 (1908), or P. Groth, *Chemische. Krystallographie* (Engelmann, Leipzig, 1910), Vol. III, p. 35.

[10] W. A. Wooster, Zeits. f. Krist. **80**, 495 (1931).

[11] See B. Orelkin and K. Lonsdale, Proc. Roy. Soc. **A144**, 630 (1934). Also iodoform with strong negative birefringence has essentially a layer type lattice. See reference 6.

LETTERS TO THE EDITOR

On the Disappearance of Hydrogen in the Presence of Positive Ions

Reference is made to a recent letter in this Journal by A. Schechter.[1] It is deemed advisable to discuss briefly some of the points raised therein in order to further clarify this field. Three distinct types of tubes or reaction chambers were used in our investigations: (1) A type which was completely immersed in liquid air,[2] this type being used both with and without a grid. The experimental results in these tests are therefore independent of the liquid-air level; (2) a tube in which the products were condensed in an attached chamber;[3] (3) the tube shown in Fig. 1 with a distance of 7½ cm between anode and collector, in which the reaction chamber was largely immersed in liquid air. This tube gave results similar in every way to those obtained by the other two types.

The liquid-air level, occluded gas, mean free path, possible dissociation of gas, etc., were recognized as factors to be considered and the apparatus was modified from time to time to study them. However, the authors were soon convinced that these factors were secondary in importance to the continued degassing of the hot ion source and the reduction or decomposition of the material composing the ion source. The Pyrex glass apparatus was thoroughly degassed by heating before the tests. The data reproduced in the plot, Fig. 2, of the Schechter letter, and published as curve 1, Fig. 3, were included in our article to show what actually happens in the experiments when a glow discharge is present within the tube. This discharge takes place under conditions similar to the well-known arc and is accompanied by a gaseous clean-up; it is a condition to be avoided in studies of collision experiments where the effect of positive ions as such are to be studied. This curve is therefore not representative of the results obtained. Reference may also be made to Schechter's results, on the synthesis of ammonia from nitrogen and hydrogen mixtures. A brief account of the results obtained by one of us in a similar experiment[4] indicated no measurable increase in the rate of decrease in the gas pressure under bombardment of K^+ ions from an iron potassium ammonia catalyst with speeds up to 330 volts. Furthermore in some of these experiments the disappearance of gas in the presence of the nitrogen-hydrogen mixture continued until the decrease in pressure was comparable to the amount of hydrogen present in the original mixture and then ceased, indicating a further reduction of the iron potassium oxides with the formation of water vapor. It was also observed after many hours of operation of the catalyst strip that it became entirely inactive as a clean-up agent in a nitrogen-hydrogen mixture, although the material was still a good emitter of positive ions.

After a further analysis of our experimental data in the light of Schechter's recent letter, we believe our previous conclusions hold although they are not in agreement with the conclusions arrived at by Schechter and his co-workers.

C. H. KUNSMAN
R. A. NELSON

Bureau of Chemistry and Soils,
U. S. Department of Agriculture,
September 14, 1935.

[1] Schechter, J. Chem. Phys. **3**, 433 (1935).
[2] Kunsman and Nelson, Phys. Rev. **40**, 936 (1932).
[3] Kunsman and Nelson, J. Chem. Phys. **2**, 752 (1934).
[4] Kunsman, J. Chem. Ed. **6**, 629 (1929).

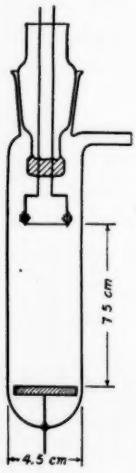

FIG. 1.

The Raman Spectrum of Arsenic Trichloride

In a recent paper[1] Brodskii and Sack apply Dennison's central force treatment[2] to the modes of vibration of $AsCl_3$ using the assignment $\omega_1=410$, $\omega_2=159$, $\omega_3=372$, $\omega_4=195$ cm^{-1}. Their calculated bond angle agrees well with electron diffraction results. It seems desirable to point out, however, that polarization experiments[3] require another assignment, namely, ω_1 (symmetrical stretching) $=410$ ($\rho=0.08$), ω_2 (symmetrical bending) $=195$ ($\rho=0.42$), ω_3 (degenerate) $=372$ ($\rho=0.86$), ω_4 (degenerate) $=159$ ($\rho=0.86$), and that until the polarization theory or experimental results have been shown to be incorrect, one has no reliable criteria for making any other assignment.

On this basis one must still conclude with previous authors[4] that central forces alone do not suffice for the treatment of the $AsCl_3$ type molecule.

DON M. YOST
THOMAS F. ANDERSON

Gates Chemical Laboratory,
California Institute of Technology,
September 16, 1935.

[1] A. E. Brodskii and A. M. Sack, J. Chem. Phys. **3**, 449 (1935).
[2] D. M. Dennison, Phil. Mag. **1**, 195 (1926).
[3] J. Cabannes and A. Rousset, Comptes rendus **194**, 79 (1931).
[4] K. W. F. Kohlrausch, *Der Smekal-Raman-Effekt* (Springer, Berlin, 1931); Don M. Yost and J. E. Sherborne, J. Chem. Phys. **2**, 125 (1934); Don M. Yost and T. F. Anderson, ibid. **2**, 624 (1934); J. B. Howard and E. B. Wilson, Jr., ibid. **2**, 630 (1934).